


Thesis submitted for the degree of  
Master of Philosophy  
at the University of Leicester

**THERMOBAROMETRY  
OF THE GARNET-BEARING ROCKS OF THE JIJAL COMPLEX  
(WESTERN HIMALAYAS, NORTHERN PAKISTAN)**



by  
Lucie Ringuette

Department of Geology, University of Leicester  
October 1996

**THERMOBAROMETRY OF THE GARNET-BEARING ROCKS OF THE JIJAL COMPLEX (WESTERN HIMALAYAS, NORTHERN PAKISTAN)**

by Lucie Ringuette

---

**ABSTRACT**

The Kohistan terrane located in the western Himalayas is an oceanic arc of Early Cretaceous age accreted to the Asian plate and then obducted onto the Indian plate. It can be observed along a complete oblique section from ultramafic/mafic rocks to supracrustal volcanics. The 150 sq km Jijal complex constitutes the lowermost part of this arc and consists of rocks that probably crystallized near the crust/mantle boundary. Detailed petrological study of the garnet-bearing rocks of the Jijal complex indicates their magmatic origin because primary garnet, plagioclase (highly saussuritised), clinopyroxene, and amphibole occur as relicts among metamorphic grains. Plagioclase, clinopyroxene and amphibole grains are usually homogeneous in composition, contrasting with zoned garnet grains that suggest complex pressure-temperature paths. However, plagioclase composition is heterogeneous at thin section scale (from albite to anorthite = 80). An average variation of 5-10% of  $Al^{VI}$ , jadeite and Ca-tschermak content between grains of a sample indicates a major decompressional metamorphic event that post-dates the magmatic stage, hence probably related to the obduction of the arc onto the Indian plate. Phases like actinolitic hornblende, epidote, muscovite, paragonite, and chlorite are widely distributed within host rocks, veins and shear zones of the Jijal complex and result from retrogression associated with penetrative fluid circulation during late stage of the obduction. Geothermobarometry of the garnet-bearing rocks of the Jijal complex indicates disequilibrium among phases mainly including garnet, plagioclase, and clinopyroxene. Such disequilibrium is more likely to be attributed to the variability of plagioclase composition within a sample, but also to clinopyroxene  $Al^{VI}$ , jadeite and Ca-tschermak variability. Considering the magmatic assemblages, temperature-pressure conditions of crystallization can be estimated between <1100-1300°C, 13-25 kbar. A minimum pressure calculated from a high-jadeite content (16%) metamorphic clinopyroxene, normative (An = 50%) plagioclase and garnet assemblage reaches 17 kbar at 950°C, and can be related to the burial of the Jijal complex during its accretion with the Asian plate that preceded its obduction onto the Indian plate.

## TABLE OF CONTENTS

	Page
INTRODUCTION.....	7
<b>Part I: Geological setting</b>	
KOHISTAN TERRANE: AN OVERVIEW.....	9
Lithological units of the Kohistan oceanic arc and tectonic implications.....	11
The Kohistan batholith unit: implications for magmatism and cooling history of the Kohistan arc.....	17
LITHOLOGICAL UNITS OF THE JIJAL COMPLEX.....	22
1) Ultramafic cumulates.....	22
2) Garnet-bearing rocks.....	23
3) Hornblende-pyroxene gabbros.....	25
<b>Part II: Petrography and mineral chemistry</b>	
MINERAL REACTIONS AND REACTION TEXTURES IN HOST ROCKS.....	27
Magmatic cumulate assemblages.....	27
Granulite facies assemblages.....	31
Amphibolite facies assemblages.....	31
Transitional epidote-(chlorite)-amphibolite facies assemblages.....	32
MINERAL REACTIONS AND REACTION TEXTURES IN VEINS.....	32
SHEAR ZONES.....	35
MINERAL ANALYSES.....	35
MINERAL CHEMISTRY AND COMPOSITION PROFILES OF THE MAIN PHASES.....	37
Garnet.....	37
Clinopyroxene.....	39
Orthopyroxene.....	40
Plagioclase.....	40
Amphibole.....	43
Sample K27, from the Kamila amphibolitic belt/Chilas complex contact.....	43

COMPOSITION PROFILES.....	46
Garnet-zoning profiles.....	46
Zoning profiles of clinopyroxene, orthopyroxene, plagioclase, and amphibole.....	49
CALCULATION OF METAMORPHIC CONDITIONS.....	49
PRESSURE AND TEMPERATURE ESTIMATES.....	52
DISCUSSION AND CONCLUSION.....	56

## Appendices

Appendix 1: Thin section descriptions including modal composition, mineral assemblage and possible reactions.....	60
Appendix 2: Calculation of mole fractions and assignment of site occupancies.....	107
Appendix 3: Probe data including calculation of the stoichiometry of minerals and the distribution of cations within sites, according to the THEBA software.....	110
3a) Garnet probe data.....	on disk
3b) Plagioclase probe data.....	on disk
3c) Clinopyroxene probe data.....	on disk
3d) Orthopyroxene probe data.....	on disk
3e) Amphibole probe data.....	on disk
Appendix 4: Compositional triangular diagrams for garnet, clinopyroxene, orthopyroxene, and amphibole of samples from the Jijal complex and K27.....	111
4a) North to South (Grs-Alm-Prp) diagrams for garnet of the northern series.....	112
4b) North to South (Grs-Alm-Prp) diagrams for garnet of the southern series.....	115
4c) North to South (Wo-En-Fs) diagrams for clinopyroxene of the northern series.....	117
4d) North to South (Wo-En-Fs) diagrams for clinopyroxene and orthopyroxene of the southern series.....	119
4e) North to South ACF ( $\text{Al}_2\text{O}_3$ -Cao-[FeO-MgO]) diagrams for amphibole of the northern series.....	121
4f) North to South ACF ( $\text{Al}_2\text{O}_3$ -Cao-[FeO-MgO]) diagrams for amphibole of the southern series.....	123
4g) Compositional triangular diagrams for garnet, clinopyroxene, and amphibole of sample K27 from the Kamila amphibolite belt/Chilas complex contact.....	124

Appendix 5: North to South pressure-temperature diagrams from selected samples of the Jijal complex..... 125

5a) North to South pressure-temperature diagrams of selected samples of the northern series..... 126

5b) North to South pressure-temperature diagrams of selected samples of the southern series..... 133

ACKNOWLEDGMENTS..... 139

REFERENCES..... 140

## Figures

Figure 1:	Simplified geological map of the Kohistan arc (from M.A. Khan et al., 1993; Coward et al., 1986).....	10
Figure 2:	Geological map of Jijal and Patan complexes (from Miller et al., 1991).....	12
Figure 3:	ACF ( $Al_2O_3$ -CaO-[FeO-MgO]) diagram including the bulk chemical composition of rocks from the Jijal complex and the change of liquidus surface with pressure, according to Moudden (1991).....	28
Figure 4:	Compositional triangular diagrams for garnet of the Jijal complex.....	38
Figure 5:	(Q-Jd-Ae) diagram according to Morimoto (1988) for clinopyroxene of the Jijal complex.....	41
Figure 6:	Fields of eclogite and granulite clinopyroxenes of the Jijal complex, according to White (1964).....	42
Figure 7:	Garnet zoning profiles:.....	47
7a)	N629b - almandine.....	47
7b)	GI11 - almandine.....	47
7c)	P23a - pyrope.....	47
7d)	N639b - (almandine-pyrope-grossular) garnet.....	47
7e)	N616 - garnet with "compositional grain shapes".....	48
7f)	N601a - garnet with growth appendices.....	48
7g)	N601a - homogeneous garnet.....	48
Figure 8:	Pressure-Temperature diagram showing results of P-T estimates from rocks of the Jijal and Khawasa Khela complexes.....	58

## Tables

Table 1:	North to South distribution and modal compositions of samples from the Jijal complex (and K27).....	29
Table 2:	Textural reactions.....	33
Table 3:	Mineral formulae and symbols.....	34
Table 4:	Metamorphic facies and associated amphibole compositions of the samples from the Jijal complex (and K27).....	44
Table 5:	Compositional variations according to zoning profiles of the main phases in samples from the Jijal complex (and K27).....	50
Table 6:	Reactions used as geothermometers and geobarometers.....	52
Table 7:	Temperature and pressure calculations of selected samples of the Jijal complex.....	55
Table 8:	Contrasting magmatic and metamorphic garnets of the Jijal complex.....	57

## INTRODUCTION

The determination of the conditions of pressure and temperature and eventually of pressure-temperature-time paths has proved, during the last two decades, to be a powerful tool to unravel the tectonic evolution of orogenic belts and more specifically of collision zones (*eg.* England and Richardson, 1977; St-Onge, 1987). The Kohistan terrane (Tahirikheli et al., 1979; Bard et al., 1980; Jan, 1980; Jan and Howie, 1981; Coward et al. 1982), located in the western Himalayas, is an obducted oceanic arc that is observable along an oblique section from ultramafic/mafic rocks to supracrustal volcanics. The Jijal complex constitutes the lowermost part of this arc. It rests directly on the Main Mantle Thrust and consists of rocks that probably crystallized near the crust/mantle boundary.

The aim of this study is to bring a better understanding to the petrologic evolution of the base of the arc from magmatic crystallization to cooling after obduction. This evolution will help understand this part of the Himalayan collisional belt. Geothermobarometry applied to the rocks of the Jijal complex should enable us to better constrain:

- 1) the late magmatic pressure-temperature conditions within or at the base of the arc;
- 2) the temperature and depth of burial during its accretion to the Asian plate;
- 3) the retrograde metamorphic conditions recorded during the obduction of the arc onto the Indian plate.

In order to do so, a general overview will be given of previous work pertaining to the Kohistan terrane and to the Jijal complex followed by traditional petrographic observations and microprobe analyses from the (garnet-pyroxenes-plagioclase +/- hornblende)-bearing rocks of the Jijal complex. Data treatment, including calculation of the stoichiometry of minerals, composition profiles and P-T curves will be undertaken with the THEBA software (Martignole et al., unpublished). These data will provide the basis for a geodynamic interpretation of the Jijal complex.

Part I:

**Geological setting**



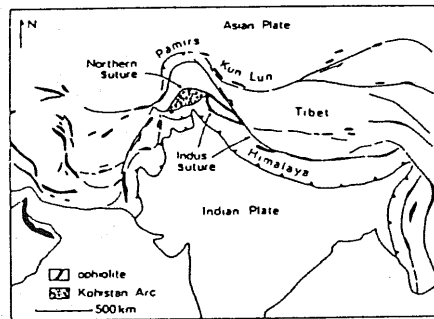
## KOHISTAN TERRANE: AN OVERVIEW

The Kohistan terrane of Northern Pakistan was first recognized as a distinct tectonic zone by Desio (1964). It is unique for its high proportion and thickness (> 45 km, Miller et al., 1994) of mafic and intermediate magmatic rocks. It covers more than 36,000 sq km in the western branch of the Himalayan syntaxis between 71°E (Kunar River) and 75°E (Nanga Parbat Massif), and is situated on the north side of the Indus-Tsangpo Suture zone, which is a crustal lineament separating the Asian Plate from the Indian Plate. In western India the latter splits into two branches represented by the northward-dipping "Main Mantle Thrust" (MMT) which separates Kohistan from the Indian Plate, and the subvertical Main Karakorum Thrust (MKT), alternatively called the Northern Megashear (Tahirkheli and Jan, 1979), the Northern Suture (Coward et al., 1982, 1986; Pudsey, 1986), or the Shyok Suture (Rex et al., 1988; Searle et al., 1989; Sullivan et al., 1993), which separates Kohistan from the Asian Plate.

The Kohistan sequence forms as a thick, more or less monoclinial slab that dips 30° to 60° NW (Bard et al., 1980). It is composed of calcalkaline plutonic and volcanosedimentary rocks, which underwent low- to high-grade metamorphism; the metamorphic grade decreases upward. This sequence is currently divided from bottom to top into the following main E-W trending units, recognized by research teams from Pakistan, France, Britain, and the United States (Tahirkheli et al., 1979; Bard et al., 1980; Jan, 1980; Jan and Howie, 1981; Coward et al. 1982; Loucks et al., 1990; Treloar et al., 1990): the Kamila Amphibolite belt with basal ultramafic-mafic cumulates, the Chilas complex, the Kohistan batholith, the Chalt volcanic belt and the Yasin Group (see figure 1).

Based on lithological and geochemical data the Kohistan sequence has been interpreted as a Cretaceous intra-oceanic arc (Tahirkheli et al., 1979; Bard et al., 1980; Coward et al., 1982; Jan et al., 1982 and 1990; Coward et al., 1986). Miller and Christensen (1994) pointed out the presence of a thick lower crustal, high-velocity zone in Kohistan which is characteristic of island arcs and provides geophysical corroboration of the island arc origin of Kohistan.

The arc developed in neo-Tethys (>120-80 Ma) due to northward subduction of the Tethys ocean. In the Karakorum which represented the continental margin at that time, calcalkaline plutons such as the Hunza and the Ghamu Bar, and sub-alkaline plutons such as the Darkot Pass were dated at ca. 110 to 95 Ma (Rb-Sr and K-Ar ages, Debon et al., 1987) and provide evidence for northward subduction of oceanic lithosphere at the leading edge of the Indian plate. Hence, the Kohistan arc probably formed on the northern side of Tethys during Cretaceous time and was separated from the Asian plate by a back-arc basin (Pudsey, 1986). Northward subduction of the back arc basin in the early Late Cretaceous (Johnson et



The position of the Kohistan Arc in the Himalayan and Tibet collision zones.

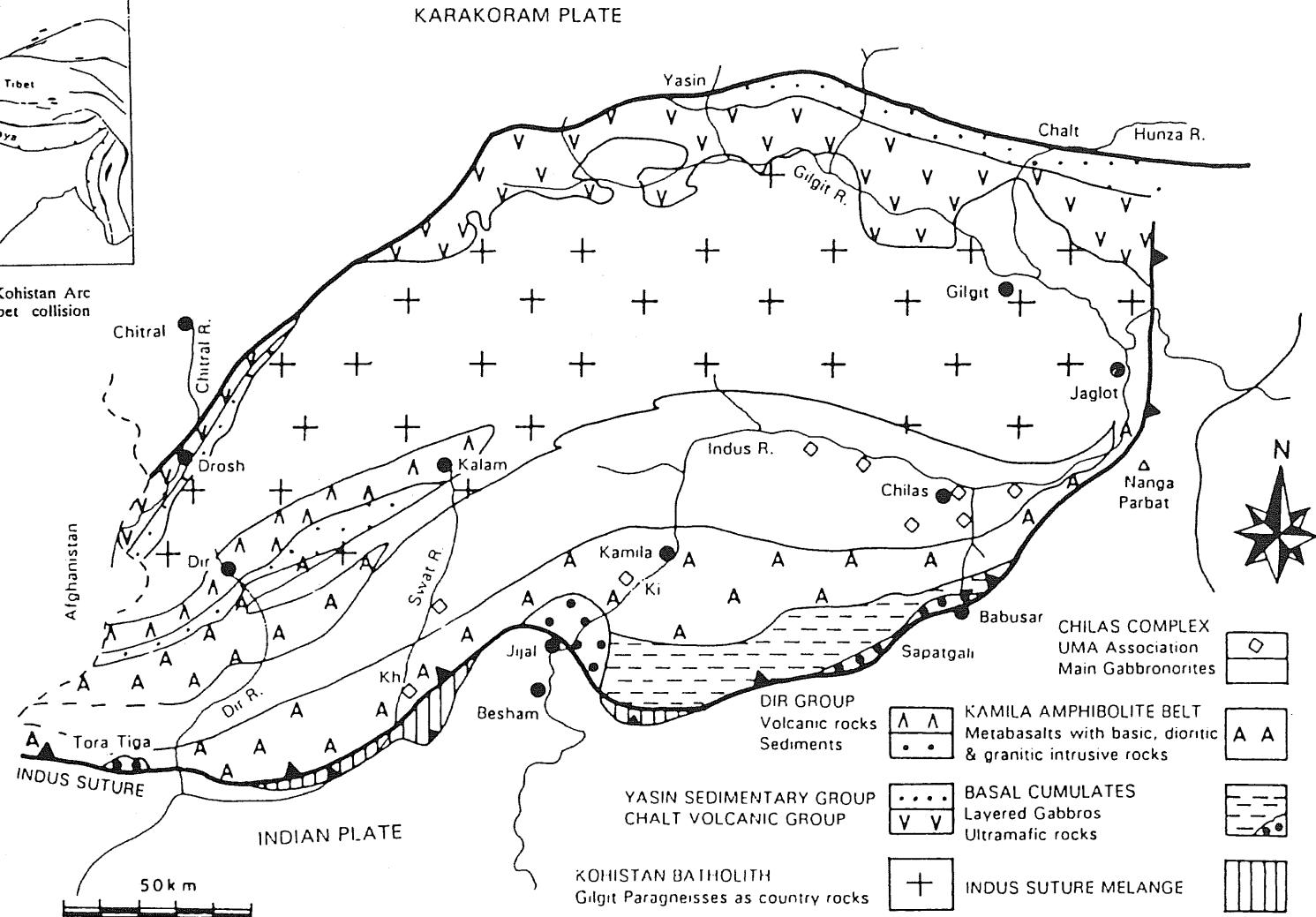


Figure 1. Simplified geological map of the Kohistan arc (from M.A. Khan et al., 1993; Coward et al., 1986).

Kh: Khawasa Khela, Ki: Kiru, UMA: ultramafic-mafic-anorthosite.

al., 1976) welded the arc to the Asian (Karakorum) plate with consequent formation of the Shyok suture in the period 102-85 Ma (Tahirkheli, 1983; Petterson and Windley, 1985; Pudsey et al., 1985; Coward et al., 1986; Searle et al., 1987). Further subduction of Tethys below the arc and the leading edge of Asia converted Kohistan into an Andean-type margin (Petterson and Windley, 1985) that predates 60 Ma (Treloar et al., 1989). Currently available age data place all continental margin sedimentation and volcanic activity in Kohistan within a 7 M.y. period (Sullivan et al., 1993). Complete consumption of Tethys resulted in the Palaeocene to mid-Eocene (between 65-49 Ma) continental collision of India with the Kohistan arc along the Indus suture (Allègre et al., 1984; Mattauer, 1986). The arc, already deformed by its accretion to the Asian plate, was partially thrust under it and then obducted onto the Indian plate. Consequently, a virtually complete oblique section of a tilted oceanic arc, from its ultramafic underpinnings at the crust/mantle boundary to surface volcanic rocks and sediments is exposed in Kohistan (Tahirkheli et al., 1980; Coward et al., 1986).

## LITHOLOGICAL UNITS OF THE KOHISTAN OCEANIC ARC AND TECTONIC IMPLICATIONS

The exposed intermediate to lower crust in southern Kohistan formed in an intraoceanic arc stage and represents a life-span of 40 M.y. (Khan et al., 1993) which is constrained by the maximum age of 120 Ma from the Jijal complex and the minimum age of 80 Ma from the mafic dykes of the Chilas complex that represent the last magmatic phase in Kohistan before its accretion with the Asian plate (Khan, 1988; Treloar et al., 1989). This wedge of lower crust consists of basal ultramafic and gabbroic cumulates emplaced into amphibolites derived from basaltic to andesitic volcanics (Jan, 1988), exposed in the Kamila amphibolite belt with basal ultramafic-mafic cumulates, together with the Chilas complex. The intermediate to upper arc crust of the northern part of Kohistan, although dominated by a range of calcalkaline intrusives that form the Kohistan batholith unit dated at c. 102-30 Ma (see next section of this chapter), includes sedimentary and volcanic rocks that formed in the intraoceanic stage of the arc. The metasedimentary and metavolcanic rocks comprise the Gilgit paragneisses overlain by the Chalt volcanic belt and the Yasin Group which is the uppermost lithological unit of Kohistan.

The **basal ultramafic-mafic cumulates** include, from east to west, the **Babusar, Sapatgali, Jijal, Patan and Tora Tiga** complexes (figures 1 and 2). They outcrop on the immediate hanging wall of the MMT and are related in space and time to the growth of the intraoceanic arc; they are considered as cumulates of magma(s) of the Kohistan arc (Jan and Jabeen, 1990). Plutons are predominantly tholeiitic in composition (Jan and Windley, 1990; Jan et al., 1993) and could be equivalent to the metavolcanic component of

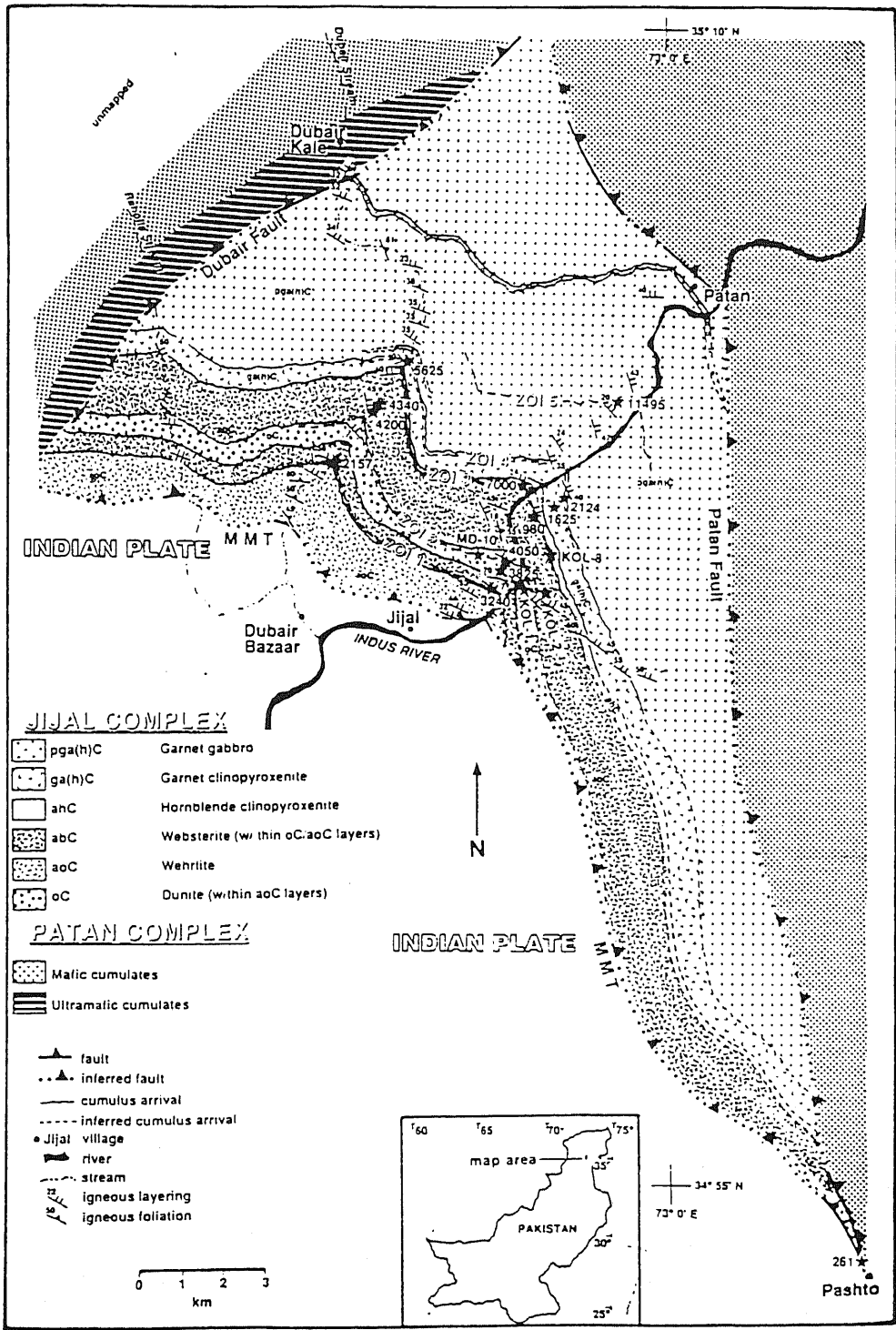


Figure 2. Geological map of Jijal and Patan complexes (from Miller et al., 1991).

the Kamila amphibolite belt to the north (Khan et al., 1993). The Jijal complex has an  $^{40}\text{Ar}/^{39}\text{Ar}$  hornblende cooling age of approximately 120 Ma (Treloar et al., 1989) which gives a maximum age for the southern part of the Kohistan arc.

Tectonic mélanges of the Indus suture zone include ultramafic-mafic plutonic complexes like that at Shangla and may represent sub-arc/oceanic crust/mantle (Jan et al., 1993). The Dargai ophiolite (like that of Spontang in western Ladakh) may be a klippe that overrode the Indian plate some 30 km to the south of the suture (Ahmed, 1988).

The **Kamila amphibolite belt** including the basal ultramafic-mafic cumulates is composed of mafic to dioritic sills and metamorphosed volcanic rocks grouped within a 38 km-wide shear zone (Treloar et al., 1990) which consists of a series of anastomosing high strain zones: the **Kamila Shear Zone**. The latter may have formed as a result of the southward propagation of shortening across the Kohistan complex following suturing with Asia, but prior to collision with India (Treloar et al., 1990). Jan (1988) interpreted banded amphibolites which form the bulk of the Kamila Amphibolite belt, as retrogressed gabbro-norites, amphibole schists and pelitic schists. It may be the higher grade equivalent of the Chalt volcanics and metasediments to the north (Coward et al., 1986). It includes two areas in which garnet is sporadically present due to compositional control: one is just to the north of Patan along the southern margin of the shear zone in an 8 km wide belt; and the second is 14 km wide and is largely coincident with a granite belt along the northern margin of the shear zone.

The metavolcanic amphibolites of the Kamila amphibolite belt can be subdivided into two different geochemical types (Khan et al., 1993): 1) fine to medium grained, homogeneous or banded amphibolite with relict pillow structures (Jan, 1988 and Treloar et al. 1990). This type is enriched in high-field-strength elements (HFSE) and heavy-rare-earth elements (HREE) and is transitional in character between N- and E-MORB types, and has a minor subducted-related component. Khan et al. (1993) identified this type to be the earliest arc basement in Kohistan; 2) medium to coarse grained and homogeneous (Jan, 1988; Treloar et al., 1990) metavolcanic amphibolites together with deformed and amphibolitised intrusive mafic plutons. Amphibolites of the second group are depleted in HFSE and HREE, have a distinct negative Nb anomaly, and are transitional tholeiitic to calcalkaline in nature. The plutons were probably emplaced in the early to mature stages of oceanic arc growth. Hence, a highly deformed and recrystallized volcanic basement intruded by mafic plutons appears to be a logical interpretation for the Kamila amphibolite belt (Khan et al., 1993). A well preserved and weakly deformed equivalent at pumpellyite grade is the Dras Unit in Ladakh (Honegger et al., 1982). A minimum K-Ar hornblende age is concordant with  $^{40}\text{Ar}/^{39}\text{Ar}$  hornblende minima at approximately 83 Ma (Treloar et al., 1989) and is similar to a  $^{40}\text{Ar}/^{39}\text{Ar}$  hornblende age of 86 Ma given by Zeitler (1985). Undeformed mafic dykes

cross-cut all the above structures and are similar to those in the Chilas complex (dated at 80-85 Ma by  $^{40}\text{Ar}/^{39}\text{Ar}$  on hornblende; Khan, 1988; Treloar et al., 1989).

The **Chilas complex** is 300 km long and up to 40 km broad and occupies the axis of the Kohistan arc along its east-west extent. It is a 10 km to 15 km thick stratiform intrusion of calcalkaline gabbro-norites (more than 85% of the complex), and massive two-pyroxene diorites. The former locally grade into pyroxenite and anorthosite ultramafic associations (Khan et al., 1993). Minor chromite-layered dunites also occur in several bodies of ultramafic rocks, commonly less than 5 sq km. The gabbro-norites grade southward into medium-pressure hydrated granulites (Khan and Coward, 1990). Based on the presence of inverted polarity in graded layers, the complex appears to be isoclinally folded with a number of widely spaced narrow, steeply dipping, shear zones of limited displacement at its southern margin. The complex is dated at 104 Ma (Sm-Nd garnet age, Coward et al., 1986) and a minimum K-Ar hornblende age is concordant with  $^{40}\text{Ar}/^{39}\text{Ar}$  hornblende minima for the hydration and shearing at approximately 80 Ma, which may be related to the collision between the Kohistan arc and the Asian plate (Treloar et al., 1989).

According to Khan et al. (1993) mutual field relations can be established between the Chilas complex and the Kamila amphibolite belt because more than two thirds of the rocks in the Kamila belt are identical to those of the Chilas complex, and the ultramafic-mafic-anorthosite associations are very similar to the rocks at Khawasa Khela and Kiru (figure 1). Metasedimentary xenoliths in the Chilas complex can also be related to the rocks of the Kamila belt, and both (see above) are intruded by similar cross-cutting mafic dykes. Khan et al. (1993) suggested that the Chilas complex formed during a period of magmatism subsequent to the formation of the Kamila amphibolite belt, which can be divided in two stages: the first one is represented by the extensive and typical calcalkaline gabbro-norites which are enriched in LILE and LREE, depleted in HFSE and HREE, and have negative Nb and positive Sr anomalies. They could be the products of partial melting of a mantle diapir emplaced into a mature back-arc environment, or more probably formed through early rifting of a mature island arc (Khan et al., 1989). The second stage of magmatism includes the ultramafic-mafic-anorthosite associations (UMA) which are depleted in incompatible trace elements, suggesting a higher degree of melting of sub-arc mantle. The UMA crystallized from tholeiitic picritic to high-Mg basalts probably generated in an advanced stage of intra-arc rifting. According to Khan et al. (1993) the absence of ophiolitic rocks, which might be expected to be related to the postulated intra-arc rift in Kohistan, may be explained by the lack of evidence for the existence of a fully fledged oceanic basin.

Mafic dykes of the Chilas complex represent a continuation of the magmatism associated with the last stages of intra-arc rifting, because they are tholeiitic to picritic and LILE depleted relative to HFSE. They have a  $^{40}\text{Ar}/^{39}\text{Ar}$  age of 80-85 Ma on hornblende

(Khan, 1988; Treloar et al., 1989), and thus may be coeval with the Jutal dykes (ca. 75 Ma, D. Rex in Petterson and Windley, 1985 and 1992) in the Kohistan batholith; they formed in the last magmatic phase of Kohistan, in the waning stages of collision of the arc with the Asian plate. The imbrication related to the collision gave rise to the Jaglot syncline (in the Kohistan batholith) and its associated folds that deformed the Chilas complex, the Chalt Volcanic belt and the Yasin Group (Petterson and Windley, 1985; Coward et al., 1986). It may have affected the entire island arc as similar subduction-related ages (80-75 Ma,  $^{40}\text{Ar}/^{39}\text{Ar}$  on phengite, Maluski and Matte, 1984) from a blueschist at Shangla Pass along the southern MMT suggest that these imbricate rocks were detached within the subduction zone itself. This collision is hence responsible for most of the deformation within the arc and is referred to as "the main phase of deformation" (Coward et al., 1986; Petterson and Windley, 1985; Treloar et al., 1989) for which a minimum age is given by a fabric cutting pegmatite at 66 Ma (K-Ar muscovite age, Treloar et al., 1989). Actinolite and chlorite within the shear zones formed during continued deformation after the Shyok suture formation.

Trondhjemites similar in composition to those of the Kohistan batholith (dated at 102 Ma, Rb-Sr whole rock isochrons, Petterson and Windley, 1985) locally intrude the Chilas complex (Khan et al., 1993).

The **Gilgit paragneisses** represent the lower levels of the sedimentary and volcanic rocks of northern Kohistan. They comprise high-grade metasediments including siltstones, semi-pelites and minor carbonates, intercalated with amphibolites of the Kamila amphibolite belt (T. Khan, pers. comm. 1991 in Khan M.A. et al., 1993), and overlain by the Chalt Volcanic belt.

The vertical **Chalt Volcanic belt** trends east-west, has an area of 330 km x 30 km, and is 6-8 km thick. It contains high-Mg (15-6%) pillowed metabasalts, andesites, dacites, pyroclastics, all intruded by various late kinematic diorites, granodiorites and mafic dykes that formed during the stage I of growth of the Kohistan batholith (see next section). The belt is metamorphosed to greenschist facies to the west and low amphibolite facies to the east (Coward et al., 1986; Petterson and Windley, 1991). Some immature turbidites are also associated with these volcanics. According to Petterson and Windley (1991) volcanics of the eastern Hunza valley are predominantly high-Mg tholeiites with subordinate andesites, boninites and komatiitic basalts, whereas the volcanics exposed in the Gilgit, Ishkuman and Yasin river valleys to the west are all low-intermediate MgO (< 6%) calcalkaline andesites to dacites. The former are characterised by a low absolute abundance of trace elements and by near constant concentrations of many trace elements through a range of major element compositions. Their strong negative Nb anomaly combined with their enrichment in LILE/HFSE give them a distinctive subduction zone signature that implies a "depleted" harzburgite-type source. In order to produce melts with a MgO content similar to boninite,

Green (1976) demonstrated that temperatures above 1200°C are required, hence a depleted harzburgite source would not melt under “normal” subduction conditions. Petterson and Windley (1991) suggested subduction of young, hot oceanic crust and/or spreading center as a possible way of achieving such required liquidus temperatures. As boninite can form in early stages of subduction (Baker, 1982), in fore-arc settings (Cameron et al., 1979), or in intraoceanic - intra-arc rifts (Beccaluva and Serri, 1988), it is interesting to note that the latter possibility can be correlated with the previous interpretation given by Khan et al. (1989, 1993) for high-Mg magmatism in the Chilas complex.

The calcalkaline andesites are enriched in incompatible trace elements but depleted in compatible elements such as Cr and Ni compared with the high-Mg tholeiites. They are also enriched in LILE/HFSE and in LREE/HREE with a distinct negative Nb anomaly, thus displaying typical subduction zone signatures. Considering their geochemical similarities and the ca. 110 Ma minimum age constrained by fossil evidence in overlying sediments interbedded with the upper volcanics of the Yasin Group, and the 72 Ma maximum age of  $^{40}\text{Ar}/^{39}\text{Ar}$  on hornblende (Treloar et al., 1989), Khan et al. (1993) suggested that the calcalkaline andesites could have formed during early arc magmatism in the Kamila amphibolite belt.

The **Yasin Group** occurring in a synclinal belt nearly 20 km long, and up to 3 km thick, contains Orbitolina and Rudists of Aptian/Albian age ( $\approx 110$  Ma) (Pudsey et al., 1986). It comprises the overlying arc sediments that are divisible into a lower sedimentary unit (over 1 km thick) and an upper fine-grained volcanic unit (up to 2 km thick) (Pudsey, 1986). The sediments consist of slates and some silty quartzites that coarsen northwards to pebble-cobble conglomerates in the vicinity of the Shyok suture and they are almost devoid of carbonates. The volcanic rocks have a high proportion of epidote-rich volcanoclastics (and a 500 m thick limestone) and terrigenous clastics that occur in the form of distal turbidites and slates with massive greywackes.

Coward et al. (1987), Khan and Coward (1990), Treloar et al. (1990) presented the Kohistan as a composite arc system that includes a northern or Chilas arc and a southern or Jijal arc, accreted along the Kamila shear zone. However Khan et al. (1993) recently demonstrated the lateral continuity and the regional extent of the Kamila shear zone which, combined with the absence of oceanic sediments and ophiolites, rules out the previous model. Considering the fact that the Chilas complex as a laterally continuous mass of closely related igneous rocks virtually divides the Kohistan arc into two entities, they suggested that the arc crust exposed on either side of the complex represents rifted parts of a single arc: the basal ultramafic-mafic complexes overlain by the Kamila amphibolite belt in southern Kohistan represent the fore arc, and the Gilgit paragneisses, the Chalt Volcanic belt and the



Yasin Group in northern Kohistan represent the back arc. Similar intra-arc rifting has been documented from modern arcs like Mariana in the western Pacific (Karig et al., 1978; Stern et al., 1990) and New-Hebrides, Fiji (Karig, 1971; Marcelot et al., 1983).

## THE KOHISTAN BATHOLITH UNIT: IMPLICATIONS FOR MAGMATISM AND COOLING HISTORY OF THE KOHISTAN ARC

The 60 km wide Trans-Himalayan batholith belt extends almost continuously for about 2700 km from Afghanistan to Burma and formed in response to the northward subduction of Tethyan oceanic lithosphere. It is represented in the Kohistan sequence by the Kohistan batholith, a range of calcalkaline plutonites that occur as major plutons (over 250 sq km in area), minor stocks, sills, sheets and dykes with a Rb-Sr age span from 102 Ma to 30 Ma (Honegger et al., 1982; Petterson and Windley, 1985, 1991). The batholith has been variably affected by regional greenschist to local amphibolite facies metamorphism. On the basis of their fabric, which is the most fundamental criterion by which the plutonic rocks were first subdivided, Petterson and Windley (1991) recognised three stages of growth within the batholith represented by compositionally distinct phases of magmatism from three magmatic source regions: stage I of growth belonged to the intraoceanic development of the arc (102-80 Ma), stage II to post-collisional Andean-continental-margin magmatism within the arc (85-40 Ma), and stage III to post-collisional magmatism (ca. 30 Ma). Sedimentary and volcanic formations such as the Dir Group and the Shamram Volcanic rocks were intruded by some second-stage plutons, and record the resumption of volcanic activity along the southern margin of the Asian plate, after a prolonged period of uplift and erosion (Sullivan et al., 1993).

The **first-stage plutonic rocks of the Kohistan batholith** occur within plutons intruded in the intraoceanic arc at its mature stage in mid-Cretaceous time, as confirmed by a Rb-Sr whole rock isochron of  $102 \pm 12$  Ma from the Matum Das trondhjemitic (Petterson and Windley, 1985). They consist of a bimodal series of gabbro-diorite quartz-tonalite-trondhjemitic, both modes being represented in approximately equal proportions. The plutons were converted into orthogneisses following the formation of the Shyok suture which gave rise to the Jaglot syncline and associated structures.

The mafic-intermediate plutons are dominated by coarse grained medium- to high-K hornblende gabbros and diorites dated at 94-80 Ma and 80-71 Ma (K-Ar ages on hornblende and biotite respectively, Treloar et al., 1989) associated with ultramafic and monomineralic hornblende pods. According to Petterson and Windley (1991) they are especially enriched in the LILE such as K, Ba and Rb and display high LILE/HFSE and LREE/HREE ratios

characteristic of subduction zone-related magmas. The felsic plutonic rocks are represented by low-K deformed trondhjemites such as the Matum Das pluton, which includes several disrupted mafic dykes dated between 81 Ma and 97 Ma (K-Ar hornblende ages, Treloar et al., 1989), that formed as a minor component in the first stage of growth. The felsic plutonics have a restricted and consistent major and trace element chemistry characterised by a lack of enrichment in LILE/HFSE and in LREE/HREE that may represent the end product of a partial melt which underwent little subsequent fractionation. Considering their low  $^{87}\text{Sr}/^{86}\text{Sr}_0$  ratios ( $0.7039 \pm 0.0001$  for the Matum Das pluton), Petterson and Windley (1991) suggested that the source of the felsic plutonics of stage I of growth was primitive arc crust, which had depleted incompatible element chemistry similar to that of the high-Mg volcanics of the Chalt Volcanic belt.

The **second stage plutonic rocks of the Kohistan batholith** are undeformed and were intruded during later northward subduction of the Tethyan plate under the island arc when it was attached to the leading edge of the Asian Plate, resulting in the formation of Andean-type plutons that represent two thirds of the Kohistan batholith.

Although most of the second stage plutonic rocks have a medium to high-K calcalkaline chemistry, they evolved with time from mafic-intermediate (85-60 Ma) to more felsic compositions (60-40 Ma). The least enriched calcalkaline magmas within stage II are represented by medium-fine grained, mafic and undeformed, NE-SW trending Jutal-Nomal dykes, generally 50 cm-1 m wide, that crosscut the Chalt Volcanics and the stage I plutonic rocks; they are dated at 75 Ma ( $^{40}\text{Ar}/^{39}\text{Ar}$  hornblende age, Petterson et al., 1985). Intermediate compositions are represented by very coarse grained cumulate hornblendites (similar to stage I), sometimes forming monomineralic associated pods with medium-coarse-grained gabbros and diorites. Medium to coarse-grained and undeformed plutons of felsic, medium- to high-K composition dominate stage II of growth. They vary from granodiorite to leucogranite (e.g. Shirot, dated at  $40 \pm 6$  Ma, Rb-Sr whole rock, Treloar et al., 1989) or they are essentially uniform in composition (e.g. Gilgit, dated at  $54 \pm 4$  Ma, *idem*), and they contain variable amounts of volcanic, sedimentary and plutonic xenoliths. According to Treloar et al. (1989) the regional cooling that postdated the suturing of Kohistan to Asia can be constrained by a K-Ar age of 80 Ma given by a hornblende from a xenolith within the pluton and by biotite K-Ar ages between 45 Ma and 34 Ma.

Although a mafic to felsic magmatic trend is observed with time, all rocks are enriched in LILE/HFSE and in LREE/HREE with ratios increasing with fractionation. Most samples also display a negative Nb anomaly. Petterson and Windley (1991) suggested that all plutons from the stage II of growth, together with the medium- to high-K stage I plutons and the calcalkaline andesites of the Chalt Volcanic belt have a typical subduction-related

calcalkaline chemistry and originated from a variably metasomatised mantle wedge situated above an active subduction zone.

Late Palaeocene volcano-sedimentary rocks of the **Dir Group** are located between the plutons of the first stage of growth whereas the others are related to the second and third stages of growth of the arc. They occur in the Baraul Banda Slate Formation and the Utror Volcanic Formation which crop out in the hanging wall of the Dir Thrust that separates the two formations. The **Baraul Banda Slate Formation** comprises 2700 m of basal conglomerates, pelites and interbedded limestones that unconformably overlie an erosion surface that cuts deep into stage I plutons. The erosion surface formed during a prolonged post-collisional period of uplift and erosion along the continental margin of Asia; it is dated at ca. 78-75 Ma ( $^{40}\text{Ar}/^{39}\text{Ar}$ , Treloar et al., 1989). The formation records rapid forearc basin accumulation during the collapse of the Kohistan continental margin within a restricted deep-water environment (Sullivan et al., 1993). The **Utror Volcanic Formation** comprises 3000 m of basaltic andesites, dacites, rhyolites and ignimbritic tuffs. It is interpreted as a complex association of lavas and volcanoclastic material that accumulated within a tectonically active ring-plain or flanking facies distal to the main focus of volcanic activity. According to Sullivan et al. (1993) the abundance of silicic lavas and pyroclastic flows, and the sedimentary thickness of the formation imply an extensional tectonic control even though the volcanic arc developed at a convergent margin. It was intruded by some ca. 48-45 Ma ( $^{40}\text{Ar}/^{39}\text{Ar}$  age) calcalkaline Andean-type plutons, which mark the approximate location of the magmatic front at that time, and which indicate a progressive northward migration of magmatic activity within the arc between Late Cretaceous and Early Eocene times (Sullivan et al., 1993).

The **Shamran Volcanic rocks** in the vicinity of the Chalt volcanic belt consist of north and northwest dipping basalt-rhyolite lava flows with abundant volcanoclastic breccias and sandstones. Unlike the Chalt Volcanic belt, strata are essentially unmetamorphosed and undeformed. Although originally correlated with the latter, dated at ca. 110-72 Ma (see above), the volcanic rocks are now identified as a northern continuation of the Late Palaeocene volcanic arc on the basis of a  $58 \pm 1$  Ma,  $^{40}\text{Ar}/^{39}\text{Ar}$  hornblende age in an andesite (Treloar et al., 1989). This age indicates that the associated plutons at Gupis and Gindai dated at 61 Ma (K-Ar hornblende age) and at 59 Ma (Rb-Sr age) respectively (Treloar et al., 1989) have undergone rapid cooling.

Considering the fact that the Baraul Banda Slate Formation received very little volcanic input, Sullivan et al. (1993) suggested that it predates the major explosive volcanic phase such as that indicated by the even broadly contemporaneous Utror Volcanic Formation and by the Shamran Volcanic rocks, basaltic andesites cooling ages of which show that

volcanism spanned a maximum period of 6 M.y. between  $58 \pm 1$  and  $55 \pm 2$  Ma ( $^{40}\text{Ar}/^{39}\text{Ar}$  hornblende age, Treloar et al., 1989).

According to Treloar et al. (1989, 1990) uplift and cooling of the accreted arc, which could result from the subduction of a young buoyant feature such as a ridge or young oceanic crust (Sullivan et al., 1993) started soon after the amphibolite facies metamorphism because much of southern Kohistan had cooled below  $500^\circ\text{C}$  by 75 Ma and below  $300^\circ\text{C}$  at about 45 Ma. However uplift and cooling occurred later to the east of Gilgit than to the west because increasingly young biotite (Treloar et al., 1989), zircon and apatite (Zeitler, 1985) ages occur in the easternmost part of the arc. This uplift/cooling history is hence well documented in the microstructures and greenschist facies assemblages of superimposed shear zones, as the principal thrust-related uplift in the Kohistan is associated with its obduction subsequent to the collision with India.

The continental collision and formation of the Indus Suture took place perhaps as early as 65 Ma (Smith et al., 1994) and certainly before 49 Ma (Beck et al., 1995). Recent paleomagnetic results identify a distinct reduction in India's northward movement rate at 55 Ma. This age was first interpreted as the initial contact between the Kohistan-Ladakh island arc and the Indian plate (Klootwijk, 1979), but now it is related to the completion of suturing between India and Asia (Klootwijk et al., 1992). The arc, partially thrust below the Asian Plate has been upturned on a crustal scale ramp to its present position, due to Eocene to Recent suture development related to the obduction of the island arc over India which took place along the MMT and underlying thrusts with a minimum displacement of 470 km (Coward et al., 1987). This requires the Kohistan region to be underlain by a slab of Indian crust.

The **third stage plutonic rocks of the Kohistan batholith** volumetrically form a minor part of this unit but provide important information on post-continental collisional magmatic processes. This intrusive stage is characterised by aplite and pegmatite swarms that occur in thin 1-3 m wide sub-horizontal sheets and extended sheets 30-40 m thick which exhibit well developed internal layering, with garnet as a common accessory phase, especially in the pegmatites (Petterson et al., 1990). The third stage plutonic rocks are represented by biotite granite sheets of the **Indus-Confluence Acid Sheets** emplaced between 50-30 Ma (Rb-Sr whole rock ages, George et al., 1993) followed by the **Parri Acid Sheets** dated at ca. 26 Ma (Rb-Sr errorchron age, Petterson, 1984). Because K-Ar and  $^{40}\text{Ar}/^{39}\text{Ar}$  cooling ages follow closely after Rb-Sr ages, Treloar et al. (1989) assumed that regional cooling did not long postdate intrusion of the late granite sheets.

The Indus-Confluence Acid Sheets are distinct geochemically as they are enriched in Sr, Ba and LREE, and depleted in Rb, Mn, HREE and Y relative to the Parri Acid Sheets.

Their geochemical compositions are also broadly similar to relatively large, evolved plutons such as the Shirot granite. Geochemical similarities with the Baltoro plutonic suite in the Karakoram dated at 21-25 Ma (U-Pb zircon age, Parish and Tirrul, 1989; Schärer et al., 1990) confirm that the northern migration of magmatic activity within Kohistan (England and Searle, 1986) occurred at least from Late Cretaceous (Sullivan et al., 1993) to Oligocene time (George et al., 1993).

According to George et al. (1993) undeformed granites in both suites have similar low ( $^{87}\text{Sr}/^{86}\text{Sr}$ )<sub>i</sub> that suggest their derivation from juvenile arc sources and lead to the conclusion that significant underthrusting of northern Kohistan by the Indian continental crust could not have occurred until after 26 Ma, and that the Kohistan terrane is hence a major juvenile addition to the continental crust (Pettersen and Windley, 1991). Deformed granite sheets that occur along the western margin of the Nanga-Parbat Massif show a marked increase in their ( $^{87}\text{Sr}/^{86}\text{Sr}$ )<sub>i</sub> ratios which can be related to a combination of sub-solidus fluid infiltrations and assimilation of crustal material. Tourmaline leucogranite dykes and plutons with U-Pb zircon ages between 12 Ma and 2 Ma (Zeitler and Chamberlain, 1991; Zeitler et al., 1993) and some structures even younger than 2 Ma cut by numerous quartz veins in the Nanga-Parbat Massif attest to widespread recent fluid flow (Craw et al., 1994) related to rapid exhumation of metasediments characterised by unusually high heat productivity (George et al., 1993).

Fission-track and  $^{40}\text{Ar}/^{39}\text{Ar}$  cooling ages indicate that late Tertiary cooling in northern Pakistan is largely a function of uplift and erosion, and thus show systematic regional variations. Hence, the Kohistan Arc has been uplifted less than 6 km over the past 35 Ma, while the Nanga-Parbat Massif in the east has been uplifted over 10 km in less than 10 Ma (Zeitler, 1985). According to Treloar et al. (1989) this rapid uplift of the Nanga-Parbat syntaxis that formed due to interference of thrust transport directions between Kohistan and the western Himalayan systems (Coward et al., 1987) was locally achieved by the reactivation of the Main Mantle Thrust with a reversed sense of motion, and is responsible for the global easterly decrease in cooling ages and the increase in cooling rate in the Kohistan terrane during the last 20 Ma.

## LITHOLOGICAL UNITS OF THE JIJAL COMPLEX

The 150 sq km ultramafic-mafic cumulate Jijal complex (35°N, 73°E) lies on the hanging-wall of the MMT (Main Mantle Thrust) between Jijal and Patan on the southern margin of the Kohistan terrane. It represents the least metamorphosed, last emplaced, deepest, and best preserved, virtually complete section through a magma chamber from an oceanic island arc. It occurs in a stack of at least four north-dipping layered cumulate complexes (including the Dasu, the Kayal and the Patan complexes) that developed along the frontal part of the Kohistan arc by precipitation from subduction-generated, hydrous, low-K, picritic, high-Mg tholeiitic magmas (Loucks et al., 1990). This 12 km thick, NW-trending tectonic wedge is separated from the Palaeozoic and older metasediments of the Indo-Pakistan plate by the MMT which crosses the Indus River at that place. Occurrence of ophiolitic *mélange* (Gansser, 1964 and 1979), and tectonic slices of granulite, glaucophane schist, harzburgite, and serpentinite (Desio, 1977; Bard et al. 1979; Shams, 1980; Jan and Howie, 1981) along or near this contact is suggestive of major tectonic activity related to the subduction of the Indian Plate below the Asian Plate (Coward et al., 1987).

Mid-Cretaceous accretion to the Asian plate together with later tilting and erosion have exposed the Jijal ultramafic-mafic sequence with along-strike continuity and relatively constant stratigraphic separation between cyclic cumulate units (Miller et al., 1991). Following Loucks et al. (1990) it is divisible into several distinct stratigraphic units which are from the base upwards: ultramafic cumulates (~3.5 km thick), garnet-bearing rocks (~4.5 km thick), hornblende-pyroxenes gabbros (~4 km thick).

### 1) ULTRAMAFIC CUMULATES

This lowermost unit is represented by multiple-cyclic units of relatively unmetamorphosed garnet- and plagioclase-free **ultramafic cumulates** that appear to be continuous with the Alpurai and the Kashora ultramafic bodies that occur not far (about 25 to 50 km) to the west along the MMT, and may represent detached slices that were continuous with the Jijal complex (Miller et al., 1991). The latter is characterised by exceptionally well preserved modal layering of pyroxenites (diopsidites > websterites), dunites, gradational lithologies that are dominantly olivine-pyroxenites, and layers, lenses and streaks of chromite in the dunitic rocks. One chromitite lens contains green chromian andradite grains that formed during the retrograde greenschist facies metamorphism associated with post-collisional uplift of the Kohistan arc (Jan et al., 1984). According to Jan and Windley (1990) at least 60 chromite ore bodies occur in the ultramafic part of the Jijal complex, and are concentrated near Shungial (Duber area) and Manidara (2 km north of Jijal). According to the classification

of Dick and Bullen (1984) the chromites have high Cr-numbers ( $> 60$ ) that are characteristic of type III alpine-type peridotites and suggest, in agreement with Miyashiro (1973), that the chromites crystallized in the earliest stages of arc-formation in an oceanic crust environment. Such rocks are locally preserved as tectonized harzburgites and enstatite-rich dunites in the forearc of many modern island arcs. The chemistry of such rocks, their olivines ( $\text{Fo}_{92-89}$ ) and clinopyroxenes ( $\text{Mg}_{49.5-48.0} \text{Fe}_{2.8-5.2} \text{Ca}_{47.4-46.8}$ ) (Jan and Howie, 1981) are also similar to those of this alpine-type spinel peridotite.

On the other hand, the abundance of diopsidite (more than 50% of the outcrop) contrasts with other alpine ultramafic complexes where olivine-rich rocks are the most abundant. Occurrence of secondary diopsidite veins and bands in the peridotites is suggestive of Ca and Si metasomatism during or before the granulite facies metamorphism that ended before 80 Ma (Treloar et al., 1989). This could explain the abundance of diopsidites. According to Jan and Windley (1990) the ultramafic rocks may be the products of an arc-related basaltic magma crystallized at pressures sufficiently high ( $> 16$  kbar, according to Green, 1982) to eliminate the formation of plagioclase and promote the crystallization of abundant ortho- and clinopyroxene, olivine, and some chromite. The crystallization of cumulus magnetite in the upper part of the ultramafic sequence prior to hornblende, garnet and plagioclase of the next unit implies that the parental magmas of the Jijal complex had relatively elevated oxygen fugacities. Appearance of hornblende as a cumulus phase prior to garnet and plagioclase is also consistent with the hydrous nature of these magmas (Loucks et al., 1990).

## 2) GARNET-BEARING ROCKS

The second unit is represented by **garnet-bearing rocks**. The contact with the first unit below is gradational or interfingering. Minor bodies of ultramafic rocks, sometimes with serpentized sheared contacts, occur sporadically throughout the garnet-bearing rocks; some with conformable contacts appear to be layers of cumulate origin, others are discordant bodies and lenses, similar to those in the Chilas mafic-ultramafic complex. Previously characterized as garnet granulites (Jan, 1980; Bard et al., 1980; Jan and Howie, 1981; Bard, 1983 and also Treloar et al., 1989, 1990; Jan and Windley, 1990; Yamamoto, 1993), these garnet-bearing rocks are more likely to be igneous (garnet)-pyroxene and (garnet)-pyroxene-plagioclase cumulates, because of the preservation of primary igneous textures (Loucks et al., 1990), density-graded modal layering, local cross-bedding, and concentrically zoned orbicular structures, as well as a lack of a metamorphic fabric.

According to Jan and Windley (1990) the small ultramafic bodies found in the garnet-bearing rocks have the characteristics of island arc plutonic rocks, but it is still not clear

whether the garnet-bearing rocks are part of a continuous sequence of arc cumulates with the adjacent principal ultramafic mass, or if the two are products of different source magmas. According to the first hypothesis, the garnet-bearing rocks would have formed when the magma had evolved to a "calcalkaline" character after extraction of the ultramafic cumulates. Alternatively, and as first proposed by Jan (1980), the ultramafic rocks would have been emplaced in the garnet-bearing rocks as solid material capable of plastic flow, resulting in the observed interfingered or gradational contacts between the two genetically unrelated units. According to Bard (1983), intensely developed foliation and isoclinal folding affected the primary layering. Sharp contacts between the garnet-bearing rocks and ultramafic rocks suggest that the former were locally injected by ultramafic dykes prior to deformation, folding and boudinage possibly related to the continental collision, when the Kohistan arc was partially thrust below the Asian plate. This partial thrust of the Kohistan arc occurred before the development of the suture followed by obduction of the arc onto the Indian plate along the MMT.

The transition from plagioclase-bearing to plagioclase-free garnet-bearing rocks at 40 km depth is well defined by a jump in Vp from 7.2 to greater than 8.0 km/s (Miller and Christensen, 1994). Also according to them, the base of the crust would lie at least 4 km below this transition, and would now be either obscured by the MMT, or would have been stripped off during obduction of the arc onto the Indian plate. The lowermost part of the Jijal complex hence provides one of the few windows through the crust/mantle transition zone. Following geophysical data, it crystallized at a depth near 45 km (14.5 kbar) and the upper part of the Jijal complex equilibrated around 36 km (12 kbar). This leads to the conclusion that the southern plagioclase-free cumulate part of the garnet-bearing rocks should be less than 0.5 km thick, according to geophysical velocity profiles and following the subdivision of the Jijal complex by Loucks et al. (1990) .

Moving northwards from the main ultramafic contact, there is a decrease in proportion of clinopyroxenites and hornblendites. The latter occur as layers consisting of hornblendite, hornblende-garnet, garnetite, and garnet-plagioclase. Hornblendites that occur as lenses, boudins and locally as deformed dykes post-dating the previously described fine-scale layering, are mostly present in the southern part of the Jijal complex (Coward et al., 1982). According to Bard et al. (1980), garnet hornblendites include in places patches of inherited clinopyroxene-orthopyroxene granulite-like rocks that are invaded by discordant feldspar-garnet-hornblende veinlets. Garnet-plagioclase veins are folded isoclinally, and cut across hornblende-bearing rocks that grade into gneissose, layered, garnet-anorthosites. The massive garnet-amphibolites show numerous blastomylonitic shear zones, some of which have formed prior to the emplacement of garnet-plagioclase veinlets. Post-tectonic leucocratic veins contain garnet megablasts up to 8 cm across that are abundant in the uppermost part of the garnet-bearing rock unit, but have locally developed in the lowermost part. Garnet-



plagioclase-bearing rocks in the uppermost part that contain relics of norite traversed by garnet granulite veins lend support to the view that garnet-bearing rocks may represent a high pressure equivalent of the Chilas complex (Jan and Howie, 1981; Coward et al., 1982).

### 3) HORNBLENDE-PYROXENE GABBROS

According to Loucks et al. (1990), the transition from garnet-bearing to garnet-free hornblende gabbro grading up into quartz diorite is smooth, with local preservation of igneous layering and a capping agmatite that represents the stooped roof of the complex. Hence, the upper 4 km of the Jijal complex including these dioritic units correspond to the **hornblende-pyroxene gabbros** of the third unit, which has not been previously considered to be part of the Jijal complex, but was rather ascribed to the overlying Kamila Amphibolite belt. Confusion can be avoided assuming with Loucks et al. (1990) that the nature of the northern contact of the Jijal complex is petrological, as defined by the capping agmatite (caught in heterogeneously deformed rocks), in contrast to the structural nature of the contact indicated by a thrust fault and associated sheared rocks, according to Jan and Howie (1981) and Coward et al. (1982 and 1987).

Part II:

**Petrography and  
mineral chemistry**

All the samples studied here were collected along the Karakorum Highway between Jijal and Patan (except for sample **K27** that comes from the contact between the Kamila amphibolite belt and the Chilas complex). They include garnet-bearing host rocks, veins, and shear zones as listed in Table 1. No specific UTM (Universal Transverse Mercator) coordinates were given for any of them but their relative position is known. The **N** series (which will be referred to as the northern series in further sections) comes from Prof Brian F. Windley's collection (University of Leicester), with numbers grading from North to South, and extending from the northern contact with the Kamila Amphibolite belt to the southern gradational and interfingering contact with the ultramafic cumulates of the complex. The **GI**, **KI**, and **P** series (which will be referred to and grouped into the southern series) come from Prof Jean-Pierre Bard's collection (Université Montpellier II). Because samples were collected during several expeditions, the numbers do not have any logical order but their relative position is known from North to South (see Table 1). Their locations extend from the southern contact with the blueschists of the MMT to about two thirds of the distance between Jijal and Patan.

The phases that occur in host rocks, veins, and shear zones include garnet, clinopyroxene, amphibole, plagioclase, quartz, epidote, zoisite, clinozoisite, chlorite, opaque oxides, rutile, and sphene, with local orthopyroxene, K-felspar, scapolite, apatite, white mica, biotite, and kyanite. The bulk chemical composition of the garnet-bearing rocks is plotted in figure 3, according to Moudden (1991). A complete description including the modal composition and possible reactions is given for each sample in appendix 1. Petrological features supported by textural evidence suggest that the phases listed above can be grouped into typical sub-assemblages related to their metamorphic grade and to the type of sample. Due to their complex history, most of the samples cannot be defined as a unique assemblage at equilibrium, but rather as a combination of different sub-assemblages that formed in response to various metamorphic conditions. They include: granulite, amphibolite, and transitional epidote-(chlorite)-amphibolite facies assemblages that overprint the primary magmatic cumulate assemblage.

## MINERAL REACTIONS AND REACTION TEXTURES IN HOST ROCKS

### MAGMATIC CUMULATE ASSEMBLAGES

The magmatic cumulate assemblages include the following phases: plagioclase, clinopyroxene, amphibole, spinel, apatite, +/- garnet. The garnet is poor in inclusions (**P23**), coarse (sometimes up to 2 cm across - **N631**) and forms in a diablastic texture (**P23**). In contrast to metamorphic garnet, it is not associated with quartz. Magmatic clinopyroxene

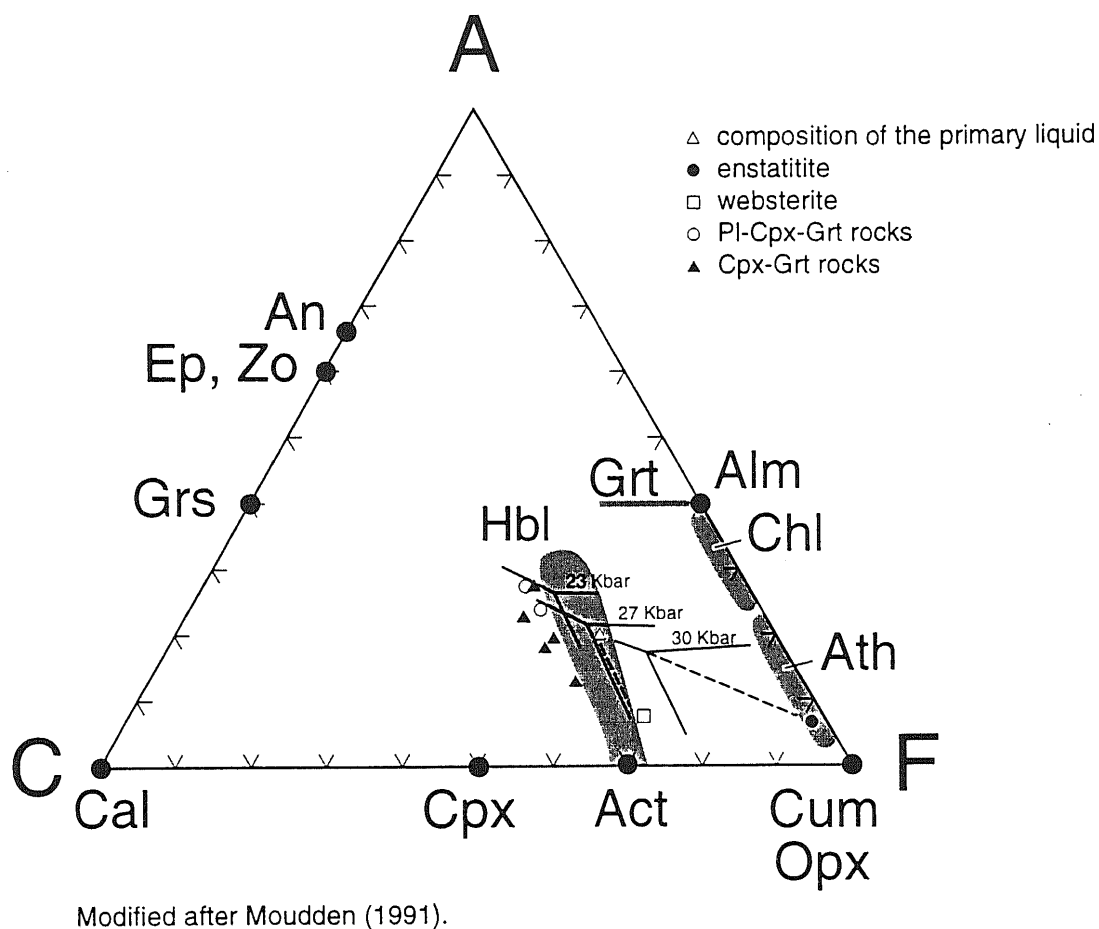


**Figure 3.** ACF ( $\text{Al}_2\text{O}_3$ -CaO-[FeO-MgO]) diagram including the bulk chemical composition of rocks from the Jijal complex and the change of liquidus surface with pressure, according to Moudden (1991).

Table 1. North to South distribution and modal compositions of samples from the Jijai complex (and K27)

NORTH		Modal composition (%)																		
Sample	Assemblage(s)	Grt	cpx	opx	amph	Pl	Kfs	Qtz	Scp	Ep	Zo, CZo	Chl	wmica	Bt	Ky	Ap	oxi	Rt	Spn	Cal
N 588	shear zone	5			40	25		15		10	5							trace		
N 589	amphibolite	15			35	47		trace		trace		2							1	
	V	40			57			trace				2					trace		1	
N 593	cumulate + granulite	30	15			35		15		trace		trace					trace	trace		
	V		trace			20		30		35		15								
N 601a	tonalite	40				32		27		1		trace					trace	trace		
N 601b	granulite	25	20		1	45		5									4	trace		
N 605	cumulate + granulite	35	10			50		5										trace		
	V	45	37		10					3		5								
N 610a	igneous?	11				75				7		trace					0.5	0.5		
N 610b	cumulate + retrograde	30	10		20	35		5		trace							trace	trace	trace	
N 614	cumulate + granulite	25	8		trace	50		4		6	1	5						1		
	V	trace	10		trace	27				35	3	25						trace		
N 616	igneous + retrograde	30	45		25					trace		trace					trace	trace		
N 617	amphibolite				100	trace				trace										
	V	10			3	65		trace	7	5	10	0						trace		
N 618	in V	30	4		42	2	0	3		5	10	3	trace						1	
N 621	shear zone	15			40	4		15			20		5				0.5	0.5	trace	
N 626	granulite + retrograde	30	6		4	50		3	1	2.5	2.5	1					trace	trace		
N 627b	cumulate + granulite	30	15		9	30		10		0.5	5	0.5					trace	trace		
N 627a, c	V	30	7		5	50			trace	1	1				trace		1	1		
N 629a, b, c	granulite?	25	20		15	30		3		2	5						trace		trace	
N 631	cumulate? + retrograde	60			20	8		trace		trace	5	5					0.5		0.5	
N 632	shear zone	20			30	3		25		12	5		5				trace	trace		
N 633	shear zone	25			25	5		30		7.5	7.5		trace				trace	trace		
N 634a	V	40	5		35	10		7	trace	1	1	1								
N 634b	cumulate + granulite	30			57			3	5	0.5	0.5	3					0.5	0.5		
N 636a, c	cumulate + granulite	25	40			35					trace						trace	trace		
N 636b	V	15	5			77				3										
N 638	granulite	15			30	3		20		20	7		4				0.5	0.5		
N 639a	cumulate + retrograde	45	20		5	16		trace	5	4	3		2				trace	trace		
N 639b	cumulate + retrograde	45	20		5	16		trace	5	4	3		2				trace	trace		
N 640	V	5			55	trace				15	15	10					trace			
SOUTH																				

NORTH		Modal composition (%)																		
Sample	Assemblage(s)	Grt	cpx	opx	amph	Pl	Kfs	Qtz	Scp	Ep	Zo, CZo	Chl	wmica	Bt	Ky	Ap	oxi	Rt	Spn	Cal
Kamila amphibolite belt/Chilas complex contact																				
K 27	V amphibolite	7	trace		25	60	0	5		trace		2					0.5	0.5		trace
P 24c	granulite	25	10		15	30		20									trace	trace		
KI 153	amphibolite + granulite	30	20		15	25		10						trace			0.5	0.5		
KI 158	granulite	35	4	2	5	40	10	3									1	1		
P 573	granulite	20	20		8	47	trace	3												
GI 11b	cumulate + granulite	30	6		10	45		8			1					trace	trace	trace		
GI 13	cumulate + granulite	35	15		2	40	0	8									trace	trace		
GI 11	epidote-amph	20			25	15		7		20	10		3				trace	trace		
GI 11a	epidote-amph	20			30	20	0	10		trace	18		2				trace	trace		
GI 18	cumulate + granulite	40			30	20	0	5		2	trace					trace	3	trace		
P 576	(V) granulite	55	10		16	12		trace	5	1	1	trace				trace		trace		
P 577	cumulate + granulite	45	10		20	15		3		0.5	5	0.5					0.5	0.5		trace
P 577a	cumulate in granulite	55	24		20			trace										1		
P 574	cumulate + granulite	35	14	??	15	20		15		trace	trace						0.5	0.5		
P 572	cumulate + retrograde	45	20	5	10	15		3			trace	trace					1	1		
PK 23b	granulite + retrograde	45	5		15	25		10											trace	
P 23	cumulate	80	10		9	trace												trace	trace	
KI 16	granulite + amphibolite	55	10		13	10		trace		1	8	2				trace	trace	trace		
GI 10	cumulate + granulite	60	25	5		10	0									trace	trace			trace
P 570	epidote-amph-chl	15			25					35	15	10					trace	trace		
P 23a	cumulate + granulite + retrograde	25	15	5	44			trace				10				1	trace	trace		
KI 189	amphibolite	25			51			trace		2.5	15	2.5				trace	1		3	
P 166	V epidote-amph-chl	15			10	35	15	15		1	5	2	trace	2			trace		trace	
P 142	epidote-amph	15			40	5		19		trace	20					1	trace		trace	
SOUTH																				

SZ = shear zone, V = vein, cpx = clinopyroxene, opx = orthopyroxene, amph = amphibole, wmica = white mica, oxi = opaque oxides.

Other mineral symbols according to Kretz (1983)

grains (**P23a**) are relatively coarse (3 mm), hypidiomorphic and have Schiller plates, indicative of high  $T^{\circ}$  (~800-850  $^{\circ}\text{C}$ ) (Brown, 1957). They are sometimes closely associated with garnet with evidence of simultaneous growth (**P577a**). Some samples have a mesocumulate texture and plagioclase was the last major phase to crystallize in the magma (**P24c**, **N610**). Amphiboles that appear to be of magmatic origin are relatively coarse and have hematite exsolution along cleavages similar to Schiller plates in the clinopyroxenes. In most samples, the magmatic cumulate assemblage has been overprinted by various metamorphic assemblages, but relic mesocumulate zones are preserved at thin section scale.

## GRANULITE FACIES ASSEMBLAGES

The reaction textures that define the granulite assemblages are mainly related to the formation of garnet according to reaction 1 (see Table 2). These metamorphic garnets may be small (a few mm across) euhedral neoblasts (**P23**) or coarse, up to 4.5 cm across (**N629**). They can be anhedral with lobate to embayed boundaries (**P23a**), hollow (**GI11b**), or form as atoll garnets (**N601**). They are closely associated with quartz that forms mosaics with serrated boundaries (**N593**) or aggregates around garnet (**N638**). Symplectites of garnet with quartz occur in contact with clinopyroxene. Metamorphic garnets usually have inclusions of amphibole, clinopyroxene, plagioclase, opaque oxides and rutile; clinopyroxene inclusions in optical continuity with the surrounding clinopyroxene grains occur in **P23a**. As observed in the cumulate assemblage, garnet can have a diablastic texture due to metamorphic growth between previous magmatic grains (**PK23b**). Deformation, kinked and mechanical twins occur locally in plagioclase (600-700  $^{\circ}\text{C}$ ). Because all typical phases of the granulite assemblage were already in the cumulate assemblage, mineral composition changes such as in exchange reaction 3 may have occurred without changes in the magmatic textures. This provides an explanation for the preservation of primary igneous textures in the Jijal complex, despite its complex history.

## AMPHIBOLITE FACIES ASSEMBLAGES

The amphibolite facies assemblages can be defined by reactions involving the formation of amphiboles by retrogression from a previous amphibole-free assemblage or, if amphibole was formed, by changes in composition during retrograde conditions. The uralitization process is observable as amphibole grains locally include symplectitic garnet with clinopyroxene relicts (**P23a**), or garnet with amphibole symplectites included in clinopyroxene grains (**P23**) defined by reactions 7, 8, and 13. When two different populations of amphiboles (usually brownish-green to bluish-green) (**N589**) are present, they occur either as inclusions that can be in optical continuity, or as coronas around previous

grains (N629). The occurrence of relatively smaller, inclusion-free grains of clinopyroxene and amphibole can also be related to reactions 9, 14, 15, 16, 17, 18, 19, 20, and 22.

## TRANSITIONAL EPIDOTE-(CHLORITE)-AMPHIBOLITE FACIES ASSEMBLAGES

A first subdivision within this facies includes the only appearance of epidote (zoisite, clinozoisite) from the previous amphibolitic assemblage, according to reactions 24, 26, 27, 28, 29, 30, 31, 32, 33, 34, 35, 36, 37, 38, and 39. The zoisite and clinozoisite mainly occur in plagioclase (saussuritization), but also form symplectites with albite or quartz along plagioclase, clinopyroxene or amphibole grains. They can also be pseudomorphic after plagioclase with twinning relicts (K1189), poikilitic with inclusions of quartz, apatite, opaque oxides, sphene or rutile and altered plagioclase, kelyphitic or nematoblastic. Symplectites of epidote and opaque oxides occur locally (N639). Scapolite which probably formed by retrogression and as a pseudomorph of plagioclase can be altered to epidote (P576) according to reaction 27. White mica often associated with zoisite is mainly acicular, locally with a preferred orientation, and is concentrated in plagioclase- and quartz-rich zones (N638) and/or is locally superimposed on zoisite, plagioclase, amphibole and garnet grains.

A second subdivision within this facies includes chlorite, which together with zoisite forms at  $T^{\circ} \sim 550^{\circ}\text{C}$  and  $P < 3.3$  kbar (Spear, 1993). According to reactions 41, 43, and 44, zoisite and chlorite form simultaneously as alteration products of amphiboles. With further retrogression, chlorite locally altered epidote according to reactions 40, 42, 45, and 46. In epidote-free assemblages, or where epidote does not react with chlorite, reactions 42, 48, 49, 50, 52, 53, 54, and 55 can be associated with the following textures: chlorite that locally occurs in optical continuity within amphibole can be present as veinlets within garnet grains (P23) or may crosscut a previous assemblage (N605); as a pseudomorph it replaces garnet (N593) or plagioclase (N640). Where nematoblastic, chlorite can be closely associated with biotite and hematite (P166), or it can form elongated aggregates and spherulites (N593).

## MINERAL REACTIONS AND REACTION TEXTURES IN VEINS

In most of the veins, retrograde minerals such as epidote, chlorite and white micas are overprinted on a previous assemblage of plagioclase, amphibole, clinopyroxene and garnet, with reaction textures similar to those of the host rocks. Hence, besides veins or veinlets exclusively composed of retrograde hydrated minerals (N617), the veins include most of the



**Table 2. Textural reactions**

- 1) 3 anorthite + 6 diopside = 2 grossular + pyrope + 3 quartz
- 2) 3 anorthite + 6 enstatite = grossular + 2 pyrope + 3 quartz
- 3) pyrope + 3 hedenbergite = almandine + 3 diopside
- 4) 2 pyrope + 6 ferrosilite = 2 almandine + 6 enstatite
- 5) grossular + 2 almandine + 6 rutile = 6 ilmenite + 3 anorthite + 3 quartz
- 6) 2 magnetite + 3 diopside + 3 anorthite = 6 hedenbergite + 3 spinel + O<sub>2</sub>
  
- 7) 4 tremolite + 3 anorthite = 3 pyrope + 11 diopside + 7 quartz + 4 fluid
- 8) 6 tremolite + 7 grossular = 27 diopside + 6 anorthite + pyrope + 6 fluid
- 9) cummingtonite = 7 orthopyroxene + quartz + fluid
- 10) biotite + 3 quartz = orthoclase + 3 orthopyroxene + fluid
- 11) muscovite + quartz = orthoclase + sillimanite + fluid
- 12) meionite = 3 anorthite + calcite
- 13) tremolite = 2 diopside + 5 enstatite + fluid
- 14) tremolite + albite = edenite + quartz
- 15) 3 pargasite + 12 anorthite + 18 diopside = 3 tremolite + 5 pyrope + 10 grossular + 3 albite
- 16) 3 tremolite + 6 anorthite + 3 albite = 3 pargasite + 2 grossular + pyrope + 18 quartz
- 17) 3 Fe-tremolite + 6 anorthite + 3 albite = 3 Fe-pargasite + almandine + 2 grossular + 18 quartz
- 18) tremolite + 2 anorthite = tschermakite + 2 diopside + 2 quartz
- 19) tremolite + albite + anorthite = pargasite + diopside + 5 quartz
- 20) Fe-tremolite + albite + anorthite = Fe-pargasite + hedenbergite + 5 quartz
- 21) grossular + 2 paragonite + 3 quartz = 3 anorthite + 2 albite + 2 fluid
- 22) 3 diopside + 2 paragonite = pyrope + grossular + 2 albite + 2 fluid
- 23) 4 quartz + 4 Fe-pargasite + 3 O<sub>2</sub> = 6 hematite + 4 hedenbergite + 4 anorthite + 4 albite + 4 fluid
  
- 24) 54 clinozoisite + 3 tremolite = 5 pyrope + 19 grossular + 57 anorthite + 30 fluid
- 25) 2 zoisite = 3 anorthite + Ca(OH)<sub>2</sub>
- 26) albite + zoisite = oligoclase + fluid
- 27) 2 epidote + CO<sub>2</sub> = meionite + fluid
- 28) hornblende + epidote + quartz = clinopyroxene + plagioclase + fluid
- 29) amphibole + epidote = garnet + fluid
- 30) zoisite + quartz = anorthite + fluid
- 31) 4 zoisite + quartz = 5 anorthite + grossular + 2 fluid
- 32) paragonite + 2 quartz + 2 zoisite = 4 anorthite + albite + 2 fluid
- 33) 2 zoisite + CO<sub>2</sub> = meionite + fluid
- 34) 4 grossular + 5 paragonite + 6 quartz = 6 zoisite + 5 albite + 2 fluid
- 35) 6 ilmenite + 6 quartz + 12 zoisite + O<sub>2</sub> = 6 sphene + 2 magnetite + 18 anorthite + 6 fluid
- 36) 4 quartz + spinel + 4 zoisite = diopside + 7 anorthite + 2 fluid
- 37) 2 anthophyllite + 4 zoisite = 3 tschermakite + 2 tremolite + 2 quartz
- 38) clinozoisite = zoisite
- 39) 4 quartz + spinel + 4 clinozoisite = diopside + 7 anorthite + 2 fluid
  
- 40) 16 anorthite + chlorite = 8 zoisite + 5 spinel + 11 quartz
- 41) 3 chlorite + 6 epidote = tschermakite + 2 anorthite + 10 fluid
- 42) 6 epidote + chlorite + 7 quartz = actinolite + 10 anorthite + 6 fluid
- 43) 3 chlorite + 12 Al-epidote + 4 quartz = 10 tschermakitic hornblende + 4 anorthite + 2 fluid
- 44) chlorite + epidote = Al-amphibole
- 45) chlorite + quartz + CaO = actinolitic hornblende + epidote
- 46) crossite + epidote + quartz = actinolite + albite + chlorite + magnetite + fluid
  
- 47) chlorite + 6 hedenbergite + 6 hematite = 3 quartz + 6 magnetite + 5 diopside + anorthite + 4 fluid
- 48) chlorite + actinolite = hornblende + anorthite
- 49) chlorite + quartz + CaO = hornblende + anorthite
- 50) actinolite + chlorite + 11 quartz + 9 CaO = 10 pyroxene + anorthite + 5 fluid
- 51) Fe-chlorite + orthoclase + K<sup>+</sup> = annite + 2 fluid
- 52) diopside + chlorite + 2 anorthite = grossular + 2 pyrope + 4 fluid
- 53) 3 chlorite + grossular + 6 quartz = 4 pyrope + 3 diopside + 12 fluid
- 54) 3 quartz + 3 chlorite + 3 anorthite = grossular + 5 pyrope + 12 fluid
- 55) anorthite + 2 chlorite + 3 quartz = 3 pyrope + diopside + 8 fluid
- 56) 4 chlorite + 36 rutile + 9 Fe-pargasite = 5 pargasite + 8 quartz + 36 ilmenite + 4 albite + 20 fluid
- 57) 6 Fe-pargasite + 3 quartz + 24 hematite + chlorite = 6 albite + 7 anorthite + 5 diopside + 24 magnetite + 10 fluid
- 58) 6 hematite = 4 magnetite + O<sub>2</sub>

**Table 3. Mineral formulae and symbols\***

NaFeSi <sub>2</sub> O <sub>6</sub>	acmite	Acm
Ca <sub>2</sub> (Mg, Fe) <sub>5</sub> Si <sub>8</sub> O <sub>22</sub> (OH) <sub>2</sub>	actinolite	Act
Ca <sub>2</sub> Fe <sub>5</sub> Si <sub>8</sub> O <sub>22</sub> (OH) <sub>2</sub>	Fe-actinolite	Fe-Act (= Fe-Tr)
NaAlSi <sub>3</sub> O <sub>8</sub>	albite	Ab
Fe <sub>3</sub> Al <sub>2</sub> Si <sub>3</sub> O <sub>12</sub>	almandine	Alm
CaAl <sub>2</sub> Si <sub>2</sub> O <sub>8</sub>	anorthite	An
K(Mg, Fe <sup>2+</sup> ) <sub>3</sub> AlSi <sub>3</sub> O <sub>10</sub> (OH) <sub>2</sub>	biotite	Bt
KFe <sub>3</sub> AlSi <sub>3</sub> O <sub>10</sub> (OH) <sub>2</sub>	Fe-biotite	Fe-Bt
CaCO <sub>3</sub>	calcite	Cal
Mg <sub>5</sub> Al <sub>2</sub> Si <sub>3</sub> O <sub>10</sub> (OH) <sub>8</sub>	chlorite	Chl
Fe <sub>5</sub> Fe <sup>3+</sup> AlSi <sub>3</sub> O <sub>10</sub> (OH) <sub>8</sub>	Fe-chlorite	Fe-Chl
Ca <sub>2</sub> Al <sub>3</sub> Si <sub>3</sub> O <sub>12</sub> (OH)	clinozoisite	Czo
(CaM <sub>4</sub> ) amphibole	crossite	
(Mg, Fe <sup>2+</sup> ) <sub>7</sub> Si <sub>8</sub> O <sub>22</sub> (OH) <sub>2</sub>	cummingtonite	Cum
CaMgSi <sub>2</sub> O <sub>6</sub>	diopside	Di
NaCa <sub>2</sub> Mg <sub>5</sub> Si <sub>8</sub> O <sub>22</sub> (OH) <sub>2</sub>	edenite	Ed
Ca <sub>2</sub> Al <sub>3</sub> Si <sub>3</sub> O <sub>12</sub> (OH)	epidote	Ep
H <sub>2</sub> O	fluid	
Na <sub>2</sub> Mg <sub>3</sub> Al <sub>2</sub> Si <sub>8</sub> O <sub>22</sub> (OH) <sub>2</sub>	glaucofane	Gln
Ca <sub>3</sub> Al <sub>2</sub> Si <sub>3</sub> O <sub>12</sub>	grossular	Grs
CaFeSi <sub>2</sub> O <sub>6</sub>	hedenbergite	Hd
Ca <sub>4</sub> [(Mg, Fe <sup>2+</sup> ) <sub>9</sub> Al](AlSi <sub>15</sub> )O <sub>44</sub> (OH) <sub>4</sub>	hornblende	Hbl
FeTiO <sub>3</sub>	ilmenite	Ilm
NaAlSi <sub>2</sub> O <sub>6</sub>	jadeite	Jd
Fe <sub>3</sub> O <sub>4</sub>	magnetite	Mag
Ca <sub>4</sub> Al <sub>6</sub> Si <sub>6</sub> O <sub>24</sub> CO <sub>3</sub>	meionite	
KAlSi <sub>3</sub> O <sub>8</sub>	orthoclase	Or
(Mg, Fe <sup>2+</sup> )SiO <sub>3</sub>	orthopyroxene	Opx
Na <sub>2</sub> Al <sub>4</sub> [Si <sub>6</sub> Al <sub>2</sub> O <sub>20</sub> ](OH) <sub>2</sub>	paragonite	Pg
NaCa <sub>2</sub> Mg <sub>4</sub> Al <sub>3</sub> Si <sub>6</sub> O <sub>22</sub> (OH) <sub>2</sub>	pargasite	Prg
NaCa <sub>2</sub> Fe <sub>4</sub> Al <sub>3</sub> Si <sub>6</sub> O <sub>22</sub> (OH) <sub>2</sub>	Fe-pargasite	Fe-Prg
KMg <sub>3</sub> AlSi <sub>3</sub> O <sub>10</sub> (OH) <sub>2</sub>	phlogopite	Phl
Mg <sub>3</sub> Al <sub>2</sub> Si <sub>3</sub> O <sub>12</sub>	pyrope	Prp
Ca(Mg, Fe)Si <sub>2</sub> O <sub>6</sub>	pyroxene	
SiO <sub>2</sub>	quartz	Qtz
Na(Ca, Na)(Mg, Fe, Mn) <sub>5</sub> Si <sub>8</sub> O <sub>22</sub> (OH) <sub>2</sub>	richterite	
TiO <sub>2</sub>	rutile	Rt
CaTi[SiO <sub>4</sub> ](O, OH, F)	sphene	Spn
MgAl <sub>2</sub> O <sub>4</sub>	spinel	Spl
Ca <sub>2</sub> Mg <sub>5</sub> Si <sub>8</sub> O <sub>22</sub> (OH) <sub>2</sub>	tremolite	Tr
Ca <sub>2</sub> Fe <sub>5</sub> Si <sub>8</sub> O <sub>22</sub> (OH) <sub>2</sub>	Fe-tremolite	Fe-Tr
Ca <sub>2</sub> Mg <sub>3</sub> Al <sub>4</sub> Si <sub>6</sub> O <sub>22</sub> (OH) <sub>2</sub>	tschermakite	Ts
Ca <sub>2</sub> (Mg, Fe) <sub>3</sub> Al <sub>4</sub> Si <sub>6</sub> O <sub>22</sub> (OH) <sub>2</sub>	Fe-tschermakite	Fe-Ts
Ca <sub>2</sub> Mg <sub>3</sub> Al <sub>2</sub> Si <sub>8</sub> O <sub>22</sub> (OH) <sub>2</sub>	tschermakitic hornblende	
CaAlSi <sub>2</sub> O <sub>6</sub>	Ca-tschermak	
Ca <sub>2</sub> Al <sub>3</sub> Si <sub>3</sub> O <sub>12</sub> (OH)	zoisite	Zo

\* Mineral symbols according to Kretz (1983)

main phases that occur in the host rocks, although they have a different modal composition, or grain size (N627). Some veins include magmatic relics such as clinopyroxene grains with Schiller plates (N634), and garnet with growth appendices that formed during the granulite facies metamorphism (N601a). The borders of the veins are often defined by a single grain reactive layer of hypidiomorphic garnets (N589, N610, N617, N636); this relationship is compatible with intrusion and/or crystallization of the veins during the magmatic stage or before the end of the granulite facies metamorphism. The general increase of hydrated minerals near the contact of the veins and their relatively higher concentration in the veins are indicative of late fluid circulation that principally occurred within former veins or at their contacts with the host rocks.

## SHEAR ZONES

In the samples collected within shear zones, nematoblastic paragonite lies parallel to the fabric of the rock, tends to surround hypidiomorphic garnet, and/or is superimposed on plagioclase that has been severely altered by abundant poikiloblastic zoisite with albite inclusions. Quartz is heterogranular occurring as neoblasts with serrated boundaries. Fractures occur in hornblende porphyroclasts reoriented in the sense of shear (N621). Heterogranular porphyroclasts of garnet, up to 1 cm across (N633), are surrounded by hornblende-rich tails with a sigmoidal shape. In shear bands, foliation (from S or C?) is well defined by elongated neoblasts or aggregates and by acicular paragonite (N632). Sample N588 contains garnet + quartz-rich and amphibole-rich layers with epidote porphyroclasts.

## MINERAL ANALYSES

Garnet, clinopyroxene, amphibole, plagioclase, epidote (including zoisite and clinozoisite), white mica, chlorite, biotite, scapolite, rutile, spinel, apatite, calcite, and kyanite were analysed for Si, Al, Fe, Mg, Mn, Ti, Cr, Ni, Ca, Na, K, F, and Cl on a JEOL JXA-8600S electron microprobe with LiF, PET, and TAP analysing crystals at the University of Leicester (UK). Standard operating conditions were: 30 nA specimen current, 15 kV accelerating potential, and counting time of 20 s. Data were reduced using a ZAF correction program. A unique set of standards, including natural wollastonite, rutile, jadeite, rhodonite, microcline, and scapolite was used respectively for the following elements: (Si, Ca), Ti, (Al, Na), Mn, K, and Cl. Synthetic oxides ( $\text{Fe}_3\text{O}_4$  and  $\text{MgO}$ ) and  $\text{SrF}_2$  were used for Fe, Mg, and F, and pure metals for Cr and Ni standards. A beam size of 10  $\mu\text{m}$  was used for all

analyses in order to avoid any loss of material, and because all minerals were analysed with a unique beam size for each run.

Artificially high totals (up to 102.93%) were obtained for garnets, but did not yield to non-stoichiometric analysis. This could be due to a general mass problem related to the available set of standards while analysing heavy phases like garnet in this case or olivine. Therefore, analyses were selected according to their stoichiometry.

Garnet, clinopyroxene, orthopyroxene, amphibole, and plagioclase of samples P573, P574, P577, KI158, N601a, and N601b were analysed on a JEOL JXA-8900L electron microprobe with LiFH, PET, PETj, and TAP analysing crystals at McGill University (Canada). Standard operating conditions were: 20 nA specimen current, 15 kV accelerating potential, and counting time of 20 s. Different sets of standards were used for different elements depending on the analysed phase as following:

- garnet: Si, Al, Mg, Ca, and Fe: **GAR1**; Mn: **SPES**; Na: **ALBI**; Ti: **TiO<sub>2</sub>**; Cr: **CHRO**.
- ortho- and clinopyroxene: Si, Mg, Ca: **DIOP**; Al, K: **ORTH**; Na: **ALBI**; Fe: **ANDR**; Mn: **MnTi**; Ti: **TiO<sub>2</sub>**; Cr: **CHRO**.
- amphibole: *idem*, F: **CaF<sub>2</sub>**; Cl: **VANA**.
- plagioclase: Si, Al, K: **ORTH**; Na: **ALBI**; Mg, Ca: **DIOP**; Fe: **ANDR**.

Except for (TiO<sub>2</sub>) and (CaF<sub>2</sub>) that are synthetic, all the standards are natural, including albite (ALBI), orthoclase (ORTH), Fe-Mg-rich garnet (GAR1), andradite (ANDR), spessartine (SPES), diopside (DIOP), chromite (CHRO), vanadinite (VANA), and pyrophanite (MnTi). A beam size of 5 µm was used for all elements except for Na and F where a defocused beam of 10 µm was used to limit material loss.

Comparative composition ratios for oxides, and cation totals were obtained for clinopyroxene, amphibole, and plagioclase from samples P573 and P577 analysed with both microprobes. Garnet oxide totals range from 98 to 100% but cation totals for formula calculated on a basis of 12 oxygens held values approximately 0.03 higher than the "high oxide totals" obtained at Leicester University, and hence are relatively not as stoichiometric. This fact illustrates the important point that high (or low) oxide totals obtained from microprobe analyses are not always directly caused by the stoichiometry of the mineral itself, but can be related to other factors like the nature of the standards or/and the nature of the analysed mineral itself.

Analyses of garnet, amphibole, pyroxene and plagioclase were performed from rim to core with an ideal spacing ranging from 35 to approximately 200 µm in order to obtain

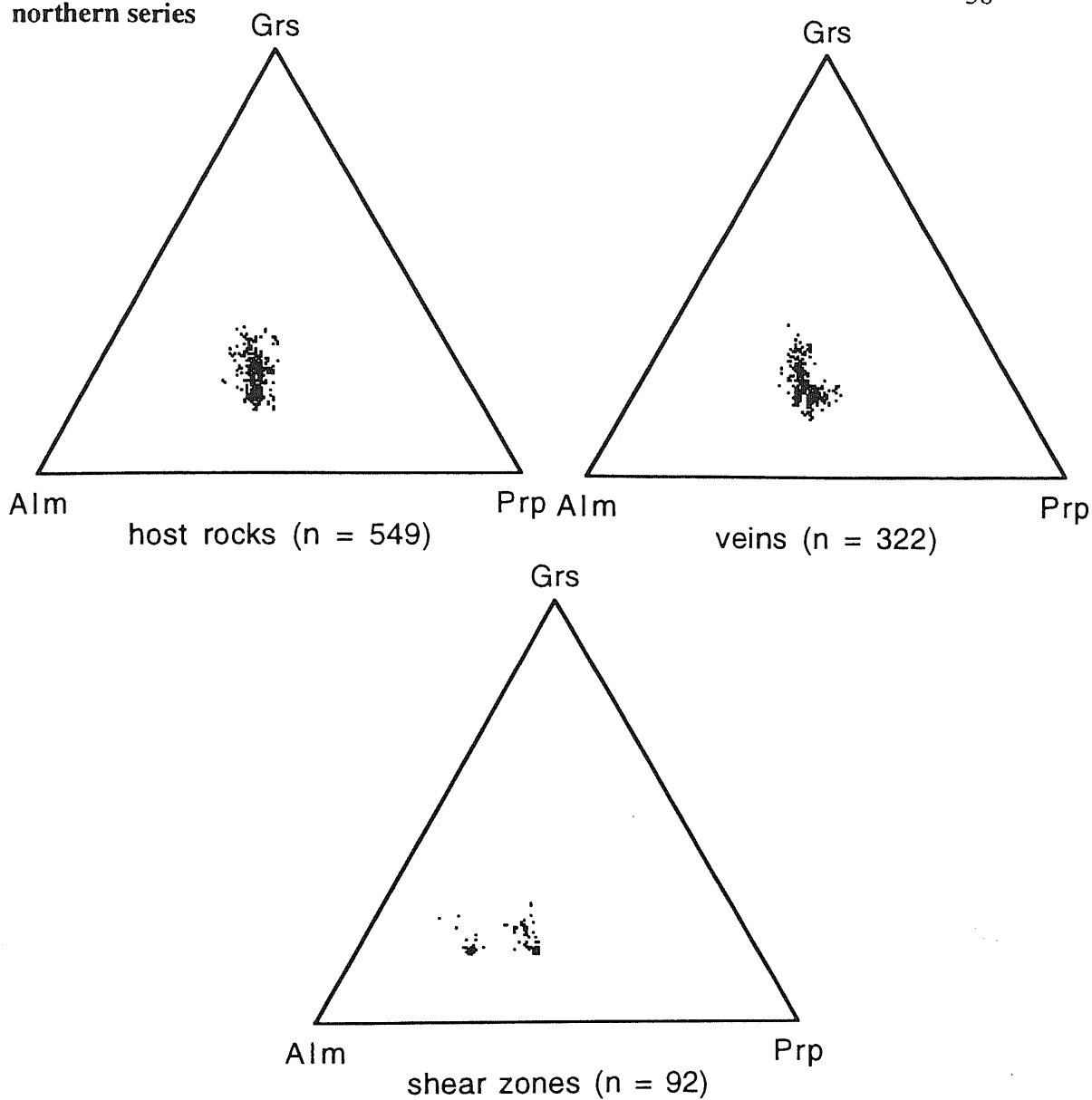
smooth composition profiles. Isolated grains were also analysed in pairs of at least two points corresponding to core and rim.

## MINERAL CHEMISTRY AND COMPOSITION PROFILES OF THE MAIN PHASES

All the data obtained from microprobe analyses are listed in appendix 3. They also include calculations of the stoichiometry of minerals and the distribution of cations within sites (see appendix 2), according to the THEBA software (Martignole et al., unpublished). Composition diagrams for garnet, clinopyroxene, orthopyroxene and amphiboles for each sample are presented in appendix 4.

### GARNET

The garnet composition range of the host rocks is ( $\text{Alm}_{32.5-61.3} \text{Prp}_{17.4-47.3} \text{Grs}_{12.2-34.1} \text{Adr}_{0.0-5.8}$ ). Figure 4 shows that compositions of the southern series are more heterogeneous than those of the northern series. In most samples the amount of grossular ( $X_{\text{Ca}}$ ) is similarly distributed in both series and probably varies positively as reactions **1**, **2**, **5**, **15**, **16**, and **17** (Table 2) proceed. According to these reactions (which have positive slopes in P-T space) reequilibration of primary garnet or formation of new garnet could therefore be associated with either an increase in pressure, or have formed under isobaric cooling conditions. Because variations in the almandine-pyrope ratios are minor to non-existent and that such ratio increases with decreasing temperature (see Table 2., reaction **3** and **4**), it is more likely to be incompatible with the hypothesis of isobaric cooling. It is therefore suggested that the reequilibration of primary garnet or the formation of new garnet occurred under increasing pressure conditions within a similar range of pressure that involved the entire complex. The almandine/pyrope ratios have a greater extent in the southern series. This implies that some of the garnets in this series were more likely to preserve relict compositions (high pyrope content) or reequilibrate in higher temperature environments which do not correspond to the maximum content of grossular, and mainly occur in samples closer to the MMT (see **P23** in appendix 4b). Relatively almandine-rich garnets which do not have the maximum grossular content either (see sample **GI18**) could have reequilibrated under lower temperatures, but are more likely representative of a local change in the overall composition towards Fe-richer compositions, in keeping with the high amount of oxides (3%) present in the rock. This suggests that partial reequilibration according to reactions such as **3** and **4** may have occurred.



southern series

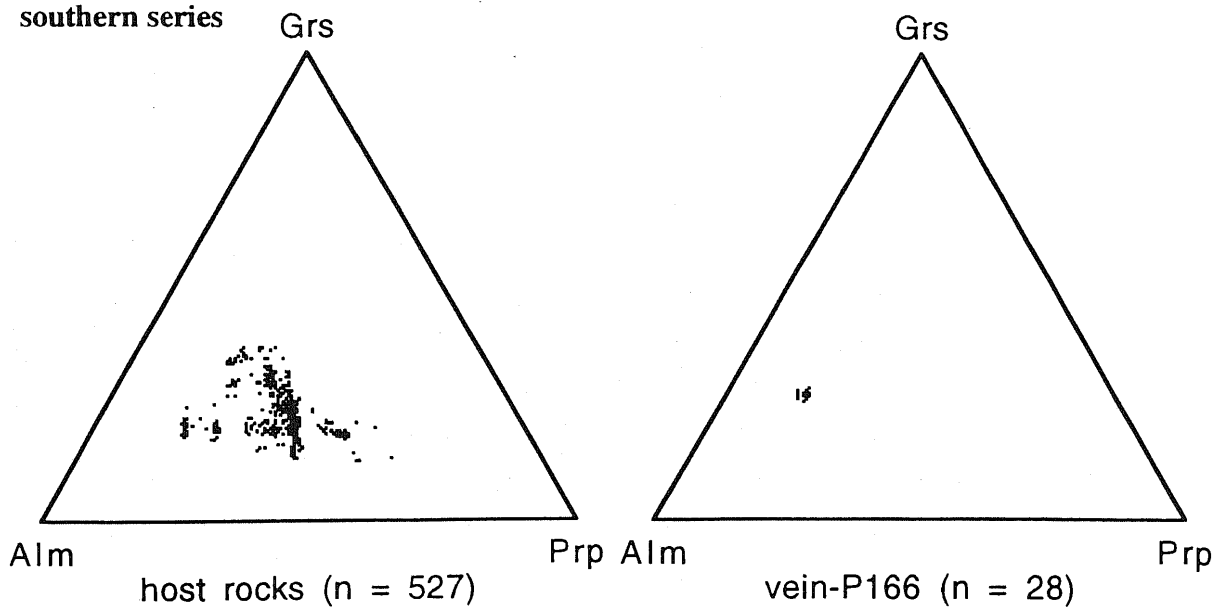


Figure 4. Compositional triangular diagrams for garnet of the Jijal complex.

The garnet composition range of the veins which mainly belong to the northern series is (Alm<sub>35.4-55.6</sub> Prp<sub>12.1-41.1</sub> Grs<sub>13.0-35.9</sub> Adr<sub>0.3-5.7</sub>). In comparison with the composition of garnet in the host rocks, garnets in the veins tend to be richer in pyrope (see **N616**, **N640**) whereas their compositional range for grossular is similar. Hence, garnets in the veins might have formed under the same pressure conditions as the host rocks probably during the initial magmatic stage. In contrast, garnets from a vein situated close to the MMT (**P166**) are almandine- and grossular-rich and cannot be related to any other samples of the southern series, but to some analyses in the shear zone **N633**.

The garnet composition range in the shear zones (**N588**, **N621**, **N632**, **N633**) is (Alm<sub>39.8-58.1</sub> Prp<sub>12.3-35.8</sub> Grs<sub>15.1-27.3</sub> Adr<sub>0.0-4.4</sub>). Because their grossular content compared to that of host rocks and veins plots in the lower part of the range, one can suppose that shearing occurred within the granulite facies metamorphism, possibly at its later stage. The four samples have different almandine/pyrope ratios as for **N588**, which comes from the northern contact boundary of the complex and which has the most homogeneous compositions with relatively low-grossular and high-almandine ratios. Conversely, sample **N632** has heterogeneous grossular contents and except for one almandine-rich analysis, there is no variation with almandine/pyrope ratio, and the latter is similar to those of the host rocks and veins. Samples **N621** and **N633** tend to have similar grossular contents to **N588**, but the composition range is wide with almandine/pyrope ratios mostly similar to those of the host rocks and veins, but spreading to higher ratios in the shear zones. Disparities in compositions according to their localisations suggest that in contrast to sample **N588**, shearing occurred on previously formed garnets in samples **N621**, **N632** and **N633** which were already heterogeneous in composition and/or had undergone reequilibration (garnet neoblasts occur). Because of their homogeneity in composition, garnets in sample **N588** are more likely to have formed under similar shearing conditions.

## CLINOPYROXENE

Clinopyroxene compositions are homogeneous throughout the samples including host rocks and veins of both series (see appendix 4c and 4d) and are defined as diopside (Di<sub>71-97</sub>). Diopside does not occur in samples from the shear zone. The composition range of diopside is (En<sub>36.2-49.3</sub> Fs<sub>1.5-20.8</sub> Wo<sub>38.6-50.0</sub>), where (En<sub>36.2</sub>) comes from the granulite facies assemblage of **N629c**, (En<sub>49.3</sub>) from the cumulate assemblage **P23**, (Fs<sub>1.5</sub>) from the granulite facies overprinted cumulate assemblage of **GI10**, (Fs<sub>20.8</sub>) from the cumulate assemblage of **P577a**, (Wo<sub>38.6</sub>) from the granitic vein **N634a**, and (Wo<sub>50.0</sub>) from the granulite and retrograde facies overprinted cumulate assemblage of **P23a**. The fact that the majority of extreme compositions occur in samples of the southern series corroborates well with the observed relic magmatic features (as Schiller plates on coarse clinopyroxene grains)

of samples that have undergone later metamorphism. Hence, low Ca-content obtained for a few analyses which indicates high temperatures of formation (between 500 and 1200°C) are more likely to be of magmatic origin according to the liquidus curves in the clinopyroxene diagram of Lindsey (1983) and are conceivable considering the geological setting.

Clinopyroxenes contain variable amounts of Na and Al (jadeite and Ca-tschermak) but according to the IMA classification of pyroxenes (Morimoto, 1988) only rarely does data from the southern series fall into the omphacite field (see figure 5). Their Q (Wo-En-Fs) *versus* Jd composition range is wider compared to clinopyroxenes of the northern series but their Jd/Ae ratios spread is more restricted. Clinopyroxenes of the Jijal complex are highly oxidized according to  $\text{Fe}^{3+}/\text{Fe}^{2+}$  ratios, commonly  $> 1$ . They are richer in  $\text{Al}_2\text{O}_3$  (up to 11.41% - **N639b**) with high  $\text{Al}^{\text{VI}}$  over  $\text{Al}^{\text{IV}}$  (therefore rich in  $\text{Si}^{\text{IV}}$ ) which indicates substitutions of tschermak molecules into the structure of the mineral under high-pressure conditions. They are also weakly sub-calcic which suggests that they may have formed or reequilibrated at temperatures between 500 and 700°C. Figure 6 includes all clinopyroxene analyses and illustrates their composition range according to their  $\text{Al}^{\text{VI}}$  and  $\text{Al}^{\text{IV}}$  content. It is interesting to note that some of the analyses fall into the eclogite facies field as defined by White (1964).

## ORTHOPYROXENE

Orthopyroxene occurs in samples **P572**, **P574?**, **GI10**, and **P23a** but was only analysed in sample KI158, and defined as enstatite with composition ranging from 56.8 to 69.8. The triangular projection in appendix4d clearly shows that the composition range is not continuous and corresponds to the observed zoning within orthopyroxene grains, because the cores are richer in enstatite (69.4-69.8) while the borders in contact with cummingtonite forming coronas are poorer (56.8-60.9), probably due to reaction 9 (Table 2.).

## PLAGIOCLASE

The plagioclase composition range is wide ( $\text{An}_{0.3-81.6}$ ) throughout the samples of both series (including host rocks, veins, and shear zones) according to textural reactions identified in the previous section. In many cases, coarser grains most likely to be of primary origin as those forming a mesocumulate texture were too altered (saussuritised and/or cloudy) to give acceptable analyses. However, the most representative compositional range for the samples extends from  $\text{An}_{35}$  to  $\text{An}_{45}$ .



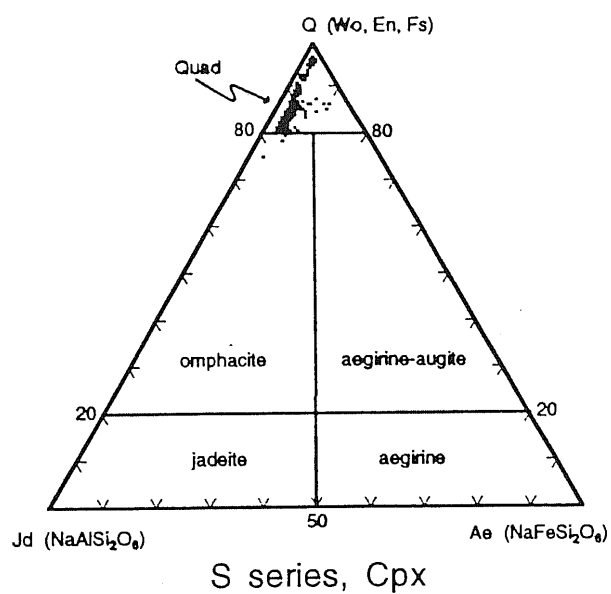
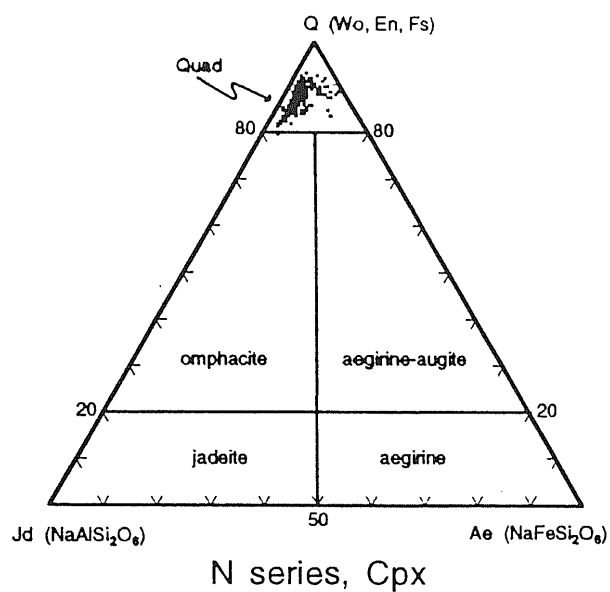
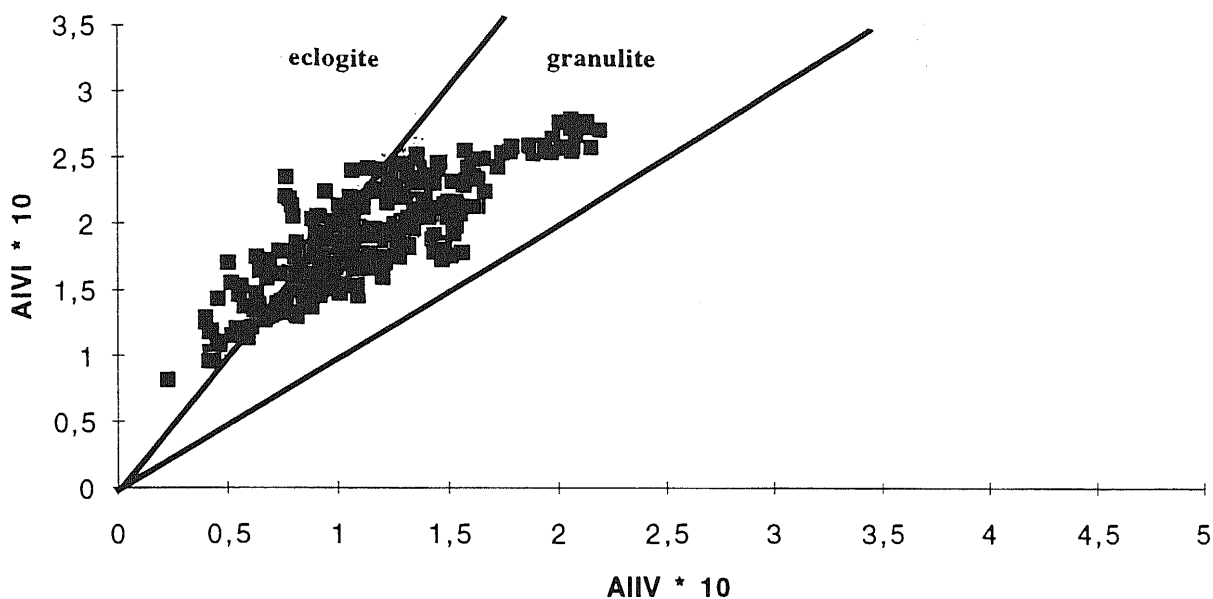


**Figure 5. (Q-Jd-Ae) diagram according to Morimoto (1988) for clinopyroxene of the Jijal complex.**

### Clinopyroxene of the northern series



### Clinopyroxene of the southern series

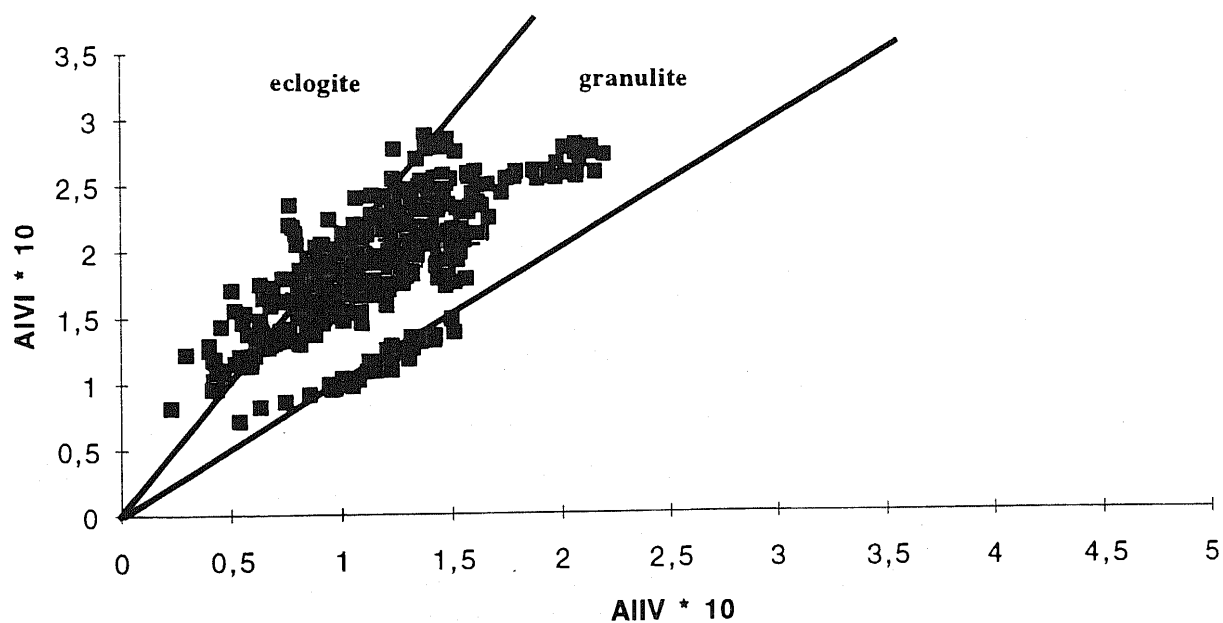


Figure 6. Fields of eclogite and granulite clinopyroxenes of the Jijal complex, according to White (1964).

## AMPHIBOLE

Amphiboles were named after the classification of Leake (1978) and include, as listed in appendix 3e: pargasite, ferroan-pargasite, pargasitic hornblende, ferroan-pargasitic hornblende, magnesio-hornblende, edenite, edenitic hornblende, actinolite, actinolitic hornblende and rare subsilicic tschermakite (**N627b**), tschermakitite hornblende (**N610a**), and cummingtonite (**KI158**). Usually amphibole grains are optically zoned and/or occur as different populations within the samples (see previous section). Because compositional variations are large enough to influence the nomenclature, more than one amphibole type usually occurs within the same sample and/or even within a single grain. ACF ( $\text{Al}_2\text{O}_3$ -CaO-FeO + MgO) projections were drawn for each sample (see appendices 4e and 4f). They show that amphiboles are more heterogeneous in the northern series than in the southern series where amphiboles of possible magmatic origin were identified. Hence, this tendency is in opposition to that previously observed from the clinopyroxene analyses, if the homogeneity of the data is considered. This may be due to the fact that post-granulite facies metamorphism has more severely affected rocks in the northern (or upper) part of the complex.

In order to define the metamorphic facies associated with amphibole compositions, different sets of criteria from Bégin et al. (1992), Spear (1993, 1980), and Abbott (1982) were taken into consideration, when applicable. Results are listed in Table 4.

### SAMPLE K27, FROM THE KAMILA AMPHIBOLITIC BELT/CHILAS COMPLEX CONTACT

Triangular projections for garnet, clinopyroxene, and amphibole are listed in appendix 4g. Their compositional ranges are: (Alm<sub>57.8-80.4</sub> Prp<sub>3.1-22.9</sub> Grs<sub>7.7-21.0</sub> Adr<sub>0.7-6.8</sub>) for garnet, (En<sub>39.0 and 39.7</sub> Fs<sub>13.7 and 13.9</sub> Wo<sub>46.6 and 47.2</sub>) for diopside (Di<sub>47</sub>), (An<sub>22.3-42.7</sub>) for plagioclase, and amphibole compositions including ferroan pargasite, ferroan-pargasitic hornblende, edenitic hornblende, and actinolite. Compared to some samples of the Jijal complex, garnet and clinopyroxene are relatively richer in Fe, and clinopyroxene has relatively low Ca content. According to compositions and solvus configuration of Linsley (1983), clinopyroxene formed at temperatures between 500 and 700°C.

**Table 4. Metamorphic facies and associated amphibole compositions of the samples from the Jijal complex (and K27)**

NORTH		Begin et al. (1992) metamorphic facies according to the compositions of coexisting plagioclase and amphibole	Spear (1993) metamorphic facies according to the Al <sub>2</sub> O <sub>3</sub> content in amphibole coexisting with epidote	Spear (1980) metamorphic facies according to the composition of plagioclase coexisting with (actinolite + hornblende)	Abbott (1982) metamorphic facies according to the presence of coexisting quartz with actinolite
Sample	Assemblage(s)				
N 588	SZ	granulite? to amphibolite			
N 589		granulite? to amphibolite, upper greenschist	amphibole incompatible with epidote		
	V				
N 593					
	V				
N 601a	V				
N 601b					
N 605					
	V				
N 610a	V	igneous?	amphibolite to greenschist with epidote in		medium to high grade
N 610b		cumulate + retrograde			
N 614		cumulate + granulite	greenschist	greenschist	greenschist
	V				
N 616	V	igneous + retrograde	amphibolite to greenschist (actinolite) with epidote in		
N 617		amphibolite	amphibolite to greenschist with epidote in		
N 617	V	anorthositic?			
N 618	in V		amphibolite (and greenschist with epidote in)	amphibolite (to greenschist)	greenschist
N 621	SZ	amphibolite to greenschist	amphibole incompatible with epidote (zoisite)		
N626		granulite + retrograde	amphibolite to greenschist		
N 627b		cumulate + granulite	amphibolite		
N 627a, c	V		amphibolite	amphibolite	medium to high grade
N 629a, b, c		granulite?	limit of amphibolite to greenschist		
N 631		cumulate? + retrograde	limit of amphibolite to greenschist		
N 632	SZ		limit of amphibolite to greenschist		
N 633	SZ	amphibolite to greenschist	amphibole incompatible with epidote		
N 634a	V	igneous	limit of amphibolite to greenschist		
N634b		cumulate + granulite	amphibole incompatible with epidote		
N 636a, c		cumulate + granulite	amphibole incompatible with epidote		
N 636b	V	anorthositic	amphibole incompatible with epidote		
N 638		granulite	amphibole incompatible with epidote		
N 639a		cumulate + retrograde	limit of amphibolite to greenschist		
N 639b		cumulate + retrograde	amphibole (except edenite) incompatible with epidote		
N 640	V	cumulate + retrograde	amphibole incompatible with epidote	greenschist	medium to high grade
		upper greenschist	upper greenschist		
SOUTH					

NORTH		Begin et al. (1992) metamorphic facies according to the compositions of coexisting plagioclase and amphibole	Spear (1993) metamorphic facies according to the Al <sub>2</sub> O <sub>3</sub> content in amphibole coexisting with epidote	Spear (1980) metamorphic facies according to the composition of plagioclase coexisting with (actinolite + hornblende)	Abbott (1982) metamorphic facies according to the presence of coexisting quartz with actinolite
Sample	Assemblage(s)				
Kamila amphibolite belt/Chilas complex contact					
K 27	V amphibolite		limit of amphibolite to greenschist	amphibolite	greenschist
P 24c	granulite				
KI 153	amphibolite + granulite	amphibolite to greenschist	greenschist with chlorite in		
KI 158	granulite	granulite? to amphibolite	amphibole compatible but no epidote		
P 573	granulite	middle amphibolite			
GI 11b	cumulate + granulite				
GI 13	cumulate + granulite				
GI 11	epidote-amphibolite	upper greenschist			
GI 11a	epidote-amphibolite	upper greenschist	amphibole incompatible with epidote (zoisite)		
GI 18	cumulate + granulite	granulite? to amphibolite	limit of amphibolite to greenschist		
P 576	(V) granulite	granulite? to amphibolite	limit of amphibolite to greenschist		
P 577	cumulate + granulite	middle amphibolite	amphibole incompatible with epidote		
P 577a	cumulate in granulite				
P 574	cumulate + granulite				
P 572	cumulate + retrograde				
PK 23b	granulite + retrograde	(granulite? to) amphibolite	(granulite? to) amphibolite		
P 23	cumulate	granulite? to amphibolite	granulite? to amphibolite		
KI 16	granulite + amphibolite		amphibolite with epidote in		
GI 10	cumulate + granulite	(high T assemblage)			
P 570	epidote-chlorite amphibolite				
P 23a	cumulate + granulite + retrograde	amphibolite	amphibolite		
KI 189	amphibolite	(high T assemblage)	limit of amphibolite to greenschist		
P 166	V epidote-chlorite amphibolite	lower to middle amphibolite	limit of amphibolite to greenschist		
P 142	epidote-amphibolite		limit of amphibolite to greenschist		
SOUTH					

SZ = shear zone, V = vein

## COMPOSITION PROFILES

### GARNET-ZONING PROFILES

Most garnet zoning profiles from the samples including host rocks, veins, and shear zones of both series tend to have flat  $X_{\text{Alm}}$ ,  $X_{\text{Prp}}$ , and  $X_{\text{Grs}}$  profiles in their cores with increasing grossular content at their rims, together with either constant or slightly (figure 7a) to drastically (figure 7b) increasing Fe/Mg ratios. Andradite and spessartine contents are low (near the detection limit) and tend to remain constant from core to rim.

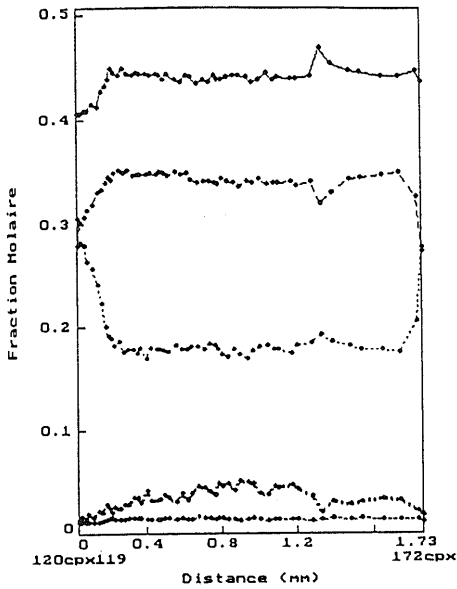
Garnets in all samples have a core composition of about  $\text{Alm}_{43}$ , except in samples **P23**, **P23a**, and **N640** which are more pyrope-rich with a composition of about  $\text{Prp}_{43}$ , and in the retrogressed cumulate **N639b** that includes ( $\text{Alm}_{34}\text{-Prp}_{31}\text{-Grs}_{31}$ ) garnets. Compared to almandine-rich zoning profiles, pyrope-rich garnets are more homogeneous from core to rim, especially for the grossular content. Fe/Mg ratios tend to decrease at the rim, and the andradite and spessartine contents remain constant. The ( $\text{Alm}_{34}\text{-Prp}_{31}\text{-Grs}_{31}$ ) garnet zoning profile is rather flat with minor increase in the Ca content and Fe/Mg ratios at rims in contact with clinopyroxene grains.

Variations in Ca content and Fe/Mg ratio from core to rim can be correlated in most cases with the reaction textures described above. An interesting feature is observed in garnet zoning profiles of sample **N616** (figure 7e), where variations in composition according to a transect across a garnet grain tend to define "compositional grain shapes", suggesting a diablatic texture. This texture, however, was not optically observed in sample **N616**, but is obviously present in **P23** and **PK23b** where composition profiles are rather flat with compositional variations only present at the "outer" rims. If no inclusions were present in the vicinity of the present transect, these contrasting and at the very first glance incoherent observations of composition profiles can tentatively be explained by the intensity of the metamorphic process involving the formation of garnet (*i.e.* reaction 1) together with later diffusion and homogenization processes within grains and/or defined by transfer reactions (*i.e.* reaction 3). Hence, the extended observable phenomena (diablatic texture in **P23** and **PK23b**) can be explained by the fact that the host rocks (cumulate and cumulate with superimposed granulite facies metamorphism) have undergone complete homogenization of compositions between former grain boundaries. Conversely, the weakly extended and non-observed nucleation of garnet in a diablatic texture phenomena has probably been restricted, as indicated by the fact that the granitic vein intruded rocks of the mid-upper northern series probably cooler and/or weakly influenced by granulite facies metamorphism.

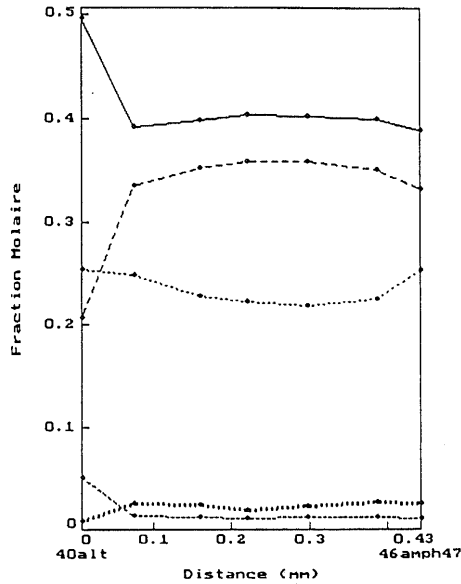
Concerning the vein **N601a**, within which appendices of garnet occur (see previous section on reactive textures of the veins), zoning profiles clearly show a net increase of about

Figure 7. Garnet zoning profiles...

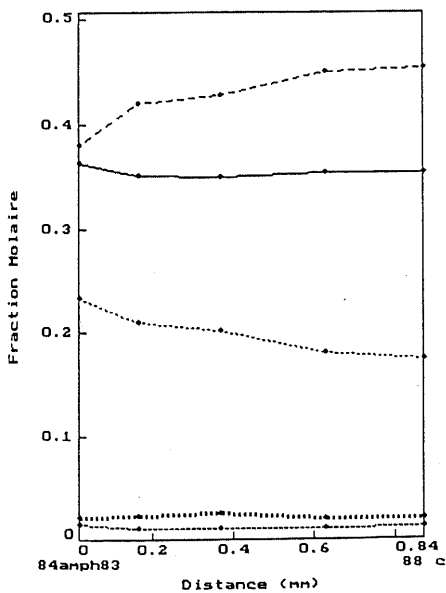
- a) N629b - host rock  
metamorphic almandine-rich garnet  
120cpx119 = Cpx (see appendix 3c)  
172cpx = Cpx



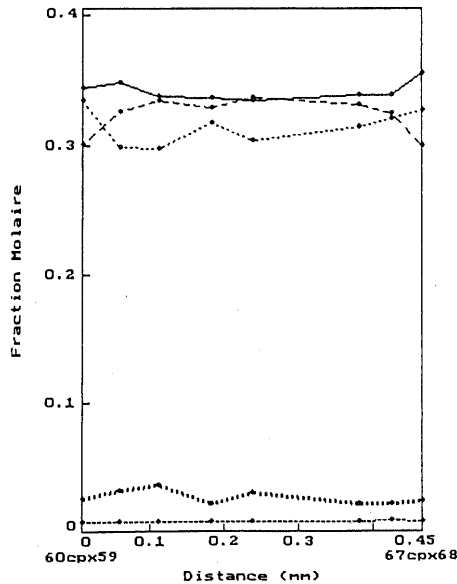
- 7b) GI11 - host rock  
metamorphic almandine-rich garnet  
40alt = alteration phases  
46amph47 = Amph (see appendix 3e)



- 7c) P23a - host rock  
metamorphic pyrope-rich garnet  
84amph83 = Amph (see appendix 3e)  
88c = Amph core

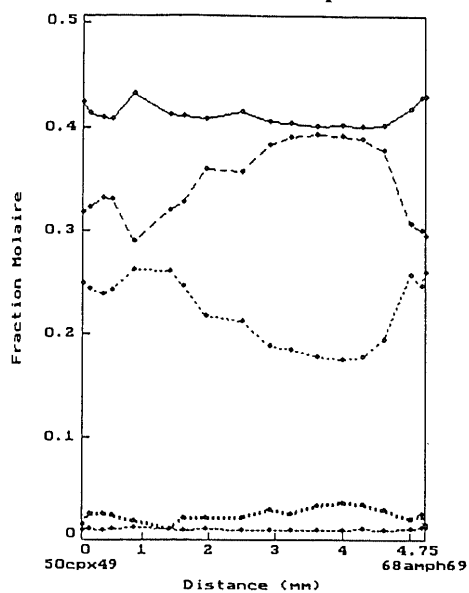


- 7d) N639b - host rock  
magmatic almandine-pyrope-grossular garnet  
60cpx59 = Cpx (see appendix 3c)  
67cpx68 = Cpx (see appendix 3c)

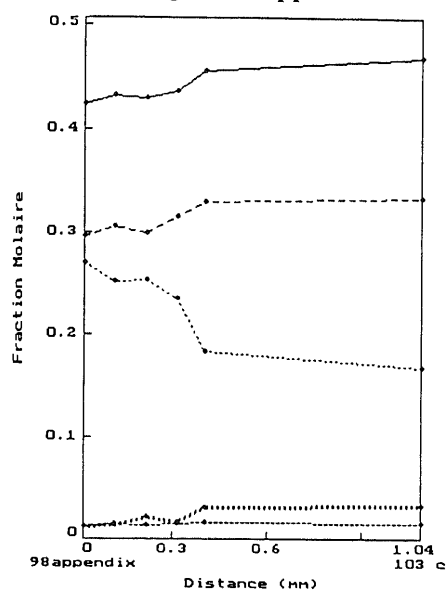


..... ADR  
----- SPS  
..... GRS  
----- PRP  
----- ALM

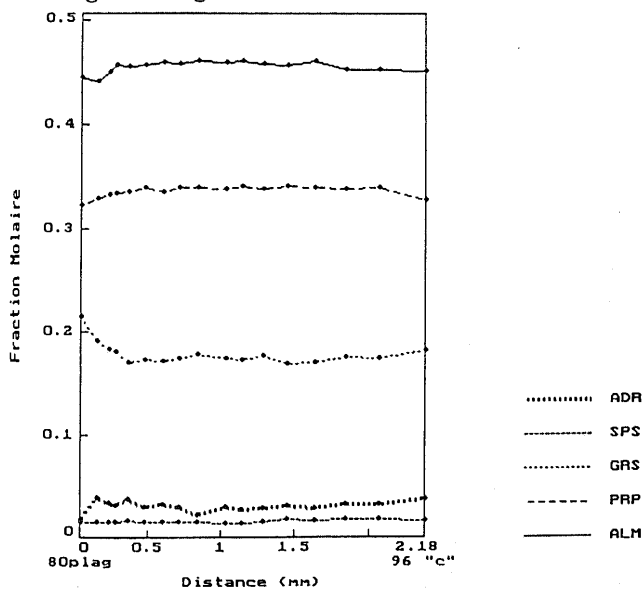
- 7e) G111 - vein  
 magmatic almandine-rich garnet  
 50cpx49 = Cpx (see appendix 3c)  
 68amph69 = Amph (see appendix 3e)  
 "compositional grain shape"



- 7f) N601a - vein  
 magmatic almandine-rich garnet  
 98appendix = growth appendix in contact with Pl  
 103c = Grt core  
 garnet with growth appendices



- 7g) N601a - vein  
 magmatic almandine-rich garnet  
 80plag = Pl  
 96 "c" = Pl core  
 homogeneous garnet



..... ADR  
 -.-.-.- SPS  
 ..... GRS  
 - - - - PRP  
 ——— ALM

Figure 7. Garnet zoning profiles



10% in the grossular content within the appendices grown on previous homogeneous garnet grains (figures 7f and 7g).

## ZONING PROFILES OF CLINOPYROXENE, ORTHOPYROXENE, PLAGIOCLASE, AND AMPHIBOLE

In contrast to garnet, minerals like clinopyroxene, orthopyroxene, plagioclase, and amphibole (?) are more likely to rehomogenize, due to volume diffusion (Freer, 1981). As a consequence, zoning profiles of the above main phases are mainly flat with minor composition variations at rims, as listed in Table 5 (samples omitted simply not showing any relevant composition changes for the listed phase(s)).

Finally, and as observed in the previous section, a relationship between mineral compositions and variations in pressure and temperature can be assumed, according to the nature of the neighboring grains and the ionic transfer or exchange reaction(s) involved. Obviously one has to be careful when giving an interpretation of the observable zoning profiles, as compositional variations at rim may only represent part of the reaction sequence. Therefore, only relic composition variations for phases, that may not have formed or reacted together within the same metamorphic event, having only undergone late partial equilibration may be shown. As mentioned previously, a list of representative compositional changes according to zoning profiles for the main phases including garnet, clinopyroxene, orthopyroxene, plagioclase, and amphibole is presented in Table 5.

## CALCULATION OF METAMORPHIC CONDITIONS

In order to minimize the uncertainties in the interpretation of pressure and temperature estimates, all calculations were performed using the same thermodynamic data base combined with a unique activity model for each phase in a given assemblage. The thermodynamic data base of Berman (1988) was used in order to insure internal consistency of data, as some activity models include excess energy parameters of Berman (*i.e.* Berman, 1990 for garnet). Mineral assemblages mainly consist of garnet-plagioclase-clinopyroxene-amphibole (+/- orthopyroxene, rutile, ilmenite, biotite, muscovite, chlorite and epidote). For a given reaction containing unaltered minerals, calculations were performed using the THEBA software (Martignole et al., unpublished) on granulite, amphibolite, and cumulate assemblages of samples including phases with available core and rim analyses within the same grain and,

Table 5. Compositional variations according to zoning profiles of the main phases in samples from the Jijal complex (and K27)

NORTH															
Sample		Contact mineral	Grt XCa	Fe/Mg	Cpx	Opx XEn	Pl mean XAn	XAn	XKfs	Amph composition	Ca	Fe3	Mg	K	Na
NORTHERN SERIES															
N 588	SZ	Pl (An37)	↑	↗											
N 589	V?	Ferroan-pargasite	↑	↓			An36	↘	→						
	V?	Magnesio-hornblende	→	↓			An45	→	→						
	V?	Grt								Ferroan-pargasite	↑	↓			
	V?	Grt								pargasitic hornblende	→	→			
	V?	Pl (An03)	↑	↓											
N 593	V?	Pl (An45)								Ferroan-pargasite	↗	↓			
	V?	Cpx					An40	↓	→						
	V?	Cpx	↗	↗											
	V	Pl (An81)	↑	↗											
	V	patte Grt	↑	→											
N 601b		Pl (An44)	→	→											
N 605	V?	Pl	↑	→											
N 610a	V	(altered) Pl	↗	→				↑	→						
		Cpx	↗	→											
N 610b															
N 614		Pl	↑	→											
N 616	V	Cpx	↗	↗											
		pargasite	↗	↗											
		pargasitic hornblende								pargasitic hornblende	↘	↗			
N 617	V?	pargasitic hornblende	→	↑											
	V?	Pl	↑	→											
N 618	ln V														
N 621	SZ														
N 626		magnesio-hornblende	↑	→											
N 627a	V	epidote	↑	→											
N 627b		Cpx	↑	→											
		epidote	↑	→											
N 627c	V	Pl (An32-90?????)	↑	→											
		Grt					An90???	↗	→						
N 629a															
N 629b		Cpx	↑	→											
N 631		magnesio-hornblende	↗	↗											
		epidote	→	→											
N 632	SZ														
N 633	SZ	epidote	→	↓						Fe-pargasitic hornblende	↘	↑	↗	↓	↗
		Fe-pargasitic hornblende	→	↓	→										
N 634a	V	Cpx	→	→											
		Pl (An37)	↑	→											
		pargasite	→	→											
N 634b		pargasitic hornblende	↗	↗											
		edenitic hornblende	↗	→											
N 636a		Cpx	↗	→											
N 636b	V	Pl (An14)	↑	→											
		epidote	↑	→											
N 636c		Cpx	↗	↗											
N 638		Fe-pargasitic hornblende	→	→											
N 639a		Cpx	→	→											
		pargasitic hornblende	→	→											
N 639b		Cpx	↑	↑											
		white mica					An10	↗	→						
N 640	V	chlorite	→	→			An4	↘	→	actinolitic hornblende	→	→	→	→	
		epidote	↗	↗											
SOUTHERN SERIES															
Kamila amphibolite belt/Chilas complex contact															
K 27	V	Pl (An37)	→	→											
P 24c		Cpx	↑	→											
KI 153															
KI 158		Pl (An38)	↑	→			An38	↓	→						
		Grt				↑	An38	↓	→						
		cummingtonite					An44	↓	→						
P 573		Cpx	↑	↑											
GI 11b															
GI 13															
GI 11															
GI 11a															
GI 18															
P 576	(V)														
P 577		alteration of Pl					An45	↑	↑						
P 577a															
P 574		Cpx	↑	→											
P 572		Cpx	↑	↑											
PK 23b		Cpx	↗	↑											
P 23		Cpx	↑	↑											
KI 16		Pl (An34)	→	→											
		Grt					An33	↘	→						
		Cpx					An33	↘	→						
GI 10		patte Grt	↑	↗											
P 570															
P 23a		edenitic hornblende	↑	↑											
		Grt (metamorphic?)	↑	↑											
KI 189															
P 166	V	altered Pl (An40)	→	→											
P 142															
SOUTH															

SZ = shear zone, V = vein, ↑ > 5% augmentation, ↗ 5% augmentation, ↓ > 5% diminution, ↘ 5% diminution, → constant (no variation)

where possible, within a proximal assemblage. Such an approach implies that both textures and mineral chemistry are considered because complete reequilibration, especially related to low-temperature retrogression is more likely to have affected minerals at a local scale.

Besides analytical uncertainties, potential sources of error in the present calculation routines include the incorporation of  $\text{Fe}^{3+}$  recalculated as andradite in garnet, acmite and  $\text{CaFe}$ -tschermak in clinopyroxene, and given by the excess of cations over the normalization scheme for amphibole.

The stoichiometry of minerals was calculated as described in appendix 2. For clinopyroxene, the utilization of Na to form jadeite molecule first instead of acmite was preferred after considering the fact that clinopyroxene is Mg-rich and  $\text{Al}^{\text{VI}}$ - (and  $\text{Si}^{\text{IV}}$ -) rich but oxidized, and also because of the tholeiitic composition of the rocks and their high propensity to have undergone high-pressure metamorphism. Garnet activities were calculated using the excess energy parameters of Berman (1990); anorthite activities in plagioclase were calculated following the Al-avoidance mixing on sites model of Kerrick and Darken (1975), together with the mixing parameters of Fuhrmann and Lindsley (1988); pyroxenes and amphibole activities were calculated following ideal-mixing on sites.

Table 6 includes a list of 8 reactions that were used as thermometers and barometers for calculations. Only water-absent equilibria have been selected because of the difficulties in obtaining independent estimates on water activity. The accuracy concerning the use of different reactions is mainly dependent on the following factors:

- 1) phases for which excess energy parameters have been determined experimentally by calorimetry such as garnet and plagioclase are the most reliable ones, in contrast to those for which excess energy parameters have been determined empirically such as clinopyroxene (Berman, 1995). Also, reactions for which the partitioning coefficient ( $K_D$ ) had been measured experimentally (as for the clinopyroxene-garnet Fe-Mg thermometer) enabled Pattison and Newton (1988) to determine the lower limit for Fe-Mg exchange for that reaction at 600°C. Such observations can thus be very helpful as they give a link to the cooling history of rocks.
- 2) In most cases, barometers will be more reliable than thermometers because the latter usually only involve two phases, whereas barometers usually involve four phases or more. Also in contrast to thermometers, most barometers are not influenced by the degree of oxidation of the rock, or that influence is negligible *i.e.* clinopyroxene for which the Al-Si exchange is obviously dominant on the formation of  $\text{CaFe}$ -tschermak molecule with increasing pressure.
- 3) If amphibole is present, one has to remember that, as an hydrated phase, it is more sensible to variations in oxygen fugacity. It contains larger amounts of  $\text{Fe}^{3+}$  than other main

phases described above and, if the real amount of  $\text{Fe}^{3+}$  is not known, this leads to greater error on the  $\text{Fe}^{2+}/\text{Mg}$  ratios on which most calculations are based especially in thermometry.

4) The fact that blocking temperatures for Fe-Mg exchange reactions appear to be lower than for net-transfer reactions implies that pressure-temperature pairs should be treated with great care especially for medium?- to low-temperature assemblages.

5) As Fe-rich phases tend to reequilibrate more easily with decreasing temperatures compared to Mg-rich phases, reactions involving Mg end-members are preferred over their Fe analogs. Thermodynamic data for Mg end-members are also better constrained than for their Fe analogs.

**Table 6. Reactions used as geothermometers and as geobarometers**

System	Geothermometer	Initially proposed by:
Cpx-Grt	pyrope + 3 hedenbergite = almandine + 3 diopside	Ellis and Green (1979)
Opx-Grt	2 pyrope + 6 ferrosilite = 2 almandine + 6 enstatite	?
Prg-Grt	3 pargasite + 4 almandine = 3 Fe-pargasite + 4 pyrope	Graham and Powell (1984)
System	Geobarometer	Initially proposed by:
Cpx-Grt-Pl	3 anorthite + 6 diopside = 2 grossular + pyrope + 3 quartz	Perkins and Newton (1981a)
Opx-Grt-Pl	3 anorthite + 6 enstatite = grossular + 2 pyrope + 3 quartz	Perkins and Newton (1981a)
GRIPS	grossular + 2 almandine + 6 rutile = 6 ilmenite + 3 anorthite + 3 quartz	Bohlen and Liotta (1986)
Ab-Jd	albite = jadeite + quartz	Essene and Fyfe (1967)
An-Cats	anorthite = Ca-tschermak + quartz	Wood (1977)

\* Mineral symbols according to Kretz (1983)

Amph = amphibole, Cats = Ca-tschermak

## PRESSURE AND TEMPERATURE ESTIMATES

The most reliable pressure-temperature determinations were obtained from samples including rim and core analyses within the same grain from the coarsest grains of clinopyroxene, garnet, plagioclase and are presented in Table 7. Thermometer-barometers intersections indicate that analysed phases do not represent equilibrium because pressures and temperatures spread between 700-1100°C and 11-20 kbar. Such a spread can be explained considering factors like the variability within the same sample of anorthite content of the plagioclase, and Ca-tschermak and jadeite content of the clinopyroxene: such components are critical in determining the pressure for barometers like  $\text{Ab} = \text{Jd} + \text{Qtz}$  (Ab-Jd), and  $\text{An} = \text{Ca-tsch} + \text{Qtz}$  (An-Cats).

Temperatures averaging 900°C were calculated with the (Cpx-Grt) Fe-Mg exchange thermometer ( $\text{Prp} + 3 \text{Hd} = \text{Alm} + 3 \text{Di}$ ). The (Prg-Grt) Fe-Mg exchange thermometer ( $3 \text{Fe-Prg} + 4 \text{Prp} = 3 \text{Prg} + 4 \text{Alm}$ ) of Holland and Powell (1984) was used in order to constrain the temperature of formation of amphiboles. Because this thermometer is empirically calibrated against the (Cpx-Grt) thermometer, results are not totally independent from those obtained from the (Cpx-Grt) thermometer, but the average temperature of amphiboles around 900°C suggests that garnet, clinopyroxene and amphibole were part of the same equilibrium assemblage.

Variations of jadeite and Ca-tschermak content of the clinopyroxenes are listed in Table 7 for each sample; they are up to 11% for Ca-tschermak and 8% for jadeite content (both in KI16). Such disequilibrium within a sample can only be attributed to heterogeneous release of Al during decompression (dejadeitization and de-Ca-tschermakitization) according to above reactions. Figure 5 shows this global trend of jadeite decrease within samples of the Jijal complex from 20% (the omphacite limit) to less than 3%. It is interesting to note that even magmatic clinopyroxene has a variable content in jadeite e.g. **P23a** (6-7%); **P572** (5-11%); **GI10** (3-5%); **N616** (7-11%); **N636c** (11-13%), that could be representative of the buffering effect due to variable albite content of plagioclase in the rocks, but is more likely to be attributed to decompressional metamorphism by analogy to metamorphic clinopyroxene. This observation gives evidence for a post-magmatic stage decompressional metamorphic event that affected the whole complex.

An interesting point to be elucidated is whether the dejadeitization and de-Ca-tschermakitization reactions are coupled, in which case the production of albite and anorthite would not affect the initial composition of the plagioclase. Considering the reaction:  $3 \text{An} + 6 \text{Di} = 2 \text{Grs} + \text{Prp} + 3 \text{Qtz}$  (Cpx-Grt-Pl), for which intersections with clinopyroxene-garnet exchange reaction (Cpx-Grt) are listed in Table 7, it is clear that if dejadeitization-only occurs, the increase of albite component of the plagioclase would lead to artificially higher pressures calculated for that reaction. An extreme case is illustrated in appendix 5b (sample **P24c**), for which the plagioclase is represented by albite and for which the (Cpx-Grt-Pl)-(Cpx-Grt) intersection would be at about 36 kbar! Note also the extremely high position of the (An-Cats) reaction compared to a hypothetical calculation with an anorthite content in plagioclase of 50%. The asymmetrical progression of dejadeitization towards de-Ca-tschermakitization can be observed in this pressure-temperature diagram and it is more likely that de-Ca-tschermakitization proceeds preferably over dejadeitization. Hence, the albitization of plagioclase (that is also common to most retrograde trends) has more effect than the anorthitization on the equilibrium.

The extended compositional range of plagioclase among the samples of the Jijal complex (from An = 0 to 82%) is in favour of a reequilibration of this phase according to

prograde and/or retrograde processes (like uralitization) followed by alteration by late fluid circulation. Realistic normative compositions of plagioclase in gabbros (from An = 50-70%) were considered and tested on samples of evident disequilibria such as **P24c**, in order to obtain an equilibrium pressure. Because such trials have not provided anticipated results, actual clinopyroxene and garnet compositions have probably been modified since the peak of metamorphism. This assertion is confirmed by zoned composition profiles in the case of garnet but seems to be in opposition with the observed preservation of igneous textures and *quasi* homogeneous composition of the clinopyroxene. This can be explained by the fact that the Al<sup>VI</sup>, and to a lesser extent the Na content of the clinopyroxene only constitute a minor part of the molecule, therefore are negligible compared to variations in Fe/Mg content. Moreover, net transfer reactions such as (Cpx-Grt-Pl), if prograde, results in the consumption of the whole clinopyroxene molecule.

Considering that plagioclase composition is not representative of peak equilibrium conditions, reactions involving this phase (barometers) cannot lead to coherent pressure determinations. One should then consider pressures in Table 7 as indicative only. Alternatively temperature-pressure trends calculated from core and rim within the same grain (see Table 7) provide some indication of the pressure-temperature path. For most samples either from host rocks or veins, grain growth is usually accompanied by an increase in pressure with decreasing, constant or increasing temperature. Due to the lack of equilibrium, calculated pressures cannot be taken at face value, although pressure-temperature trends could be reliable.

It is interesting to consider sample **N629a** for which calculated pressures and temperatures include values for a magmatic clinopyroxene-bearing assemblage together with those obtained with a metamorphic clinopyroxene from the same assemblage. The growth of the magmatic clinopyroxene is characterized by a decrease in pressure and temperature at variance with the growth of the metamorphic clinopyroxene characterized by an increase in pressure and temperature. Even in this case, one should be careful when considering pressure trends, because in the assemblage garnet-plagioclase-clinopyroxene the anorthite content of the plagioclase is sensitive to the production of grossular, unless the modal proportion of plagioclase is such that it could be considered as an infinite reservoir. In this sample the plagioclase content is only 30%, hence cannot be considered as an infinite reservoir. Pressure trends could therefore represent artefacts in opposition with an initial unknown path in the case of the magmatic clinopyroxene-bearing assemblage, especially if extensive garnet growth (30% of the modal composition of the rock) occurred during the late magmatic stage. On the other hand, contrasting temperature trends in garnet-clinopyroxene pairs from the same sample attest to disequilibrium in exchange reactions. In this case, the only value that can be retained is an average.

Table 7. Temperature and pressure calculations of selected samples from the Jijal complex

NORTH													
Sample	Assemblage(s)	An	Jd	Cats	position	(An-Cats) / (Cpx-Grt)		(Ab-Jd) / (Cpx-Grt)		(Cpx-Grt-Pl) / (Cpx-Grt)		(GRIPS) / (Cpx-Grt)	
						T	P	T	P	T	P	T	P
northern series													
N 589	(V) amphibolite	40-47	10-12	7-8	rim	724	1234			732	1253		
					core	823	776			839	1322		
N 593	(V) cumulate + granulite	albite	10-13	4-7	rim			827	915				
					core			785	587			842	2447
N 601b	granulite	43-55	7-11	4-9	rim	923	604	771	504	852	3147	826	2278
					core	913	352	930	828	945	1318	934	946
N 610a	V igneous?	albite-28	11-13	3-6	rim	816	2231	761	401	829	2682	929	875
					core	938	1804	902	637	943	1946		
N 610b	cumulate + retrograde	8-40	12-16	1-11	rim	929	3255	851	634	921	2957		
					core	949	2731			946	2640		
N 614	(V) cumulate + granulite	albite	13-16	9	rim			907	859				
					core			878	785				
N 627a	V	26-42	10-12	8-9	rim	1015	1021	1017	1085	1040	1895	1019	1143
					core	999	981			1019	1667	1003	1109
N 629a	granulite?	19-20	10-12	3-9	rim	803	813	798	642	823	1453		
	(magmatic clinopyroxene)				core	930	1409	907	672	938	1697		
	granulite?				rim	860	1226	844	725	870	1553		
	(metamorphic clinopyroxene)				core	815	807	810	657	837	1523		
N 634a	V igneous	36-37	12-19	5-7	rim	931	929	939	1180	953	1652		
					core	911	927	918	1162	930	1559		
N 636b	V anorthositic	14-64	11-13	12-16	rim	1108	1346	1112	1520	1121	1845		
					core	1143	1346	1147	1493	1150	1604		
N 639b	cumulate + retrograde	5-10	11-14	13-15	rim	1015	3029	956	897	1009	2813	978	1653
					core			987	983	1043	3053	1009	1753
southern series													
P 24c	granulite	albite	14-16	10-13	rim			939	1012				
					core			941	988				
KI 153	amphibolite + granulite	57-60	8-11	3-12	rim	730	1001	726	868	737	1239	719	632
					core	957	837	964	1065	972	1329	957	840
KI 158	granulite	38-54	8-12	3-10	rim	779	822	778	802	792	1232		
					core	732	299	743	659	753	982		
						(An-Cats) / (Opx-Grt)		(Ab-Jd) / (Opx-Grt)		(Opx-Grt-Pl) / (Opx-Grt)			
						T	P	T	P	T	P		
						823	811	824	829	855	1196		
						797	242	840	710	875	1102		
P 573	granulite	39-45	12-17	8-13	rim	922	1307	922	1303	932	1617		
					core	1024	1116	1024	1132	1043	1762		
GI 11b	cumulate + granulite	31-41	14-16	9-11	rim	770	1195	769	1150	780	1537		
					core	805	1224	802	1150	810	1411		
GI 13	cumulate + granulite	37-40	13-15	8-10	rim	871	1172	870	1141	881	1514	862	864
					core	809	1143	807	1088	816	1368	798	767
P 576	(V) granulite	36-38	13-16	3-8	rim	778	1052	780	1133	789	1424		
					core	966	1063	972	1269	981	1552		
P 577	cumulate + granulite	33-42	11-17	7-12	rim	950	1301	948	1225	962	1700		
					core	1052	1343	1048	1203	1069	1951		
P 574	cumulate + granulite	40-46	11-17	5-12	rim	979	1408	974	1248	976	1320		
					core	1112	1200	1112	1201	1121	1521		
P 572	cumulate + retrograde	37-40	12-17	5-11	rim	1024	1350	1027	1470	1040	1904		
					core	952	1294	956	1409	965	1719		
KI 16	granulite + amphibolite	32-37	11-19	1-12	rim	944	1470	941	1379	958	1969		
					core	937	1399	939	1461	950	1838		
SOUTH													

V = vein, An = anorthite % in plagioclase, Jd = jadeite % in clinopyroxene, Cats = Ca-tschermak % in clinopyroxene  
P = pressure (MPa), T = temperature (C)

## DISCUSSION AND CONCLUSION

Recent work in geothermobarometry of gabbroic rocks from the Kamila amphibolite belt enabled Jan and Karim (1995) to suggest a regional thermotectonic event, that could be related to the collision of the Kohistan oceanic arc with the Asian plate. This took place at about 800°C, 5.5-7.5 kbar and was followed by crustal thickening and cooling at about 510-600°C, 10-12 kbar (estimated from late veins crosscutting the olivine-gabbros of Khwasa Khela). Pressure-temperature-time paths of the garnet-bearing rocks from Jijal and Chilas complexes are distinct (Yamamoto, 1993) and suggest a high-pressure anticlockwise path for the Jijal complex in contrast to a low-pressure retrograde path for the Chilas complex. Temperature and pressure estimates for the Jijal complex are about 697- 949°C, 10.2-17.0 kbar, and 607-785°C, 6.3-7.8 kbar for the Chilas complex. According to Yamamoto (1993), this difference in pressure corresponds to 25 km in crustal thickness at the last stage of the granulite facies metamorphism which brought the rocks of the Jijal complex to a depth of about 55 km.

Pressure and temperature estimations from the present study span between 719-1150°C (from Cpx-Grt thermometer) and 9.8-31.5 kbar (from Cpx-Grt-Pl barometer); this pressure-temperature range corroborates the data of Yamamoto (1993) although it is more extended (see figure 8). However, the high variability of the albite content of plagioclase in all samples is responsible for the disequilibrium and several of the pressures obtained are certainly artefacts. An important new conclusion from this study comes from petrological evidence (like the presence of primary garnet, plagioclase and clinopyroxene and probably amphibole) which point to a magmatic origin of the garnet-bearing rocks of the Jijal complex (see Table 8). According to Green (1982), dry tholeiitic basalts crystallize clinopyroxene-garnet-plagioclase on the solidus at temperatures between 1180 and 1300°C and pressures between 13 and 25 kbar. In garnet-free cumulate assemblages, the occurrence of presumably magmatic amphibole however attests for temperatures of crystallization lower than 1100°C (Essene et al., 1970).

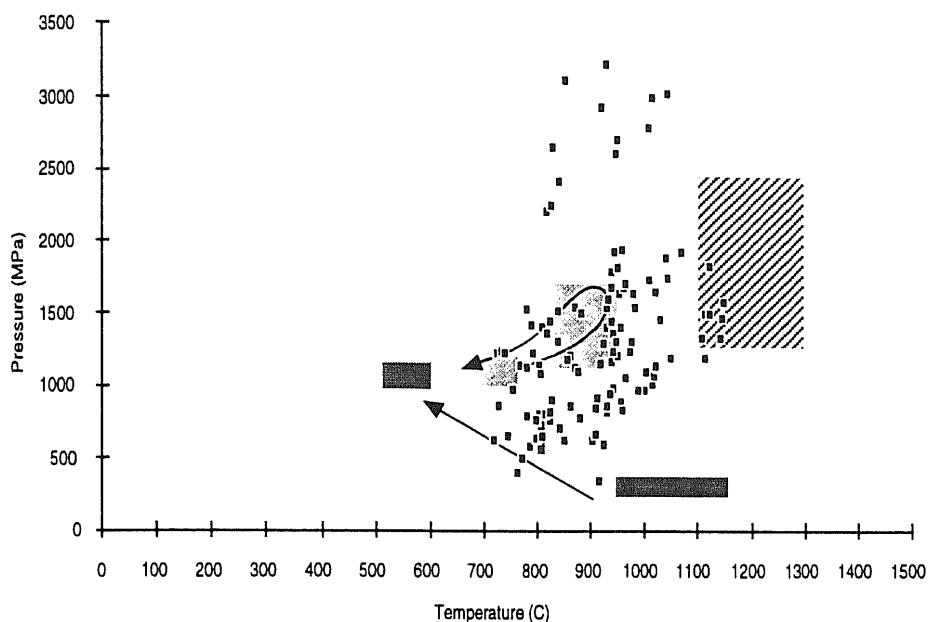
Temperature and pressure conditions of 950°C and 17 kbar calculated from anorthite = 50% content in plagioclase, with jadeite = 16% content in metamorphic clinopyroxene and garnet of sample **P24c** probably represent the best approximation for minimum pressure conditions of rocks from the Jijal complex before decompression. The variable  $Al^{VI}$ , Ca-tschermak and jadeite content of clinopyroxene within a sample including either magmatic and/or metamorphic clinopyroxene are indicative of this penetrative decompressional metamorphic event that post-dated the magmatic stage.



Table 8. Contrasting magmatic and metamorphic garnets of the Jijal complex

MAGMATIC	METAMORPHIC
Assemblage: Pl, Cpx, Amph, Spl, Ap, +/- Grt	Assemblage: Pl, Cpx, Opx, Amph, Rt, opaque oxides, Ep, Chl, white mica, Scp, Grt
poor in inclusions	usually have inclusions of Amph, Cpx, Pl, and opaque oxides
grains can be coarse (up to 2 cm across) not associated with Qtz locally associated with magmatic Cpx with evidence of simultaneous growth	grains occur as small (a few mm across) euhedral neoblasts, or coarse, up to 4.5 cm across hypidiomorphic grains anhedral with lobate to embayed boundaries hollow, or forming atoll garnets associated with Qtz that forms mosaics with serrated boundaries, or aggregates around Grt. Symplectites with Qtz occur in contact with Cpx
some samples with a mesocumulate texture (Pl is the last phase to crystallize in the magma) Relic zones preserved at thin section scale, overprinted by various metamorphic assemblages	garnet grows forming a diablastic texture
Process: Cpx-Pl-Grt crystallization between 1180-1300 C, 13-25 kbar (Green, 1982)	Process: Grt growth according mainly to reaction 1 (Table 2), but also 2, 5, 15, 16, and 17 OR Reequilibration of the Grt due to Ca-Si metasomatism like that observed in the ultramafic rocks below (Treloar, 1989) according to reaction such as: 8, 21, 34, and 53  followed by retrogression to greenschist facies involving Grt consumption: 22, 24, 29, 31, 52, 54, but also: 8 and 53.

cpx = clinopyroxene, opx = orthopyroxene, amph = amphibole  
Other mineral symbols according to Kretz (1983)



**Figure 8. Pressure-Temperature diagram showing results of P-T estimates from rocks of the Jijal and Khawasa Khela complexes.**

Points are plotted according to the thermobarometric data listed in Table 7. Light gray shaded areas indicate estimated P-T conditions for rocks of the Jijal complex according to their anticlockwise path (from Yamamoto, 1993). Dark gray shaded areas indicate estimated P-T conditions and path of the ultramafic rocks of the Khawasa Khela complex according to Jan and Karim (1995). The stripe box represents P-T conditions of crystallization for the Grt-Cpx-Pl magmatic assemblage according to Green (1982).

In conclusion, the magmatic garnet-bearing rocks of the Jijal complex might have formed in temperature-pressure conditions between  $<1100$  and  $1300^{\circ}\text{C}$  and between 13 and 25 kbar. Metamorphism related to the accretion of the arc with the Asian plate that resulted in the burial of the complex most likely occurred under estimated minimum pressure conditions of  $950^{\circ}\text{C}$ , 17 kbar, and was followed by decompression associated with the obduction of the Jijal complex onto the Indian plate during continental collision.

## Appendix 1:

**Thin section descriptions  
including modal composition,  
mineral assemblage  
and possible reactions**

**P23: Garnetite**Modal composition:

garnet	80%
green pargasite	9%
clinopyroxene	10%
clinozoisite	1%
plagioclase	trace
apatite, chlorite	trace
opaque oxides & rutile	trace

Coarse, but heterogranular garnets in a diablastic texture form 80% of the rock. They are poor in inclusions but may include fresh clinopyroxene, green pargasite, and opaque oxides aggregates that are usually coarse grained, with lobate to serrated boundaries. Aggregates have a granoblastic texture. Rare alteration is present as chlorite may locally form veinlets in garnet (54). Rare trace of clinozoisite may be

associated with chlorite or slightly alter pargasite at grain boundaries (41). A few mm-large euhedral neoblasts of garnet may form in aggregates, showing that metamorphism was still in progress during final crystallization. Rare garnet with tremolite symplectite may be included in clinopyroxene grains (8), suggesting that a "plagioclase + clinopyroxene" cumulate was the protolith of the garnetite.

Mineral assemblage and possible reactions:

- 8)        6 tremolite + 7 grossular  $\leftarrow$  27 diopside + 6 anorthite + pyrope + 6 fluid  
 41)       3 chlorite + 6 epidote  $\leftarrow$  tschermakite + 2 anorthite + 10 fluid  
 54)       3 quartz + 3 chlorite + 3 anorthite  $\leftarrow$  grossular + 5 pyrope + 12 fluid

### P23a: Retrogressed garnet pyroxenite

#### Modal composition:

pale green amphibole	44%
garnet	25%
clinopyroxene	15%
chlorite	10%
orthopyroxene?	5%
apatite	1%
quartz	trace
opaque oxides & rutile	trace

The holocrystalline thin section shows an heterogeneous distribution of heterogranular minerals without any preferred orientation. Large, green hypidiomorphic clinopyroxene grains with Schiller plates (indicative of high  $T^{\circ}$  ~800-850 °C) and spinel inclusions remain as patches on the metamorphic assemblage. There is textural evidence that the primary assemblage (possibly plagioclase + clinopyroxene + pargasite) cumulate was prograded to

granulite facies until disappearance of plagioclase (1, 7). Granulite facies minerals appear as pseudo-aggregates between the large cumulate pargasite and clinopyroxene grains. Garnets are anhedral with lobated to embayed boundaries. Symplectites of garnet with quartz also occur in contact with pyroxenes (1). Interstitial quartz neoblasts occur between garnet and orthopyroxene? (2). Inclusions in garnet are of oxide (rutile, ilmenite?), orthopyroxene, clinopyroxene as round inclusions or in optical continuity with surrounding grains, and amphibole. Garnets are altered by chlorite propagating in fractures (54). Amphibole grains locally include symplectitic garnet with clinopyroxene relict (7, 15). Orthopyroxene grains are altered and plagioclase is absent. Clear and small amphibole grains occur. It is suggested that they might be metamorphic amphiboles contrasting with the coarse grained cumulate ones (48).

#### Mineral assemblage and possible reactions:

- 1)  $3 \text{ anorthite} + 6 \text{ diopside} \rightarrow 2 \text{ grossular} + \text{pyrope} + 3 \text{ quartz}$
- 2)  $3 \text{ anorthite} + 6 \text{ enstatite} \rightarrow \text{grossular} + 2 \text{ pyrope} + 3 \text{ quartz}$
- 7)  $4 \text{ tremolite} + 3 \text{ anorthite} \leftarrow 3 \text{ pyrope} + 11 \text{ diopside} + 7 \text{ quartz} + 4 \text{ fluid}$
- 15)  $3 \text{ pargasite} + 12 \text{ anorthite} + 18 \text{ diopside} \rightarrow 3 \text{ tremolite} + 5 \text{ pyrope} + 10 \text{ grossular} + 3 \text{ albite}$
- 48)  $\text{chlorite} + \text{actinolite} \leftarrow \text{hornblende} + \text{anorthite}$
- 54)  $3 \text{ quartz} + 3 \text{ chlorite} + 3 \text{ anorthite} \leftarrow \text{grossular} + 5 \text{ pyrope} + 12 \text{ fluid}$

**PK 23b: Garnet granulite**

<u>Modal composition:</u>	
garnet	45%
plagioclase	25%
green ferroan pargasite	15%
quartz	10%
clinopyroxene	5%
rutile, chlorite	trace

The global texture is granoblastic with an heterogeneous distribution of minerals, as garnets tend to agglomerate in a matrix roughly composed of plagioclase. Garnets are hypidiomorphic to euhedral with usually straight boundaries when in contact with plagioclase and lobated to embayed boundaries when in contact with clinopyroxene, quartz, and ferroan

pargasite (7, 17). Garnets tend to agglomerate as neoblasts form and may include large inclusions of hornblende, clinopyroxene, quartz mosaic, apatite, and rutile. Garnets are altered by chlorite filling the cracks (54). Plagioclase are cloudy and/or strongly saussuritizised (25). Uralitization as a retrogression process can be observed (7).

Mineral assemblage and possible reactions:

- 7) 4 tremolite + 3 anorthite ← 3 pyrope + 11 diopside + 7 quartz + 4 fluid
- 17) 3 Fe-tremolite + 6 anorthite + 3 albite ← 3 Fe-pargasite + almandine + 2 grossular + 18 quartz
- 25) 2 zoisite ← 3 anorthite + Ca(OH)<sub>2</sub>
- 54) 3 quartz + 3 chlorite + 3 anorthite ← grossular + 5 pyrope + 12 fluid

**P24c: Retrogressed garnet granulite**

<u>Modal composition:</u>	
plagioclase	30%
garnet	25%
quartz	20%
pale green amphibole	15%
clinopyroxene	10%
opaque oxides & rutile	trace
zoisite	trace

A homogeneous distribution of minerals is observable at thin section scale. Minerals are isogranular, except for euhedral garnets. Contact boundaries between garnet and quartz or amphibole are lobate. Garnets are altered by chlorite (54), as well as clinopyroxenes (55). Apatite, quartz, clinopyroxene (which can be surrounded by quartz), opaque oxides & rutile

and amphibole occur as round inclusions in garnet. All plagioclase grains are cloudy and sometimes saussuritizised (25). Rare symplectitic zoisite + albite appears in contact with plagioclase (26), as retrograde reaction progressed. Contact boundaries with garnet are straight. Clinopyroxenes are anhedral and altered by chlorite. Uralization may have affected some grains (7). Lobate contact boundaries between amphibole and clinopyroxene clearly show the transformation of one to the other.

Mineral assemblage and possible reactions:

- 7) 4 tremolite + 3 anorthite  $\leftarrow$  3 pyrope + 11 diopside + 7 quartz + 4 fluid  
 25) 2 zoisite  $\leftarrow$  3 anorthite + Ca(OH)<sub>2</sub>  
 26) albite + zoisite  $\leftarrow$  oligoclase + fluid  
 54) 3 quartz + 3 chlorite + 3 anorthite  $\leftarrow$  grossular + 5 pyrope + 12 fluid  
 55) anorthite + 2 chlorite + 3 quartz  $\leftarrow$  3 pyrope + diopside + 8 fluid

**P142: Garnet and zoisite amphibolite**Modal composition:

bluish to green amphibole	40%
zoisite	20%
quartz	19%
garnet	15%
plagioclase	5%
apatite	1%
epidote, chlorite	trace
opaque oxides & sphene	trace

A slight preferred orientation of hypidiomorphic zoisite and ferroan pargasite can be seen in thin section. Ferroan pargasite and zoisite are usually poikilitic with round inclusions of quartz, apatite, opaque oxides & sphene, and altered plagioclase. Porphyroclastic garnets (1mm to 2.5mm) are slightly altered by chlorite (54), are rare in inclusions or inclusion-free, and contrast with coarser garnets that are hypidiomorphic and poikilitic with rounded inclusions of quartz,

rutile? (inherited from previous granulite facies metamorphism?) or sphene, apatite, plagioclase, and rare amphibole? Foliation is preserved in garnet. Most of the plagioclase is lightly saussuritised (25) and a few grains are patched with cloudy areas. Quartz tends to form aggregates around garnets and also in the matrix. Zircon and monazite? may be present as accessory minerals. Considering the assemblage, the rock was retrogressed to the epidote/amphibolite facies with chlorite and epidote in ( $T^{\circ} < 550^{\circ}\text{C}$ ,  $P < 3.3 \text{ kbar}$ ) (17, 26, 41).

Mineral assemblage and possible reactions:

- 17) 3 Fe-tremolite + 6 anorthite + 3 albite  $\leftarrow$  3 Fe-pargasite + almandine + 2 grossular + 18 quartz  
 25) 2 zoisite  $\leftarrow$  3 anorthite + Ca(OH)<sub>2</sub>  
 26) albite + zoisite  $\leftarrow$  oligoclase + fluid  
 41) 3 chlorite + 6 epidote  $\leftarrow$  tschermakite + 2 anorthite + 10 fluid  
 54) 3 quartz + 3 chlorite + 3 anorthite  $\leftarrow$  grossular + 5 pyrope + 12 fluid



**P166: Retrogressed anatectic garnet vein**Modal composition:

plagioclase	35%
garnet	15%
quartz	15%
K feldspar	15%
bluish to green amphibole	10%
zoisite	5%
biotite	2%
chlorite	2%
epidote	1%
white mica	trace
opaque oxides	trace
sphene	trace

The sample comes from an heterogeneous diorite with skarn enclaves. It is deformed, as shown in the thin section by undulatory extinction of quartz, kinked twins in plagioclase and by a 7 mm wide plagioclase porphyroclast, surrounded by small euhedral garnet mixed with elongated ferroan pargasites, zoisites (25, 26), quartz, biotite? or hematite and opaque oxides. Acicular chlorite and biotite (from breakdown of primary hornblende? or hematite) , are alteration products of hornblende and garnet (24, 41, 49, 51). Ferro-magnesian minerals are concentrated around the plagioclase porphyroclast giving an augen texture. Euhedral garnets also occur as

aggregates with interstitial biotite (52). They are inclusions-free, except for coarser grains that have a few K feldspar? and quartz inclusions. Coarse grained plagioclases and K feldspar grains form the matrix and heterogeneously saussuritised plagioclase (25) may be slightly cloudy. Contact boundaries between the two and with quartz are lobate. The latter forms aggregates between plagioclase and K feldspar. Considering the assemblage, the rock was retrogressed to the epidote/amphibolite facies with chlorite and epidote in ( $T^{\circ} < 550^{\circ}\text{C}$ ,  $P < 3.3 \text{ kbar}$ ) (17).

Mineral assemblage and possible reactions:

- 17)  $3 \text{ Fe-tremolite} + 6 \text{ anorthite} + 3 \text{ albite} \leftarrow 3 \text{ Fe-pargasite} + \text{almandine} + 2 \text{ grossular} + 18 \text{ quartz}$
- 24)  $54 \text{ clinozoisite} + 3 \text{ tremolite} \leftarrow 5 \text{ pyrope} + 19 \text{ grossular} + 57 \text{ anorthite} + 30 \text{ fluid}$
- 25)  $2 \text{ zoisite} \leftarrow 3 \text{ anorthite} + \text{Ca(OH)}_2$
- 26)  $\text{albite} + \text{zoisite} \leftarrow \text{oligoclase} + \text{fluid}$
- 41)  $3 \text{ chlorite} + 6 \text{ epidote} \leftarrow \text{tschermakite} + 2 \text{ anorthite} + 10 \text{ fluid}$
- 49)  $\text{chlorite} + \text{quartz} + \text{CaO} \leftarrow \text{hornblende} + \text{anorthite}$
- 51)  $\text{Fe-chlorite} + \text{orthoclase} + \text{K}^+ \leftarrow \text{annite} + 2 \text{ fluid}$
- 52)  $\text{diopside} + \text{chlorite} + 2 \text{ anorthite} \leftarrow \text{grossular} + 2 \text{ pyrope} + 4 \text{ fluid}$

P570: Garnet epidote amphibolite

TYPE

Modal composition:

epidote	35%
blue-green amphibole	25%
zoisite, clinozoisite	15%
garnet	15%
chlorite	10%
opaque oxides, sphene	trace
monazite	trace

The rock has undergone strong retrograde metamorphism as shown by the heterogeneous distribution of minerals, mostly poikiloblastic and symplectitic. Hypidiomorphic garnets, poor in inclusions, are kelyphitic, and are surrounded by chlorite-epidote-amphibole symplectites (24, 25, 26, 41). Rare inclusions are epidote, and rutile. Cracks in garnet are filled by chlorite. Nematoblastic epidote is not oriented. Amphibole

is poikilitic with quartz inclusions, or altered by epidote or zoisite along cleavages (19, 25, 30). The rock has undergone epidote/amphibolite facies metamorphism, with chlorite and epidote in ( $T^{\circ} < 550^{\circ}\text{C}$ ,  $P < 3.3 \text{ kbar}$ ).

Mineral assemblage and possible reactions:

- 19) tremolite + albite + anorthite  $\leftarrow$  pargasite + diopside + 5 quartz
- 24) 54 clinozoisite + 3 tremolite  $\leftarrow$  5 pyrope + 19 grossular + 57 anorthite + 30 fluid
- 25) 2 zoisite  $\leftarrow$  3 anorthite +  $\text{Ca}(\text{OH})_2$
- 26) albite + zoisite  $\leftarrow$  oligoclase + fluid
- 30) zoisite + quartz  $\leftarrow$  anorthite + fluid
- 41) 3 chlorite + 6 epidote  $\leftarrow$  tschermakite + 2 anorthite + 10 fluid

**P572: Garnet "granulite"?**Modal composition:

garnet	45%
clinopyroxene	20%
plagioclase	15%
green amphibole	10%
orthopyroxene	5%
quartz	3%
opaque oxides & rutile	2%
zoisite, chlorite	trace

Augen-shaped clusters of orthopyroxene, clinopyroxene, green amphibole occur in this heterogranular garnet granulite. Pyroxenes are superimposed by Schiller plates which are indicative of a magmatic texture. A fine grained layer is richer in opaque oxides & rutile and poorer in plagioclase. Euhedral, 1mm to 2.5mm garnets have rounded inclusions of amphibole, clinopyroxene, quartz, opaque oxides and rutile. Cracks are filled with chlorite (52, 54) that also

occurs between garnet grains. The absence of quartz forming along garnet grains suggests that the latter are of primary magmatic origin. Coarser plagioclases are saussuritised and cloudy (25), but a few fresh grains can be found in contact with garnet and clinopyroxene. Symplectitic amphibole and zoisite surround plagioclase (15, 16, 19, 26). Contact boundaries are usually straight with a mesocumulate texture.

Mineral assemblage and possible reactions:

- 15)  $3 \text{ pargasite} + 12 \text{ anorthite} + 18 \text{ diopside} \leftarrow 3 \text{ tremolite} + 5 \text{ pyrope} + 10 \text{ grossular} + 3 \text{ albite}$
- 16)  $3 \text{ tremolite} + 6 \text{ anorthite} + 3 \text{ albite} \leftarrow 3 \text{ pargasite} + 2 \text{ grossular} + \text{pyrope} + 18 \text{ quartz}$
- 19)  $\text{tremolite} + \text{albite} + \text{anorthite} \leftarrow \text{pargasite} + \text{diopside} + 5 \text{ quartz}$
- 25)  $2 \text{ zoisite} \leftarrow 3 \text{ anorthite} + \text{Ca(OH)}_2$
- 26)  $\text{albite} + \text{zoisite} \leftarrow \text{oligoclase} + \text{fluid}$
- 52)  $\text{diopside} + \text{chlorite} + 2 \text{ anorthite} \leftarrow \text{grossular} + 2 \text{ pyrope} + 4 \text{ fluid}$
- 54)  $3 \text{ quartz} + 3 \text{ chlorite} + 3 \text{ anorthite} \leftarrow \text{grossular} + 5 \text{ pyrope} + 12 \text{ fluid}$

**P573: Garnet granulite**

Modal composition:

plagioclase	47%
garnet	20%
clinopyroxene	20%
green edenite	8%
quartz	3%
opaque oxides & rutile	2%
K feldspar	trace

Heterogranular, granoblastic texture with slightly coarser fresh plagioclase and garnet grains. Grain boundaries between plagioclase and K feldspar are straight to locally embayed. Deformation and mechanical twins occur in plagioclase. Garnets are poikiloblastic and hypidiomorphic. Inclusions in garnet are of quartz, clinopyroxene, opaque oxides, rutile, and plagioclase. Garnets may be embayed when

in contact with clinopyroxene (1) or oxides. The latter also crystallized at triple junctions. Quartz is concentrated along garnet boundaries. Clinopyroxene and green edenite form aggregates that tend to define a preferred orientation (14, 18, 19). Traces of zoisite symplectites with quartz (30) or albite (26) occur locally, as well as chlorite filling garnet cracks (54). Textural features show that the sample must have reached equilibrium. Negligable post-amphibolite facies retrograde alteration traces may appear but are not taken into account, considering the freshness of the assemblage. Thus, consistent thermodynamic data of the granulite/upper amphibolite facies metamorphism may be expected from this sample.

Mineral assemblage and possible reactions:

- 1) 3 anorthite+ 6 diopside → 2 grossular + pyrope + 3 quartz
- 14) tremolite + albite → edenite + quartz
- 18) tremolite + 2 anorthite → tschermakite + 2 diopside + 2 quartz
- 19) tremolite + albite + anorthite → pargasite + diopside + 5 quartz
- 26) albite + zoisite ← oligoclase + fluid
- 30) zoisite + quartz ← anorthite + fluid
- 54) 3 quartz + 3 chlorite + 3 anorthite ← grossular + 5 pyrope + 12 fluid

**P574: Garnet "granulite"**

Modal composition:

garnet	35%
plagioclase	20%
green amphibole	15%
quartz	15%
clinopyroxene	14%
opaque oxides & rutile	1%
zoisite and epidote	trace
orthopyroxene	??

Mineral distribution is heterogeneous with relatively coarser garnets that reach up to 6mm wide. Clinopyroxene and amphibole tend to form aggregates between hypidiomorphic garnets and plagioclase + quartz. Euhedral, smaller metamorphic garnets occur in the aggregates (1, 15). Therefore, the sample has a coarse heterogranular texture. Alteration is present (chlorite filling garnet cracks, zoisite symplectites, trace of epidote) (26, 41, 43).

Garnet in contact with quartz has embayed boundaries. It contains rounded inclusions of clinopyroxene, quartz, and green amphibole. Rutile and opaque oxide inclusions occur in hornblende. Opaque oxides & rutile also developed at 3-grain intersections. Plagioclase is fresh and has deformation twins. A second generation of clinopyroxene and amphibole may be present (15) but as smaller grains in comparison with clinopyroxene or amphibole grains of the first generation.

Mineral assemblage and possible reactions:

- 1) 3 anorthite+ 6 diopside → 2 grossular + pyrope + 3 quartz
- 15) 3 pargasite + 12 anorthite + 18 diopside → 3 tremolite + 5 pyrope + 10 grossular + 3 albite
- 26) albite + zoisite ← oligoclase + fluid
- 41) 3 chlorite + 6 epidote ← tschermakite + 2 anorthite + 10 fluid
- 43) 3 chlorite + 12 Al-epidote + 4 quartz ← 10 tsch-hornblende + 4 anorthite + 2 fluid

**P576: Garnet granulite with diffuse veinlet of clinopyroxene garnetite**Modal composition:

garnet	55%
green hornblende	16%
plagioclase	12%
clinopyroxene	10%
scapolite	5%
zoisite, epidote	2%
chlorite	trace
rutile	trace
quartz	trace

At thin section scale, patches instead of veinlets of clinopyroxene-garnetite are observed and may be attributed to the diffuse appearance of the veinlets. Distribution of minerals is therefore heterogeneous, as plagioclase is not found in the veinlets. The granoblastic texture is more pronounced in the host rock as garnet in contact with plagioclase has straight boundaries. In contrast, garnet is embayed when next to clinopyroxene or hornblende which clearly show a reaction in progress (8). (This observation is

also valid for the veinlet). Symplectites of epidote + albite, and zoisite + albite? (26, 41, 42, 48, 49) occur locally between garnet and hornblende. Plagioclase is fresh but may be locally saussuritised (25, 26) and/or cloudy. Poikiloblastic garnets of the veinlet are relatively coarser but hypidiomorphic. Coarser inclusions are of clinopyroxene, hornblende, quartz, and rutile. Inclusions of a few microns are very common and usually define trails or sheaf-like patterns. Scapolite is altered by epidote (27). Alteration in garnet by chlorite is common (54).

Mineral assemblage and possible reactions:

- 8)  $6 \text{ tremolite} + 7 \text{ grossular} \leftarrow 27 \text{ diopside} + 6 \text{ anorthite} + \text{pyrope} + 6 \text{ fluid}$
- 25)  $2 \text{ zoisite} \leftarrow 3 \text{ anorthite} + \text{Ca(OH)}_2$
- 26)  $\text{albite} + \text{zoisite} \leftarrow \text{oligoclase} + \text{fluid}$
- 27)  $2 \text{ epidote} + \text{CO}_2 \leftarrow \text{meionite} + \text{fluid}$
- 41)  $3 \text{ chlorite} + 6 \text{ epidote} \leftarrow \text{tschermakite} + 2 \text{ anorthite} + 10 \text{ fluid}$
- 42)  $6 \text{ epidote} + \text{chlorite} + 7 \text{ quartz} \leftarrow \text{actinolite} + 10 \text{ anorthite} + 6 \text{ fluid}$
- 48)  $\text{chlorite} + \text{actinolite} \leftarrow \text{hornblende} + \text{anorthite}$
- 49)  $\text{chlorite} + \text{quartz} + \text{CaO} \leftarrow \text{hornblende} + \text{anorthite}$
- 54)  $3 \text{ quartz} + 3 \text{ chlorite} + 3 \text{ anorthite} \leftarrow \text{grossular} + 5 \text{ pyrope} + 12 \text{ fluid}$

**P577: Garnet "granulite", garnet gabbro**Modal composition:

garnet	45%
pale green pargasite	20%
plagioclase	15%
clinopyroxene	10%
zoisite	5%
quartz	3%
epidote, chlorite	1%
opaque oxides & rutile	1%
calcite?	

In thin section, the sample is heterogranular with garnets (or garnet aggregates) of 1 mm to 15 mm. Small garnets tend to be euhedral, whereas coarser ones are poikilitic with inclusions of clinopyroxene, pargasite, rutile, and quartz. Inclusions of a few microns, sometimes defining rows, also appear in garnet. Boundaries are straight in contact with plagioclase, but tend to be curved or embayed when in contact with clinopyroxene or pargasite (1, 8, 15). Garnets

are altered by chlorite and epidote filling the cracks and at grain boundaries (29, 54). Plagioclase is usually fresh with deformation twins but grains may be locally severely saussuritised (25, 26) and cloudy as a result of local fluid circulation. Epidote may have crystallized at grain boundaries (41). Epidote and quartz symplectites also occur along plagioclase grains (30).

**P577a: Plagioclase-free zone of P577 "garnet granulite"**Modal composition:

garnet	55%
pale green amphibole	20%
clinopyroxene	24%
rutile	1%
quartz	trace

Garnets have embayed boundaries when in contact with clinopyroxene. Small euhedral neoblasts of garnet can be included in clinopyroxene, but clinopyroxene inclusions also occur in garnet. Textural evidence shows that garnet may grow simultaneously with clinopyroxene, suggesting possible solidus assemblage from a high-P garnet gabbro.

Mineral assemblage and possible reactions:

- 1) 3 anorthite + 6 diopside → 2 grossular + pyrope + 3 quartz
- 8) 6 tremolite + 7 grossular ← 27 diopside + 6 anorthite + pyrope + 6 fluid
- 15) 3 pargasite + 12 anorthite + 18 diopside ← 3 tremolite + 5 pyrope + 10 grossular + 3 albite
- 25) 2 zoisite ← 3 anorthite + Ca(OH)<sub>2</sub>
- 26) albite + zoisite ← oligoclase + fluid
- 29) amphibole + epidote ← garnet + fluid
- 30) zoisite + quartz ← anorthite + fluid
- 41) 3 chlorite + 6 epidote ← tschermakite + 2 anorthite + 10 fluid
- 54) 3 quartz + 3 chlorite + 3 anorthite ← grossular + 5 pyrope + 12 fluid

## GI 10: Garnet granulite

### Modal composition:

garnet	60%
clinopyroxene	25%
K feldspar or plagioclase?	10%
pargasite	5%
apatite	trace
opaque oxides	trace

Garnet size at thin section scale is hard to evaluate because garnet crystallized in grains up to a few cm across from surrounding minerals like primary clinopyroxene, K feldspar, and pargasite, in a diablastic texture (**1, 15: cpx1**). Therefore, large anhedral and rounded inclusions of these minerals are numerous in garnet.

Minerals are heterogeneously distributed because

fresh clinopyroxene-rich zones appear in the thin section. Secondary pyroxene and garnet symplectites form in contact with amphibole grains (**8: cpx2**). Opaque minerals are also concentrated in these zones. Minerals are generally hypidiomorphic in a granoblastic texture. The assemblage and textures suggest a clinopyroxene + plagioclase protolith that has undergone granulite facies metamorphism.

### Mineral assemblage and possible reactions:

- 1) 3 anorthite + 6 diopside → 2 grossular + pyrope + 3 quartz
- 8) 6 tremolite + 7 grossular → 27 diopside + 6 anorthite + pyrope + 6 fluid
- 15) 3 pargasite + 12 anorthite + 18 diopside → 3 tremolite + 5 pyrope + 10 grossular + 3 albite



## GI 11: Garnet and epidote amphibolite

### Modal composition:

green hornblende	25%
garnet	20%
epidote	20%
plagioclase	15%
zoisite	10%
quartz	7%
white mica	3%
opaque oxides	trace

The sample shows a preferred orientation defined by poikilitic elongated green hornblende and zoisite grains (30). Both contain rounded quartz and epidote inclusions (28), with superimposed white mica needles (31, 34). Porphyroblastic garnets are heterogeneously distributed in the thin section. They are porphyroblastic to poikiloblastic with irregular sized inclusions of quartz, opaque oxides and rutile, poikiloblastic hornblende, apatite, and plagioclase. Opaque

oxides & rutile may be surrounded by hornblende. Plagioclase grains are fresh but masked by superimposed epidote and acicular white mica (32, 36). The latter might have formed after deformation, because they are not oriented. Quartz forms aggregates with serrated boundaries that concentrate between garnets and embay them (relic textures of 1, 14, 17). Assemblage and textures suggest an epidote-amphibolite facies rock that was slightly deformed during metamorphism.

### Mineral assemblage and possible reactions:

- 1)  $3 \text{ anorthite} + 6 \text{ diopside} \rightarrow 2 \text{ grossular} + \text{pyrope} + 3 \text{ quartz}$
- 14)  $\text{tremolite} + \text{albite} \leftarrow \text{edenite} + \text{quartz}$
- 17)  $3 \text{ Fe-tremolite} + 6 \text{ anorthite} + 3 \text{ albite} \leftarrow 3 \text{ Fe-pargasite} + \text{almandine} + 2 \text{ grossular} + 18 \text{ quartz}$
- 28)  $\text{hornblende} + \text{epidote} + \text{quartz} \leftarrow \text{clinopyroxene} + \text{plagioclase} + \text{fluid}$
- 30)  $\text{zoisite} + \text{quartz} \leftarrow \text{anorthite} + \text{fluid}$
- 31)  $4 \text{ zoisite} + \text{quartz} \leftarrow 5 \text{ anorthite} + \text{grossular} + 2 \text{ fluid}$
- 32)  $\text{paragonite} + 2 \text{ quartz} + 2 \text{ zoisite} \leftarrow 4 \text{ anorthite} + \text{albite} + 2 \text{ fluid}$
- 34)  $4 \text{ grossular} + 5 \text{ paragonite} + 6 \text{ quartz} \leftarrow 6 \text{ zoisite} + 5 \text{ albite} + 2 \text{ fluid}$
- 36)  $4 \text{ quartz} + \text{spinel} + 4 \text{ zoisite} \leftarrow \text{diopside} + 7 \text{ anorthite} + 2 \text{ fluid}$

## GI 11a: Garnet-zoisite amphibolite

### Modal composition:

green hornblende	30%
garnet	20%
plagioclase (& K feldspar)	20%
zoisite, clinozoisite?	18%
quartz	10%
white mica	2%
epidote	trace
opaque oxides & rutile	trace
monazite?	

Compared with **GI 11**, this sample seems less deformed, in spite of the tendency for zoisite and hornblende to be rearranged in oriented elongated crystals. Note also the quasi-absence of epidote and the larger amount of zoisite (**31**). Garnet is more homogeneously distributed. It may be embayed by quartz that usually concentrates along garnet boundaries, but also by poikilitic hornblende. Some neoblasts of hornblende and zoisite are poikilitic which include quartz grains, or are free of inclusions (**17, 30**). Zoisite may

also form symplectites with albite (**26**). Unoriented white mica needles concentrate on plagioclase (**32**). The latter is also superimposed by zoisite (**31**), but still remains fresh. The metamorphic facies of the rock is epidote-amphibolite.

### Mineral assemblage and possible reactions:

- 17)  $3 \text{ Fe-tremolite} + 6 \text{ anorthite} + 3 \text{ albite} \leftarrow 3 \text{ Fe-pargasite} + \text{almandine} + 2 \text{ grossular} + 18 \text{ quartz}$
- 26)  $\text{albite} + \text{zoisite} \leftarrow \text{oligoclase} + \text{fluid}$
- 30)  $\text{zoisite} + \text{quartz} \leftarrow \text{anorthite} + \text{fluid}$
- 31)  $4 \text{ zoisite} + \text{quartz} \leftarrow 5 \text{ anorthite} + \text{grossular} + 2 \text{ fluid}$
- 32)  $\text{paragonite} + 2 \text{ quartz} + 2 \text{ zoisite} \leftarrow 4 \text{ anorthite} + \text{albite} + 2 \text{ fluid}$

## GI 11b: Garnet "granulite", garnet gabbro

### Modal composition:

plagioclase	45%
garnet	30%
amphibole	10%
quartz	8%
clinopyroxene	6%
zoisite	1%
opaque oxides and rutile	trace
apatite	trace

Hypidioblastic garnets have straight boundaries when in contact with plagioclase but may be lobated, embayed or even hollow when in contact with interstitial quartz neoblasts and clinopyroxene or hornblende (1, 15). They may contain rounded inclusions of quartz, amphibole, opaque oxides, rutile, and plagioclase. The latter is heterogranular with deformation twins, and may be fresh or partly saussuritised (25) and/or cloudy. Boundaries

are lobate except when in contact with garnet, which gives usually an anhedral shape to the grains. Pyroxenes may be altered (7, 30, 44) and mostly anhedral. Predominant texture is granoblastic with coarse grained zones, which tend to define a preferred orientation.

### Mineral assemblage and possible reactions:

- 1)  $3 \text{ anorthite} + 6 \text{ diopside} \rightarrow 2 \text{ grossular} + \text{pyrope} + 3 \text{ quartz}$
- 7)  $4 \text{ tremolite} + 3 \text{ anorthite} \leftarrow 3 \text{ pyrope} + 11 \text{ diopside} + 7 \text{ quartz} + 4 \text{ fluid}$
- 15)  $3 \text{ pargasite} + 12 \text{ anorthite} + 18 \text{ diopside} \rightarrow 3 \text{ tremolite} + 5 \text{ pyrope} + 10 \text{ grossular} + 3 \text{ albite}$
- 25)  $2 \text{ zoisite} \leftarrow 3 \text{ anorthite} + \text{Ca(OH)}_2$
- 30)  $\text{zoisite} + \text{quartz} \leftarrow \text{anorthite} + \text{fluid}$
- 44)  $\text{chlorite} + \text{epidote} \leftarrow \text{Al-amphibole}$

### GI 13: Garnet "granulite", garnet gabbro

#### Modal composition:

plagioclase, K feldspar	40%
garnet	35%
clinopyroxene, opx?	15%
quartz	8%
amphibole	2%
opaque oxides & rutile	trace

Mineral distribution is quite homogeneous although plagioclase tends to be coarser and clinopyroxene, quartz, amphibole and rutile usually surround garnets. The latter are euhedral to anhedral when embayed by quartz, but very altered. Rounded inclusions of quartz (1), rutile, plagioclase and clinopyroxene occur in garnets. Plagioclases are hypidiomorphic with lobate

boundaries. They may be partly saussuritised (25) and/or cloudy. Orthopyroxenes (?) are slightly pleochroic to pale pink. Rutile may be included in amphibole with surrounding quartz (?). In general, minerals are not very fresh and are severely cracked.

#### Mineral assemblage and possible reactions:

- 1) 3 anorthite + 6 diopside  $\rightarrow$  2 grossular + pyrope + 3 quartz  
 25) 2 zoisite  $\leftarrow$  3 anorthite + Ca(OH)<sub>2</sub>

### GI 18: Amphibole, garnet and plagioclase cumulate

#### Modal composition:

garnet	40%
green to blue amphibole	30%
plagioclase & K feldspar	20%
quartz	5%
magnetite	3%
epidote	2%
zoisite	trace
apatite	trace
rutile	trace

At thin section scale, the sample is divisible into amphibole, garnet and plagioclase layers; these are most likely magmatic cumulate layers. This assumption is also reinforced by the presence of apatite in the rock. The "amphibole" layer is granoblastic with equigranular, pleochroic, dark green to blue, ferroan pargasite and ferroan-pargasitic hornblende grains that tend to be elongated, defining a preferred orientation. Rare epidote and plagioclase grains occur at triple junctions (20, 26). The latter are fresh but may

include round inclusions of epidote. Magnetite is abundant, and tends to agglomerate to form elongated neoblasts parallel to the layering. Some larger elongated neoblasts may be poikiloblastic with inclusions of amphibole and rare rutile.

The contact between the "amphibole" and "garnet" layers is very well defined and tends to be straight. Elongated neoblasts of magnetite occur systematically along the contact border.

Garnets of the diablastic "garnet" layer are poikiloblastic and contain inclusions of hornblende, plagioclase, quartz, zoisite, epidote and magnetite. The latter is abundant and defines layers parallel to the amphibole, garnet and plagioclase layers, but with a weaker tendency to agglomerate. Hence, they are hypidiomorphic to euhedral. To a lesser extent, they tend to form along old garnet grain boundaries. Alteration by chlorite associated with magnetite is present but heterogeneous (57). Therefore, plagioclase inclusions may be fresh or cloudy.

The contact between the "garnet" and "plagioclase" layers is gradual as euhedral neoblasts of garnet are gradually but heterogeneously dispersed into the "plagioclase" layer. The garnets neoblasts tend to be free of inclusions but may be associated with altered amphibole (17, 29) and magnetite when they are part of small aggregates.

The "plagioclase" layer also includes quartz in a quasi-equigranular texture. Grains are usually hypidiomorphic to euhedral but may have serrated or embayed boundaries. They may be locally saussuritised (25) but are usually very fresh. Scarse aggregates are of anhedral magnetite grains and hornblende.

#### Mineral assemblage and possible reactions:

- 17)  $3 \text{ Fe-tremolite} + 6 \text{ anorthite} + 3 \text{ albite} \rightarrow 3 \text{ Fe-pargasite} + \text{almandine} + 2 \text{ grossular} + 18 \text{ quartz}$
- 20)  $\text{Fe-tremolite} + \text{albite} + \text{anorthite} \leftarrow \text{Fe-pargasite} + \text{hedenbergite} + 5 \text{ quartz}$
- 25)  $2 \text{ zoisite} \leftarrow 3 \text{ anorthite} + \text{Ca(OH)}_2$
- 26)  $\text{albite} + \text{zoisite} \leftarrow \text{oligoclase} + \text{fluid}$
- 29)  $\text{amphibole} + \text{epidote} \leftarrow \text{garnet} + \text{fluid}$
- 57)  $6 \text{ Fe-pargasite} + 3 \text{ quartz} + 24 \text{ hematite} + \text{chlorite} \leftarrow 6 \text{ albite} + 7 \text{ anorthite} + 5 \text{ diopside} + 24 \text{ magnetite} +$
- 10  $\text{fluid}$

## K27: Amphibolite crosscut by a garnet granite vein

### Modal composition:

K feldspar and plagioclase	60%
green hornblende	25%
garnet	7%
quartz	5%
chlorite	2%
opaque oxides and rutile	1%
clinopyroxene	trace
epidote	trace
calcite	trace

A 1.5cm "granitic" vein of K feldspar, plagioclase, quartz, and garnet crosscuts the green hornblende-plagioclase-quartz host rock, which is altered by chlorite (forming also veinlets) (44, 48, 49). Hornblende tends to form aggregates and may be poikilitic and anhedral with quartz and opaque oxides and rutile inclusions, or hypidiomorphic and free of inclusions. Quartz appears as neoblasts with lobate to serrate boundaries (49). Plagioclase and K feldspar are slightly saussuritised (25) and may have deformation twins.

In the vein, K feldspar and plagioclase are coarser (up to 4 mm wide) but still slightly altered (25). Garnets are anhedral and strongly altered by chlorite (54) and cracked. Rutile may be present where chlorite and opaque oxides are in contact. Contact borders of the vein tend to be straight and are related to the major change in grain size of plagioclases and K feldspars, which are much coarser in the vein. Calcite, quartz, plagioclase? and epidote occur in 0.5 mm wide veinlets that crosscut the previous assemblages.

### Mineral assemblage and possible reactions in the host rock:

- 25)  $2 \text{ zoisite} \leftarrow 3 \text{ anorthite} + \text{Ca(OH)}_2$
- 44)  $\text{chlorite} + \text{epidote} \leftarrow \text{Al-amphibole}$
- 48)  $\text{chlorite} + \text{actinolite} \leftarrow \text{hornblende} + \text{anorthite}$
- 49)  $\text{chlorite} + \text{quartz} + \text{CaO} \leftarrow \text{hornblende} + \text{anorthite}$

### Mineral assemblage and possible reactions in the vein:

- 25)  $2 \text{ zoisite} \leftarrow 3 \text{ anorthite} + \text{Ca(OH)}_2$
- 54)  $3 \text{ quartz} + 3 \text{ chlorite} + 3 \text{ anorthite} \leftarrow \text{grossular} + 5 \text{ pyrope} + 12 \text{ fluid}$

## KI 16: Garnet granulite (partly retrogressed to amphibolite facies)

### Modal composition:

garnet	55%
pale green amphibole	13%
clinopyroxene	10%
plagioclase	10%
zoisite, clinozoisite?	8%
chlorite	2%
epidote	1%
quartz, rutile	1%
apatite	trace

A heterogeneous distribution of minerals except for garnet in thin section clearly shows a "zoned" cumulate texture. The first zone is characterized by hypidiomorphic to euhedral garnets, and clinopyroxene assemblage, with a granoblastic texture. Contact boundaries between garnet and pyroxenes are locally serrated. Chlorite surrounds a few grains.

A second zone consists of the same assemblage combined with amphibole and zoisite. It is therefore suggests that part of the rock has

undergone amphibolite facies retrogression (8, 28, 45, 50). Garnets are still euhedral with rare inclusions of clinopyroxene, rutile, apatite and quartz. Zoisite can be acicular, symplectitic with albite (26) and amphiboles (+ rare white mica) or pseudomorphous after plagioclase (30). Acicular chlorite also appears as an alteration phase and is more developed filling cracks in garnet (54). Pyroxenes have reaction rims of quartz when in contact with garnet (1). Contact borders with amphiboles are clearly defined. Altered pyroxenes may be altered by chlorite along their cleavages (55).

A third zone is characterized by its relatively high content of coarse plagioclase, and zoisite symplectites (26). Rare quartz grains occur between garnet and plagioclase. The latter is saussuritised (25) and heterogeneously cloudy.

The rock therefore is heterogranular with a holocrystalline mesocumulate-type texture.

### Mineral assemblage and possible reactions:

- 1)  $3 \text{ anorthite} + 6 \text{ diopside} \rightarrow 2 \text{ grossular} + \text{pyrope} + 3 \text{ quartz}$
- 8)  $6 \text{ tremolite} + 7 \text{ grossular} \leftarrow 27 \text{ diopside} + 6 \text{ anorthite} + \text{pyrope} + 6 \text{ fluid}$
- 25)  $2 \text{ zoisite} \leftarrow 3 \text{ anorthite} + \text{Ca(OH)}_2$
- 26)  $\text{albite} + \text{zoisite} \leftarrow \text{oligoclase} + \text{fluid}$
- 28)  $\text{hornblende} + \text{epidote} + \text{quartz} \leftarrow \text{clinopyroxene} + \text{plagioclase} + \text{fluid}$
- 30)  $\text{zoisite} + \text{quartz} \leftarrow \text{anorthite} + \text{fluid}$
- 45)  $\text{chlorite} + \text{quartz} + \text{CaO} \leftarrow \text{actinolitic hornblende} + \text{epidote}$
- 50)  $\text{actinolite} + \text{chlorite} + 11 \text{ quartz} + 9 \text{ CaO} \leftarrow 10 \text{ pyroxene} + \text{anorthite} + 5 \text{ fluid}$
- 54)  $3 \text{ quartz} + 3 \text{ chlorite} + 3 \text{ anorthite} \leftarrow \text{grossular} + 5 \text{ pyrope} + 12 \text{ fluid}$
- 55)  $\text{anorthite} + 2 \text{ chlorite} + 3 \text{ quartz} \leftarrow 3 \text{ pyrope} + \text{diopside} + 8 \text{ fluid}$

**KI 153: Garnet-plagioclase granulite (vein?)**Assemblage:

garnet	30%
plagioclase	25%
clinopyroxene	20%
green hornblende	15%
quartz	10%
rutile	trace

This garnet-plagioclase granulite appears to be a 4.5 cm wide vein that crosscuts a green plagioclase-free clinopyroxene-hornblende assemblage. Contact between the two is irregular without appearance of contact metamorphism. Nevertheless, these assumptions cannot be conclusive because a larger sample would have been necessary to define the geological setting.

The main texture of the granulite is heterogranular with clinopyroxene-hornblende-quartz forming aggregates between coarser garnet and plagioclase grains. The latter are cloudy and saussuritised (25) but a few relatively fresh grains can be found. Garnet tends to agglomerate in a diablastic-like texture as crystal growth proceeds between the grains (8). Contact boundaries with plagioclase are straight, whereas garnets are embayed when in contact with clinopyroxene or hornblende (1, 7). Irregular-shaped coarse inclusions are numerous and are of rutile, clinopyroxene, hornblende, and quartz.

Clinopyroxene and hornblende grains of the "green" rock are hypidiomorphic with quartz forming round neoblasts at grain boundaries (from 18?). Mineral assemblage and textures suggest an overprint of amphibolite facies metamorphism on previous granulite facies assemblage.

Mineral assemblage and possible reactions:

- 1)  $3 \text{ anorthite} + 6 \text{ diopside} \leftarrow 2 \text{ grossular} + \text{pyrope} + 3 \text{ quartz}$
- 7)  $4 \text{ tremolite} + 3 \text{ anorthite} \leftarrow 3 \text{ pyrope} + 11 \text{ diopside} + 7 \text{ quartz} + 4 \text{ fluid}$
- 8)  $6 \text{ tremolite} + 7 \text{ grossular} \leftarrow 27 \text{ diopside} + 6 \text{ anorthite} + \text{pyrope} + 6 \text{ fluid}$
- 18)  $\text{tremolite} + 2 \text{ anorthite} \rightarrow \text{tschermakite} + 2 \text{ diopside} + 2 \text{ quartz}$
- 25)  $2 \text{ zoisite} \leftarrow 3 \text{ anorthite} + \text{Ca(OH)}_2$



**KI 158: Garnet granulite****TYPICAL SUB-SOLIDUS**Modal composition:

plagioclase (K-Feldspar)	50%
garnet	35%
green amphibole	5%
clinopyroxene	4%
quartz	3%
orthopyroxene	2%
opaque oxides & rutile	1%
biotite	trace

The sample is heterogranular and minerals tend to be oriented. The mineral distribution is heterogeneous. Hence, garnet-poor zones contain coarser K feldspar and plagioclase with elongated relict orthopyroxene sometimes altered by biotite? and surrounded by opaque oxides and amphibole reaction corona (9, 10). Orthopyroxene is pleochroic from yellowish brown to pink. Some garnets are especially poikiloblastic with quartz, but many contain amphibole, clinopyroxene and

rutile. Garnets locally form coronas surrounding clinopyroxene grains (8). Hollow garnets to atoll garnets are filled with growth-mosaic substructured quartz. On the other hand, most garnets are symplectitic with quartz and are euhedral (1). Quartz appears as neoblasts, strongly associated with garnet. Plagioclase is fresh or hardly saussuritised (25) at grain boundaries. Deformation twins can be seen, as well as undulatory extinction in K feldspar and quartz. Traces of biotite occur around opaque oxide grains.

Mineral assemblage and possible reactions:

- 1)  $3 \text{ anorthite} + 6 \text{ diopside} \rightarrow 2 \text{ grossular} + \text{pyrope} + 3 \text{ quartz}$
- 8)  $6 \text{ tremolite} + 7 \text{ grossular} \leftarrow 27 \text{ diopside} + 6 \text{ anorthite} + \text{pyrope} + 6 \text{ fluid}$
- 9)  $\text{cummingtonite} \leftarrow 7 \text{ orthopyroxene} + \text{quartz} + \text{fluid}$
- 10)  $\text{biotite} + 3 \text{ quartz} \leftarrow \text{orthoclase} + 3 \text{ orthopyroxene} + \text{fluid}$
- 25)  $2 \text{ zoisite} \leftarrow 3 \text{ anorthite} + \text{Ca(OH)}_2$

**KI 189: Garnet hornblendite**Modal composition:

bluish-green hornblende	51%
garnet	25%
zoisite	15%
epidote, chlorite	5%
sphene	3%
opaque oxides	1%
apatite, zircon	trace
quartz	trace

Heterogranular grains tend to show a preferred orientation due to hornblende. Chlorite alteration occurs between the grains as well as filling the cracks in anhedral garnets (54). The latter have rare inclusions of quartz. Rare quartz neoblasts only occur in contact with garnet and hornblende (17, 30). Epidote replaces garnet (29), or is a pseudomorph of plagioclase (twinning relics sometimes remain) (26). Zoisite-epidote, and chlorite alteration

(44) superimpose previous garnet-hornblende-(plagioclase-quartz?) assemblage. Zoisite sometimes has undergone dendritic crystallization. The rock is titanium-rich, with coarse sphene grains.

Mineral assemblage and possible reactions:

- 17)  $3 \text{ Fe-tremolite} + 6 \text{ anorthite} + 3 \text{ albite} \leftarrow 3 \text{ Fe-pargasite} + \text{almandine} + 2 \text{ grossular} + 18 \text{ quartz}$
- 26)  $\text{albite} + \text{zoisite} \leftarrow \text{oligoclase} + \text{fluid}$
- 29)  $\text{amphibole} + \text{epidote} \leftarrow \text{garnet} + \text{fluid}$
- 30)  $\text{zoisite} + \text{quartz} \leftarrow \text{anorthite} + \text{fluid}$
- 44)  $\text{chlorite} + \text{epidote} \leftarrow \text{Al-amphibole}$
- 54)  $3 \text{ quartz} + 3 \text{ chlorite} + 3 \text{ anorthite} \leftarrow \text{grossular} + 5 \text{ pyrope} + 12 \text{ fluid}$

**N588: SHEAR ZONE with garnet and amphibole close to Jijal northern contact**Modal composition:

bluish-green ferroan pargasite

40%

plagioclase

25%

quartz

15%

epidote

10%

garnet

5%

zoisite

5%

rutile

trace

monazite?

The rock divides into garnet + quartz-rich layers and ferroan pargasite-rich layers. The latter contain porphyroclasts of epidote grains that tend to form symplectites with quartz when in contact with plagioclase (30), or have quartz, plagioclase, and/or green hornblende inclusions. Coarser grains of epidote are zoned. Coarse ferroan pargasite grains are poikiloblastic with quartz inclusions and tend to be elongated. Small, inclusion-free clasts locally have exsolution lamellae of hematite. Coarse, up to 2.5 mm wide,

garnets are free of inclusions (but exceptionally with inclusions of quartz) and hypidiomorphic to euhedral with straight boundaries. Plagioclase grains are fresh to saussuritised (25) with local deformation twins. Zoisite is also present (30).

The garnet + quartz-rich layers (from 1?) are relatively coarse grained with fresh or saussuritised plagioclase grains and small elongated quartz neoblasts. The latter have serrated boundaries and locally form mosaics which contain small grains of fresh plagioclase. Coarse green ferroan pargasite and a few zoisite grains also occur in this layer. Fine clasts of ferroan pargasite tend to agglomerate and be oriented along the quartz neoblasts preferred orientation.

It is likely, considering the assemblage, that the rock belongs to the epidote-amphibolite facies, and that shearing occurred after the formation of epidote.

Mineral assemblage and possible reactions:

- 1)  $3 \text{ anorthite} + 6 \text{ diopside} \rightarrow 2 \text{ grossular} + \text{pyrope} + 3 \text{ quartz}$   
 25)  $2 \text{ zoisite} \leftarrow 3 \text{ anorthite} + \text{Ca(OH)}_2$   
 30)  $\text{zoisite} + \text{quartz} \leftarrow \text{anorthite} + \text{fluid}$

## N589: Vein crosscutting a garnet amphibolite

### Modal composition of the host-rock:

plagioclase	47%
brownish- to bluish-green	
hornblende	35%
garnet	15%
chlorite	2%
sphene	1%
quartz, epidote	trace

### Modal composition of the vein:

brownish- to bluish-green	
hornblende	57%
garnet	40%
chlorite	2%
sphene	1%
quartz	trace
opaque oxides	trace

The host rock shows a granoblastic texture with garnet hypidiomorphic grains that tend to agglomerate. They have inclusions of quartz, rutile and hornblende. Plagioclase is relatively fresh to highly saussuritised (25) or cloudy. Traces of symplectitic epidote locally occur on plagioclase grains (26, 30). Hornblende grains are altered by chlorite (42, 48, 49). Two different populations of hornblende may be present; bluish-green hornblende grains (lower amphibolite facies?) contrast with brownish-green hornblende (48). Textural evidence suggests that garnet formed by progression into the initial amphibolite facies assemblage of this amphibole + plagioclase mesocumulate (17), before retrogression. The whole rock is very altered and garnet grains are highly cracked.

The contact between the host rock and the vein is clearly defined by a single-grain layer of hypidiomorphic garnet grains formed as a reaction product between the plagioclase of the host rock and the hornblende of the vein (17). The vein is relatively coarse grained and essentially composed of brownish-green hornblende and garnet (hypidiomorphic to euhedral neoblasts?). Plagioclase as a restrictive reactant phase occurs only as inclusions within garnet. Hornblende grains have inclusions of quartz, opaque oxides, clinopyroxene?, plagioclase, and sphene. Hornblende is altered by chlorite (48, 49, 31) and hematite (58) and garnet by chlorite in cracks (54).

### Mineral assemblage and possible reactions of the host rock:

- 17)  $3 \text{ Fe-tremolite} + 6 \text{ anorthite} + 3 \text{ albite} \rightarrow 3 \text{ Fe-pargasite} + \text{almandine} + 2 \text{ grossular} + 18 \text{ quartz}$
- 25)  $2 \text{ zoisite} \leftarrow 3 \text{ anorthite} + \text{Ca(OH)}_2$
- 26)  $\text{albite} + \text{zoisite} \leftarrow \text{oligoclase} + \text{fluid}$
- 30)  $\text{zoisite} + \text{quartz} \leftarrow \text{anorthite} + \text{fluid}$
- 42)  $6 \text{ epidote} + \text{chlorite} + 7 \text{ quartz} \leftarrow \text{actinolite} + 10 \text{ anorthite} + 6 \text{ fluid}$
- 48)  $\text{chlorite} + \text{actinolite} \leftarrow \text{hornblende} + \text{anorthite}$
- 49)  $\text{chlorite} + \text{quartz} + \text{CaO} \leftarrow \text{hornblende} + \text{anorthite}$

Mineral assemblage and possible reactions of the vein:

- 17)  $3 \text{ Fe-tremolite} + 6 \text{ anorthite} + 3 \text{ albite} \rightarrow 3 \text{ Fe-pargasite} + \text{almandine} + 2 \text{ grossular} + 18 \text{ quartz}$
- 31)  $4 \text{ zoisite} + \text{quartz} \leftarrow 5 \text{ anorthite} + \text{grossular} + 2 \text{ fluid}$
- 48)  $\text{chlorite} + \text{actinolite} \leftarrow \text{hornblende} + \text{anorthite}$
- 49)  $\text{chlorite} + \text{quartz} + \text{CaO} \leftarrow \text{hornblende} + \text{anorthite}$
- 54)  $3 \text{ quartz} + 3 \text{ chlorite} + 3 \text{ anorthite} \leftarrow \text{grossular} + 5 \text{ pyrope} + 12 \text{ fluid}$
- 58)  $6 \text{ hematite} \leftarrow 4 \text{ magnetite} + \text{O}_2$

**N593: Epidote-quartz-plagioclase vein crosscutting a garnet****clinopyroxenite****Typical prograde (Cpx + plag) CUMULATE**Modal composition of the host-rock:

plagioclase	35%
garnet	30%
quartz	15%
clinopyroxene	15%
rutile, hematite and opaque oxides,	
epidote, chlorite	trace

Modal composition of the vein:

epidote (pistacite?)	35%
quartz	30%
plagioclase	20%
chlorite	15%
clinopyroxene	trace

The host rock has a granoblastic texture but is altered. Hematite, opaque oxide and chlorite overprint clinopyroxene (47), plagioclase is saussuritised (25) and cloudy, and chlorite fills cracks in garnet (54). The latter is hypidiomorphic to euhedral and closely associated with quartz. It can reach over 1 cm across and is usually poikilitic with quartz, cloudy plagioclase, rutile and opaque oxide, clinopyroxene, and epidote inclusions and tend to form symplectites with quartz. Quartz forms mosaics with serrated boundaries. Textural evidence suggests the prograde formation of quartz + garnet from a former mesocumulate assemblage of clinopyroxene and plagioclase (1).

The contact between the vein and the host rock is not sharp, but it is outlined by progressive mineralogical and structural differences. Garnet is absent in the vein and the overprinted, retrogressive assemblage occurs as elongated aggregates; quartz neoblasts with serrated boundaries form a mosaic, epidote (probably pistacite) with quartz inclusions overprints plagioclase (30?), and chlorite locally neoblastic forms spherulites, Plagioclase is heterogeneously saussuritised (25) and overprinted by epidote and quartz neoblasts (30). Kinked twins and deformation twins locally occur in plagioclase. Pseudomorphic chlorite, replacing garnet, appears with quartz in symplectites that include altered clinopyroxene grains with embayed boundaries (55).

Mineral assemblage and possible reactions of the host rock:

- 1)  $3 \text{ anorthite} + 6 \text{ diopside} \rightarrow 2 \text{ grossular} + \text{pyrope} + 3 \text{ quartz}$

- 25) 2 zoisite ← 3 anorthite + Ca(OH)<sub>2</sub>
- 47) chlorite + 6 hedengergite + 6 hematite ← 3 quartz + 6 magnetite + 5 diopside + anorthite + 4 fluid
- 54) 3 quartz + 3 chlorite + 3 anorthite ← grossular + 5 pyrope + 12 fluid

Mineral assemblage and possible reactions of the vein:

- 25) 2 zoisite ← 3 anorthite + Ca(OH)<sub>2</sub>
- 30) zoisite + quartz ← anorthite + fluid
- 55) anorthite + 2 chlorite + 3 quartz ← 3 pyrope + diopside + 8 fluid

N601: Garnet granulite cut by a coarse garnet tonalite vein

(N601b)

Modal composition of the host rock:

plagioclase	45%
garnet	25%
clinopyroxene	20%
quartz	5%
spinelles	4%
brown amphibole	1%
opaque oxide & rutile	trace

(N601a)

Modal composition of the vein:

garnet	40%
plagioclase	32%
quartz	27%
epidote	1%
chlorite	trace
rutile, spinelle	trace

Minerals in the thin section are quite homogeneously distributed even if textural evidence strongly suggests disequilibria, with garnet and quartz neoblasts crystallizing from clinopyroxene and plagioclase (1). Garnet grain boundaries are straight except when in contact with quartz where they are lobate to strongly embayed, forming atoll garnets. Coarse plagioclase grains with deformation twins form a granoblastic texture, but are locally superimposed by diffuse spinel aggregates (39) or they are saussuritizised (25). Rutile is dark and usually included in garnet. Local rare brown amphibole grains have crystallized at triple junctions of plagioclase (8). The contact boundary of the host rock with the vein is curved and only defined by the absence of clinopyroxene and the occurrence of coarse garnet containing a few inclusions.

Garnets in the vein are coarse (up to 6 mm across) and slightly altered by chlorite (54) and epidote in cracks. They are hypidiomorphic with lobate boundaries and "appendices": this texture suggests that crystallization switched from grain expansion growth to crystallization restricted along grain boundaries (1 from mobile Mg and Fe instead of cpx). Mosaic heterogranular quartz with lobate to serrated boundaries occurs principally around garnet. Quartz also occurs as rare inclusions with plagioclase and epidote in garnet grains. Granoblastic plagioclase with straight grain boundaries is locally altered by epidote (26), or invaded by opaque minerals and locally saussuritizised (25). Coarser plagioclase grains

show deformation twins. Textural evidence suggests that the vein is magmatic and has undergone granulite facies metamorphism that produced the garnet appendices. Retrogressive processes gave rise to epidote (26, 29, with amphibole from the rock, 30).

Mineral assemblage and possible reactions of the host rock:

- 1) 3 anorthite + 6 diopside  $\rightarrow$  2 grossular + pyrope + 3 quartz
- 8) 6 tremolite + 7 grossular  $\leftarrow$  27 diopside + 6 anorthite + pyrope + 6 fluid
- 25) 2 zoisite  $\leftarrow$  3 anorthite +  $\text{Ca}(\text{OH})_2$
- 39) 4 quartz + spinel + 4 clinozoisite  $\leftarrow$  diopside + 7 anorthite + 2 fluid

Mineral assemblage and possible reactions of the vein:

- 1) 3 anorthite + 6 diopside  $\rightarrow$  2 grossular + pyrope + 3 quartz
- 25) 2 zoisite  $\leftarrow$  3 anorthite +  $\text{Ca}(\text{OH})_2$
- 26) albite + zoisite  $\leftarrow$  oligoclase + fluid
- 29) amphibole + epidote  $\leftarrow$  garnet + fluid
- 30) zoisite + quartz  $\leftarrow$  anorthite + fluid
- 54) 3 quartz + 3 chlorite + 3 anorthite  $\leftarrow$  grossular + 5 pyrope + 12 fluid

**N605: Narrow clinopyroxene-chlorite-garnet vein crosscutting a garnet granulite**

Modal composition of the host-rock:

plagioclase	50%
garnet	35%
clinopyroxene	10%
quartz	5%
rutile	trace

Modal composition of the vein:

garnet	45%
clinopyroxene	37%
brownish green pargasite	10%
chlorite	5%
epidote	3%

The host rock has a typical granulite facies assemblage of elongate garnet, clinopyroxene and quartz aggregates. Minerals have a weak preferred orientation. Garnet is hypidiomorphic with embayed boundaries and has inclusions of quartz, clinopyroxene and rutile. Plagioclase is relatively coarsely grained but cloudy or highly saussuritised (25).

Clinopyroxene grains are smaller and locally include rutile and rounded quartz. Grain boundaries are usually straight defining a mesocumulate texture.

The vein is narrow (5-7 mm) and has diffuse contacts. The assemblage differs from the

host rock because plagioclase is absent and pyroxenes are more heavily altered to chlorite (7, 36, 44). Brownish-green pargasite may be altered by epidote (37, 44). Hornblende locally contains inclusions of clinopyroxene (18). Garnet seems to have grown along the

boundaries between plagioclase grains outside of the vein and clinopyroxene grains in the vein, and thus follows the main prograde tendency of the host rock (1).

Textural evidence suggests that the vein had intruded the rock before the end of the prograde granulite facies metamorphism. Epidote-greenschist facies metamorphism is related to late cooling.

Mineral assemblage and possible reactions of the host rock:

- 1)  $3 \text{ anorthite} + 6 \text{ diopside} = 2 \text{ grossular} + \text{pyrope} + 3 \text{ quartz}$   
 25)  $2 \text{ zoisite} \leftarrow 3 \text{ anorthite} + \text{Ca(OH)}_2$

Mineral assemblage and possible reactions of the vein:

- 1)  $3 \text{ anorthite} + 6 \text{ diopside} \rightarrow 2 \text{ grossular} + \text{pyrope} + 3 \text{ quartz}$   
 7)  $4 \text{ tremolite} + 3 \text{ anorthite} \leftarrow 3 \text{ pyrope} + 11 \text{ diopside} + 7 \text{ quartz} + 4 \text{ fluid}$   
 18)  $\text{tremolite} + 2 \text{ anorthite} \leftarrow \text{tschermakite} + 2 \text{ diopside} + 2 \text{ quartz}$   
 36)  $4 \text{ quartz} + \text{spinel} + 4 \text{ zoisite} \leftarrow \text{diopside} + 7 \text{ anorthite} + 2 \text{ fluid}$   
 37)  $2 \text{ anthophyllite} + 4 \text{ zoisite} \leftarrow 3 \text{ tschermakite} + 2 \text{ tremolite} + 2 \text{ quartz}$   
 44)  $\text{chlorite} + \text{epidote} \leftarrow \text{Al-amphibole}$



## N610: Retrogressed garnet granulite

### (N610b)

#### Modal composition of the host rock:

plagioclase	35%
garnet	30%
pale green hornblende	20%
clinopyroxene	10%
quartz	5%
epidote	trace
opaque oxides & rutile	trace
sphene	trace
orthopyroxene?	

### (N610a)

#### Modal composition of the vein:

plagioclase	75%
garnet	11%
epidote	7%
opaque oxides and rutile	1%
chlorite	trace

Minerals in the host rock are quite homogeneously distributed but tend to have a preferred orientation because garnet, pale green hornblende, and clinopyroxene form elongate aggregates. Garnets have straight boundaries when in contact with plagioclase, but are lobate, embayed, or in some cases hollow when in contact with clinopyroxene or hornblende (1, 7, 16). Hence, garnets are euhedral (small neoblasts) to anhedral and may have inclusions of hornblende, clinopyroxene, opaque oxides, rutile, and plagioclase. They are altered by chlorite infilling the cracks (53, 54). Quartz forms essentially as neoblasts around garnet and may have crystallized in a mosaic. Plagioclases are cloudy and a few may also be saussuritised (25) with rare epidote neoblasts (30) that usually occur in the plagioclase-free zone that occupies 10% of the thin section. Textural

evidence suggests that clinopyroxene and garnet crystallized before plagioclase in a magmatic environment. Textural similarities and the assemblage suggest this sample is similar to **P24c**.

In the vein, relicts of garnet occur between epidote and chlorite (54). Opaque oxides and rutile are concentrated in epidote which pseudomorphs hornblende (41, 44). Zoisite combined with epidote forms aggregates which seem to replace hornblende as pseudomorphs (41). Hence, this anorthositic vein in sample N610 seems to be a highly altered and retrogressed zone of the former garnet cumulate, perhaps caused by local fluid circulation. The high degree of saussuritization (25, 26) of minerals enables us to identify them from one to the other. Hence, they have been counted in the plagioclase fraction.

#### Mineral assemblage and possible reactions in the host rock:

- 1) 3 anorthite + 6 diopside  $\leftarrow$  2 grossular + pyrope + 3 quartz
- 7) 4 tremolite + 3 anorthite  $\leftarrow$  3 pyrope + 11 diopside + 7 quartz + 4 fluid
- 16) 3 tremolite + 6 anorthite + 3 albite  $\leftarrow$  3 pargasite + 2 grossular + pyrope + 18 quartz
- 25) 2 zoisite  $\leftarrow$  3 anorthite +  $\text{Ca(OH)}_2$

- 30) zoisite + quartz  $\leftarrow$  anorthite + fluid  
 53) 3 chlorite + grossular + 6 quartz  $\leftarrow$  4 pyrope + 3 diopside + 12 fluid  
 54) 3 quartz + 3 chlorite + 3 anorthite  $\leftarrow$  grossular + 5 pyrope + 12 fluid

Mineral assemblage and possible reactions in the vein:

- 25) 2 zoisite  $\leftarrow$  3 anorthite +  $\text{Ca}(\text{OH})_2$   
 26) albite + zoisite  $\leftarrow$  oligoclase + fluid  
 41) 3 chlorite + 6 epidote  $\leftarrow$  tschermakite + 2 anorthite + 10 fluid  
 44) chlorite + epidote  $\leftarrow$  Al-amphibole  
 54) 3 quartz + 3 chlorite + 3 anorthite  $\leftarrow$  grossular + 5 pyrope + 12 fluid

**N614: Epidote- and clinopyroxene-rich vein crosscutting a garnet clinopyroxenite.**

Modal composition of the host-rock:

plagioclase	50%
garnet	25%
clinopyroxene	8%
epidote	6%
chlorite	5%
quartz	4%
zoisite	1%
rutile	1%
actinolite	trace

Modal composition of the vein:

epidote	35%
plagioclase	27%
chlorite	25%
clinopyroxene	10%
zoisite	3%
amphibole, garnet and rutile	trace

The host rock has a granoblastic texture with a quite homogeneous distribution of minerals. Plagioclase grains, which are the most important constituent of the rock (50%), are relatively coarse, but completely saussuritised (25) and cloudy. Clinopyroxenes are brownish to bluish-green but severely altered to partly replaced by pseudomorphic epidote and chlorite (29, 45, 50, 53). In contact with plagioclase are intergrain symplectites of epidote and albite. Zoisite with albite symplectites also locally occur in plagioclase (26). Garnet grains are euhedral to hypidiomorphic and contain a few inclusions of quartz, altered plagioclase, rutile and rare actinolite. Garnets are strongly associated with quartz neoblasts, suggesting their prograde formation from a previous plagioclase-clinopyroxene mesocumulate assemblage (1). They are altered by chlorite filling the cracks (54) or replacing garnet as a pseudomorph along the vein contact (52).

The vein has a well defined, 2 mm wide, border of mostly continuous plagioclase. A transitional 5-6 mm wide zone in the vein consists of coarse altered plagioclase (25, 26, 30), clinopyroxene, and local garnet relics combined with pseudomorphic chlorite (53, 55), which are remnants of the host assemblage. Well developed heterogranular chlorite, zoisite and epidote are the main components of the vein. The core of the vein is essentially composed of highly symplectitic epidote with albite that sometimes forms relatively coarse grains with serrated boundaries, and which is superimposed by nematoblastic epidote (26, 29, 30).

Textural evidence suggests that the initial plagioclase + clinopyroxene cumulate underwent prograde granulite facies metamorphism, responsible for the formation of garnet + quartz in the host rock (1). Intrusion of the vein and retrograde metamorphism to epidote-amphibolite with chlorite-in facies could be related to late cooling during further uplift.

Mineral assemblage and possible reactions of the host rock:

- 1)  $3 \text{ anorthite} + 6 \text{ diopside} \rightarrow 2 \text{ grossular} + \text{pyrope} + 3 \text{ quartz}$
- 25)  $2 \text{ zoisite} \leftarrow 3 \text{ anorthite} + \text{Ca(OH)}_2$
- 26)  $\text{albite} + \text{zoisite} \leftarrow \text{oligoclase} + \text{fluid}$
- 29)  $\text{amphibole} + \text{epidote} \leftarrow \text{garnet} + \text{fluid}$
- 50)  $\text{actinolite} + \text{chlorite} + 11 \text{ quartz} + 9 \text{ CaO} \leftarrow 10 \text{ pyroxene} + \text{anorthite} + 5 \text{ fluid}$
- 52)  $\text{diopside} + \text{chlorite} + 2 \text{ anorthite} \leftarrow \text{grossular} + 2 \text{ pyrope} + 4 \text{ fluid}$
- 53)  $3 \text{ chlorite} + \text{grossular} + 6 \text{ quartz} \leftarrow 4 \text{ pyrope} + 3 \text{ diopside} + 12 \text{ fluid}$
- 54)  $3 \text{ quartz} + 3 \text{ chlorite} + 3 \text{ anorthite} \leftarrow \text{grossular} + 5 \text{ pyrope} + 12 \text{ fluid}$

Mineral assemblage and possible reactions of the vein:

- 25)  $2 \text{ zoisite} \leftarrow 3 \text{ anorthite} + \text{Ca(OH)}_2$
- 26)  $\text{albite} + \text{zoisite} \leftarrow \text{oligoclase} + \text{fluid}$
- 29)  $\text{amphibole} + \text{epidote} \leftarrow \text{garnet} + \text{fluid}$
- 30)  $\text{zoisite} + \text{quartz} \leftarrow \text{anorthite} + \text{fluid}$
- 53)  $3 \text{ chlorite} + \text{grossular} + 6 \text{ quartz} \leftarrow 4 \text{ pyrope} + 3 \text{ diopside} + 12 \text{ fluid}$
- 55)  $\text{anorthite} + 2 \text{ chlorite} + 3 \text{ quartz} \leftarrow 3 \text{ pyrope} + \text{diopside} + 8 \text{ fluid}$

**N616: Magmatic hornblende-pyroxene-garnet vein that cuts a garnet hornblendite**Modal composition of the vein:

clinopyroxene	45%
garnet	30%
brownish green amphibole	25%
epidote and chlorite	trace
opaque oxides & rutile,	trace

The rock is coarse grained with a granoblastic texture. Pyroxenes and large, hypidiomorphic brownish-green hornblendes contain Schiller plates and spinel, which are an indication of high T (~800-850°C) of formation. Amphibole inclusions occur locally in pyroxenes (15). In hornblende-rich areas pyroxenes (?) occur as

smaller grains at triple junctions with amphibole grains which locally has inclusions of epidote (44). Garnets are euhedral with straight boundaries or locally embayed. They have inclusions of hornblende, pyroxene, opaque oxides and rutile. Plagioclase and quartz are absent. Thus, garnet is not associated with quartz and is probably not metamorphic. Considering the assemblage and the textures of this sample, it is suggested that they have a primary, magmatic cumulate origin. The presence of epidote and chlorite overprinting the assemblage occurred during late greenschist facies retrograde metamorphism, which is responsible for compositional changes in amphiboles (7, 41, 44, 48).

Mineral assemblage and possible reactions:

- 7)  $4 \text{ tremolite} + 3 \text{ anorthite} \leftarrow 3 \text{ pyrope} + 11 \text{ diopside} + 7 \text{ quartz} + 4 \text{ fluid}$
- 15)  $3 \text{ pargasite} + 12 \text{ anorthite} + 18 \text{ diopside} \leftarrow 3 \text{ tremolite} + 5 \text{ pyrope} + 10 \text{ grossular} + 3 \text{ albite}$
- 41)  $3 \text{ chlorite} + 6 \text{ epidote} \leftarrow \text{tschermakite} + 2 \text{ anorthite} + 10 \text{ fluid}$
- 44)  $\text{chlorite} + \text{epidote} \leftarrow \text{Al-amphibole}$
- 48)  $\text{chlorite} + \text{actinolite} \leftarrow \text{hornblende} + \text{anorthite}$

## N617: Plagioclase-rich vein in hornblendite

### Modal composition of the host rock:

brownish-green hornblende	100%
epidote, plagioclase	trace
chlorite?	

### Modal composition of the vein:

plagioclase	65%
garnet	10%
zoisite	10%
scapolite	7%
epidote, clinozoisite	5%
brownish-green hornblende	3%
quartz, rutile	trace

The host rock is composed of brownish-green hornblende. It is coarse grained and has a granoblastic texture. Traces of epidote and plagioclase locally occur at triple junctions (30). Plagioclase is severely saussuritised (25). Hornblende contains Schiller plates and can be considered to be magmatic.

The contact with the plagioclase-rich vein is marked by a more or less diffuse layer of reactive (prograde?) garnets (16), that locally have altered plagioclase, hornblende, and epidote inclusions. Garnets are euhedral to hypidiomorphic and contain white mica inclusions (32).

The vein is essentially composed of cloudy and saussuritised plagioclase (25) with minor coarse pseudomorphic? epidote (30) and scapolite (27). Small grains of scapolite also tend to agglomerate into mosaics. They are superimposed by clinozoisite (26) that has a preferred orientation parallel to the contact of the vein with the host rock. Small aggregates of garnet and hornblende form hypidiomorphic grains that may be related to those described above. They could represent part of the contact that was incorporated into the vein during its formation.

### Mineral assemblage and possible reactions in the host rock:

- 16)  $3 \text{ tremolite} + 6 \text{ anorthite} + 3 \text{ albite} \rightarrow 3 \text{ pargasite} + 2 \text{ grossular} + \text{pyrope} + 18 \text{ quartz}$
- 25)  $2 \text{ zoisite} \leftarrow 3 \text{ anorthite} + \text{Ca(OH)}_2$
- 30)  $\text{zoisite} + \text{quartz} \leftarrow \text{anorthite} + \text{fluid}$
- 32)  $\text{paragonite} + 2 \text{ quartz} + 2 \text{ zoisite} \leftarrow 4 \text{ anorthite} + \text{albite} + 2 \text{ fluid}$

### Mineral assemblage and possible reactions in the vein:

- 25)  $2 \text{ zoisite} \leftarrow 3 \text{ anorthite} + \text{Ca(OH)}_2$
- 26)  $\text{albite} + \text{zoisite} \leftarrow \text{oligoclase} + \text{fluid}$
- 27)  $2 \text{ epidote} + \text{CO}_2 \leftarrow \text{meionite} + \text{fluid}$
- 30)  $\text{zoisite} + \text{quartz} \leftarrow \text{anorthite} + \text{fluid}$

## N618: Amphibole-garnet lens in an anorthositic vein with paragonite

### Modal composition:

zoned brownish to blue-green	
amphibole	42%
garnet	30%
zoisite, clinozoisite	10%
epidote	5%
clinopyroxene	4%
quartz	3%
chlorite, ilmenite	3%
plagioclase & K feldspar	2%
sphene	1%
paragonite	trace

The thin section contains a amphibole lens, in which heterogeneous distributed heterogranular grains are partly surrounded by a vein consisting of white epidote (?), zoisite, clinopyroxene, quartz, plagioclase, and paragonite.

The contact zone between the two is gradual over 2 to 5 mm. Amphibole grains in contact with garnet in that zone are replaced by darker green chlorite (49, 55). Amphibole grains in the vein are strongly altered by epidote and zoisite that form hypidiomorphic and coarse neoblasts (26, 41, 42, 44). There are relics of fresh plagioclase between zoisite grains of the vein

(26). The matrix also contains anhedral quartz and chlorite. Acicular paragonite, locally superimposed on zoisite (34) and plagioclase (21) is concentrated between grains, but superimposed needles are not oriented. Paragonite also occurs in the amphibolitic contact.

Coarse, anhedral garnet grains, with many inclusions, a few microns wide, are heterogeneously distributed in the contact zone. Inclusions are of epidote, quartz, amphibole, and plagioclase?, and also garnet which is partly altered by chlorite and epidote (29, 54). Coarse (up to 1.5mm wide) sphene is usually in contact with garnet or amphibole. Some grains have a corona of radial epidote (35). Brownish-green amphibole grains are rimmed by blue-green amphibole (18, 19).

Considering the general assemblage and appearance in thin section, the amphibolite zone of N618 could be associated with P23a, in spite of the fact that N618 has been more affected by retrograde metamorphism, giving rise to zoisite and epidote. Traces of the primary assemblage and textures are preserved and consist of the brown-amphibole + plagioclase + garnet + rutile assemblage. The secondary assemblage consists of bluish amphibole + sphene + epidote + paragonite + chlorite.

### Mineral assemblage and possible reactions:

- 18) tremolite + 2 anorthite  $\leftarrow$  tschermakite + 2 diopside + 2 quartz
- 19) tremolite + albite + anorthite  $\leftarrow$  pargasite + diopside + 5 quartz
- 26) albite + zoisite  $\leftarrow$  oligoclase + fluid
- 29) amphibole + epidote  $\leftarrow$  garnet + fluid
- 35) 6 ilmenite + 6 quartz + 12 zoisite + O<sub>2</sub>  $\leftarrow$  6 sphene + 2 magnetite + 18 anorthite + 6 fluid

- 41) 3 chlorite + 6 epidote  $\leftarrow$  tschermakite + 2 anorthite + 10 fluid  
 42) 6 epidote + chlorite + 7 quartz  $\leftarrow$  actinolite + 10 anorthite + 6 fluid  
 44) chlorite + epidote  $\leftarrow$  Al-amphibole  
 49) chlorite + quartz + CaO  $\leftarrow$  hornblende + anorthite  
 54) 3 quartz + 3 chlorite + 3 anorthite  $\leftarrow$  grossular + 5 pyrope + 12 fluid  
 55) anorthite + 2 chlorite + 3 quartz  $\leftarrow$  3 pyrope + diopside + 8 fluid

## N621: SHEAR ZONE: Hornblendite with paragonite

### Modal composition:

bluish-green hornblende	40%
zoisite	20%
garnet	15%
quartz	15%
paragonite	5%
plagioclase	4%
opaque oxides & rutile?	1%
sphene	trace

Nemoblastic paragonite is oriented and tends to surround hypidiomorphic garnet (34). Bluish-green hornblende and zoisite have been reoriented and fractures might have formed during shearing. Quartz is heterogranular and appears as neoblasts with serrated boundaries. It tends to form aggregates around garnet grains. Plagioclase grains are small but fresh with superimposed paragonite (32). Most grains have been replaced by abundant poikiloblastic zoisite with albite

inclusions (26). Hornblende also tends to be poikiloblastic. Garnets are poor in inclusions but may include quartz, opaque oxides, rutile, and clinopyroxene? and they are altered by chlorite (54). Sphene occurs in the matrix.

N621 can be related to GI 11a considering the assemblage, but may be more deformed and paragonite-rich.

### Mineral assemblage and possible reactions:

- 26) albite + zoisite  $\leftarrow$  oligoclase + fluid  
 32) paragonite + 2 quartz + 2 zoisite  $\leftarrow$  4 anorthite + albite + 2 fluid  
 34) 4 grossular + 5 paragonite + 6 quartz  $\leftarrow$  6 zoisite + 5 albite + 2 fluid  
 54) 3 quartz + 3 chlorite + 3 anorthite  $\leftarrow$  grossular + 5 pyrope + 12 fluid

## N626: Coarse plagioclase-garnet-clinopyroxene-hornblende rock

### Modal composition:

plagioclase	50%
garnet	30%
clinopyroxene	6%
epidote, clinozoisite,	5%
green hornblende	4%
quartz	3%
chlorite, scapolite	2%
opaque oxides & rutile	trace

The rock is heterogranular with an heterogeneous distribution of minerals. Garnets are up to approximately 1.5 cm wide. They are hypidiomorphic usually with straight boundaries and tend to agglomerate to form a diablastic texture. Small grains of hornblende, clinopyroxene, quartz, epidote, chlorite, opaque oxides and rutile occur as interstitial grains or as inclusions. Considering the close association between garnets and clinopyroxenes, it is

suggested that garnets might have crystallized from a previous cumulate assemblage of plagioclase + clinopyroxene (1). Clinopyroxene grains locally reach 2 cm wide and are associated with mm-size garnets as the prograde reaction proceeds. Plagioclase is the most abundant phase in the rock and is coarse grained with straight boundaries. It is cloudy and saussuritised (25), and partly replaced by chlorite (26, 49), epidote (30), and clinozoisite (locally symplectitic with albite: 26, 38). Hornblende is also altered by chlorite, epidote, and clinozoisite (41, 44, 48).

### Mineral assemblage and possible reactions:

- 1)  $3 \text{ anorthite} + 6 \text{ diopside} \leftarrow 2 \text{ grossular} + \text{pyrope} + 3 \text{ quartz}$
- 25)  $2 \text{ zoisite} \leftarrow 3 \text{ anorthite} + \text{Ca(OH)}_2$
- 26)  $\text{albite} + \text{zoisite} \leftarrow \text{oligoclase} + \text{fluid}$
- 30)  $\text{zoisite} + \text{quartz} \leftarrow \text{anorthite} + \text{fluid}$
- 38)  $\text{clinozoisite} \leftarrow \text{zoisite}$
- 41)  $3 \text{ chlorite} + 6 \text{ epidote} \leftarrow \text{tschermakite} + 2 \text{ anorthite} + 10 \text{ fluid}$
- 44)  $\text{chlorite} + \text{epidote} \leftarrow \text{Al-amphibole}$
- 48)  $\text{chlorite} + \text{actinolite} \leftarrow \text{hornblende} + \text{anorthite}$
- 49)  $\text{chlorite} + \text{quartz} + \text{CaO} \leftarrow \text{hornblende} + \text{anorthite}$



## N627: Coarse plagioclase-garnet-clinopyroxene-hornblende vein in fine-grained garnet-plagioclase-clinopyroxene-hornblende rock

(N627b)

### Modal composition of the host-rock:

plagioclase	30%
garnet	30%
clinopyroxene	15%
quartz	10%
green hornblende	9%
zoisite, clinozoisite	5%
chlorite, epidote	1%
opaque oxides & rutile	trace

(N627a, c)

### Modal composition of the vein:

plagioclase	50%
garnet	30%
clinopyroxene	7%
green hornblende	5%
opaque oxides & rutile	2%
epidote, clinozoisite	1%
scapolite, kyanite	trace

The host rock has a 1-2 mm grain size, a granoblastic texture and a homogeneous distribution of minerals. Plagioclase is cloudy and/or saussuritised (25), with deformation and kinked twins. Fresh, fine-grained plagioclase also occurs between garnet and clinopyroxene grains. It forms a mosaic with serrated boundaries. Replacement of plagioclase by pseudomorphic epidote increases towards the contact of the vein (36). Symplectites of zoisite + albite are well developed between plagioclase and hornblende grains near the contact of the vein (26). Green hornblende and clinopyroxene grains are hypidiomorphic with lobate boundaries and are altered by epidote and chlorite (30, 36, 42, 48, 55). Garnets are hypidiomorphic to euhedral and tend to agglomerate with interstitial hornblende, clinopyroxene, quartz, and rutile. They are locally embayed when in contact with quartz. Considering the assemblage and the textures, it is suggested that garnets are metamorphic and formed from the clinopyroxene + amphibole? + plagioclase cumulate assemblage

(1).

The vein is coarse grained with garnets up to 1 cm across. It is essentially composed of plagioclase which is heterogeneously altered and which is fresh to cloudy, saussuritised (25) and partly replaced by epidote or clinozoisite (24, 32, 38). Hypidiomorphic garnets with straight boundaries tend to agglomerate in a diablastic texture, enclosing clinopyroxene, amphibole, altered plagioclase and epidote inclusions (8). Relatively large, up to 1 mm wide, anhedral rutile grains are included in garnet. They also occur together with altered plagioclase inclusions. Atoll garnets are locally embayed by altered plagioclase or epidote (8). Coarse grains of green hornblende (or Cpx?) are severely altered by epidote and are cloudy (36, 39). Nematoblastic clinozoisite grains (in optical continuity) are superimposed on the assemblage (24). Uralitization (8) indicates the destabilization of anorthite in plagioclase. Aluminium silicate was found in one analysis.

Mineral assemblage and possible reactions of the host rock:

- 1) 3 anorthite + 6 diopside  $\rightarrow$  2 grossular + pyrope + 3 quartz
- 25) 2 zoisite  $\leftarrow$  3 anorthite +  $\text{Ca}(\text{OH})_2$
- 26) albite + zoisite  $\leftarrow$  oligoclase + fluid
- 30) zoisite + quartz  $\leftarrow$  anorthite + fluid
- 36) 4 quartz + spinel + 4 zoisite  $\leftarrow$  diopside + 7 anorthite + 2 fluid
- 42) 6 epidote + chlorite + 7 quartz  $\leftarrow$  actinolite + 10 anorthite + 6 fluid
- 48) chlorite + actinolite  $\leftarrow$  hornblende + anorthite
- 55) anorthite + 2 chlorite + 3 quartz  $\leftarrow$  3 pyrope + diopside + 8 fluid

Mineral assemblage and possible reactions of the vein:

- 8) 6 tremolite + 7 grossular  $\leftarrow$  27 diopside + 6 anorthite + pyrope + 6 fluid
- 24) 54 clinozoisite + 3 tremolite  $\leftarrow$  5 pyrope + 19 grossular + 57 anorthite + 30 fluid
- 25) 2 zoisite  $\leftarrow$  3 anorthite +  $\text{Ca}(\text{OH})_2$
- 32) paragonite + 2 quartz + 2 zoisite  $\leftarrow$  4 anorthite + albite + 2 fluid
- 36) 4 quartz + spinel + 4 zoisite  $\leftarrow$  diopside + 7 anorthite + 2 fluid
- 38) clinozoisite  $\leftarrow$  zoisite
- 39) 4 quartz + spinel + 4 clinozoisite  $\leftarrow$  diopside + 7 anorthite + 2 fluid

**N629: Coarse clinopyroxene-plagioclase-garnet rock**Modal composition:

plagioclase	30%
clinopyroxene	20%
amphibole	15%
garnet	25%
zoisite	5%
quartz	3%
epidote	2%
opaque oxides & sphene	trace

The rock is essentially composed of coarse, up to 4,5 cm wide garnet, clinopyroxene granoblastic aggregates and plagioclase. Alteration is heterogeneously present in the sample.

Hornblende can be fresh to severely altered by epidote (37). Symplectites with zoisite, albite? and hornblende also occur (26). It is suggested that two generations of clinopyroxene and amphibole(?) might be present in the rock as inclusions in optical continuity, and as coronas

around previous grains (14, 16, 48). Plagioclase is cloudy, saussuritised (25) and locally forms fine-grained mosaics with embayed boundaries (recrystallization?).

Garnets are hypidiomorphic with a few inclusions of amphibole, opaque oxide, sphene, epidote, and altered plagioclase. They are superimposed by oriented needles of white mica? (22, 37) at the angle of about 30°. Quartz is usually in contact with garnet suggesting its prograde formation before subsequent retrograde metamorphism (1, 15).

Mineral assemblage and possible reactions:

- 1) 3 anorthite + 6 diopside  $\rightarrow$  2 grossular + pyrope + 3 quartz
- 14) tremolite + albite  $\leftarrow$  edenite + quartz
- 15) 3 pargasite + 12 anorthite + 18 diopside  $\leftarrow$  3 tremolite + 5 pyrope + 10 grossular + 3 albite
- 16) 3 tremolite + 6 anorthite + 3 albite  $\leftarrow$  3 pargasite + 2 grossular + pyrope + 18 quartz
- 22) 3 diopside + 2 paragonite  $\leftarrow$  pyrope + grossular + 2 albite + 2 fluid
- 25) 2 zoisite  $\leftarrow$  3 anorthite +  $\text{Ca}(\text{OH})_2$
- 26) albite + zoisite  $\leftarrow$  oligoclase + fluid
- 36) 4 quartz + spinel + 4 zoisite  $\leftarrow$  diopside + 7 anorthite + 2 fluid
- 37) 2 anthophyllite + 4 zoisite  $\leftarrow$  3 tschermakite + 2 tremolite + 2 quartz
- 48) chlorite + actinolite  $\leftarrow$  hornblende + anorthite

**N631: Coarse garnet-hornblende-plagioclase rock**Modal composition:

garnet	60%
hornblende	20%
plagioclase	8%
zoisite	5%
chlorite	5%
opaque oxides & sphene	1%
scapolite?	1%
quartz, epidote	trace

The rock is coarse grained with hypidiomorphic garnets up to 2 cm across. Garnets have straight boundaries and contain only a few inclusions of hornblende, zoisite, epidote, quartz, opaque oxides and sphene. They are altered by chlorite in cracks (54). Interstitial symplectites of zoisite + albite? and/or epidote + chlorite + albite? occur at contacts of garnet with plagioclase (26, 29, 45). Hornblendes between garnet grains form heterogranular interstitial grains in aggregates

with zoisite (epidote), albite? (26, 30, 45), chlorite, and quartz. Fine-grained hornblendes probably of a second generation (48) are fresh in contrast with coarser grains that are usually altered by epidote. Chlorite locally occurs as superimposed lamellae and inclusions in optical continuity in amphibole (probably actinolitic hornblende). Plagioclase is cloudy and/or saussuritised (25) with superimposed epidote or nematoblastic zoisite (30) that also crosscuts some zoisite symplectites (26, 30). Opaque oxides are usually included in hornblende and form compact aggregates with inclusions of amphibole, epidote, and quartz. It is not obvious whether garnet is magmatic or metamorphic.

Mineral assemblage and possible reactions:

- 25) 2 zoisite  $\leftarrow$  3 anorthite +  $\text{Ca}(\text{OH})_2$
- 26) albite + zoisite  $\leftarrow$  oligoclase + fluid
- 29) amphibole + epidote  $\leftarrow$  garnet + fluid
- 30) zoisite + quartz  $\leftarrow$  anorthite + fluid
- 45) chlorite + quartz +  $\text{CaO}$   $\leftarrow$  actinolitic hornblende + epidote

- 48) chlorite + actinolite  $\leftarrow$  hornblende + anorthite  
 54) 3 quartz + 3 chlorite + 3 anorthite  $\leftarrow$  grossular + 5 pyrope + 12 fluid

### N632d: MYLONITE: Hornblendite with paragonite

#### Modal composition:

green hornblende	30%
quartz	25%
garnet	20%
epidote	12%
zoisite	5%
paragonite	5%
plagioclase	3%
opaque oxides & rutile	trace

The sample is mylonitic with shear bands and heterogranular porphyroclasts of garnet (1mm to 8mm wide) surrounded by hornblende-rich tails with a sigmoidal shape. Foliation is well defined by acicular paragonite and elongate neoblasts or aggregates. Distinct aggregates of small garnets surrounded by hornblende, quartz, paragonite, epidote, zoisite and plagioclase tend to form sigmoids which define the shear bands. Coarser garnets are hypidiomorphic with serrated

to embayed grain boundaries when in contact with quartz (1). Large inclusions of quartz with hornblende, plagioclase, opaque oxides and rutile are combined with numerous inclusions a few microns wide. Smaller garnets may be free of inclusions, but are still altered by chlorite (54). Zoisite is poikilitic with quartz (30). Opaque oxide inclusions in hornblende are embayed but elsewhere these minerals form a graphic texture (23). Quartz tends to form elongate aggregates and mosaic quartz may occur in coarser grains.

#### Mineral assemblage and possible reactions:

- 1) 3 anorthite + 6 diopside  $\rightarrow$  2 grossular + pyrope + 3 quartz  
 23) 4 quartz + 4 Fe-pargasite + 3 O<sub>2</sub>  $\rightarrow$  6 hematite + 4 hedenbergite + 4 anorthite + 4 albite + 4 fluid  
 30) zoisite + quartz  $\leftarrow$  anorthite + fluid  
 54) 3 quartz + 3 chlorite + 3 anorthite  $\leftarrow$  grossular + 5 pyrope + 12 fluid

**N633c: SHEAR ZONE: Mylonite with garnets**Modal composition:

quartz	30%
garnet	25%
green hornblende & ferroan pargasite	20%
epidote, zoisite	15%
brown hornblende	5%
plagioclase?	5%
opaque oxides & rutile	trace
white mica	trace

The mylonite is essentially composed of sigmoidal garnet porphyroclasts (up to 1 cm across) with green hornblende in a hairy? matrix composed of elongated neoblasts of quartz, green hornblende, epidote and plagioclase. In the matrix are remnants, most likely of a magmatic stage, of brown hornblende with Schiller plates (23?) that is relatively coarser than the matrix clasts, and of hornblende zoned from brown to green from core to rim (17). Green hornblende in the matrix is locally poikilitic with inclusions

of quartz and is most likely to be metamorphic (17). Nemoblastic and oriented zoisite is superimposed on plagioclase + quartz-rich zones (30). Quartz forms mosaics with serrated grain boundaries. Garnet clasts locally contain hornblende, quartz or plagioclase, and rutile inclusions. They are also locally superimposed by white mica? needles (21).

Mineral assemblage and possible reactions:

- 17)  $3 \text{ Fe-tremolite} + 6 \text{ anorthite} + 3 \text{ albite} \leftarrow 3 \text{ Fe-pargasite} + \text{almandine} + 2 \text{ grossular} + 18 \text{ quartz}$
- 21)  $\text{grossular} + 2 \text{ paragonite} + 3 \text{ quartz} \leftarrow 3 \text{ anorthite} + 2 \text{ albite} + 2 \text{ fluid}$
- 23)  $4 \text{ quartz} + 4 \text{ Fe-pargasite} + 3 \text{ O}_2 \rightarrow 6 \text{ hematite} + 4 \text{ hedenbergite} + 4 \text{ anorthite} + 4 \text{ albite} + 4 \text{ fluid}$
- 30)  $\text{zoisite} + \text{quartz} \leftarrow \text{anorthite} + \text{fluid}$

## N634: Granitic vein that crosscuts a garnet hornblendite

(N634b)

### Modal composition of the host-rock:

brownish-green hornblende	57%
garnet	30%
scapolite	5%
quartz	3%
chlorite	3%
zoisite, epidote	1%
opaque oxides & sphene	1%

(N634a)

### Modal composition of the vein:

garnet	40%
green hornblende	35%
plagioclase	10%
quartz	7%
clinopyroxene	5%
epidote, zoisite, chlorite	3%
scapolite	trace

The host rock is locally porphyroblastic (?) containing coarse, up to 5 mm wide, hypidiomorphic, brownish-green hornblende porphyroclasts. Except for their size, they are not different from the grains of the matrix. They locally have chlorite? (44) and hornblende inclusions (19), and also Schiller plates (23) that suggest a magmatic origin. Garnets are hypidiomorphic to euhedral and usually poikiloblastic with inclusions of hornblende, opaque oxides and sphene. They tend to form aggregates with embayed boundaries when in contact with hornblende where they are locally surrounded by interstitial and small neoblasts of quartz (16). The amount of scapolite increases towards the vein. Sphene is usually included or surrounded by opaque oxides. Plagioclase is absent.

The granite vein has a granoblastic texture and coarse, up to 4 mm wide, garnets that have

hornblende inclusions of opaque oxides, sphene, quartz, and plagioclase?. Garnet grains tend to agglomerate to form a diablastic texture. Grains are euhedral to hypidiomorphic. It is likely that pyroxenes show Schiller plates, but they locally occur in brownish-green hornblende (23). Plagioclase is coarse grained and cloudy or saussuritised (25), but fresh grains locally occur. Alteration by epidote, zoisite, and chlorite is present between the grains (26, 42). Quartz is associated with garnet and occurs as small neoblasts with embayed boundaries (1, 16).

### Mineral assemblage and possible reactions of the host rock:

- 16)  $3 \text{ tremolite} + 6 \text{ anorthite} + 3 \text{ albite} \rightarrow 3 \text{ pargasite} + 2 \text{ grossular} + \text{pyrope} + 18 \text{ quartz}$
- 19)  $\text{tremolite} + \text{albite} + \text{anorthite} \leftarrow \text{pargasite} + \text{diopside} + 5 \text{ quartz}$
- 23)  $4 \text{ quartz} + 4 \text{ Fe-pargasite} + 3 \text{ O}_2 \rightarrow 6 \text{ hematite} + 4 \text{ hedenbergite} + 4 \text{ anorthite} + 4 \text{ albite} + 4 \text{ fluid}$
- 44)  $\text{chlorite} + \text{epidote} \leftarrow \text{Al-amphibole}$

### Mineral assemblage and possible reactions of the vein:

- 1)  $3 \text{ anorthite} + 6 \text{ diopside} \rightarrow 2 \text{ grossular} + \text{pyrope} + 3 \text{ quartz}$
- 16)  $3 \text{ tremolite} + 6 \text{ anorthite} + 3 \text{ albite} \rightarrow 3 \text{ pargasite} + 2 \text{ grossular} + \text{pyrope} + 18 \text{ quartz}$

- 23)  $4 \text{ quartz} + 4 \text{ Fe-pargasite} + 3 \text{ O}_2 \rightarrow 6 \text{ hematite} + 4 \text{ hedenbergite} + 4 \text{ anorthite} + 4 \text{ albite} + 4 \text{ fluid}$
- 25)  $2 \text{ zoisite} \leftarrow 3 \text{ anorthite} + \text{Ca(OH)}_2$
- 26)  $\text{albite} + \text{zoisite} \leftarrow \text{oligoclase} + \text{fluid}$
- 42)  $6 \text{ epidote} + \text{chlorite} + 7 \text{ quartz} \leftarrow \text{actinolite} + 10 \text{ anorthite} + 6 \text{ fluid}$

**N636: Anorthositic vein that crosscuts a garnet- and clinopyroxene-rich vein, and is crosscut by an epidote-rich veinlet.**

(N636a, c)

Modal composition of the host vein:

clinopyroxene	40%
plagioclase	35%
garnet	25%
zoisite	trace
opaque oxides & rutile	trace

(N636b)

Modal composition of the anorthositic vein:

plagioclase	77%
garnet	15%
clinopyroxene	5%
epidote	3%

The host vein is granoblastic and relatively fresh.

Foliation is defined by elongate aggregates of clinopyroxene and garnet. Garnets are usually euhedral with inclusions of plagioclase, fresh hornblende, opaque oxides, and rutile.

Clinopyroxene, as well as plagioclase, are saussuritised (6, 25, 36) near the epidote-rich veinlet. Clinopyroxenes are anhedral and have Schiller plates. They are cracked and locally altered by epidote near the epidote-rich veinlet.

(36) Clinopyroxene grains are also locally rimmed by epidote symplectites when in contact with plagioclase (30). The latter is slightly cloudy and saussuritised (25) near the epidote-rich veinlet, but mostly fresh elsewhere in the sample. Contacts between plagioclase grains are straight to embayed and have deformation twins.

Quartz is absent. The epidote-rich veinule is partly cloudy. Textural evidence suggests that garnets may have crystallized from a clinopyroxene-plagioclase magmatic assemblage (1), and that prograde reaction was still in process during the intrusion of the epidote-rich veinlet.

Contact with the anorthosite vein is clear and marked by up to 5 mm wide garnets which have inclusions of fresh plagioclase and which are altered by epidote (26). Small nemoblastic epidote or white mica? (31, 32) is locally superimposed on garnet. Plagioclases in the vein form a granoblastic texture, are usually fresh, but sometimes altered by epidote (26) and they have deformation twins. Coarse, up to 2,5 cm garnets, surrounded or including clinopyroxene are heterogeneously distributed in the vein, together with clinopyroxene and garnet aggregates.

Mineral assemblage and possible reactions of the host vein:

- 1)  $3 \text{ anorthite} + 6 \text{ diopside} \rightarrow 2 \text{ grossular} + \text{pyrope} + 3 \text{ quartz}$

- 6)  $2 \text{ magnetite} + 3 \text{ diopside} + 3 \text{ anorthite} \leftarrow 6 \text{ hedenbergite} + 3 \text{ spinel} + \text{O}_2$   
 25)  $2 \text{ zoisite} \leftarrow 3 \text{ anorthite} + \text{Ca(OH)}_2$   
 30)  $\text{zoisite} + \text{quartz} \leftarrow \text{anorthite} + \text{fluid}$   
 36)  $4 \text{ quartz} + \text{spinel} + 4 \text{ zoisite} \leftarrow \text{diopside} + 7 \text{ anorthite} + 2 \text{ fluid}$

Mineral assemblage and possible reactions of the anorthositic vein:

- 26)  $\text{albite} + \text{zoisite} \leftarrow \text{oligoclase} + \text{fluid}$   
 31)  $4 \text{ zoisite} + \text{quartz} \leftarrow 5 \text{ anorthite} + \text{grossular} + 2 \text{ fluid}$   
 32)  $\text{paragonite} + 2 \text{ quartz} + 2 \text{ zoisite} \leftarrow 4 \text{ anorthite} + \text{albite} + 2 \text{ fluid}$

### N638: Garnet meta-gabbro

Modal composition:

bluish-green hornblende	30%
epidote	20%
quartz	20%
garnet	15%
zoisite	7%
paragonite	4%
plagioclase	3%
opaque oxides & rutile	1%

The distribution of minerals is homogeneous but they are heterogranular. Porphyroblastic garnets are anhedral to hypidiomorphic and contain rare inclusions of epidote, quartz, rutile, and hornblende. Garnets are altered by chlorite (54). Quartz neoblasts have serrated boundaries and tend to form aggregates around garnet (1, 16). It may also form mosaics. Hornblende may be poikilitic with albite inclusions (15). Zoisite usually forms symplectites with albite (26),

while epidote is rather poikilitic with albite inclusions. Acicular paragonite is concentrated in plagioclase-quartz zones (32), but the needles are not oriented. Compared to **GI 11a**, **N638** does not show any trace of shearing (no preferred orientation) and is richer in epidote.

Mineral assemblage and possible reactions:

- 1)  $3 \text{ anorthite} + 6 \text{ diopside} \rightarrow 2 \text{ grossular} + \text{pyrope} + 3 \text{ quartz}$   
 15)  $3 \text{ pargasite} + 12 \text{ anorthite} + 18 \text{ diopside} \rightarrow 3 \text{ tremolite} + 5 \text{ pyrope} + 10 \text{ grossular} + 3 \text{ albite}$   
 16)  $3 \text{ tremolite} + 6 \text{ anorthite} + 3 \text{ albite} \rightarrow 3 \text{ pargasite} + 2 \text{ grossular} + \text{pyrope} + 18 \text{ quartz}$   
 26)  $\text{albite} + \text{zoisite} \leftarrow \text{oligoclase} + \text{fluid}$   
 32)  $\text{paragonite} + 2 \text{ quartz} + 2 \text{ zoisite} \leftarrow 4 \text{ anorthite} + \text{albite} + 2 \text{ fluid}$   
 54)  $3 \text{ quartz} + 3 \text{ chlorite} + 3 \text{ anorthite} \leftarrow \text{grossular} + 5 \text{ pyrope} + 12 \text{ fluid}$



**N639: Altered garnet-clinopyroxene-plagioclase cumulate**Modal composition:

garnet	45%
clinopyroxene	20%
plagioclase	16%
brownish-green pargasite	5%
scapolite	5%
epidote	4%
zoisite	3%
paragonite	2%
opaque oxides & rutile	trace
quartz	trace

Minerals are heterogeneously distributed in the rock and epidote-zoisite alteration has locally affected the assemblage. The hand specimen appears to be part of a layered cumulate. Large elongated plagioclase aggregates are surrounded by clinopyroxene and by plagioclase-free garnet and clinopyroxene layers which contrasts with plagioclase-bearing layers. Garnets are usually euhedral and contain rare inclusions of clinopyroxene, epidote, and opaque oxides and sphene. Garnets locally tend to agglomerate in a diablastic texture. Amphibole is brownish-green

to bluish-green and can be coarse grained (19). Clinopyroxene usually has Schiller plates, suggestive of a magmatic origin. Inclusions in garnet and surrounding grains of clinopyroxene locally have the same optical orientation. When in contact with plagioclase, pargasite is locally altered in association with symplectitic zoisite and albite (26), or epidote and albite. Plagioclase is usually anhedral and can be fresh to severely saussuritised (25) and/or cloudy. Scapolite (?) (pseudomorphic after plagioclase) zoisite (26) and epidote (32) occur locally. Nematoblastic paragonite is superimposed on cloudy plagioclase (32). Symplectites of epidote and opaque oxides occur locally (35, 36).

Mineral assemblage and possible reactions:

- 19) tremolite + albite + anorthite  $\leftarrow$  pargasite + diopside + 5 quartz
- 25) 2 zoisite  $\leftarrow$  3 anorthite +  $\text{Ca}(\text{OH})_2$
- 26) albite + zoisite  $\leftarrow$  oligoclase + fluid
- 32) paragonite + 2 quartz + 2 zoisite  $\leftarrow$  4 anorthite + albite + 2 fluid
- 35) 6 ilmenite + 6 quartz + 12 zoisite +  $\text{O}_2$   $\leftarrow$  6 sphene + 2 magnetite + 18 anorthite + 6 fluid
- 36) 4 quartz + spinel + 4 zoisite  $\leftarrow$  diopside + 7 anorthite + 2 fluid

**N640: 10 cm-wide hornblendite vein, 200 m south of N639****TYPICAL EPIDOTE-CHLORITE-AMPHIBOLITE + GARNET**Modal composition of the vein:

tremolite?	35%
green hornblende	20%
epidote	15%
zoisite	15%
chlorite	10%
garnet	5%
plagioclase	trace
opaque oxides	trace

This chlorite-bearing retrogressed rock is representative of the epidote-amphibolite facies. Chlorite grains are usually pseudomorphs of plagioclase (30, 41) and zoisite, or replace garnet (29, 45, 54). Tremolite is fresh and is hypidiomorphic with serrated boundaries. It is usually superimposed on green hornblende (19, 48), which mainly occurs as relics with Schiller plates? (23). Garnets usually form elongate fragments or

relics that are free of inclusions. Plagioclase occurs mainly in a planar, 0.5 mm wide veinlet, but relics are present in the host rock. It is suggested that tremolite, epidote, chlorite, and zoisite of the epidote-amphibolite facies are retrogressed products of a primary, magmatic assemblage of green hornblende, garnet, and plagioclase (19). Minerals tend to have a preferred orientation. Opaque oxides are fine-grained and tend to agglomerate and are superimposed on the assemblage as products of alteration.

Mineral assemblage and possible reactions:

- 19) tremolite + albite + anorthite  $\leftarrow$  pargasite + diopside + 5 quartz
- 23) 4 quartz + 4 Fe-pargasite + 3 O<sub>2</sub>  $\rightarrow$  6 hematite + 4 hedenbergite + 4 anorthite + 4 albite + 4 fluid
- 29) amphibole + epidote  $\leftarrow$  garnet + fluid
- 30) zoisite + quartz  $\leftarrow$  anorthite + fluid
- 41) 3 chlorite + 6 epidote  $\leftarrow$  tschermakite + 2 anorthite + 10 fluid
- 45) chlorite + quartz + CaO  $\leftarrow$  actinolitic hornblende + epidote
- 48) chlorite + actinolite  $\leftarrow$  hornblende + anorthite
- 54) 3 quartz + 3 chlorite + 3 anorthite  $\leftarrow$  grossular + 5 pyrope + 12 fluid

## Appendix 2:

### **Calculation of mole fractions and assignment of site occupancies**

**Plagioclase (Al-avoidance mixing on sites)****A(T1)<sub>2</sub>(T2)<sub>2</sub>O<sub>8</sub>**

A: Ca, Na, K

T1: Si, Al<sup>IV</sup>

T2: Si

$$A = Ca + Na + K$$

$$T1 = [(Si - SiT2) + Al^{IV}]$$

$$T2 = SiT2 = 2$$

$$Al^{IV} = 4 - Si$$

$$Al^{VI} = Al - Al^{IV}$$

$$^AXCa = XAn = Ca / (Ca + Na + K)$$

$$^AXNa = XAb = Na / (Ca + Na + K)$$

$$^AXK = XKfs = K / (Ca + Na + K)$$

$$XSi = Si / (Si + Al^{IV})$$

$$T2XSi = 1$$

$$T1XSi = [(Si - SiT2) / (Si - SiT2) + Al^{IV}]$$

**Garnet (ideal mixing on sites)****X<sub>3</sub>Y<sub>2</sub>Z<sub>3</sub>O<sub>12</sub>**X: Fe<sub>2</sub>, Mg, Mn, CaY: Fe<sub>3</sub>, Al<sup>VI</sup>, CrZ: Si, Al<sup>IV</sup>

$$X = XAlm + XPrp + XGrs + XSps + XUva$$

$$Y = Fe_3 + Al^{VI} + Cr$$

$$Z = Si + Al^{IV} = 3$$

$$Al^{IV} = 3 - Si$$

$$Al^{VI} = Al - Al^{IV}$$

$$ratioFe2Mg = Fe_2 / Mg$$

$$^XXFe_2 = XAlm = Fe_2 / (Fe_2 + Mg + Ca + Mn)$$

$$^XXMg = XPrp = Mg / (Fe_2 + Mg + Ca + Mn)$$

$$^XXCa = XGrs = Ca / (Fe_2 + Mg + Ca + Mn)$$

$$^XXMn = XSps = Mn / (Fe_2 + Mg + Ca + Mn)$$

$$XAdr = 1 - (XAlm + XPrp + XGrs + XSps + XUva)$$

$$XUva = Cr / (Fe_3 + Al^{VI} + Cr)$$

$$XUgr = Al^{VI} + XUva + XAdr$$

$$^YXFe_3 = Fe_3 / (Fe_3 + Al^{VI} + Cr)$$

$$XFe_2 = Fe_2 / (Fe_2 + Mg)$$

**Pyroxenes: (ideal mixing on sites)**

$$M2[Fe_2 / (Fe_2 + Mg)] = M1[Fe_2 / (Fe_2 + Mg)]$$

**Clinopyroxene**

$$(M2)(M1)T_2O_6$$

**Orthopyroxene**

$$(M2)_{0.5}(M1)_{0.5}TO_3$$

M2: Ca, Na, K, Mn, Mg, Fe<sub>2</sub>M1: Fe<sub>3</sub>, Al<sup>VI</sup>, Ti, Cr, Mg, Fe<sub>2</sub>T: Si, Al<sup>IV</sup>

$$CaTitsch = CaTiAl_2O_6$$

$$CaFetsch = CaFe_2SiO_6$$

$$Catsch = CaAl_2SiO_6$$

$$(Mg-tscherma) = CaMgAl_2O_6$$

$$Jd = NaAlSi_2O_6$$

$$Ac = NaFeSi_2O_6$$

$$CaW_0 = Ca - (Ca \text{ in tsch})$$

$$Al^{VI} = M1Al = (Al \text{ of } Jd) + (Al \text{ in tsch} / 2)$$

$$M1Fe_2 = [1 - (Al^{VI} + Fe_3 + Ti + Cr)] * XFe_2$$

$$M1Mg = [1 - (Al^{VI} + Fe_3 + Ti + Cr)] * XMg$$

$$M2Fe_2 = [1 - (Ca + Na + K + Mn)] * XFe_2$$

$$M2Fe_2$$

$$M2Mg = [1 - (Ca + Na + K + Mn)] * XMg$$

$$M2Fe_2$$

$$ratioFe2Mg = Fe_2 / Mg$$

$$ratioJdCat = XJd / XCats$$

$$XFe_2 = Fe_2 / (Fe_2 + Mg)$$

$$XMg = Mg / (Fe_2 + Mg)$$

$$XCaTitsch = CaTitsch / [Ca + Na + ((CaW_0 + Fe_2 + Mg + Mn) / 2)]$$

$$XCaFetsch = CaFetsch / [Ca + Na + ((CaW_0 + Fe_2 + Mg + Mn) / 2)]$$

$$XCatsch = CaTitsch / [Ca + Na + ((CaW_0 + Fe_2 + Mg + Mn) / 2)]$$

$$M2XCa = Ca$$

$$M2XNa = Na$$

$$XJd = (Na \text{ in } Jd) / [Ca + Na + ((CaW_0 + Fe_2 + Mg + Mn) / 2)]$$

$$XAc = (Na \text{ in } Ac) / [Ca + Na + ((CaW_0 + Fe_2 + Mg + Mn) / 2)]$$

$$XRdn = (Mn / 2) / [Ca + Na + ((CaW_0 + Fe_2 + Mg + Mn) / 2)]$$

$$M2XFe_2 = M2Fe_2 / (Ca + Na + K + Mn + M2Mg +$$

$$M2XMg = M2Mg / (Ca + Na + K + Mn + M2Mg +$$

$$M1XAl = Al^{VI} / (Fe_3 + Al^{VI} + Ti + Cr + M1Mg + M1Fe_2)$$

$$M1XFe_2 = M1Fe_2 / (Fe_3 + Al^{VI} + Ti + Cr + M1Mg + M1Fe_2)$$

$$\begin{aligned} XEn &= Mg / (Fe2 + Mg + Ca_{Wo}) \\ XF_s &= Fe2 / (Fe2 + Mg + Ca_{Wo}) \\ XWo &= Ca_{Wo} / (Fe2 + Mg + Ca_{Wo}) \\ XDi &= XEn / (XF_s + XEn) \\ XHd &= XF_s / (XF_s + XEn) \end{aligned}$$

$$M1XMg = M1Mg / (Fe3 + Al^{VI} + Ti + Cr + M1Mg + M1Fe2)$$

#### Calculation of the jadeite (Jd) molecule first:

All Ti forms CaTi-tschermak molecule  
 Na (+ Al<sup>VI</sup>) forms jadeite  
 Excess Na (+ Fe3) forms acmite  
 Excess Fe3 (+ Ca) forms CaFe-tschermak molecule  
 Excess Al (+ Ca) forms Ca-tschermak molecule  
 Excess Al (+ Mg) forms Mg-tschermak molecule

#### Calculation of the acmite (Ac) molecule first:

All Ti forms CaTi-tschermak molecule  
 Na (+ Fe3) forms acmite  
 Excess Fe3 (+ Ca) forms CaFe-tschermak molecule  
 Excess Na (+ Al<sup>VI</sup>) forms jadeite  
 Excess Al (+ Ca) forms Ca-tschermak molecule  
 Excess Al (+ Mg) forms Mg-tschermak molecule

#### Amphibole: (random mixing on sites)

$$M2[Fe2 / (Fe2 + Mg)] = M13[Fe2 / (Fe2 + Mg)] = M4[Fe2 / (Fe2 + Mg)]$$

$$A(M4)(M13)_5(M2)_2(T1)_4(T2)_4O_{22}(OH, Cl, F)_2$$

$$T2 = Si = 4$$

$$T1 = [(Si - 4) + Al + Fe3 + Cr3] = 4$$

$$M2 = Al^{VI} + Fe3 + Cr3 + Ti^{VI} + Fe2 + Mg = 2$$

$$M13 = Fe2 + Mg = 5$$

$$M4 = Fe2 + Mg + Mn + Ca + Na$$

$$A = Na + K + V$$

$$AlkA = Na + K$$

$$M4Alk = M4Ca + M4Na$$

$$XFe3 = Fe3 / (Fe3 + Al^{VI} + Cr3)$$

$$XMg = Mg / (Fe2 + Mg)$$

$$AXV = AV$$

$$M2XMg = Mg / (Al^{VI} + Fe3 + Cr3 + Ti^{VI} + Fe2 + Mg)$$

All abbreviations according to the ones used in the THEBA software where:

An = anorthite, Ab = albite, Kfs = K-felspar

Alm = almandine, Prp = pyrope, Grs = grossular, Sps = spessartine, Adr = andradite, Uva = uvarovite,

Ugr = ugrandite

CaTitsch = CaTi-tschermak molecule, CaFetsch = CaFe-tschermak molecule, Catsch = Ca-tschermak molecule,

Cats = all tschermak molecules, Jd = jadeite, Ac = acmite, Rdn = rhodonite, En = enstatite, Fs = ferrosilite,

Wo = wollastonite, Di = diopside, Hd = hedenbergite

AlkA = alkali in site A, V = vacancy.

### Appendix 3:

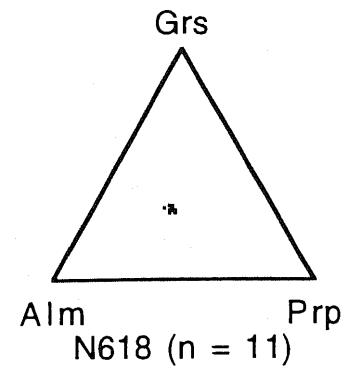
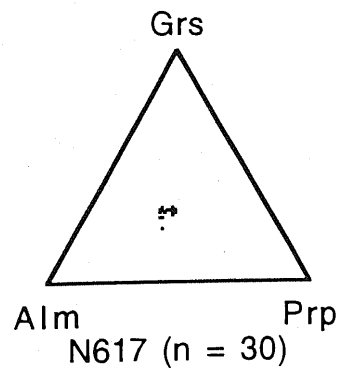
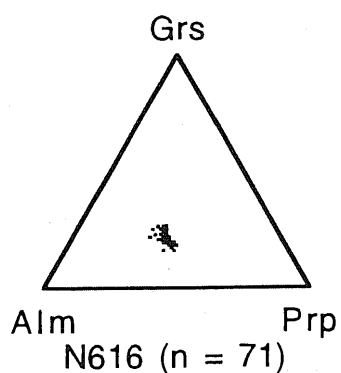
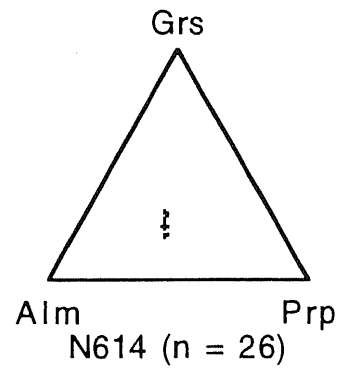
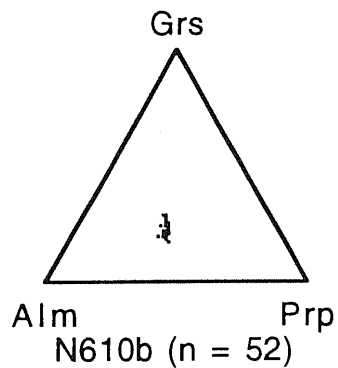
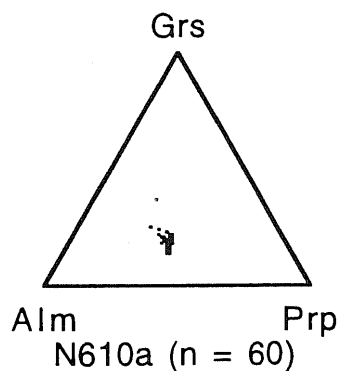
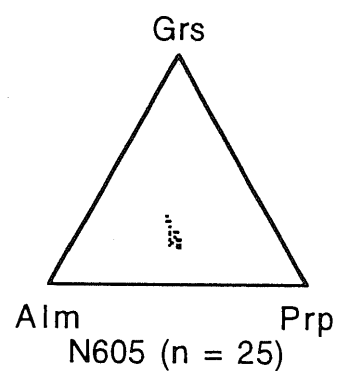
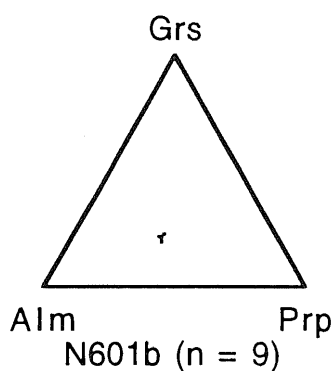
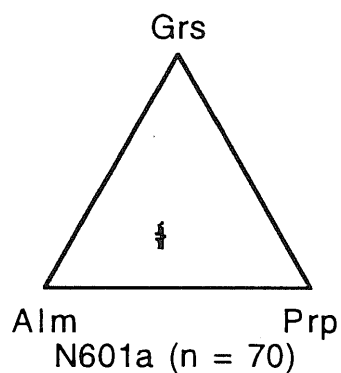
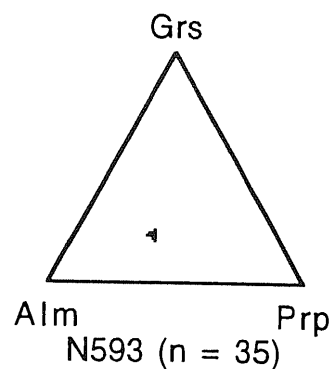
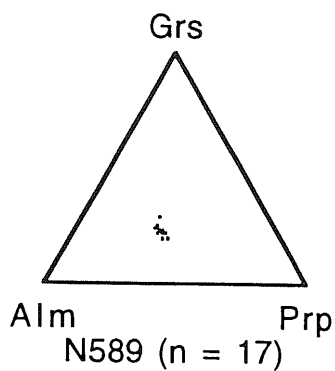
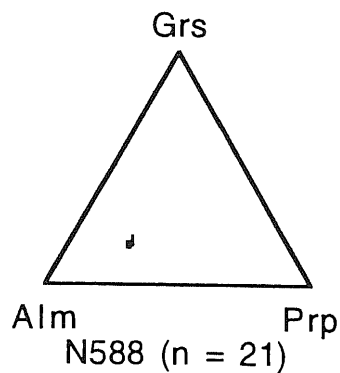
**Probe data  
including calculation of  
the stoichiometry of minerals  
and the distribution of  
cations within sites,  
according to the THEBA software  
(Martignole et al., unpublished)**

(on disks, see back cover)

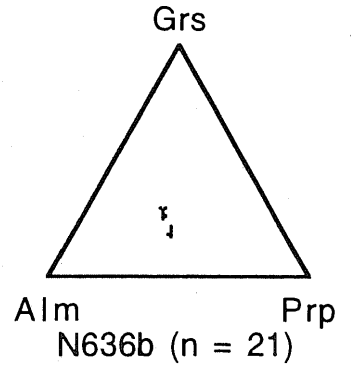
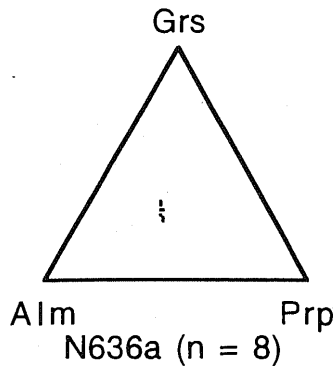
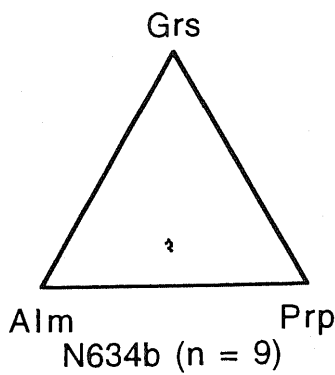
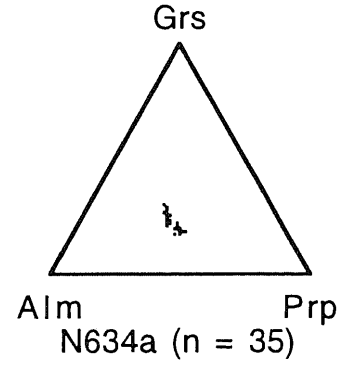
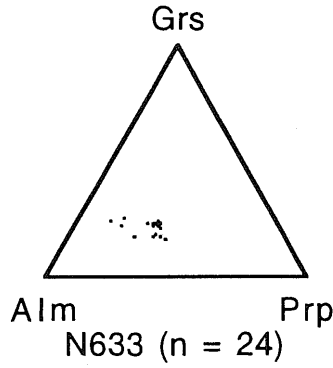
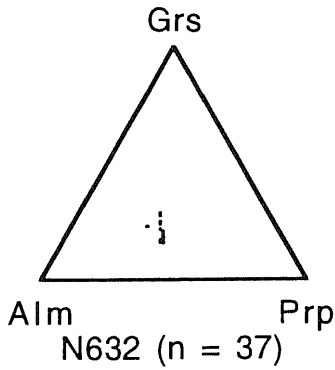
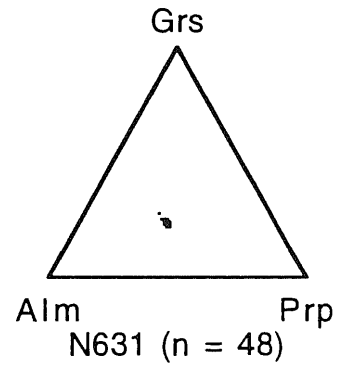
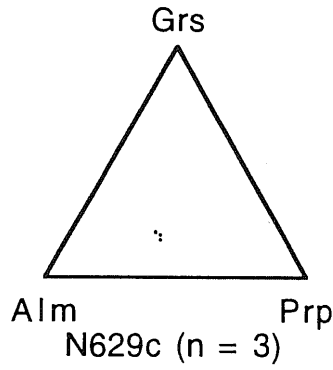
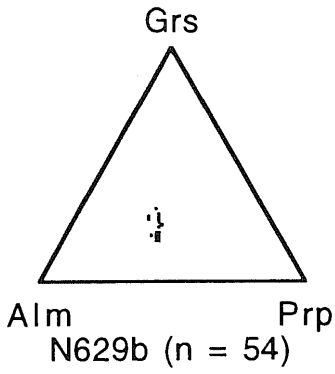
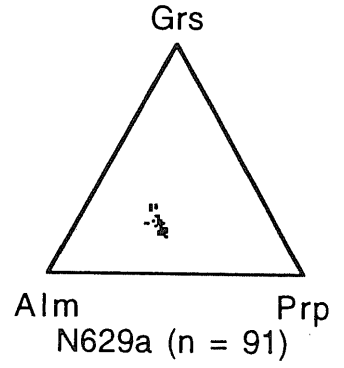
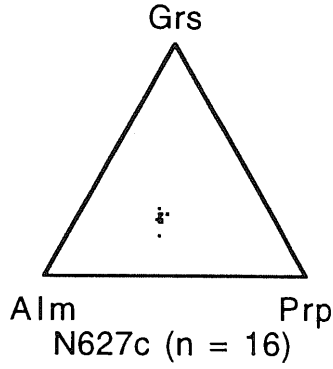
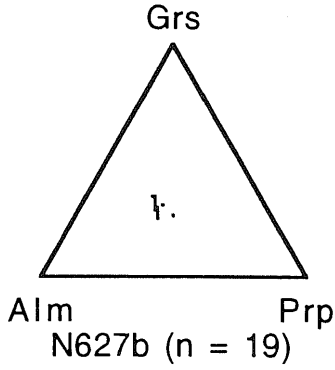
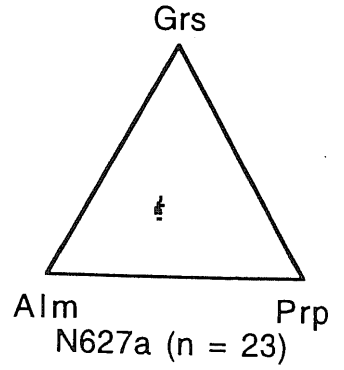
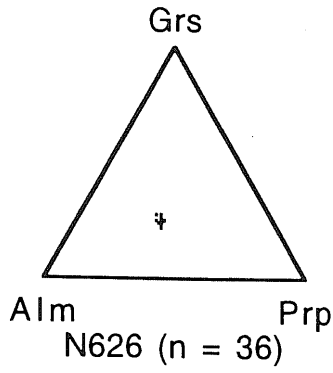
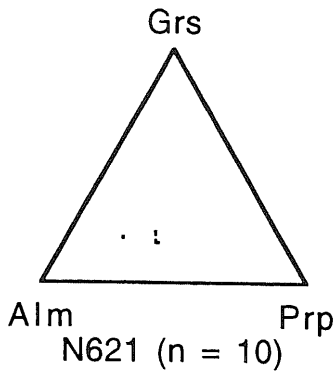
## Appendix 4:

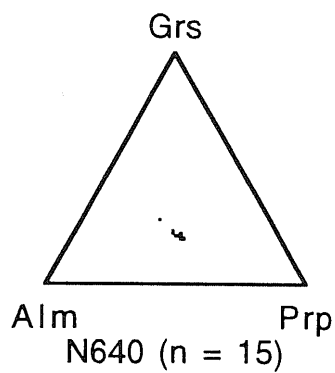
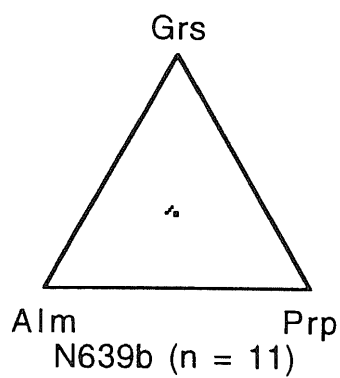
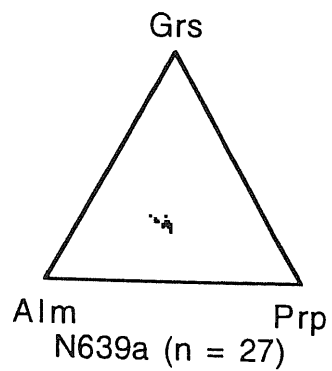
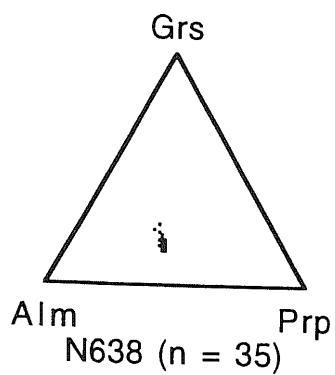
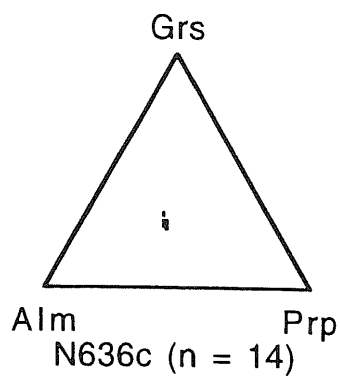
**Compositional triangular diagrams  
for garnet, clinopyroxene,  
orthopyroxene, and amphibole  
of samples from the Jijal complex  
and K27**

**4a) North to South (Grs-Alm-Prp) diagrams for garnet of the northern series**

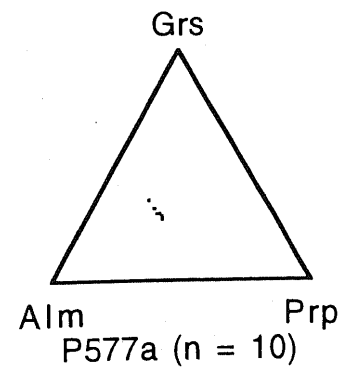
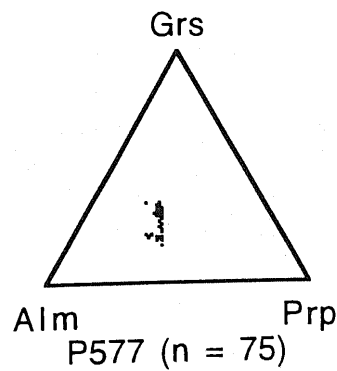
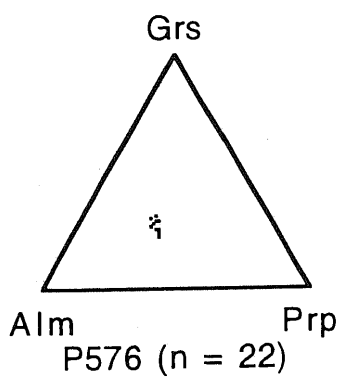
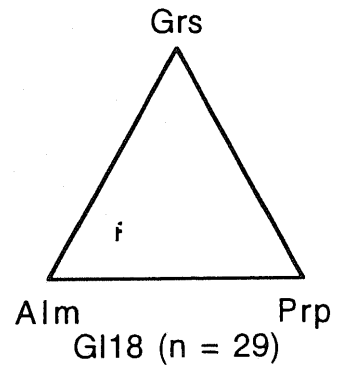
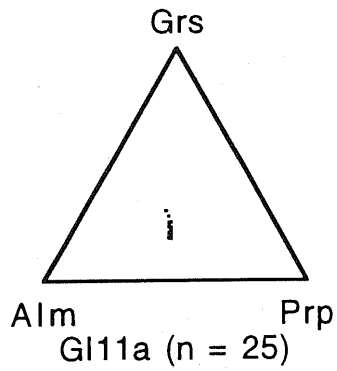
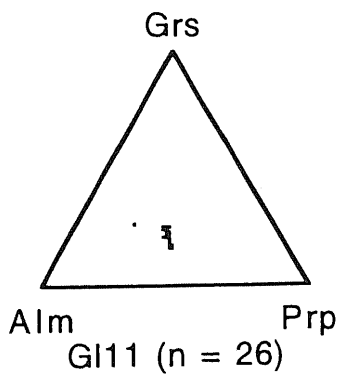
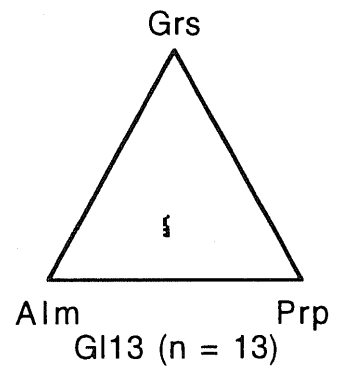
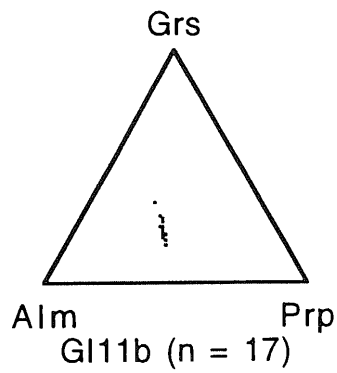
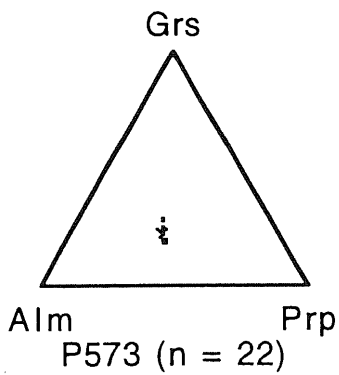
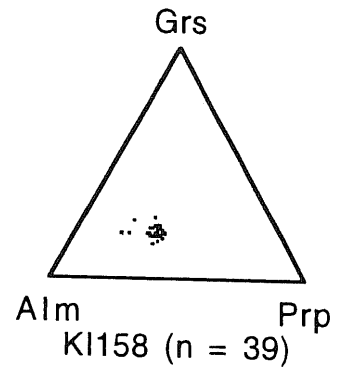
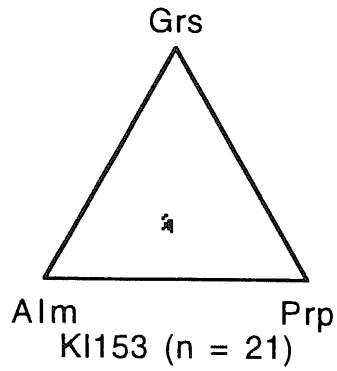
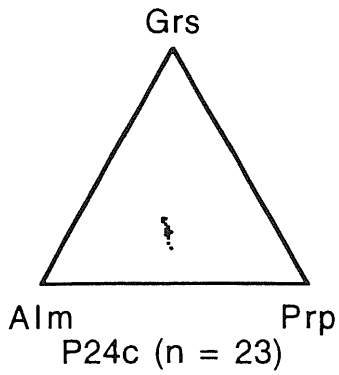


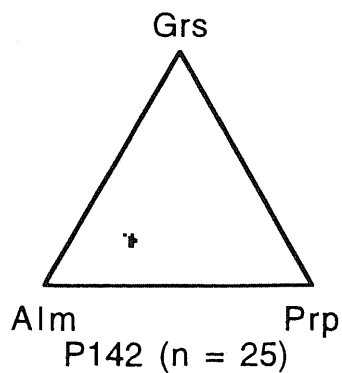
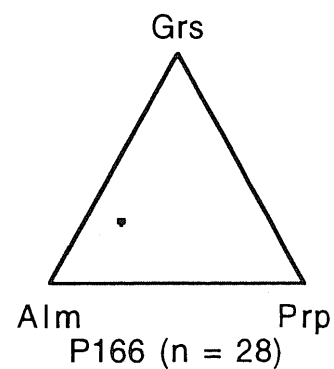
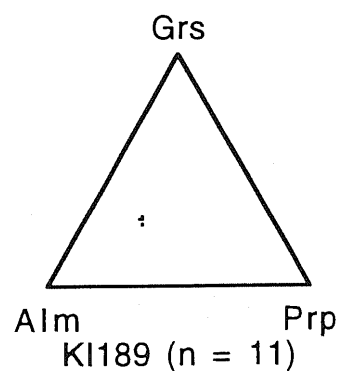
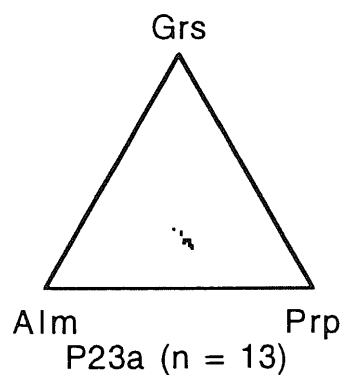
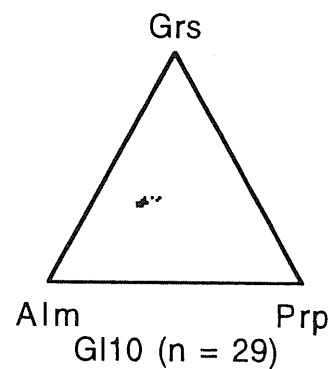
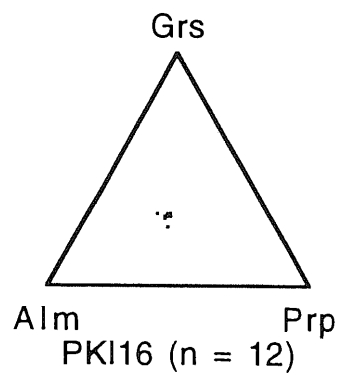
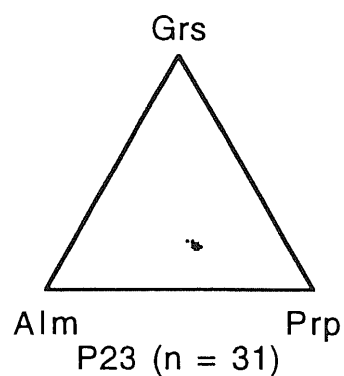
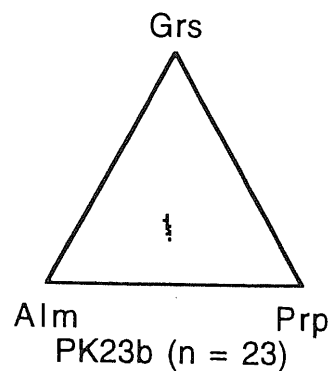
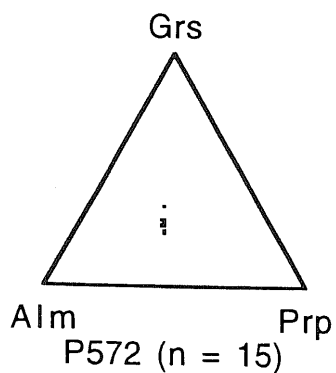
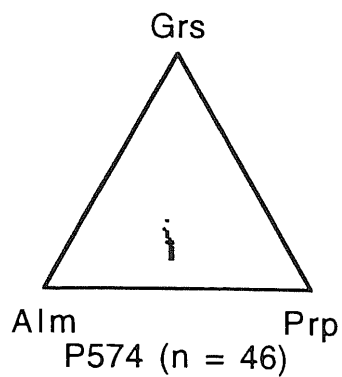




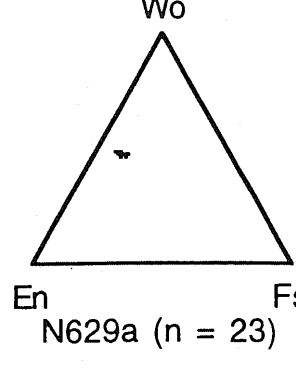
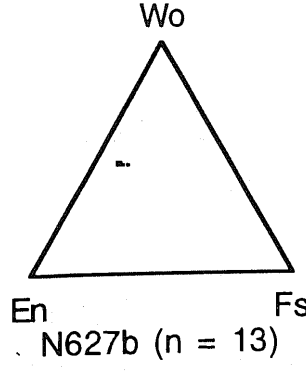
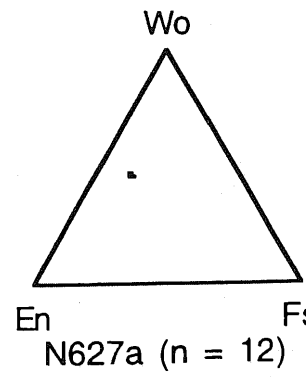
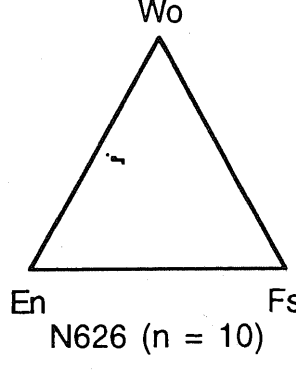
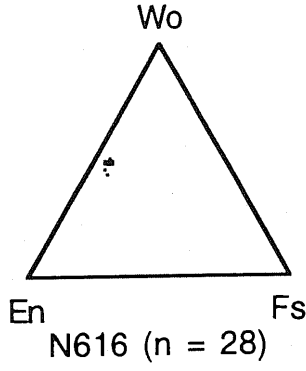
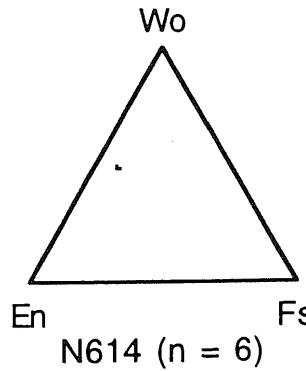
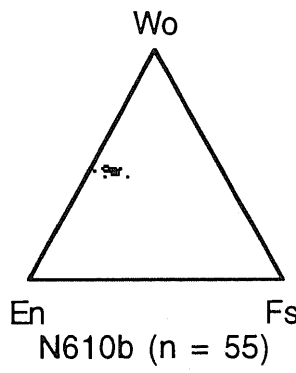
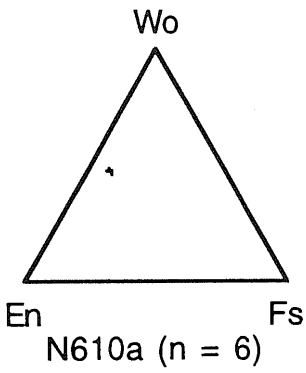
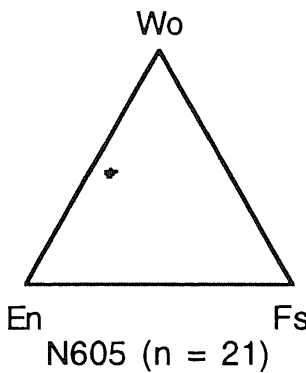
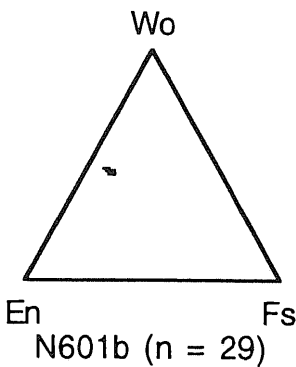
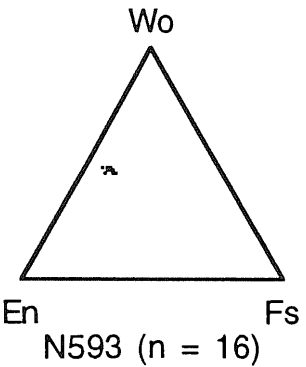
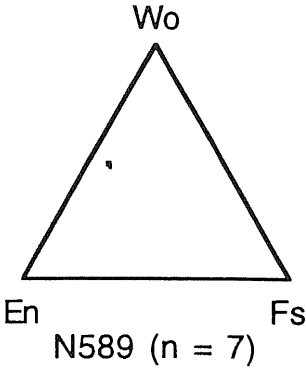


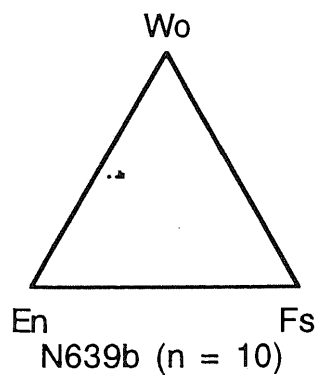
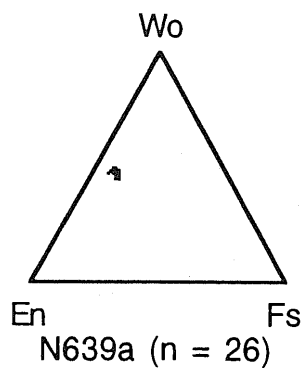
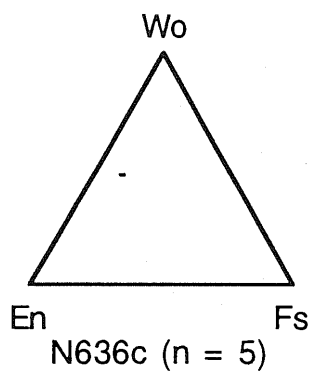
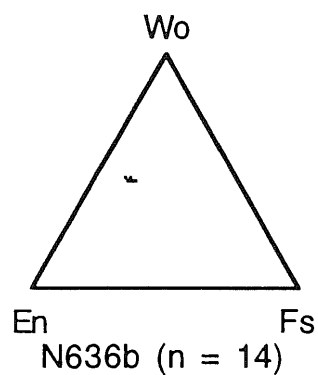
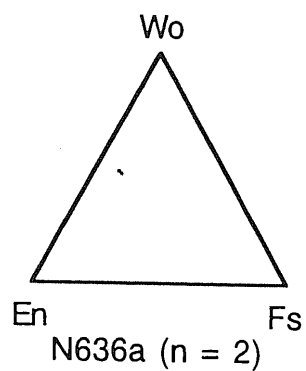
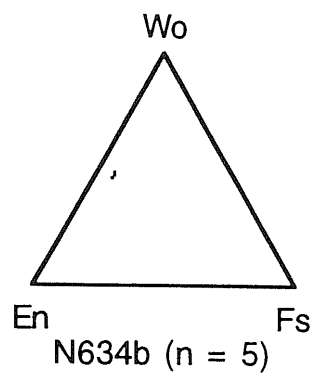
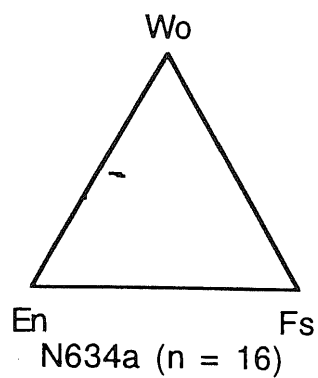
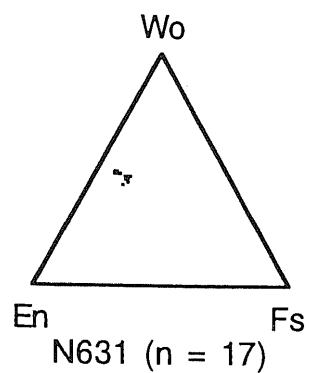
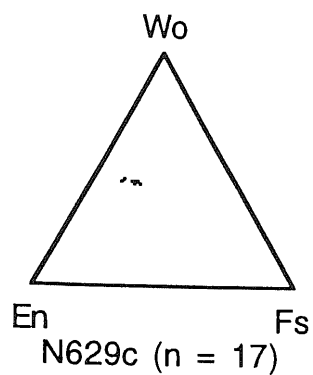
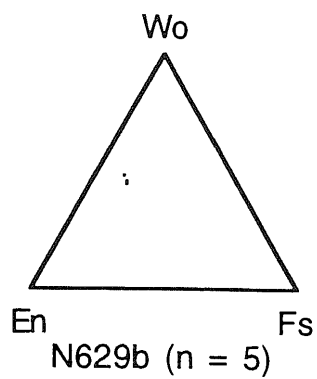
**4b) North to South (Grs-Alm-Prp) diagrams for garnet of the southern series**



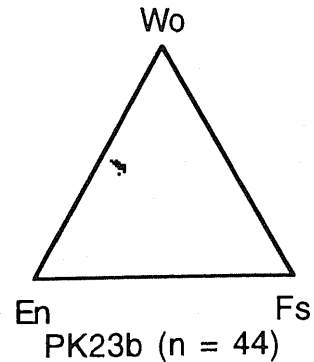
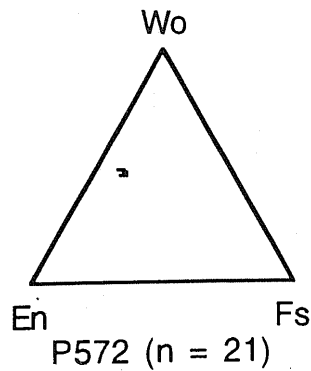
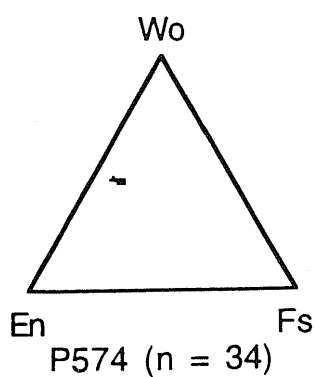
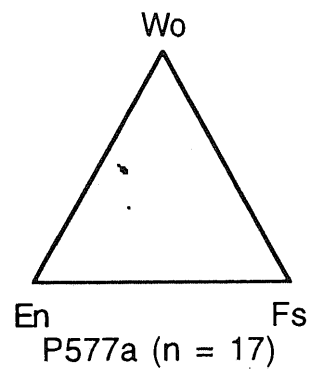
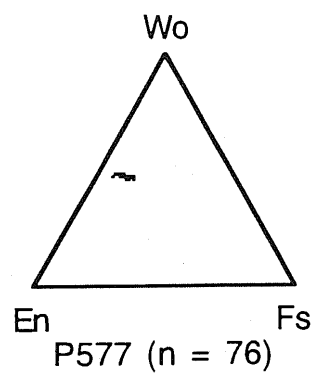
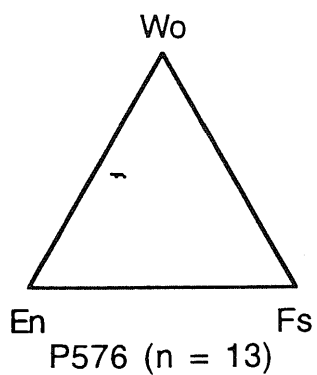
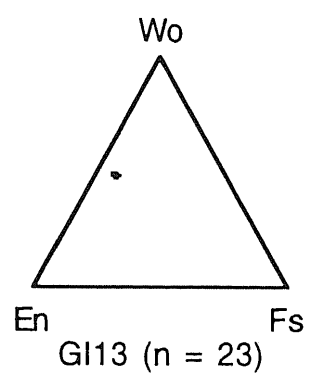
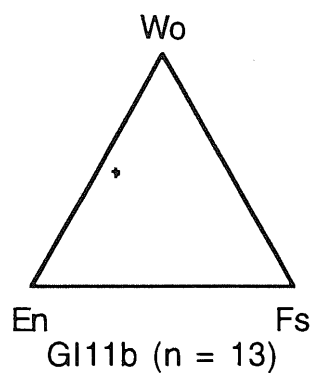
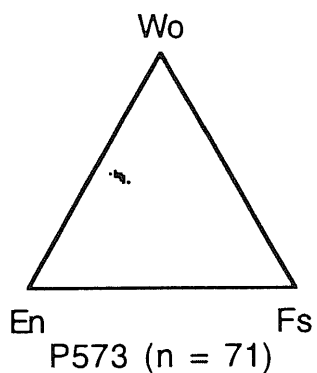
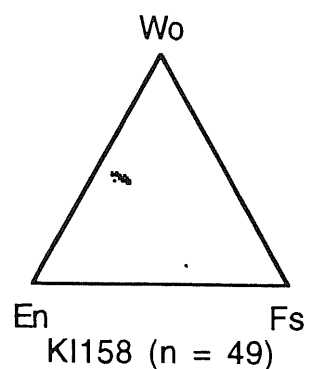
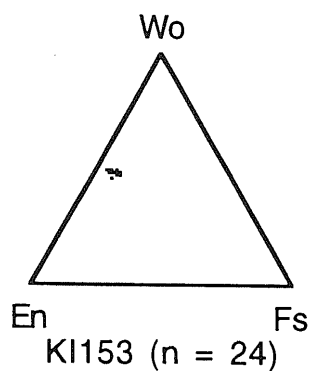
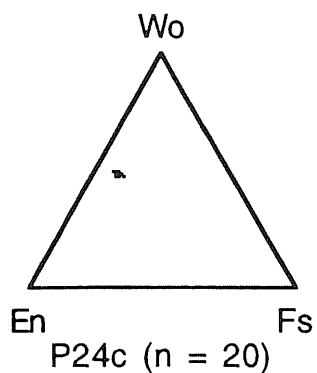


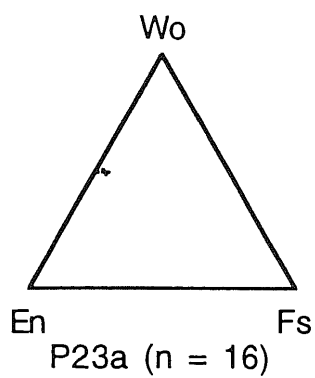
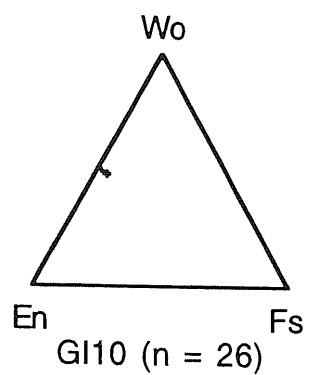
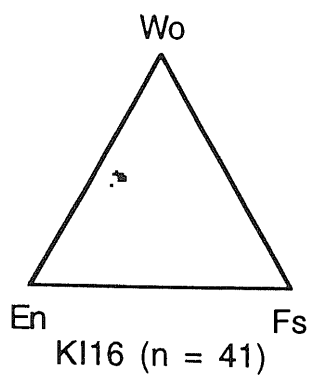
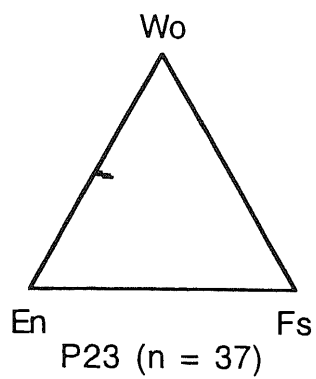
4c) North to South (Wo-En-Fs) diagrams for clinopyroxene of the northern series



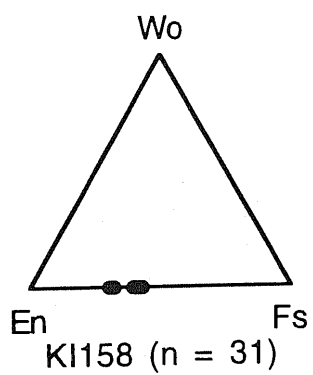


**4d) North to South (Wo-En-Fs) diagrams for clinopyroxene and orthopyroxene of the southern series**





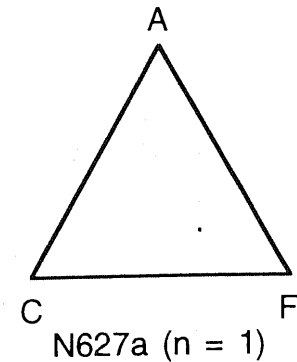
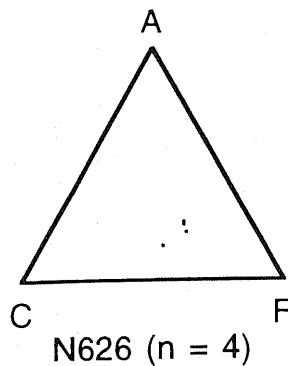
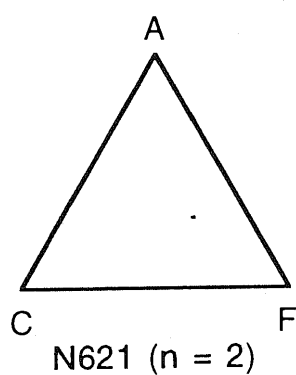
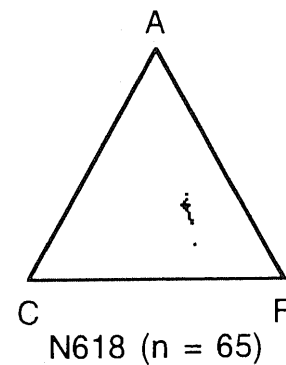
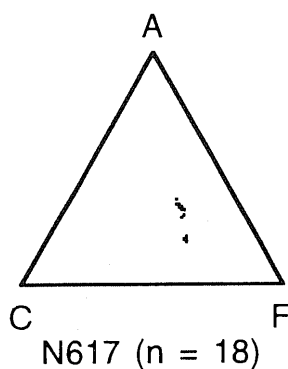
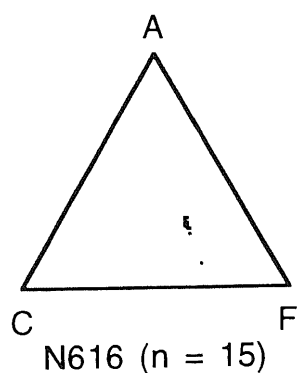
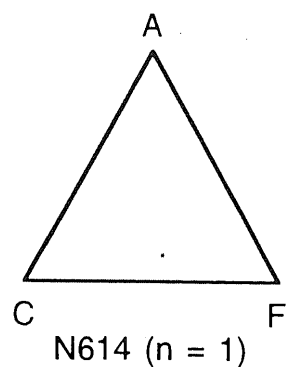
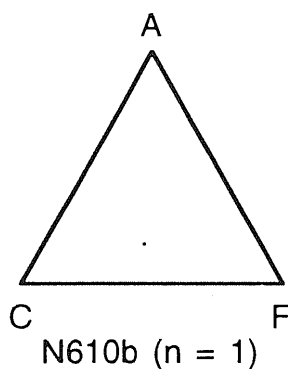
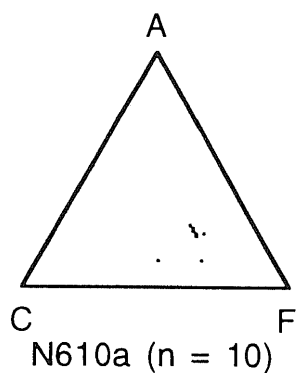
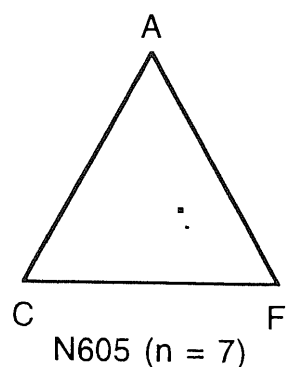
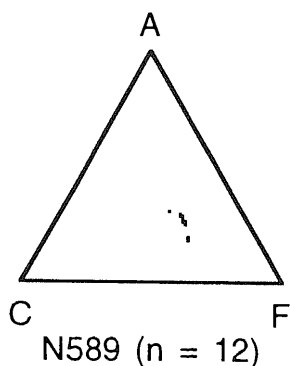
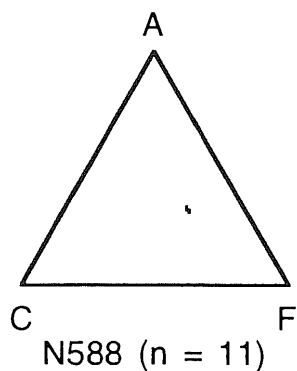
orthopyroxene:

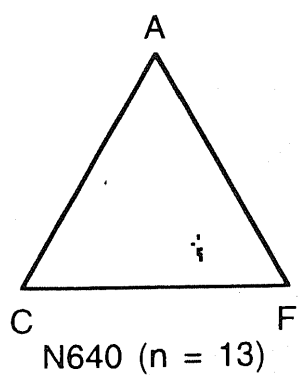
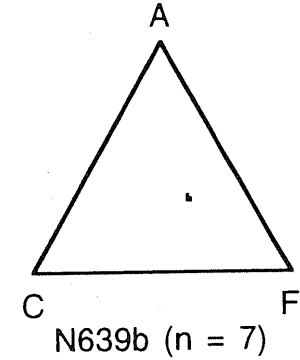
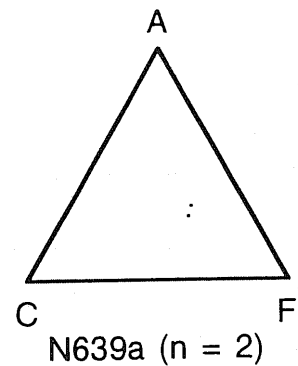
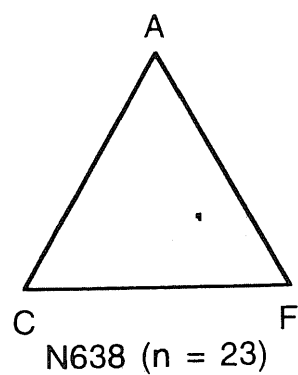
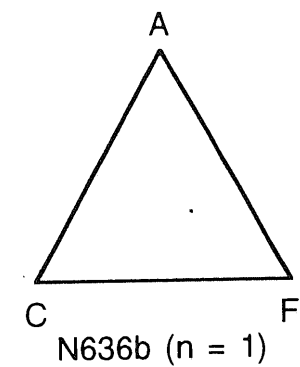
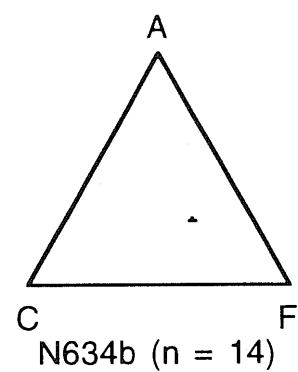
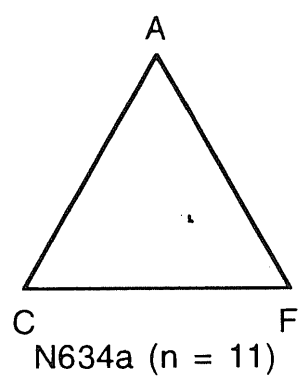
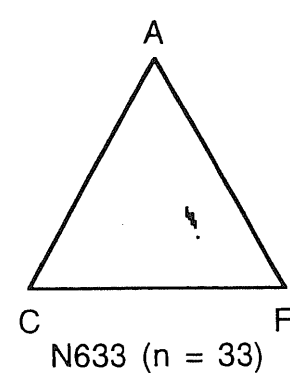
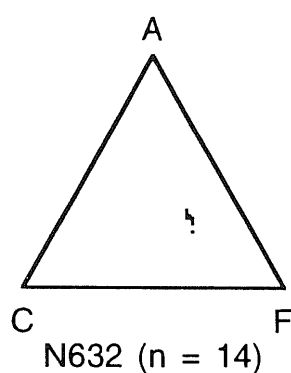
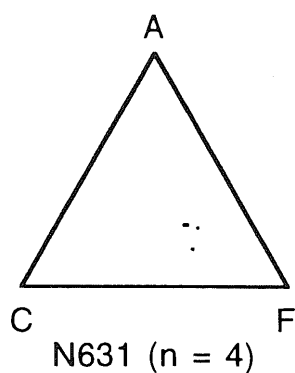
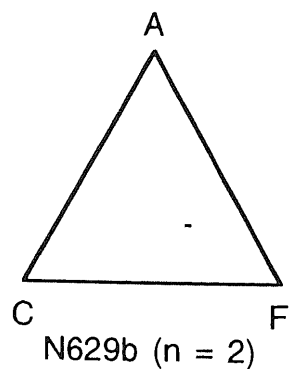
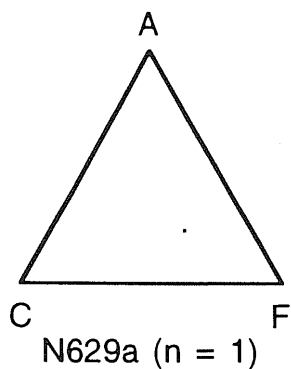
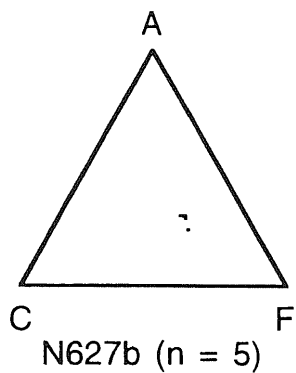




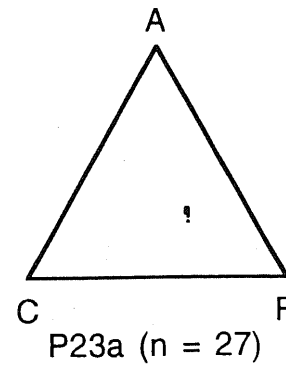
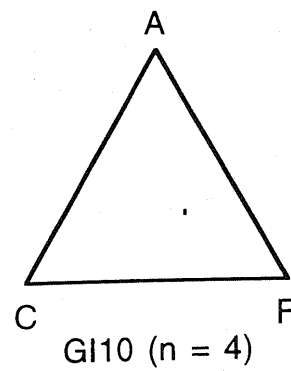
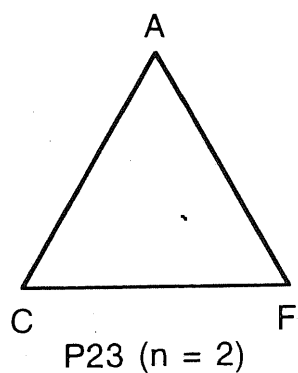
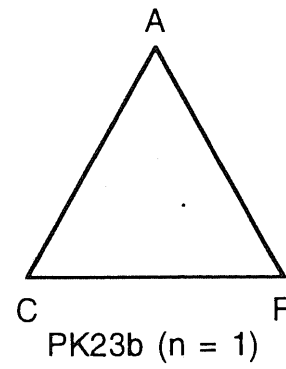
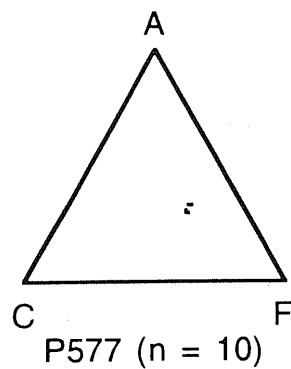
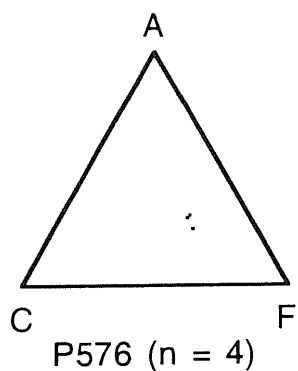
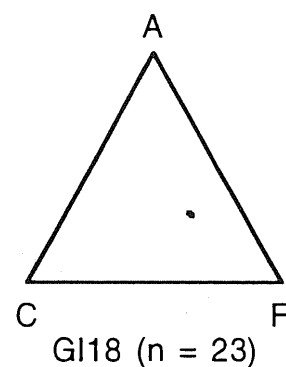
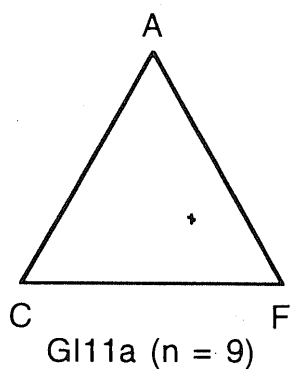
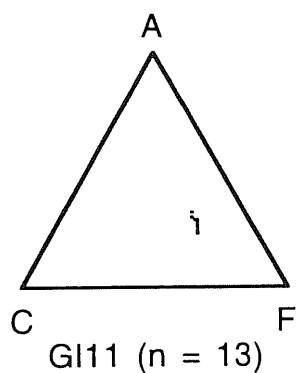
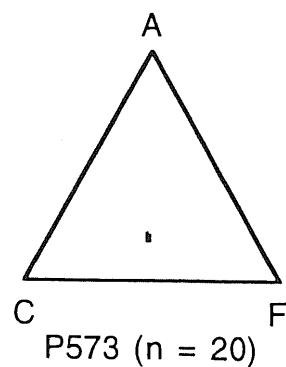
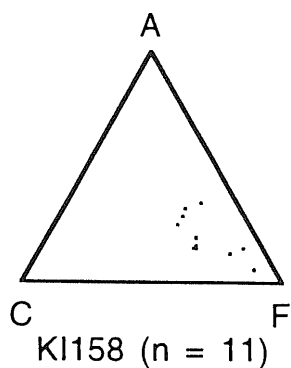
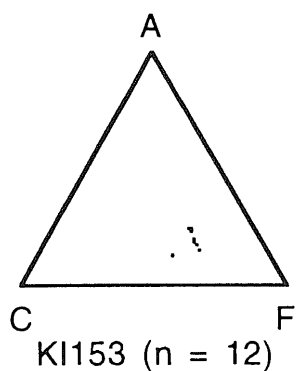
4e) North to South ACF ( $\text{Al}_2\text{O}_3\text{-CaO-[FeO-MgO]}$ ) diagrams for amphibole of the northern series

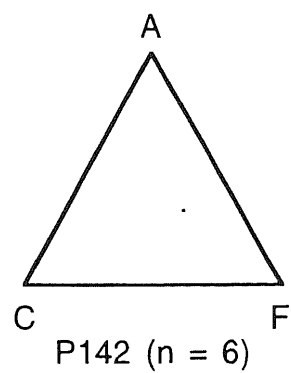
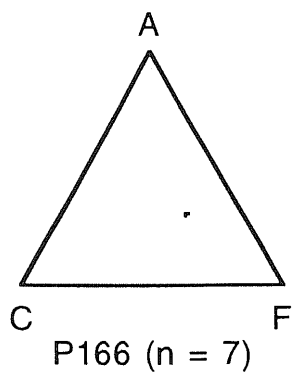
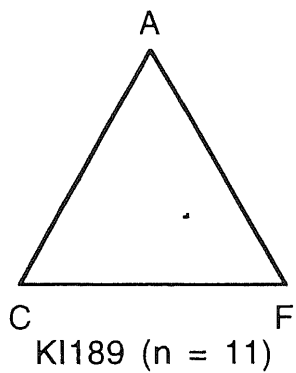
---





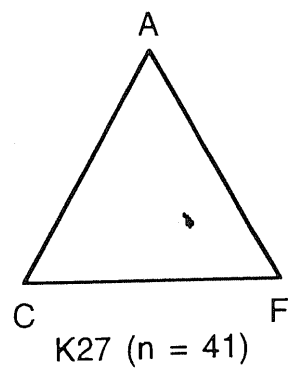
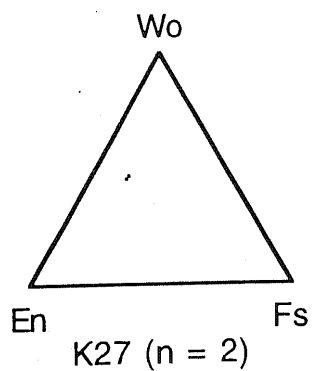
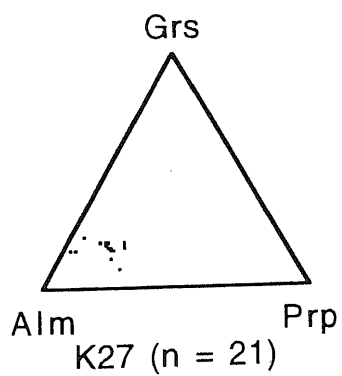
4f) North to South ACF ( $\text{Al}_2\text{O}_3$ - $\text{CaO}$ - $[\text{FeO-MgO}]$ ) diagrams for amphibole of the southern series





**4g) Compositional triangular diagrams for garnet, clinopyroxene, and amphibole of sample K27 from the Kamila amphibolite belt/Chilas complex contact**

---

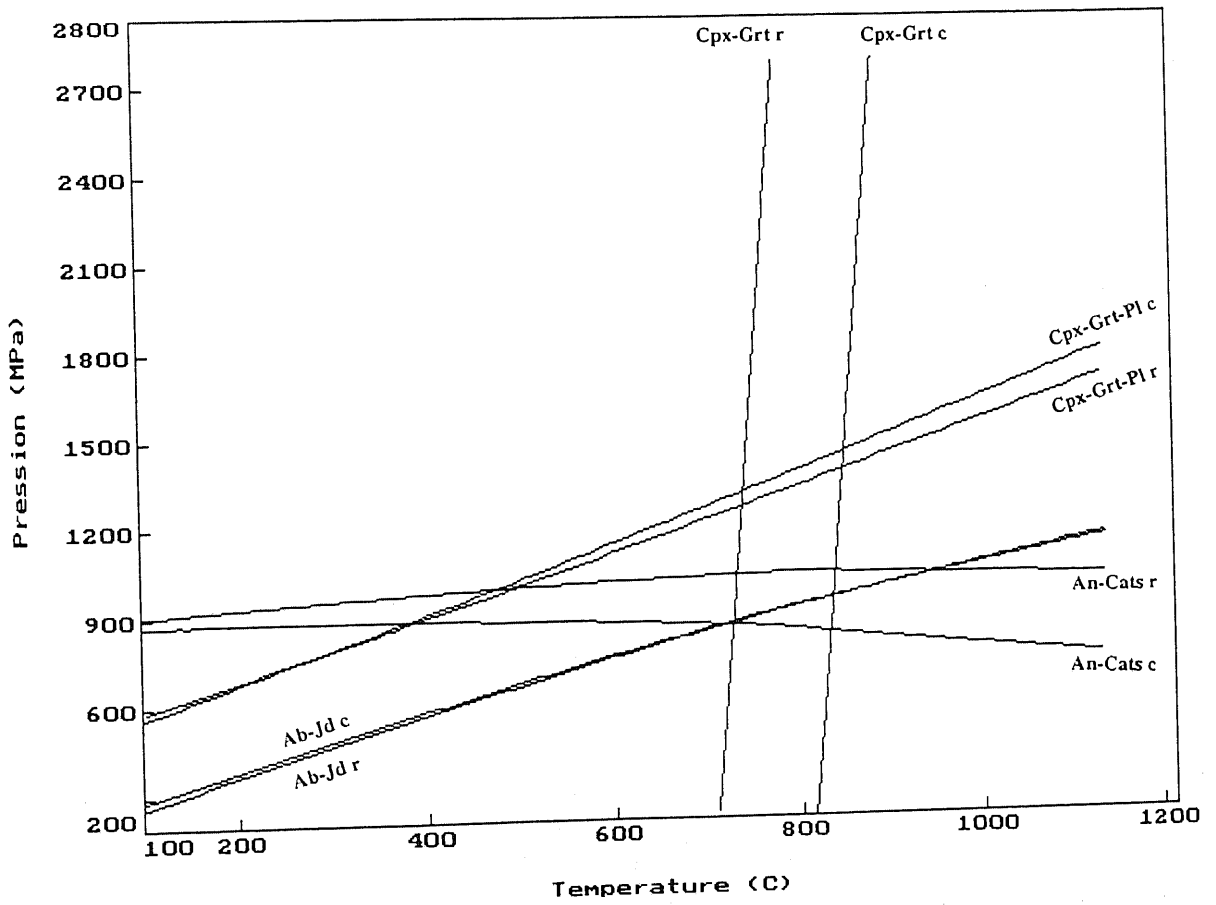


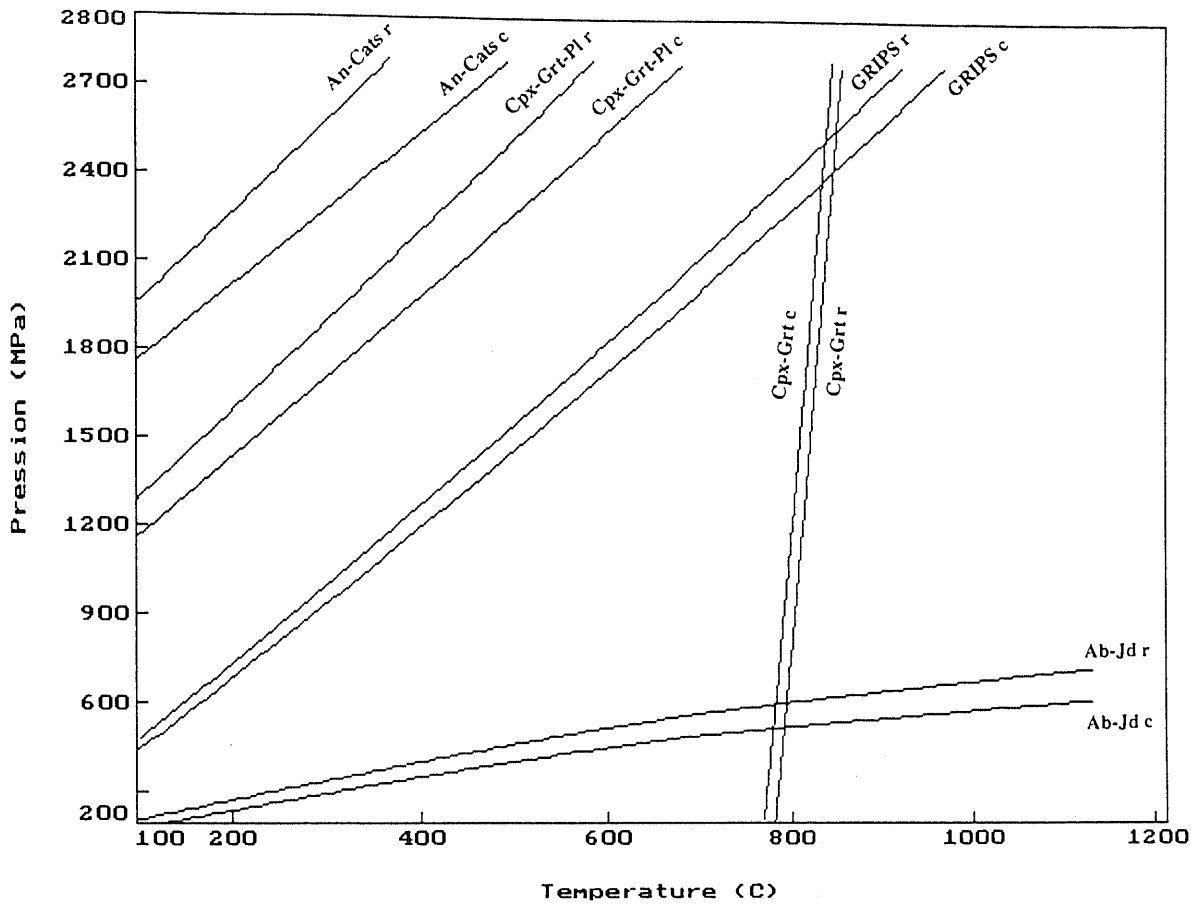
## Appendix 5:

**North to South  
pressure-temperature diagrams  
of selected samples from the Jijal complex**

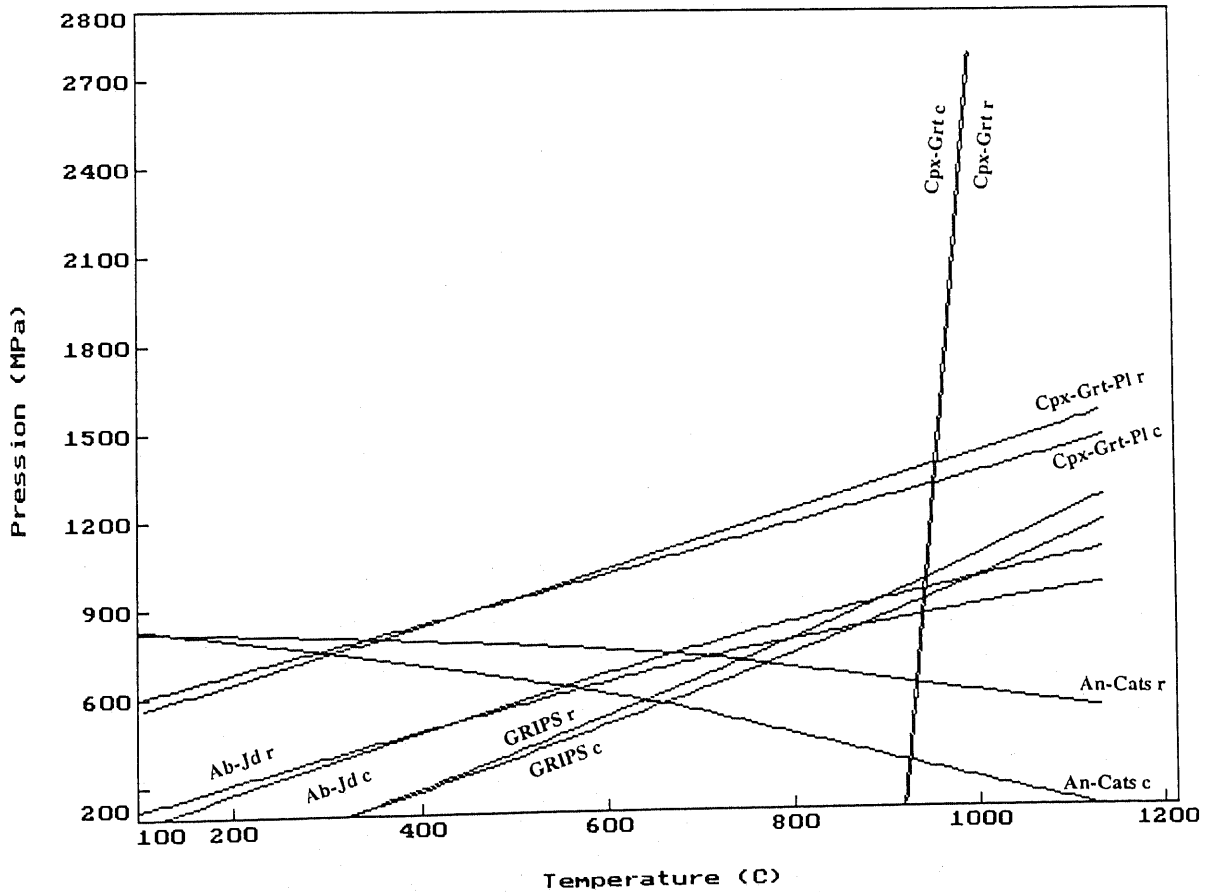
5a) North to South pressure-temperature diagrams of selected samples of the northern series

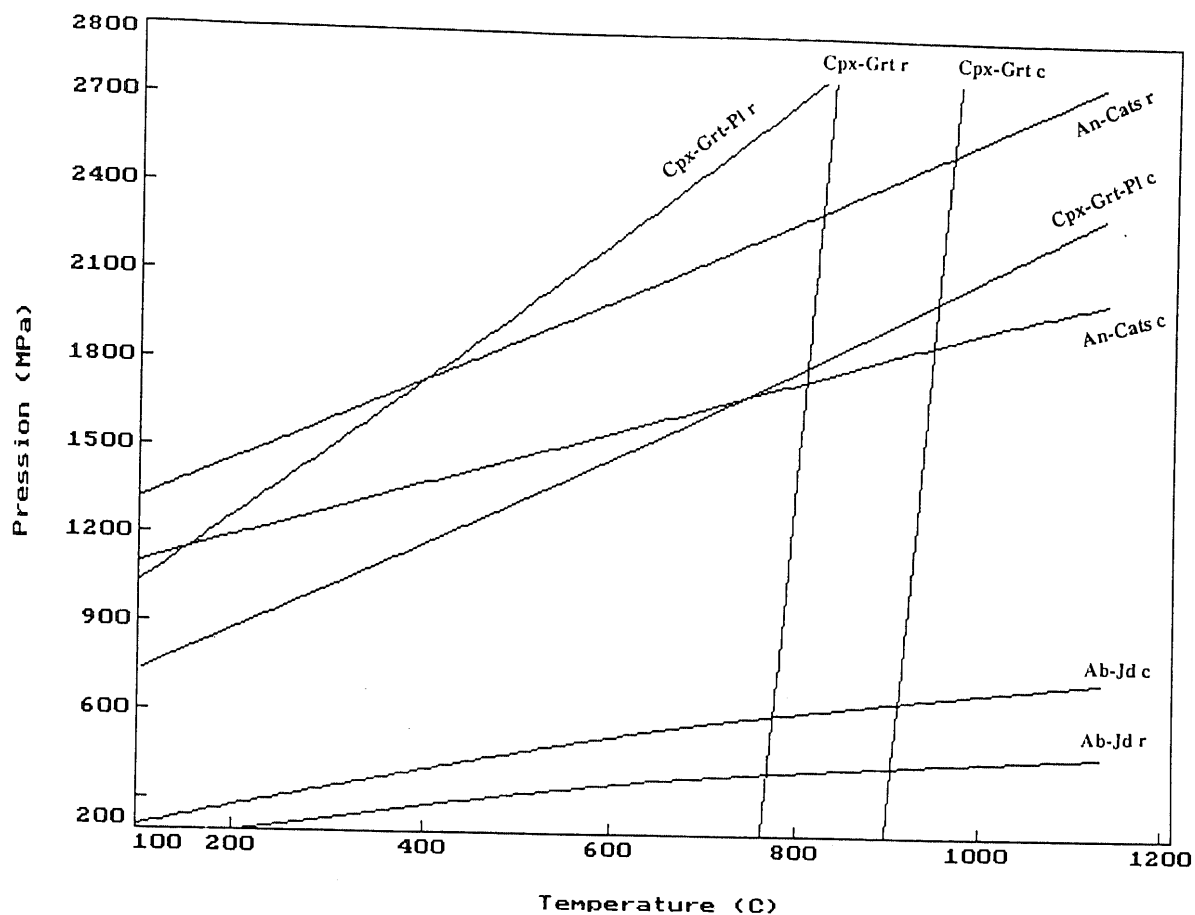
N 589



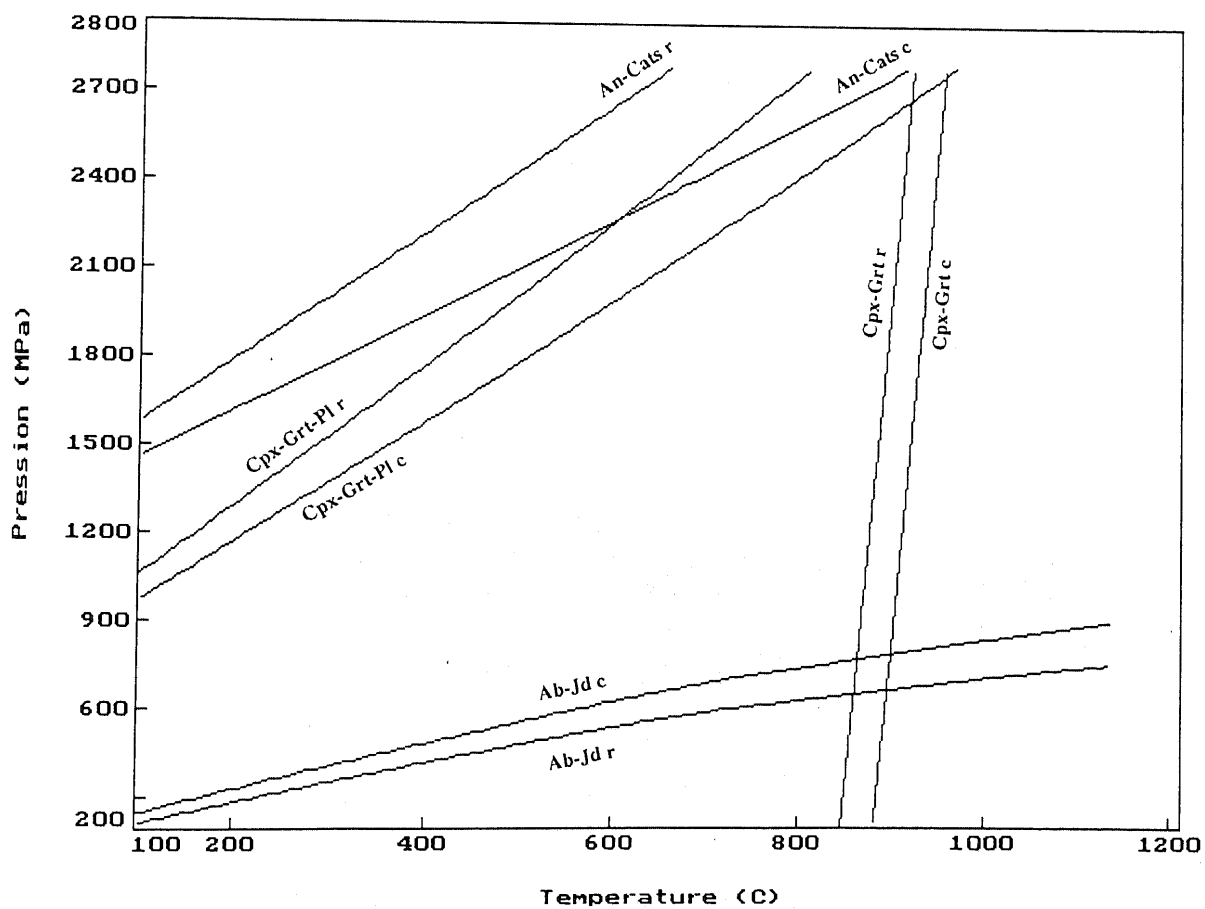


N 601b



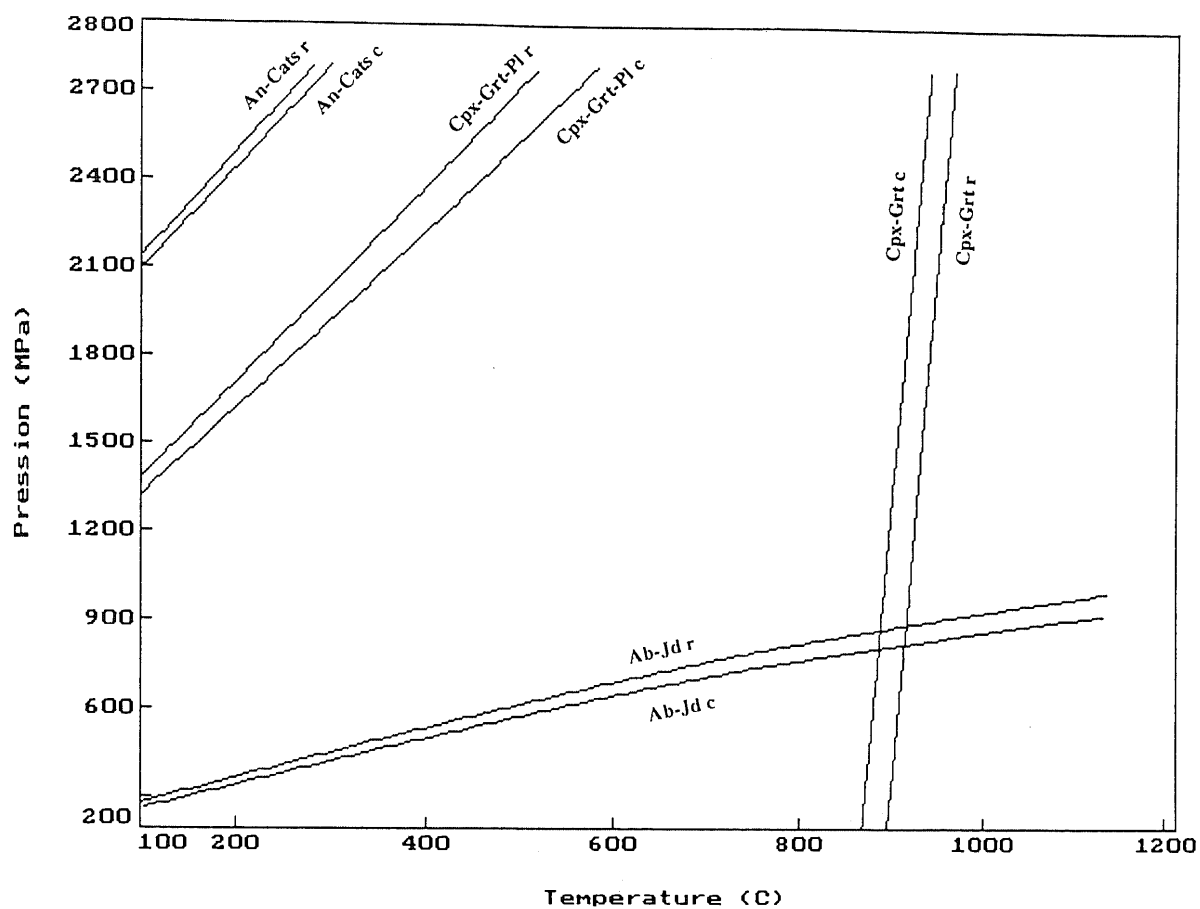


N 610b

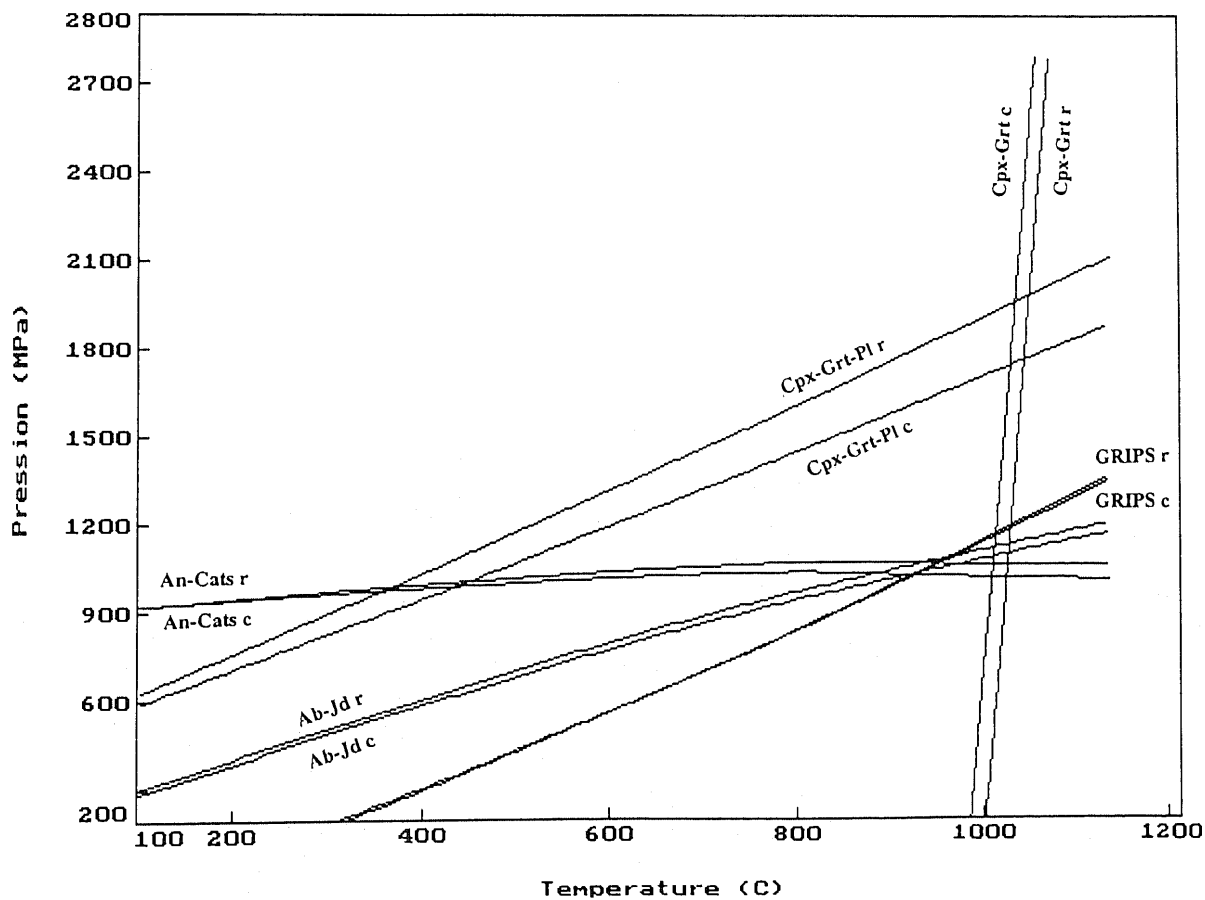




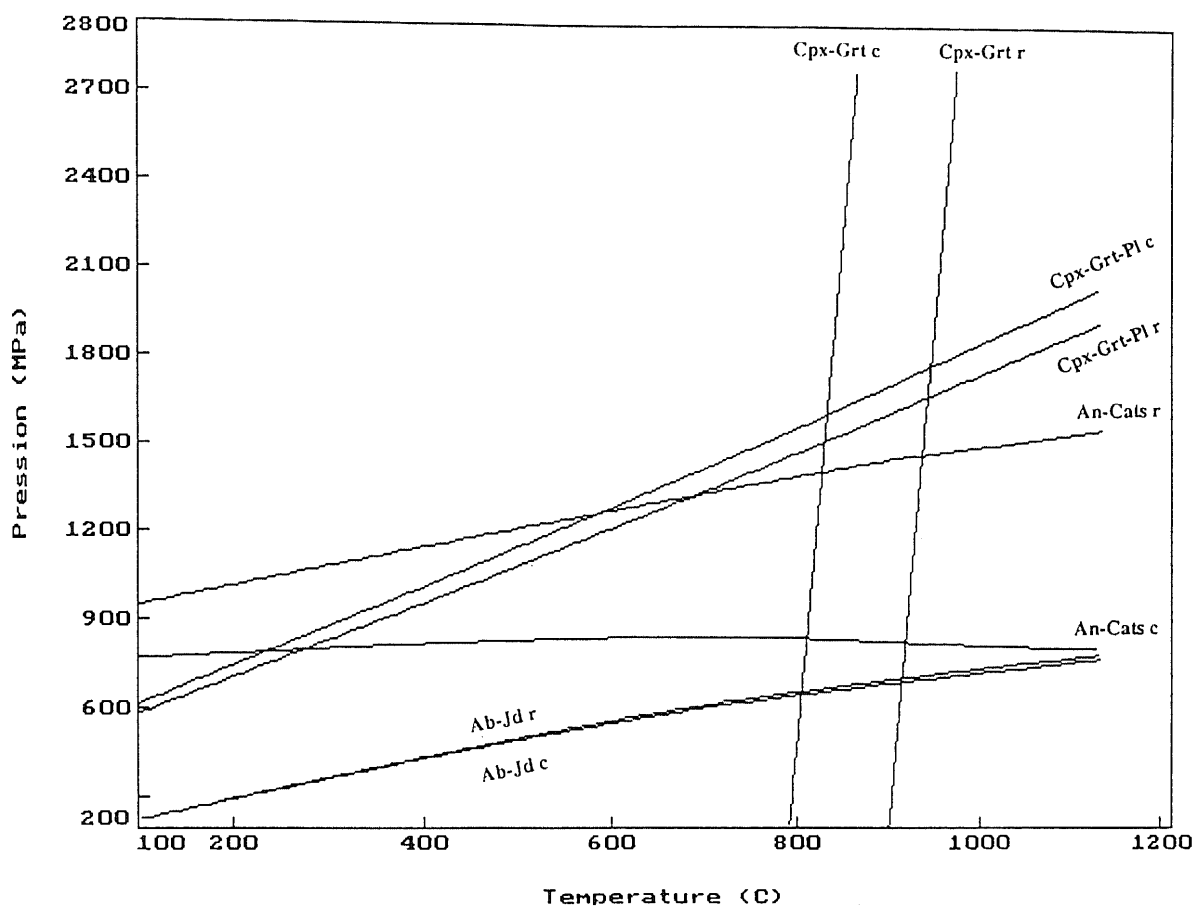
## N 614



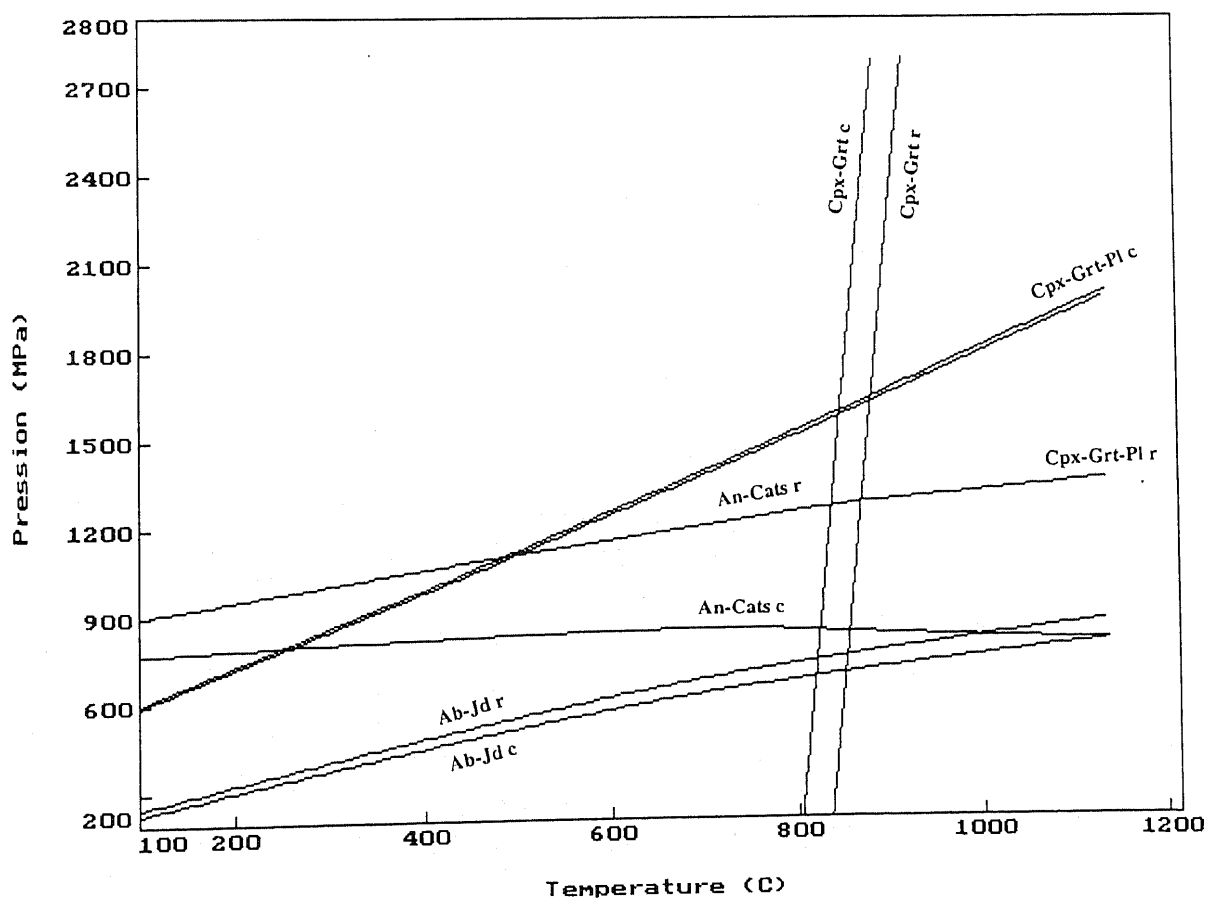
## N 627a



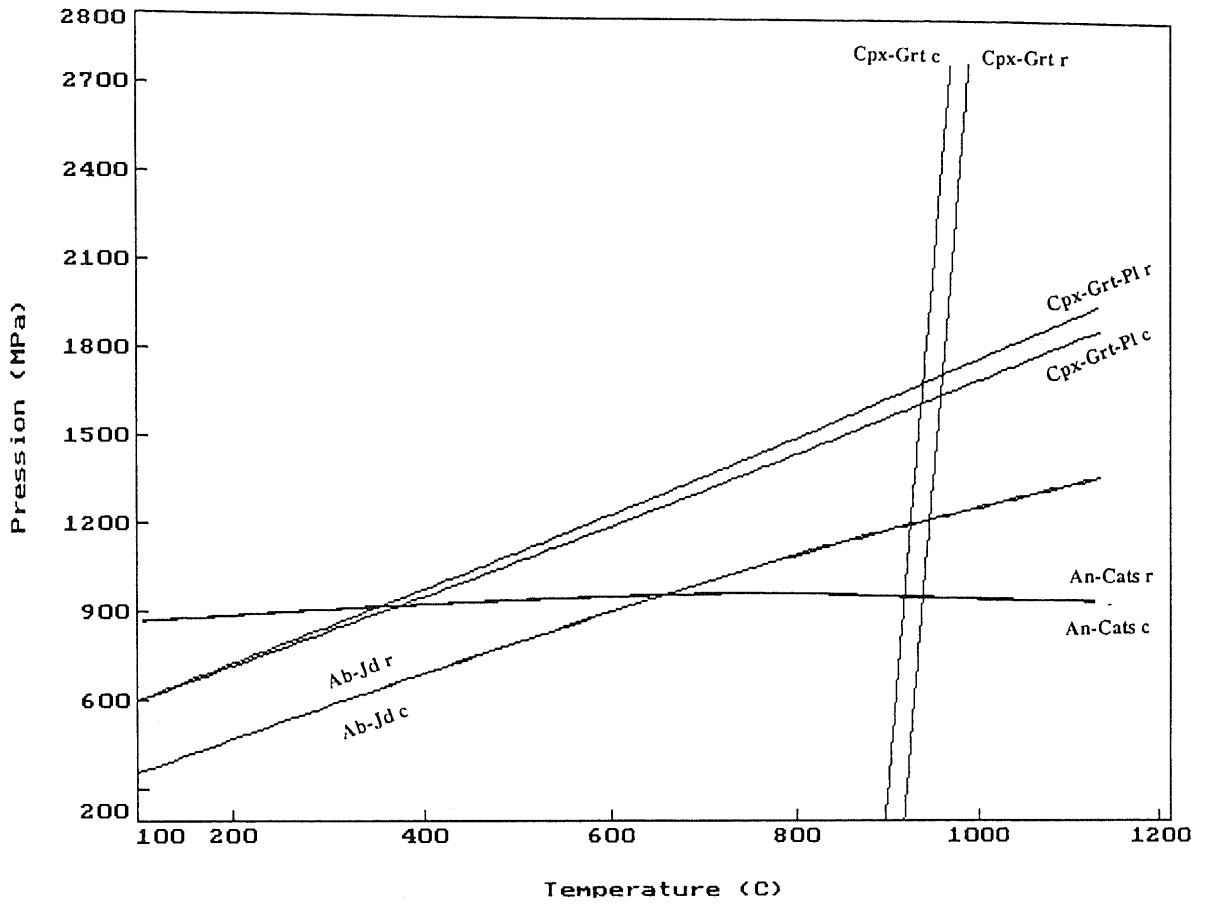
## N 629a (magmatic clinopyroxene)



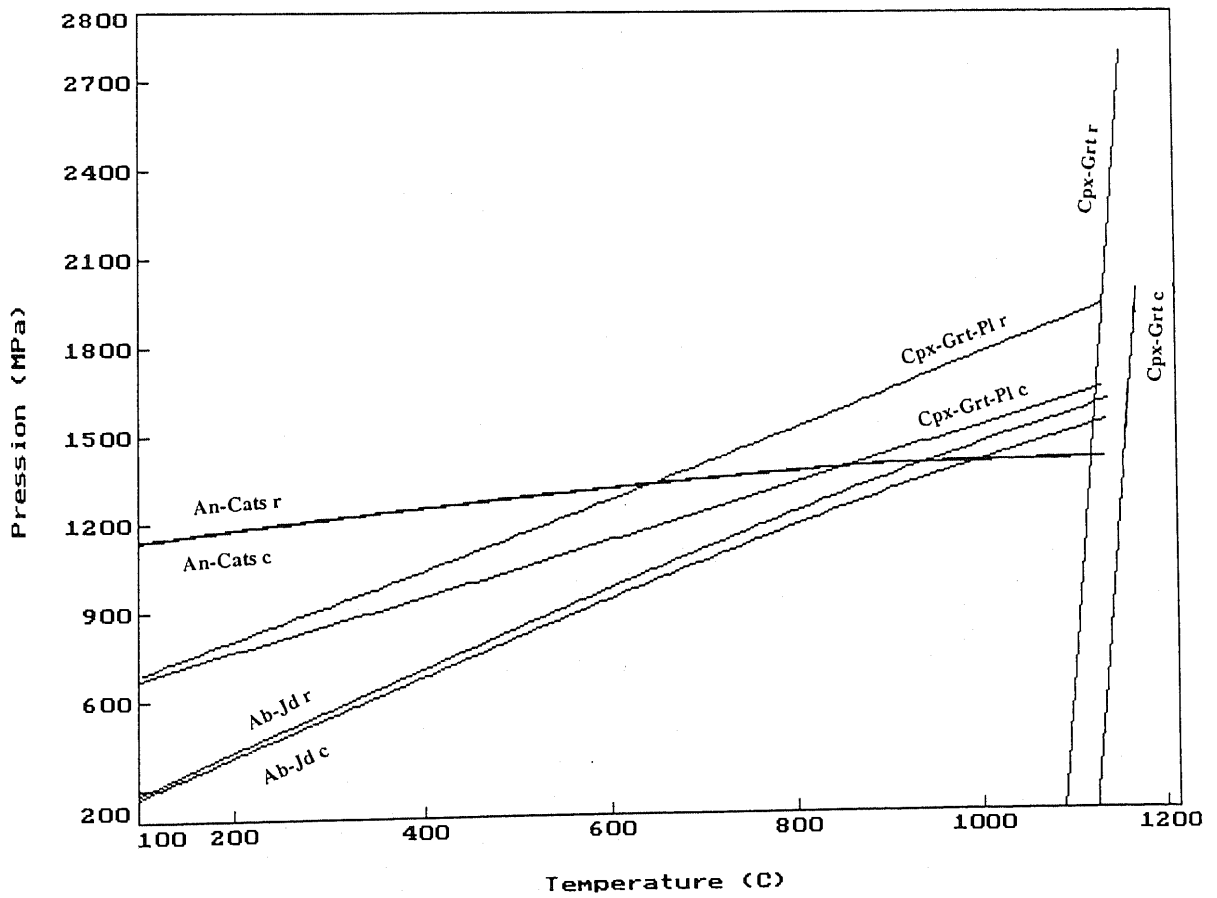
## N 629a (metamorphic clinopyroxene)

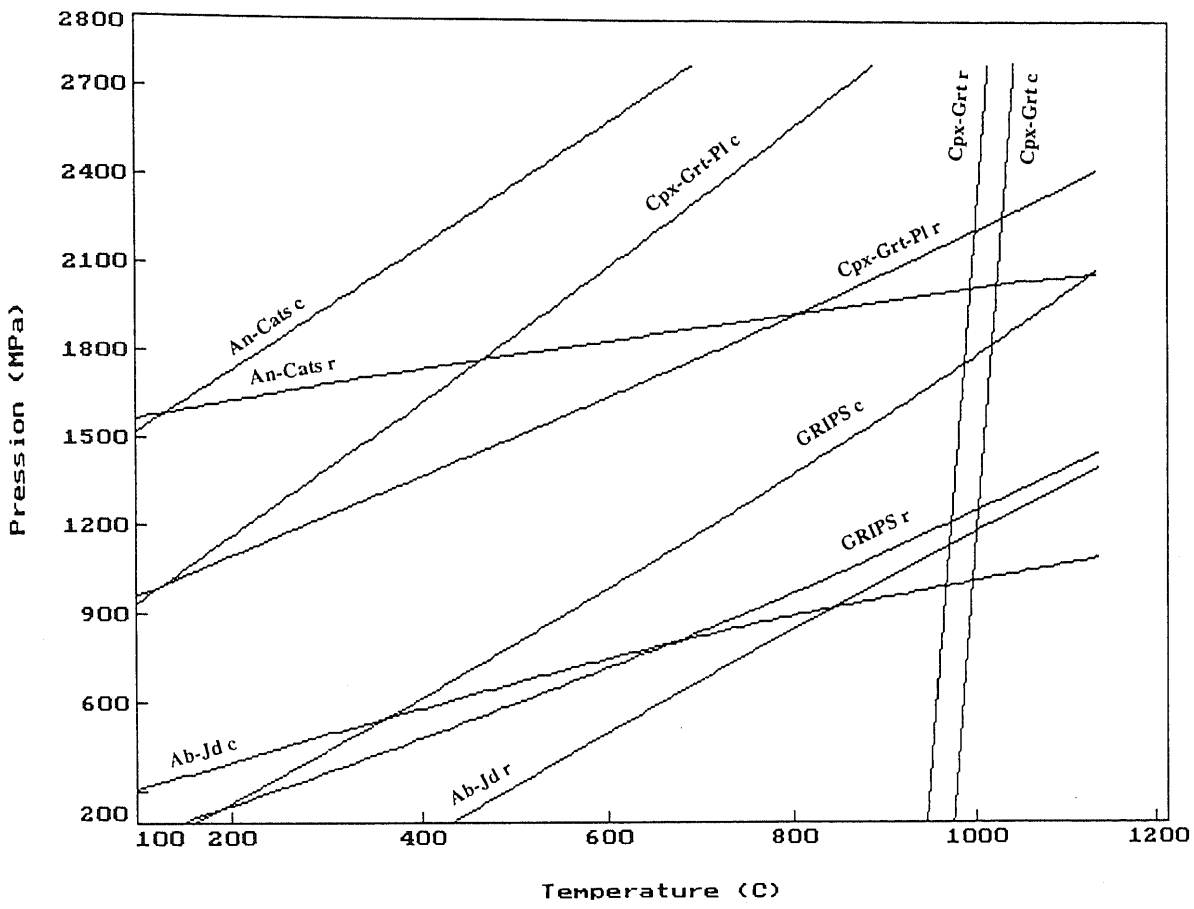


## N 634a



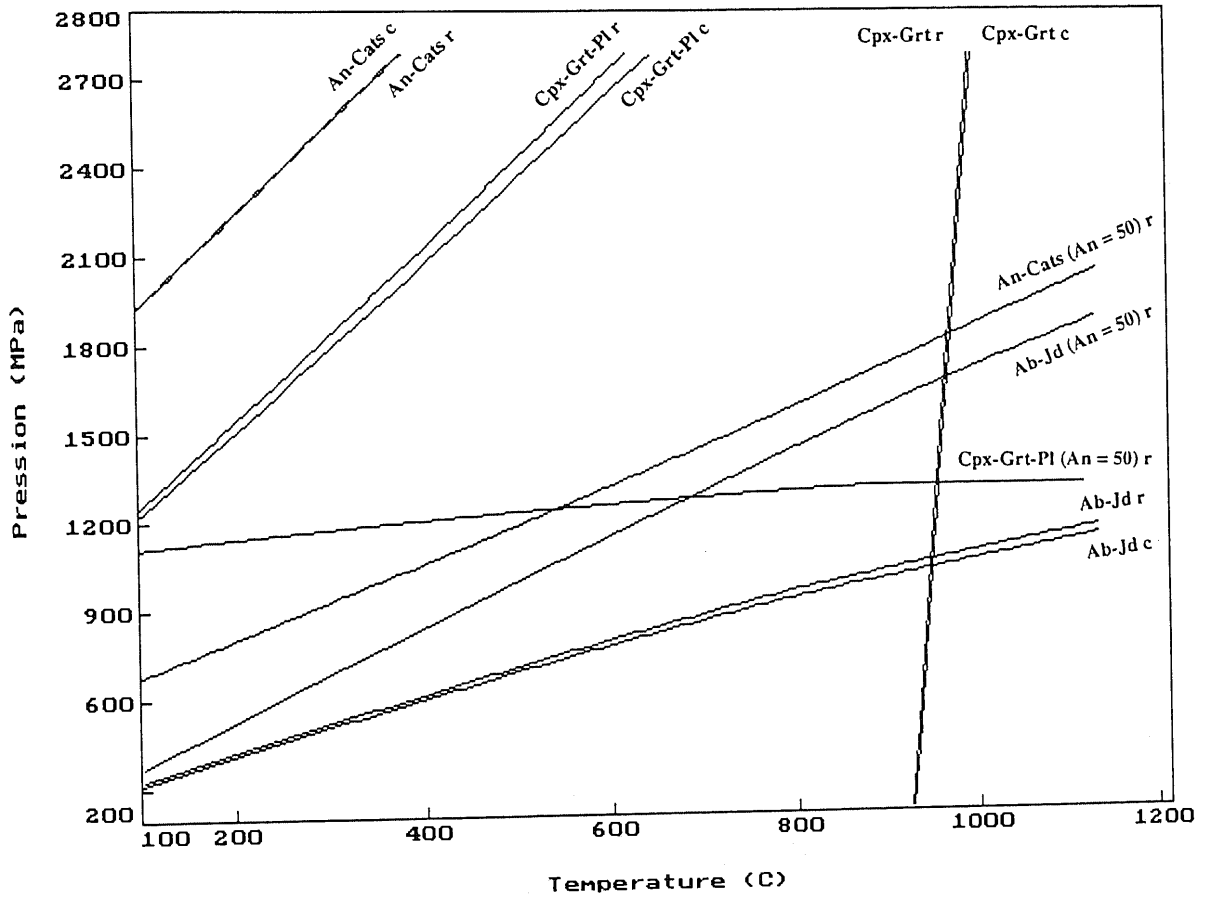
## N 636b



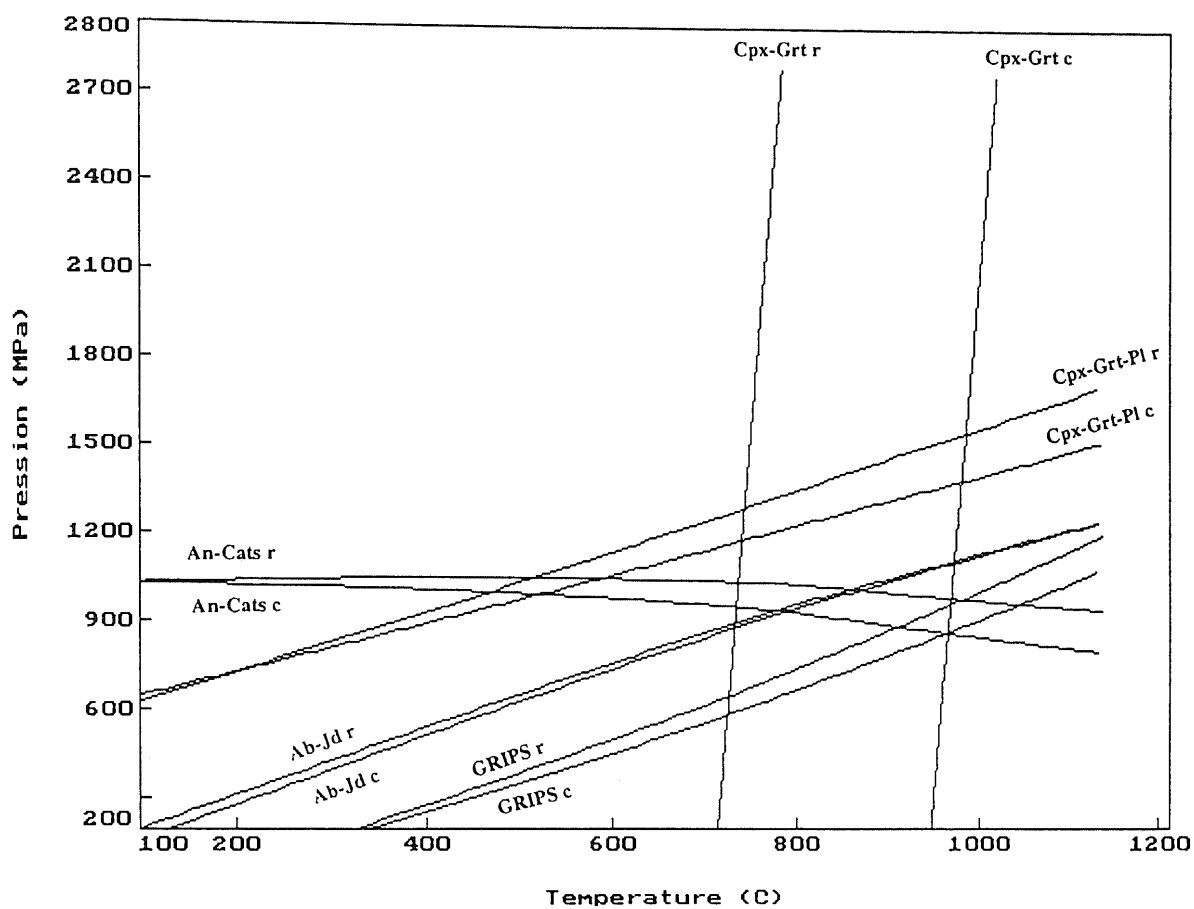


5b) North to South pressure-temperature diagrams of selected samples of the southern series

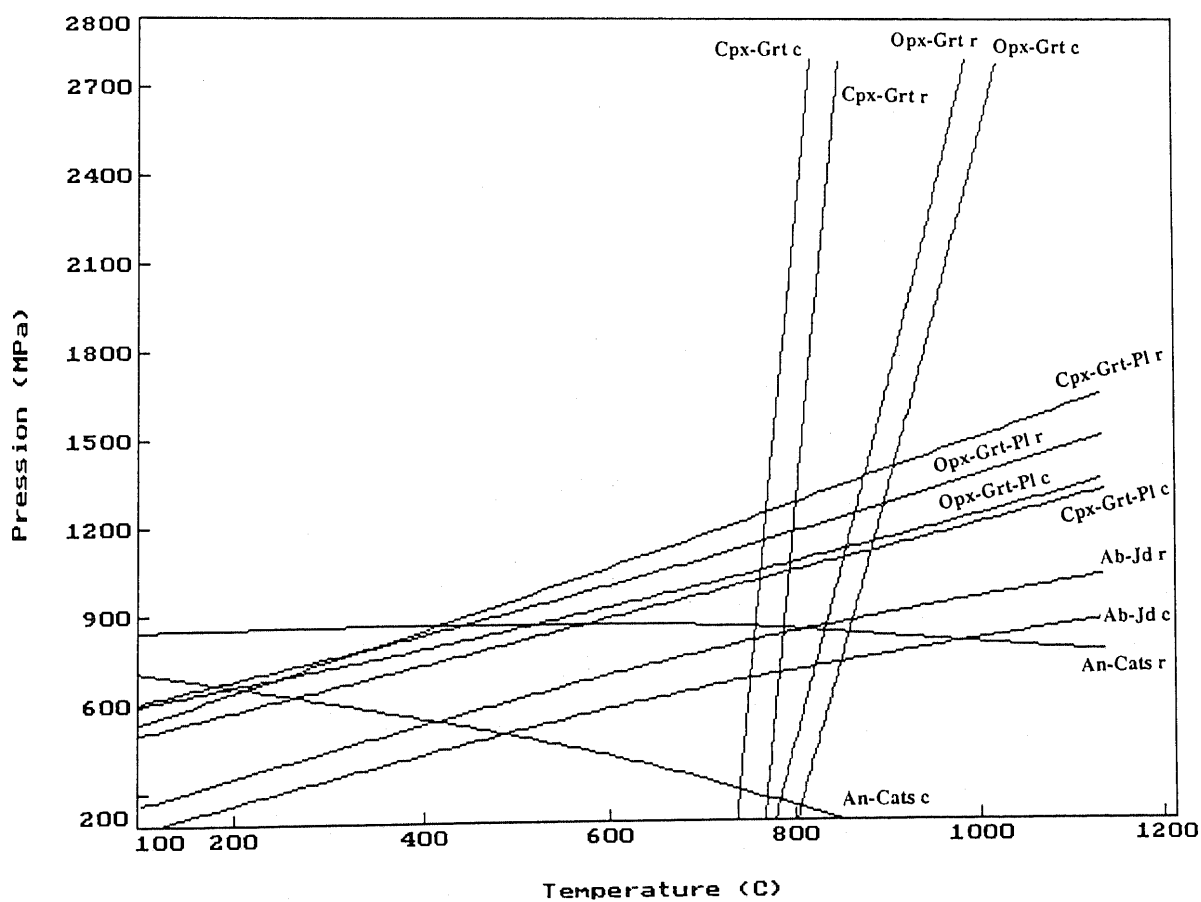
P 24c

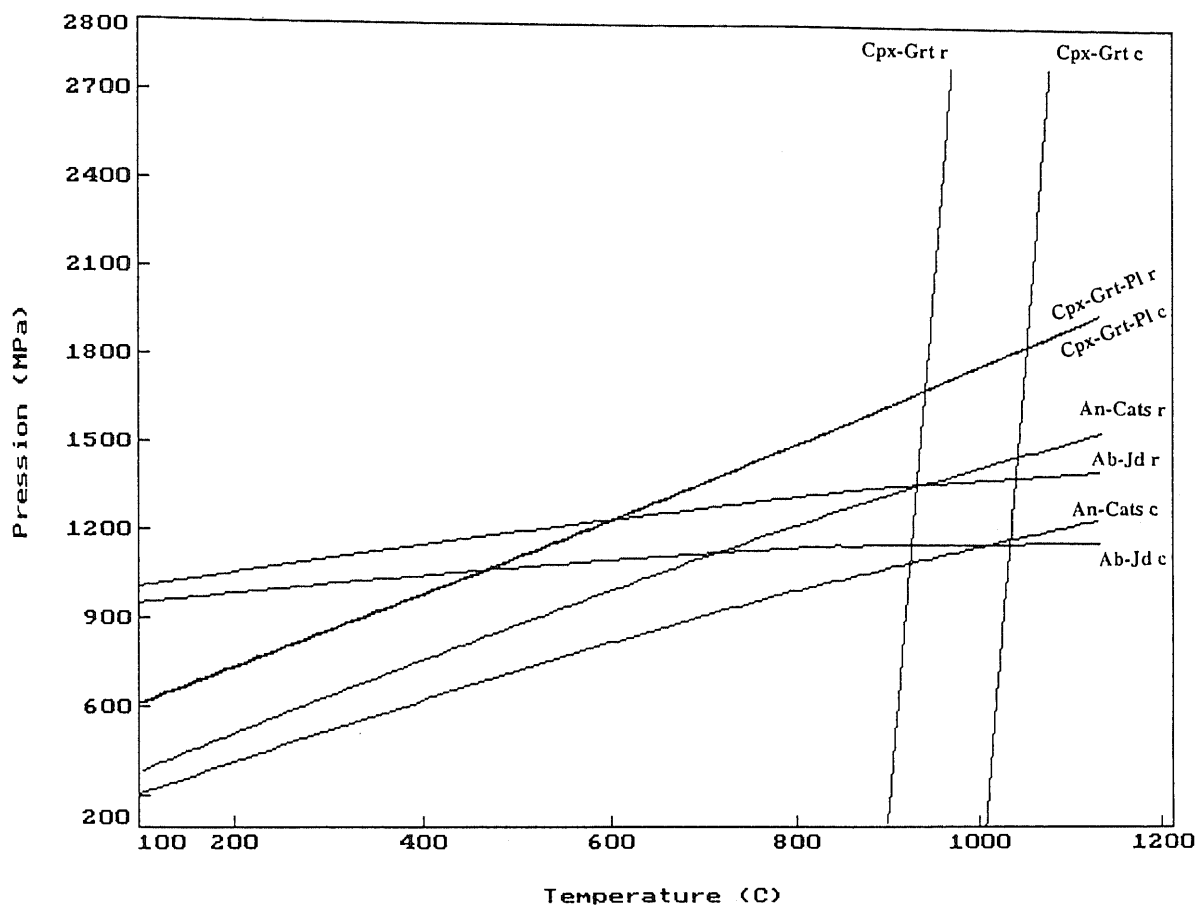


## KI 153

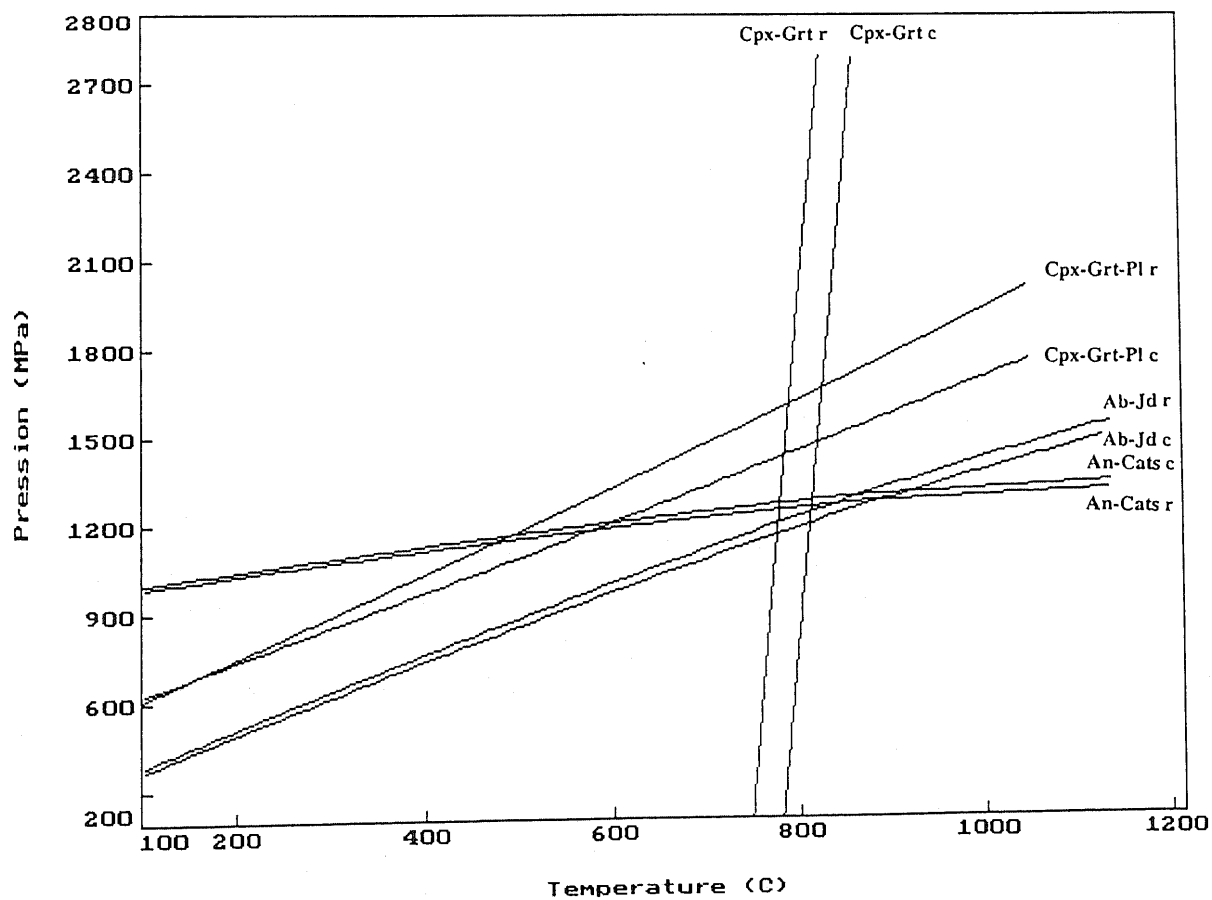


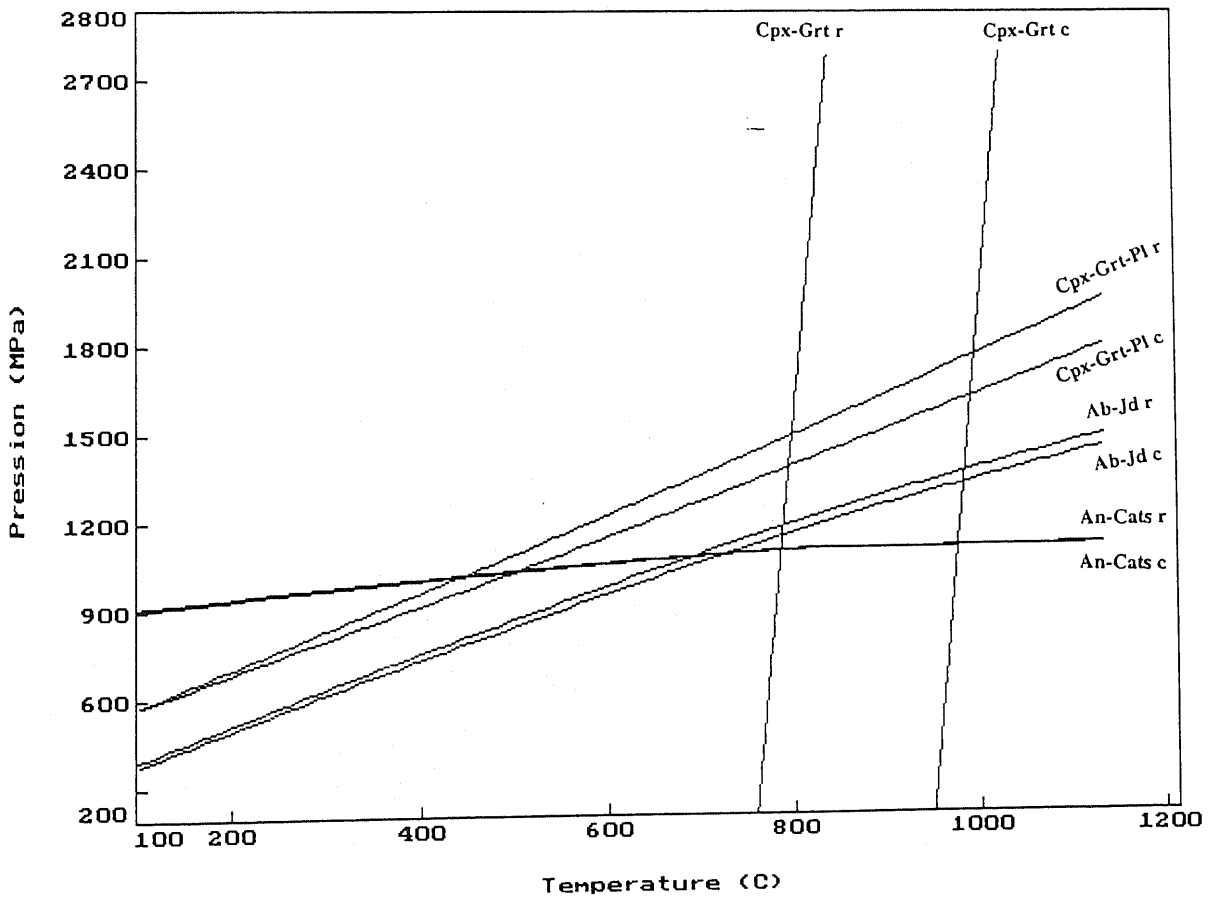
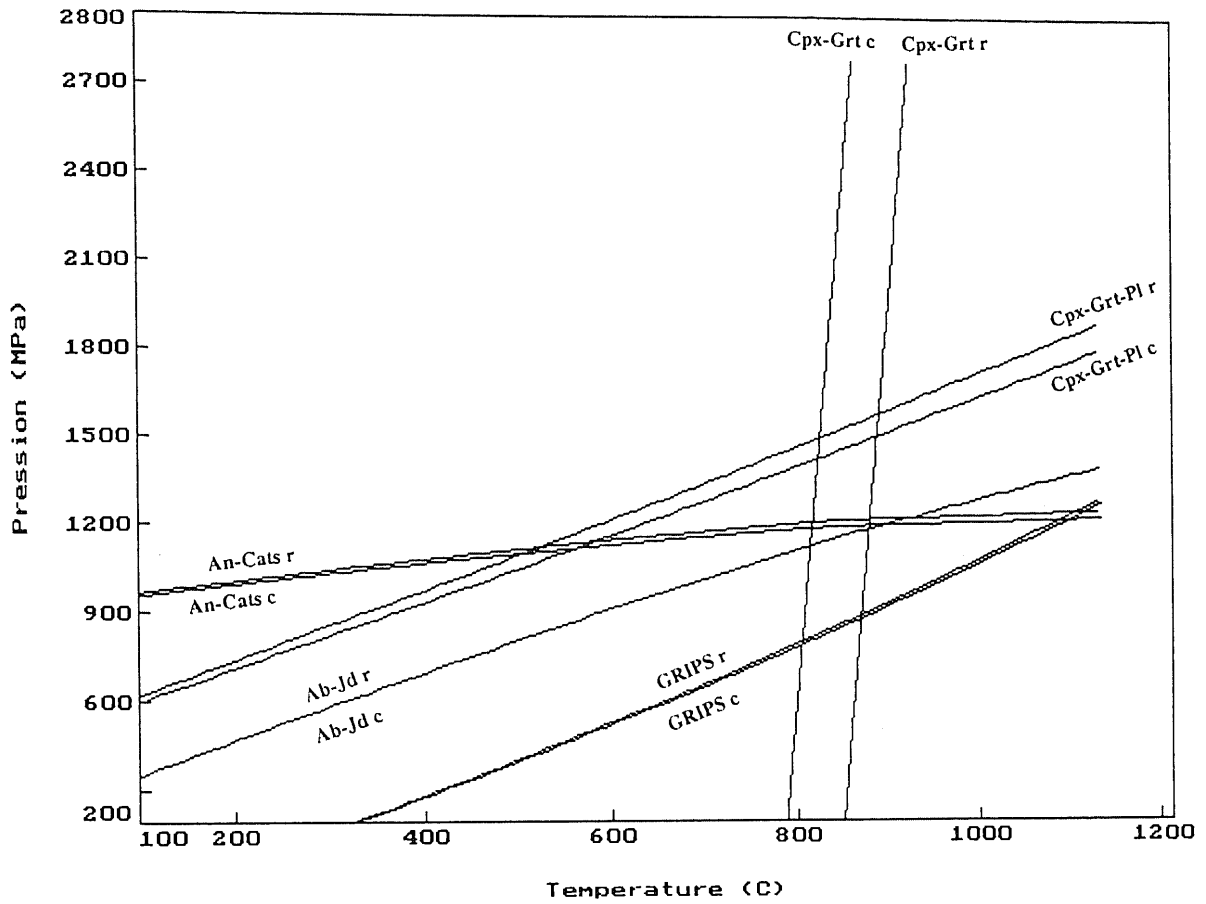
## KI 158



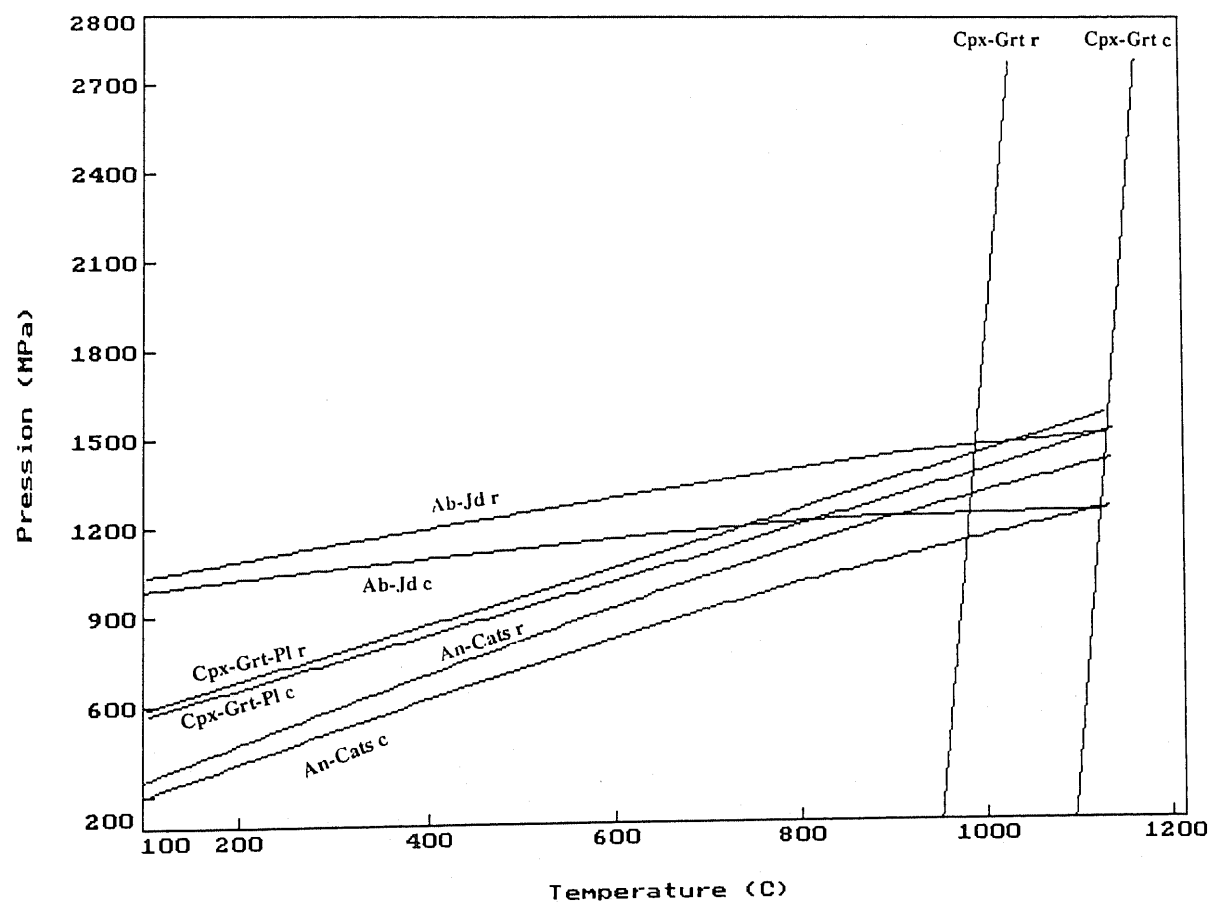
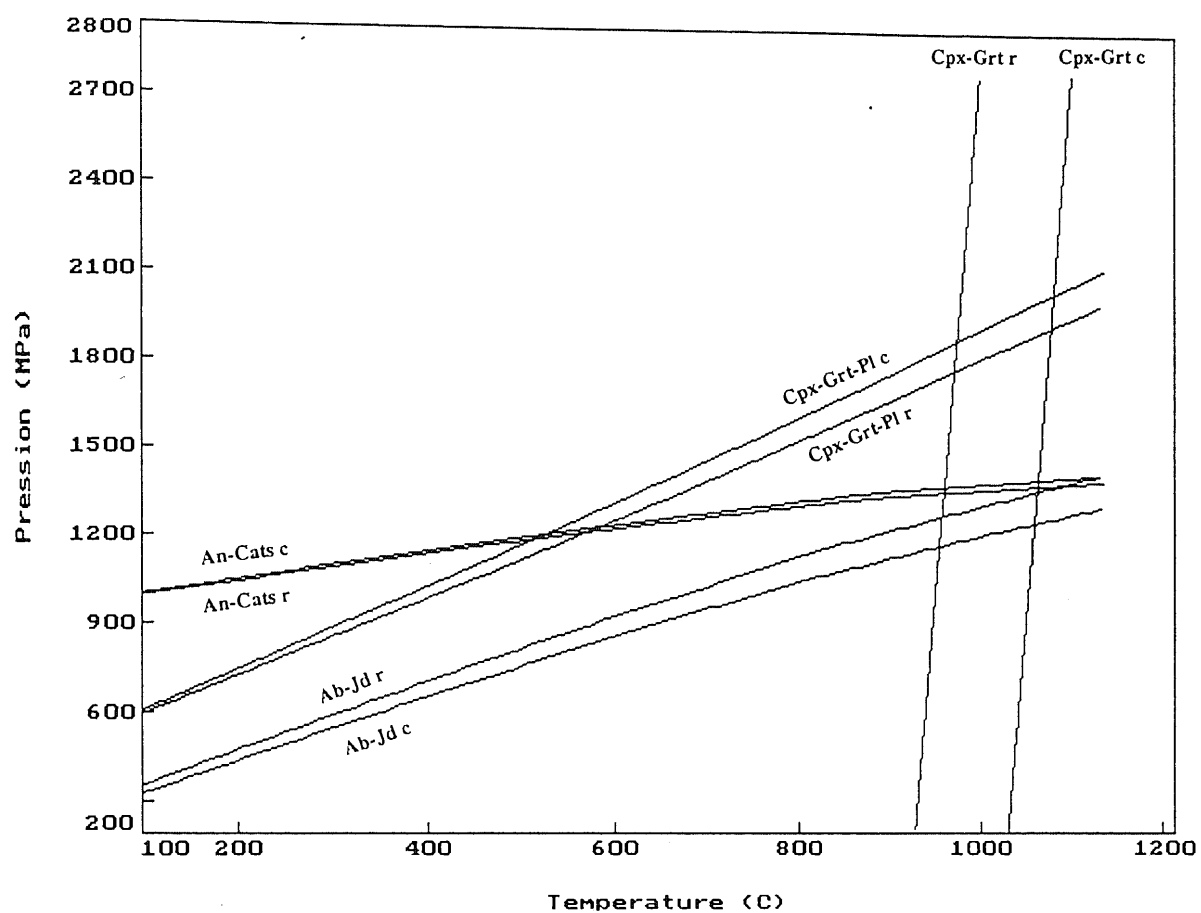


GI 11b

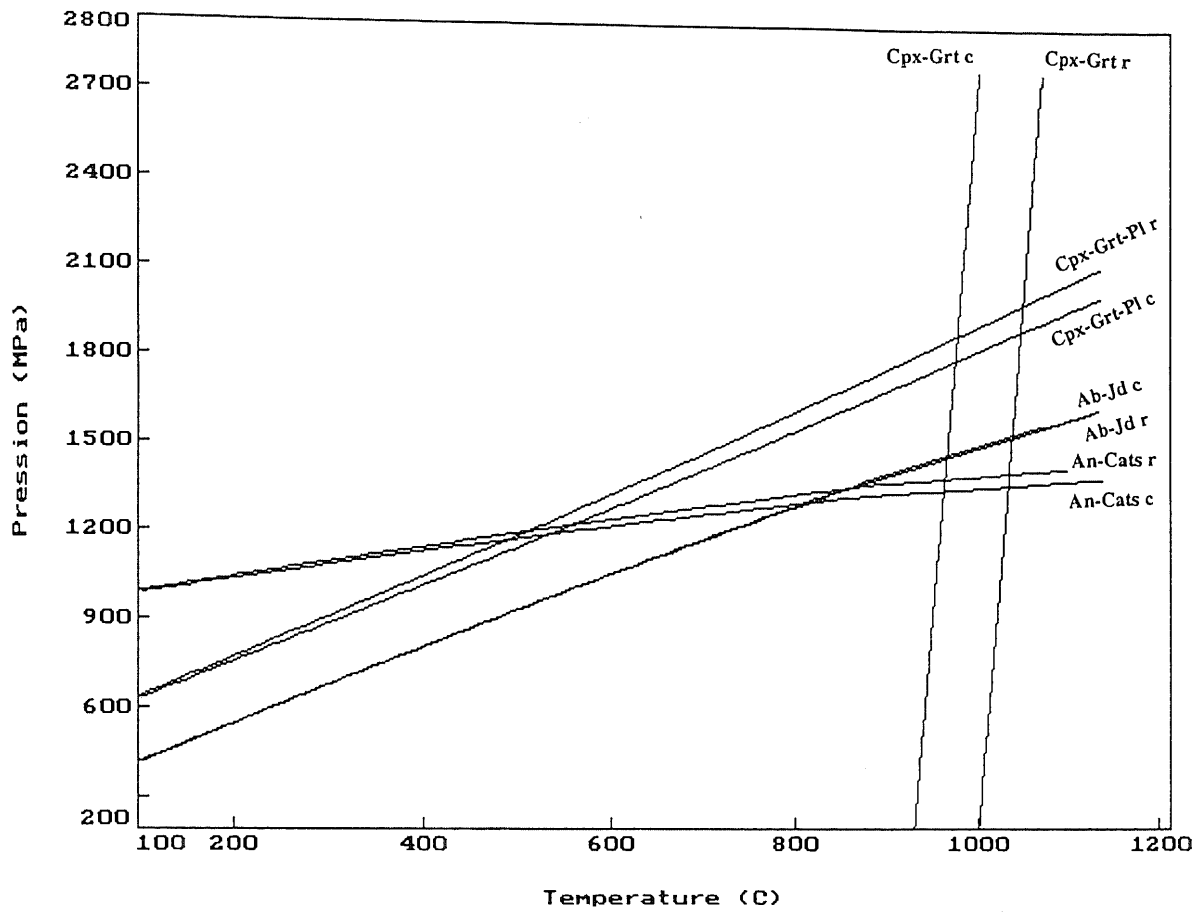




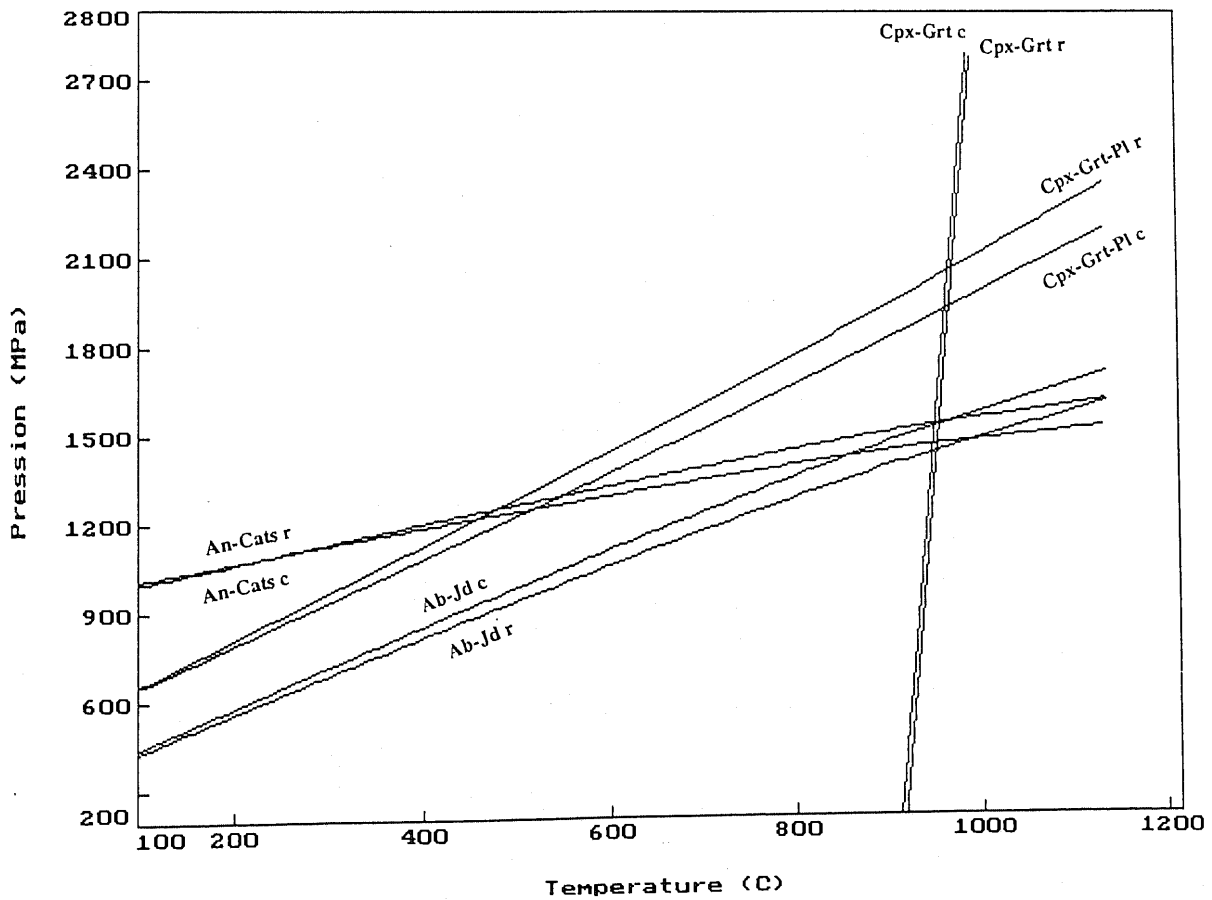




P 572



KI 16



## ACKNOWLEDGMENTS

I would like to express my great gratitude to Prof Brian F. Windley who accepted the supervision of this M.Phil. research project and manifested great interest by bringing wise guidance, encouragement and support at every instance.

I would like to cheerfully thank Prof Jean-Pierre Bard of Universite Montpellier II (France) and also Prof Brian F. Windley for giving me access to their sample collections from Kohistan and for providing me with invaluable information from their fieldwork experiences.

Special thanks are due to Dr Jacques Martignole of Université de Montréal (Canada) who was the first with Dr Bernard L. Mamet to believe in this project and helped me transform it into a reality. Dr Jacques Martignole is also thanked for helpful discussion and guidance on geothermobarometry aspects, and for letting me use the THEBA unpublished software for data treatment.

Thanks are due to Rob Wilson (from University of Leicester) and Glenn Poirier from McGill University (Canada) for their help in using the microprobes.

I gratefully acknowledge the British Council (Placer Dome Inc. Chevening Award) for their entire financial support during my M.Phil. studies.

I would also like to acknowledge the help I received from many friends from the University of Leicester, Université Montpellier II (France), and Université de Montréal (Canada).

## REFERENCES

- ABBOTT, R.N. 1982. A petrogenetic grid for medium and high grade metabasites. *American Mineralogist*, vol. 67, pp. 865-876.
- AHMED, Z. 1988. Bulk chemistry and petrography of the Sakhakot-Qila ophiolite, Pakistan. *Acta Mineralogica Pakistanica*, vol. 4, pp. 4-29.
- ALLEGRE, C.J., COURTILLOT, V., TAPPONNIER, P., HIRN, A., MATTAUER, M., COULON, C., JAEJER, J.J., MARCOUX, J. and 25 others. 1984. Structure and evolution of the Himalaya-Tibet orogenic belt. *Nature*, vol. 307, pp. 17-22.
- ANOVITZ, L.M. 1991. Al zoning in pyroxene and plagioclase: window on late prograde to early retrograde P-T paths in granulite terranes. *American Mineralogist*, vol. 76, pp. 1328-1343.
- ARANOVICH, L.Y. and PODLESSKII, K.K. 1989. Geothermobarometry of high-grade metapelites: simultaneously operating reactions. *Geological Society of London, Special Publication 43*, pp. 45-61.
- BAKER, P.E. 1982. Evolution and classification of orogenic volcanic rocks. In: *Andesites*, R.S. Thorpe (ed.), John Wiley & Sons, New York, pp. 11-24.
- BANNERT, D., BENDER, F.K., BENDER, H., GRUNEBERG, F., KAZMI, A.H., RAZA, H.A. and SHAMS, F.A. 1995. Geology of Pakistan, F.K. Bender and H.A. Raza, Gebruder Borntraeger eds., vol. 25, 414 pp.
- BARD, J.P., JAN, M.Q., MALUSKI, H., MATTE, Ph. and PROUST, F. 1979. Position et extension de la "ceinture" métamorphique à facies schistes bleus dans l'Himalaya du Pakistan Nord. *7e Réunion Annuelle des Sciences de la Terre*, Lyon, p. 29.
- BARD, J.P., MALUSKI, H., MATTE, Ph. and PROUST, F. 1980. The Kohistan sequence: crust and mantle of an obducted island arc. *Geological Bulletin of University of Peshawar, Special Issue*, vol. 13, pp. 87-94.
- BARD, J.-P. 1983. Metamorphic evolution of an obducted island arc: exemple of the Kohistan sequence (Pakistan) in the Himalayan collided range. *Geological Bulletin of University of Peshawar*, vol. 16, pp. 105-184 and *Earth and Planetary Science Letters*, vol. 65, pp. 133-144.
- BECCALUVA, L. and SERRI, G. 1988. Boninitic and low-Ti ophiolites: a reappraisal of their petrogenesis and original tectonic setting. *Tectonophysics*, vol. 146, pp. 291-315.
- BECK, R.A., BURBANK, D.W., SERCOMBE, W.J., RILEY, G.W., BARNDT, J.K., BERRY, J.R., AFZAL, J., KHAN, A.M., JURGEN, H., METJE, J., CHEEMA, A., SHAFIQUE, N.A., LAWRENCE, R.D. and KHAN, M.A. 1995. Stratigraphic evidence for an early collision between northwest India and Asia. *Nature*, vol. 373, pp. 55-58.
- BEGIN, N.J. and CARMICHAEL, D.M. 1992. Textural and compositional relationship of Ca-amphiboles in metabasites of the Cape Smith Belt, northern Québec: implication for a miscibility gap at medium pressure. *Journal of Petrology*, vol. 33, pp. 1317-1343.
- BERMAN, R.G. 1990. Mixing properties of Ca-Mg-Fe-Mn garnets. *American Mineralogist*, vol. 75, pp. 328-344.
- BERMAN, R.G. 1988. Internally consistent thermodynamic data for minerals in the system Na<sub>2</sub>O-K<sub>2</sub>O-CaO-MgO-FeO-Fe<sub>2</sub>O<sub>3</sub>-Al<sub>2</sub>O<sub>3</sub>-SiO<sub>2</sub>-TiO<sub>2</sub>-H<sub>2</sub>O-CO<sub>2</sub>. *Journal of Petrology*, vol. 29, pp. 445-522.
- BERMAN, R.G. and BROWN, T.H. 1985. Heat capacity of minerals in the system Na<sub>2</sub>O-K<sub>2</sub>O-CaO-MgO-FeO-Fe<sub>2</sub>O<sub>3</sub>-Al<sub>2</sub>O<sub>3</sub>-SiO<sub>2</sub>-TiO<sub>2</sub>-H<sub>2</sub>O-CO<sub>2</sub>: representation, estimation, and high temperature extrapolation. *Contributions to Mineralogy and Petrology*, vol. 89, pp. 168-183.
- BERMAN, R.G., ARANOVICH, L.Y. and PATTISON, D.R.M. 1995. Reassessment of the garnet-clinopyroxene Fe-Mg exchange thermometer: II. Thermodynamic analysis. *Contributions to Mineralogy and Petrology*, vol. 119, pp. 30-42.

- COWARD, M.P., BUTLER, R.W.H., ASIF KHAN, M. and KNIPE, R.J. 1987. The tectonic history of Kohistan and its implications for Himalayan structure. *Journal of the Geological Society, London*, vol. 144, pp. 377-391.
- COWARD, M.P., JAN, M.Q., REX, D., TARNEY, J., THIRLWALL, M. and WINDLEY, B.F. 1982. Geotectonic framework of the Himalaya of N Pakistan. *Journal of the geological society of London*, vol. 139, pp. 299-308.
- COWARD, M.P., WINDLEY, B.F., BROUGHTON, R.D., LUFF, I.W., PETTERSON, M.G., PUDSEY, C.J., REX, D.C. and ASIF KHAN, M. 1986. Collision tectonics in the NW Himalayas. *Geological Society of London, Special Publication*, vol. 19, pp. 203-219.
- CRAW, D., KOONS, P.O., WINSLOW, D., CHAMBERLAIN, C.P. and ZEITLER, P. 1994. Boiling fluids in a region of rapid uplift, Nanga Parbat Massif, Pakistan. *Earth and Planetary Science Letters*, vol. 128, pp. 169-182.
- DEBON, F., LEFORT, P., DAUTEL, D., SONET, J. and ZIMMERMANN, J.L. 1987. Granites of western Karakorum and northern Kohistan (Pakistan): a composite Mid-Cretaceous to Upper Cenozoic magmatism, *Lithos*, vol. 20, pp. 19-40.
- DESIO, A. 1977. The occurrence of blueschists between the Middle Indus and Swat valleys as an evidence of subduction (N. Pakistan). *Rendiconti della Accademia Nazionale dei Lincei*, ser. 8, vol. 62, pp. 1-9.
- DICK, H.J.B. and BULLEN, T. 1984. Chromian spinel as a petrogenetic indicator in abyssal and alpine-type peridotites and spatially associated lavas. *Contributions to Mineralogy and Petrology*, vol. 86, pp. 54-76.
- ENGLAND, P.C. and RICHARDSON, S.W. 1977. The influence of erosion upon the mineral facies of rocks from different metamorphic environments. *Journal of the Geological Society of London*, vol. 134, pp. 201-213.
- ENGLAND, P.C. and SEARLE, M.P. 1986. The Cretaceous-Tertiary deformation of the Lhasa block and its implications for crustal thickening in Tibet. *Tectonics*, vol. 5, pp. 1-14.
- ESSENE, E.J. and FYFE, W.S. 1967. Omphacite in California metamorphic rocks. *Contributions to Mineralogy and Petrology*, vol. 15, pp. 1-23.
- ESSENE, E.J., HENSEN, B.J. and GREEN, D.H. 1970. Experimental study of amphibolite and eclogite stability. *Physics of the Earth and Planetary Interiors*, vol. 3, pp. 378-384.
- FREER, R. 1981. Diffusion in silicate minerals and glasses: a data digest and guide to the literature. *Contributions to Mineralogy and Petrology*, vol. 70, pp. 440-454.
- FROST, B.R. and CHACKO, T. 1989. The granulite uncertainty principle: limitations on thermobarometry in granulites. *Journal of Geology*, vol. 97, pp. 435-450.
- FUHRMAN, M.L. and LINDSLEY, D.H. 1988. Ternary feldspar modeling and thermometry. *American Mineralogist*, vol. 73, pp. 201-215.
- GANSSER, A. 1964. *Geology of the Himalayas*. London: Wiley, 289 pp.
- GANSSER, A. 1979. Map of ophiolitic belts of Himalayan and Tibetan region. *International Geological Correlations Programme, International Atlas of Ophiolites*, 1: 500 000 Boulder, Colorado: Geological Society of America.
- GASPARIK, T. 1984. Experimental study of subsolidus phase relations and mixing properties of pyroxenes in the system  $\text{CaO-Al}_2\text{O}_3\text{-SiO}_2$ . *Geochimica et Cosmochimica Acta*, vol. 48, pp. 2537-2546.
- GEORGE, M.T., HARRIS, N.B.W. and BUTLER, R.H.W. 1993. The tectonic implications of contrasting granite magmatism between the Kohistan island arc and the Nanga Parbat-Haramosh Massif, Pakistan Himalaya. *Geological Society of London, Special Publication* 74, pp. 173-191.
- GRAHAM, C.M. and POWELL, R. 1984. A garnet-hornblende geothermometer: calibration, testing, and application to the Pelona schist, southern California. *Journal of Metamorphic Geology*, vol. 2, pp. 13-31.

- GREEN, D.H. 1976. Experimental testing of equilibrium partial melting of peridotite under water saturated, high pressure conditions. *Canadian Mineralogist*, vol. 14, pp. 255-268.
- GREEN, T.H. 1982. Anatexis of mafic crust and high pressure crystallization of andesite. In: *Andesites*, R.S. Thorpe (ed.), John Wiley & Sons, New York, pp. 465-487.
- HONEGGER, K., DIETRICH, V., FRANK, W., GANSSE, A., THONI, M. and TROMMSDORFF, V. 1982. Magmatism and metamorphism in the Ladakh Himalayas (the Indus-Tsangpo suture zone). *Earth and Planetary Science Letters*, vol. 60, pp. 253-292.
- HUDON, P., Department of Geological Sciences, McGill University. 1991. Introduction à la thermodynamique appliquée à la géothermobarométrie et à l'utilisation du logiciel Theba (Montpellier, octobre 1991).
- JAN, M.Q. 1980. Petrology of the obducted mafic and ultramafic metamorphites from the southern part of the Kohistan island arc sequence. *Geological Bulletin of University of Peshawar, Special Issue*, vol. 13, pp. 95-107.
- JAN, M.Q. and KHAN, M.A. 1992. Exsolution in Al-Cr-Fe<sup>3+</sup>-rich spinels from the Chilas mafic-ultramafic complex, Pakistan. *American Mineralogist*, vol. 77, pp. 1074-1079.
- JAN, M.Q., KHAN, M.A. and QAZI, M.S. 1993. The Sapat mafic-ultramafic complex, Kohistan arc, North Pakistan. *Geological Society of London, Special Publication*, vol. 74, pp. 113-121.
- JAN, M.Q. and HOWIE, R.A. 1981. The mineralogy and geochemistry of the metamorphosed basic and ultrabasic rocks of the Jijal Complex, Kohistan, NW Pakistan. *Journal of Petrology*, vol. 22, part 1, pp. 85-126.
- JAN, M.Q. and HOWIE, R.A. 1982. Hornblende amphiboles from basic and intermediate rocks of Swat-Kohistan, northwest Pakistan. *American Mineralogist*, vol. 67, pp. 1155-1178.
- JAN, M.Q. and JABEEN, N. 1990. A review of mafic-ultramafic plutonic complexes in the Indus Suture Zone of Pakistan. *Physics and Chemistry of the Earth*, vol. 17, pp. 93-113.
- JAN, M.Q. and KARIM, A. 1995. Coronas and high-P veins in metagabbros of the Kohistan island arc, northern Pakistan: evidence for crustal thickening during cooling. *Journal of Metamorphic Geology*, vol. 13, pp. 357-366.
- JAN, M.Q., WILSON, R.N. and WINDLEY, B.F. 1982. Paragonite paragenesis from the garnet granulites of the Jijal complex, Kohistan, N. Pakistan. *Mineralogical Magazine*, vol. 45, pp. 73-77.
- JAN, M.Q. and WINDLEY, B.F. 1990. Chromian spinel-silicate chemistry in ultramafic rocks of the Jijal complex, northwest Pakistan. *Journal of Petrology*, vol. 31, pp. 667-715.
- JAN, M.Q., WINDLEY, B.F. and WILSON, R.N. 1984. Chromian andradite and olivine-chromite relations in a chromitite layer from the Jijal complex, northwestern Pakistan. *Canadian Mineralogist*, vol. 22, pp. 341-345.
- JOHNSON, B.D., POWELL, C. McA. and VEEVERS, J.J. 1976. Spreading history of the eastern Indian Ocean, and Greater India's northward flight from Antarctica and Australia. *Bulletin of the Geological Society of America*, vol. 87, pp. 1560-1566.
- KARIG, D.E. 1971. Origin and development of marginal basins in the western Pacific. *Journal of Geophysical Research*, vol. 74, pp. 2543-2579.
- KARIG, D.E., ANDERSON, R.N. and BIBEE, L.D. 1978. Characteristics of back arc spreading in the Mariana trough. *Journal of Geophysical Research*, vol. 83, pp. 1213-1226.
- KERRICK, D.M. and DARKEN, L.S. 1975. Statistical thermodynamic models for ideal oxide and silicate solid solutions, with application to plagioclase. *Geochimica et Cosmochimica Acta*, vol. 39, pp. 1431-1442.
- KHAN, M.A. 1988. Petrology and structure of the Chilas mafic-ultramafic complex, Kohistan, NW Himalayas, Pakistan. PhD Thesis, Imperial College, University of London.

- KHAN, M.A. and COWARD, M.P. 1990. Entrapment of an island arc in collision tectonics: a review of the structural history of the Kohistan arc complex, N.W. Himalayas. *Physics and Chemistry of the Earth*, vol. 17, pp. 1-18.
- KHAN, M.A., JAN, M.Q. and WEAVER, B.L. 1993. Evolution of the lower arc crust in Kohistan, N. Pakistan: temporal arc magmatism through early, mature and intra-arc rift stages. *Geological Society of London, Special Publication 74*, pp. 123-138.
- KHAN, M.A., JAN, M.Q., WINDLEY, B.F., TARNEY, J. and THIRLWALL, M. 1989. The Chilas mafic-ultramafic igneous complex; the root of the Kohistan island arc in the Himalaya of northern Pakistan. *Geological Society of America, Special paper*, vol. 232, pp. 75-94.
- KLOOTWIJK, C.J. 1979. A summary of palaeo-magnetic data from extrapeninsular Indo-Pakistan and south-central Asia: implications for collision tectonics. *Structural Geology of the Himalaya*, Saklani P.S. (ed.), Today and Tomorrow Publications, New Delhi, pp. 307-360.
- KLOOTWIJK, C.J., GEE, J.S., PIERCE, J.W., SMITH, G.M. and McFADDEN, P.L. 1992. An early India-Asia contact: Paleomagnetic constraints from Ninetyeast Ridge, ODP Leg 121. *Geology*, vol. 20, pp. 395-398.
- KRETZ, R. 1983. Symbols for rock-forming minerals. *American Mineralogist*, vol. 68, pp. 277-279.
- LEAKE, E. 1978. Nomenclature of amphiboles. *Mineralogical Magazine*, vol. 42, pp. 533-563.
- LINDSLEY, D.H. 1983. Pyroxene thermometry. *American Mineralogist*, vol. 68, pp. 477-493.
- LOUCKS, R.R., MILLER, D.J., ASHRAF, M., AWAN, M.A. and KAHN, M.S. 1990. The Jijal Complex: Layered mafic-ultramafic arc cumulates from the crust-mantle boundary, Pakistani Himalayas (Abstract), *EOS Trans. AGU*, vol. 71, 664 pp.
- MADER, U.K. and BERMAN, R.G. 1992. Amphibole thermobarometry: a thermodynamic approach. *Current Research, part E; Geological Survey of Canada, paper 92-1E*, pp. 393-400.
- MADER, U.K., PERCIVAL, J.A. and BERMAN, R.G. 1994. Thermobarometry of garnet-clinopyroxene-hornblende granulites from the Kapuskasing structural zone. *Canadian Journal of Earth Sciences*, vol. 31, pp. 1134-1145.
- MAJID, M. and PARACHA, F.A. 1980. Calc-alkaline magmatism at destructive plate margin in Kohistan, northern Pakistan. *Geological Bulletin of University of Peshawar, Special Issue*, vol. 13, pp. 109-120.
- MALUSKI, H. and MATTE, P. 1984. Ages of alpine tectometamorphic events in the northwestern Himalaya (northern Pakistan) by  $^{40}\text{Ar}/^{39}\text{Ar}$  method. *Tectonics*, vol. 3, pp. 1-18.
- MARCELOT, G., DUPUY, C., GIROD, M. and MAURY, R.C. 1983. Petrology of Futuna island lavas (New Hebrides): an example of calc-alkaline magmatism associated with the initial stages of back-arc spreading. *Chemical Geology*, vol. 38, pp. 23-37.
- MARTIGNOLE, J. 1992. Exhumation of high-grade terranes: a review. *Canadian Journal of Earth Sciences*, vol. 29, pp. 737-745.
- MARTIGNOLE, J. and POUGET, P. 1993. Contrasting zoning profiles in high-grade garnets: evidence for the allochthonous nature of a Grenville province terrane. *Earth and Planetary Science Letters*, vol. 120, pp. 177-185.
- MATTAUER, M. 1986. Intracontinental subduction, crust-mantle decollement and crustal stacking wedge in the Himalaya and other collision belts. In: Coward M.P. & Ries A.C. (eds) *Collision Tectonics*. Geological Society of London, Special Publication 19, pp. 37-50.
- MILLER, D.J. and CHRISTENSEN, N.I. 1994. Seismic signature and geochemistry of an island arc: A multidisciplinary study of the Kohistan accreted terrane, northern Pakistan. *Journal of Geophysical Research*, vol. 99, pp. 11 623-11 642.
- MILLER, D.J., LOUCKS, R.R. and ASHRAF, M. 1991. Platinum-group element mineralization in the Jijal layered ultramafic-mafic complex, Pakistani Himalayas. *Economic Geology*, vol. 86, pp. 1093-1102.

- MIYASHIRO, A. 1973. The Troodos ophiolitic complex was probably formed in an island arc. *Earth and Planetary Science Letters*, vol. 19, pp. 218-224.
- MOECHER, D.P., ESSENE, E.J. and ANOVITZ, L.M. 1988. Calculation and application of clinopyroxene-garnet-plagioclase-quartz geobarometers. *Contributions to Mineralogy and Petrology*, vol. 100, pp. 92-106.
- MORIMOTO, N. 1988. Nomenclature of pyroxenes. *Mineralogical Magazine*, vol. 52, pp. 535-550.
- MOUDDEN, A. 1991. PhD thesis, Université Montpellier II.
- PARRISH, R. and TIRRUL, R. 1989. U-Pb age of the Baltoro granite, northwest Himalaya, and implications for monazite U-Pb systematics. *Geology*, vol. 17, pp. 1076-1079.
- PATTISON, D.R.M. and NEWTON, R.C. 1988. Reversed experimental calibration of the garnet-clinopyroxene  $K_D$  (Fe-Mg) exchange thermometer. *Contributions to Mineralogy and Petrology*, vol. 101, pp. 87-103.
- PERKINS, D. and NEWTON, R.C. 1981a. Charnockite geobarometers based on coexisting garnet-pyroxene-plagioclase-quartz. *Nature*, vol. 292, no. 5819, pp. 144-146.
- PERKINS, D. and NEWTON, R.C. 1981b. The compositions of coexisting pyroxenes and garnets in the system  $\text{CaO-MgO-Al}_2\text{O}_3\text{-SiO}_2$  at 900-1100°C and high pressure. *Contributions to Mineralogy and Petrology*, vol. 75, pp. 291-300.
- PETTERSON, M.G. 1984. The structure, petrology and geochemistry of the Kohistan batholith, Gilgit, N. Pakistan. Unpublished Ph.D. thesis, Leicester University.
- PETTERSON, M.G. and WINDLEY, B.F. 1985. Rb-Sr dating of the Kohistan arc-batholith in the Trans-Himalaya of north Pakistan, and tectonic implications. *Earth and Planetary Science Letters*, vol. 74, pp. 45-57.
- PETTERSON, M.G. and WINDLEY, B.F. 1991. Changing source regions of magmas and crustal growth in the Trans-Himalayas: evidence from the Chalt volcanics and Kohistan batholith, Kohistan, northern Pakistan. *Earth and Planetary Science Letters*, vol. 102, pp. 326-341.
- PETTERSON, M.G. and WINDLEY, B.F. 1992. Field relations, geochemistry and petrogenesis of the Cretaceous basaltic Jutal dykes, Kohistan, northern Pakistan. *Journal of the Geological Society of London*, vol. 149, pp. 299-308.
- PETTERSON, M.G., WINDLEY, B.F. and SULLIVAN, M.A. 1990. A petrological, structural and geochemical review of the Kohistan batholith and its relationship to regional tectonics. *Physics and Chemistry of the Earth*, vol. 17, pp. 47-70.
- POGNANTE, U. and SPENCER, D.A. 1991. First report of eclogites from the Himalayan belt, Kaghan valley (northern Pakistan). *European Journal of Mineralogy*, vol. 3, pp. 613-618.
- PUDSEY, C.J. 1986. The Northern Suture, Pakistan: Margin of a Cretaceous island arc. *Geological Magazine*, vol. 123, pp. 405-423.
- PUDSEY, C.J., COWARD, M.P., LUFF, I.W., SHACKLETON, R.M., WINDLEY, B.F. and JAN, M.Q. 1985. Collision zone between the Kohistan arc and the Asian plate in NW Pakistan. *Transactions of the Royal Society of Edinburgh: Earth Sciences*, vol. 76, pp. 463-479.
- PUDSEY, C.J., SCHROEDER, R. and SKELTON, P.W. 1986. Cretaceous (Aptian-Albian) age for the island-arc volcanics, Kohistan. In: GUPTA, V.J. (ed.) *Recent Researches in Geology. Palaeontology, Stratigraphy and Structure of the Western Himalayas*. Hindustani Publishing Co, Delhi, vol. 3, pp. 150-168.
- REX, A.J., SEARLE, M.P., TIRRUL, R., CRAWFORD, D.J., PRIOR, D.J., REX, D.C. and BARNICOAT, A.C. 1988. The geochemical and tectonic evolution of the central Karakorum, North Pakistan. *Philosophical Transactions of the Royal Society of London*, vol. 326, pp. 229-255.
- ROCK, N.M.S. and LEAKE, B.E. 1984. The International Mineralogical Association amphibole nomenclature scheme: computerization and its consequences. *Mineralogical Magazine*, vol. 48, pp. 211-227.



- SCHÄRER, U., COPELAND, P.Y., HARRISON, T.M. and SEARLE, M.P. 1990. Age, cooling history and origin of post-collisional leucogranites in the Karakoram batholith; a multi-system isotope study. *Journal of Geology*, vol. 98, pp. 233-251.
- SEARLE, M.P., REX, A.J., TIRRUL, R., REX, D.C. and BARNICOAT, A.C. 1989. Metamorphic, magmatic and tectonic evolution of the central Karakorum in the Biafo-Baltoro-Hushe regions of N. Pakistan. *Geological Society of America, Special Publication*, vol. 232, pp. 1989.
- SEARLE, M.P., WINDLEY, B.F., COWARD, M.P., COOPER, D.J.W., REX, A.J., REX, D.C., LI TINGDONG., XIAO XUCHANG., JAN, M.Q., THAKUR, V.C. and KUMAR, S. 1987. The closing of Tethys and tectonics of the Himalaya. *Geological Society of America Bulletin*, vol. 98, vol. 678-701.
- SHAMS, F.A. 1980. Origin of the Shangla blueschists, Swat Himalaya, Pakistan. *Proceedings of the International Commission on Geodynamics*. R.A.K. Tahirkheli, M.Q. Jan and M. Majid (eds), Special Issue, *Geological Bulletin of the University of Peshawar*, vol. 13, pp. 67-70.
- SMITH, H.A., CHAMBERLAIN, C.P. and ZEITLER, P.K. 1994. Timing and duration of Himalayan Metamorphism within the Indian Plate, Northwest Himalaya, Pakistan. *Journal of Geology*, vol. 102, pp. 493-508.
- SPEAR, F.S. 1980. NaSi=CaAl exchange equilibrium between plagioclase and amphibole. *Contributions to Mineralogy and Petrology*, vol. 72, pp. 33-41.
- SPEAR, F.S. 1993. Metamorphic phase equilibria and pressure-temperature-time path. *Mineralogical Society of America, monograph*, 799 pp.
- STERN, R.J., PING-NAN, L., MORRIS, J.D., JACKSON, M.C., FRYER, P., BLOOMER, S.H. and ITO, E. 1990. Enriched back-arc basin basalts from the northern Mariana trough: implications for the magmatic evolution of back-arc basins. *Earth and Planetary Science Letters*, vol. 100, pp. 210-225.
- ST-ONGE, M.R. 1987. Zoned poikiloblastic garnets: P-T paths and syn-metamorphic uplift through 30 km of structural depth, Wopmay Orogen, Canada. *Journal of Petrology*, vol. 28, pp. 1-21.
- SULLIVAN, M.A., WINDLEY, B.F., SAUNDERS, A.D., HAYNES, J.R. and REX, D.C. 1993. A palaeogeographic reconstruction of the Dir Group: evidence for magmatic arc migration within Kohistan, N. Pakistan. Treloar P.J. & Searle M.P. (eds), *Geological Society of London, Special Publication* 74, pp. 139-160.
- TAHIRKHELI, R.A.K. 1980. The Main Mantle Thrust: its score in metallogeny of northern Pakistan. *Geological Bulletin of University of Peshawar, Special Issue*, vol. 13, pp. 193-198.
- TAHIRKHELI, R.A.K. 1982. Geology of the Himalaya Karakoram and Hindukush in Pakistan. Special Issue, *Geological Bulletin of the University of Peshawar*, vol. 15, 51 pp.
- TAHIRKHELI, R.A.K. 1983. Geological evolution of Kohistan island arc on the southern flank of the Karakorum-Hindukush in Pakistan. *Bollettino Geofisica Tercia ed Applicata*, vol. 25, pp. 351-364.
- TAHIRKHELI, R.A.K. and JAN, M.Q. 1979. Geology of Kohistan, Karakorum Himalaya, northern Pakistan. *Geological Bulletin, University of Peshawar*, vol. 11.
- TAHIRKHELI, R.A.K., MATTAUER, M., PROUST, F. and TAPPONNIER, P. 1979. The India-Eurasia suture zone in northern Pakistan: synthesis and interpretation of data at plate scale. In: FARAH A. and DeJong K.A. (eds) *Geodynamics of Pakistan*. Geological Survey of Pakistan, Quetta, pp. 125-130.
- TONARINI, S., VILLA, I.M., OBERLI, F., MEIER, M., SPENCER, D.A., POGNANTE, U. and RAMSAY, J.G. 1993. Eocene age of eclogite metamorphism in Pakistan Himalaya: implications for India-Eurasia collision. *Terra Nova*, vol. 5, pp. 13-20.
- TRELOAR, P.J., BRODIE, K.H., COWARD, M.P., JAN, M.Q., KHAN, M.A., KNIPE, R.J., REX, D. and WILLIAMS, M.P. 1990. The evolution of the Kamila shear zone. In: *Exposed Cross-Sections of the Continental Crust*. M.H. Salisbury and D.M. Fountain (eds), Kluwer Academic, Hingham, Mass, pp. 175-214.

- TRELOAR, P.J., REX, D.C., GUISE, P.G., COWARD, M.P., SEARLE, M.P., WINDLEY, B.F., PETTERSON, M.G., JAN, M.Q and LUFF, I.W. 1989. K-Ar and Ar-Ar geochronology of the Himalayan collision in NW Pakistan: constraints on the timing of suturing, deformation, metamorphism and uplift. *Tectonics*, vol. 8, pp. 881-909.
- WHITE, A.J.R. 1964. Clinopyroxenes from eclogites and basic granulites. *American Mineralogist*, vol. 49, pp. 883-888.
- WINSLOW, D.M., CHAMBERLAIN, C.P. and ZEITLER, P.K. 1995. Metamorphism and melting of the lithosphere due to rapid denudation, Nanga Parbat Massif, Himalaya. *Journal of Geology*, vol. 103, pp. 395-409.
- WOOD, B.J. 1977. The activities of components in clinopyroxene and garnet solid solutions and their application to rocks. *Philosophical Transactions of the Royal Society of London*, vol. 286, pp. 331-342.
- WOOD, B.J. and BANNO, S. 1973. Garnet-orthopyroxene and orthopyroxene-clinopyroxene relationships in simple and complex systems. *Contributions to Mineralogy and Petrology*, vol. 42, pp. 109-124.
- YAMAMOTO, H. 1993. Contrasting metamorphic P-T-time paths of the Kohistan granulites and tectonics of the western Himalayas. *Journal of the Geological Society, London*, vol. 150, pp. 843-856.
- ZEITLER, P.K. 1985. Cooling history of the NW Himalaya, Pakistan. *Tectonics*, vol. 4, pp. 127-151.
- ZEITLER, P.K. and CHAMBERLAIN, C.P. 1991. Petrogenetic and tectonic significance of young leucogranites from the northwestern Himalaya, Pakistan. *Tectonics*, vol. 10, pp. 729-741.
- ZEITLER, P.K., CHAMBERLAIN, C.P. and SMITH, H.A. 1993. Synchronous anatexis, metamorphism, and rapid denudation at Nanga Parbat (Pakistan Himalaya). *Geology*, vol. 21, pp. 347-350.